Advances in Clinical and Experimental Medicine

MONTHLY ISSN 1899-5276 (PRINT) ISSN 2451-2680 (ONLINE) www.advances.umed.wroc.pl

2018, Vol. 27, No. 5 (May)

Impact Factor (IF) – 1.179
Ministry of Science and Higher Education – 15 pts.
Index Copernicus (ICV) – 155.19 pts.

Wroclaw Medical University

Advances
in Clinical and Experimental Medicine

ISSN 1899-5276 (PRINT) ISSN 2451-2680 (ONLINE) www.advances.umed.wroc.pl

MONTHLY 2018
Vol. 27, No. 5
(May)

Advances in Clinical and Experimental Medicine is a peer-reviewed open access journal published by Wroclaw Medical University. Its abbreviated title is Adv Clin Exp Med. Journal publishes original papers and reviews encompassing all aspects of medicine, including molecular biology, biochemistry, genetics, biotechnology, and other areas. It is published monthly, one volume per year.

Editorial Office
ul. Marcinkowskiego 2–6
50-368 Wrocław, Poland
Tel.: +48 71 784 12 05
E-mail: redakcja@umed.wroc.pl

Publisher
Wroclaw Medical University
Wybrzeże L. Pasteura 1
50-367 Wrocław, Poland

© Copyright by Wroclaw Medical University, Wrocław 2018

Online edition is the original version of the journal

Editor-in-Chief
Maciej Bagłaj

Vice-Editor-in-Chief
Dorota Frydecka

Secretary
Katarzyna Neubauer

Editorial Board
Piotr Dzięgiel
Marian Klinger
Halina Milnerowicz
Jerzy Mozrzymas
Piotr Ponikowski
Marek Sąsiadek
Leszek Szenborn
Jacek Szepietowski

Thematic Editors
Marzenna Bartoszewicz (microbiology)
Marzena Dominiak (dentistry)
Paweł Domosławski (surgery)
Maria Ejma (neurology)
Jacek Gajek (cardiology)
Katarzyna Kapelko-Słowik (internal medicine)
Mariusz Kusztal
(nephrology and transplantology)
Rafał Matkowski (oncology)
Robert Śmigiel (pediatrics)
Paweł Tabakow (experimental medicine)
Anna Wiela-Hojeńska
(pharmaceutical sciences)
Marcin Ruciński (basic sciences)
Katarzyna Neubauer (gastroenterology)
Ewa Milnerowicz-Nabzdyk (gynecology)

Statistical Editors
Dorota Diakowska
Leszek Noga
Lesław Rusiecki

Technical Editorship
Paulina Kunicka
Joanna Gudarowska
Agnieszka Kwiatkowska
Marek Misiak

English Language Copy Editors
Sherill Howard Pociecha
Jason Schock
Marcin Tereszewski
Eric Hilton

International Advisory Board
Reinhard Berner (Germany)
Vladimir Bobek (Czech Republic)
Marcin Czyz (UK)
Buddhadeb Dawn (USA)
Kishore Kumar Jella (USA)
Pavel Kopel (Czech Republic)
Tomasz B. Owczarek (USA)
Ivan Rychlík (Czech Republic)
Anton Sculean (Switzerland)
Andriy B. Zimenkovsky (Ukraine)

Editorial Policy

Advances in Clinical and Experimental Medicine (Adv Clin Exp Med) is an independent multidisciplinary forum for exchange of scientific and clinical information, publishing original research and news encompassing all aspects of medicine, including molecular biology, biochemistry, genetics, biotechnology and other areas. During the review process, the Editorial Board conforms to the "Uniform Requirements for Manuscripts Submitted to Biomedical Journals: Writing and Editing for Biomedical Publication" approved by the International Committee of Medical Journal Editors (www.ICMJE.org/). The journal publishes (in English only) original papers and reviews. Short works considered original, novel and significant are given priority. Experimental studies must include a statement that the experimental protocol and informed consent procedure were in compliance with the Helsinki Convention and were approved by an ethics committee.

For all subscription related queries please contact our Editorial Office:

redakcja@umed.wroc.pl

For more information visit the journal's website:

www.advances.umed.wroc.pl

Pursuant to the ordinance no. 13/XV R/2017 of the Rector of Wroclaw Medical University (as of February 7, 2017) from February 8, 2017 authors are required to pay a fee amounting to 300 euros for each manuscript accepted for publication in the journal "Advances in Clinical and Experimental Medicine."

Pursuant to the ordinance no. 134/XV R/2017 of the Rector of Wroclaw Medical University (as of December 28, 2017) from January 1, 2018 authors are required to pay a fee amounting to 700 euros for each manuscript accepted for publication in the journal "Advances in Clinical and Experimental Medicine."

Indexed in: MEDLINE, Science Citation Index Expanded, Journal Citation Reports/Science Edition,

Scopus, EMBASE/Excerpta Medica, Ulrich's™ International Periodicals Directory, Index Copernicus

Typographic design: Monika Kolęda, Piotr Gil
DTP: Wydawnictwo UMW, TYPOGRAF
Cover: Monika Kolęda
Printing and binding: EXDRUK

Advances
in Clinical and Experimental Medicine

MONTHLY 2018, Vol. 27, No. 5 (May)

ISSN 1899-5276 (PRINT)
ISSN 2451-2680 (ONLINE)
www.advances.umed.wroc.pl

Contents

Original papers

© Copyright by Wroclaw Medical University, Wrocław 2018

Reviews

MiR-181a inhibits human trabecular meshwork cell apoptosis induced by H_2O_2 through the suppression of NF-κB and JNK pathways

Yuwen Wang[A,D,F], Heding Zhou[B,D,F], Xiaotian Liu[C,D,F], Yin Han[B,F], Suqi Pan[B,F], Yanyan Wang[C,F]

Ningbo Eye Hospital, Ningbo, China

A – research concept and design; B – collection and/or assembly of data; C – data analysis and interpretation;
D – writing the article; E – critical revision of the article; F – final approval of the article

Advances in Clinical and Experimental Medicine, ISSN 1899-5276 (print), ISSN 2451-2680 (online) *Adv Clin Exp Med*. 2018;27(5):577–582

Address for correspondence
Yuwen Wang
E-mail: wangyuwen12321@126.com

Funding sources
None declared

Conflict of interest
None declared

Received on January 6, 2017
Reviewed on January 17, 2017
Accepted on February 23, 2017

Abstract

Background. The trabecular meshwork (TM) plays a critical role in the outflow of aqueous humor.

Objectives. In this study, we aimed to investigate the effect of miR-181a on H_2O_2-induced apoptosis in TM cells.

Material and methods. Human primary explant-derived TM cells were cultured in fibroblast medium and then treated with different concentrations of H_2O_2 for 2 h. We used a series of methods to carry out the research, such as MTT assay, quantitative reverse transcriptase-polymerase chain reaction (qRT-PCR), apoptosis assay, and western blot methodology.

Results. The apoptosis assay and qRT-PCR showed that H_2O_2-induced apoptosis and cell viability were suppressed in a dose-dependent manner in TM cells. After the TM cells were treated with H_2O_2, miR-181a expression was significantly lower. The overexpression of miR-181a enhanced TM cells' viability, while the knockdown of miR-181a inhibited viability of cells. The overexpression of miR-181a suppressed TM cell apoptosis, while the knockdown of miR-181a induced apoptosis. H_2O_2 activated the nuclear factor-κB (NF-κB) and c-Jun N-terminal kinase (JNK) pathways and induced cell apoptosis, while the overexpression of miR-181a suppressed both pathways and decreased the rate of apoptosis.

Conclusions. In conclusion, this study indicated that miR-181a could improve the survival rate of TM cells after H_2O_2 treatment by blocking the NF-κB and JNK signaling pathways. These findings might provide novel therapeutic opportunities in the treatment of glaucoma.

Key words: cell apoptosis, H_2O_2, miR-181a, trabecular meshwork, nuclear factor-κB, c-Jun N-terminal kinase pathway

DOI
10.17219/acem/69135

Copyright
© 2018 by Wroclaw Medical University
This is an article distributed under the terms of the Creative Commons Attribution Non-Commercial License (http://creativecommons.org/licenses/by-nc-nd/4.0/)

Introduction

Worldwide, glaucoma is the one of the leading causes of irreversible blindness.[1,2] There are 60 million people diagnosed with glaucoma, of whom 8.4 million have been blinded due to glaucoma.[2] One of the major risk factors associated with glaucoma includes elevated hydrostatic pressure or intraocular pressure (IOP) in the eyes.[3] Intraocular pressure depends on the rate of formation and drainage of the aqueous humor via the trabecular meshwork.[3] The trabecular meshwork (TM), consisting of TM cells and located at the intraocular anterior chamber angle, plays a critical role in the outflow of aqueous humor.[4] Decreased outflow of aqueous humor induces an elevation in IOP and ultimately leads to glaucoma.[3,4] This in turn leads to increased oxidative DNA damage in the TM of glaucoma patients. The oxidative stress induces the activation of the nuclear factor-κB (NF-κB) and c-Jun N-terminal kinase (JNK) signaling pathways.[5] Trabecular meshwork cells play an important role in maintaining the extracellular matrix synthesis (ECM) and phagocytosis of the debris in outflow tissues which control the aqueous-outflow facility. Thus, a shortage of TM cells might result in ocular hypertension. Therefore, the elucidation of the mechanism underlying the miR-181a and primary oxidative stress response signaling pathways might reveal promising opportunities for preventing TM cell apoptosis, which can prevent glaucoma.[5] An understanding the biological functions of TM cells is then beneficial for understanding the pathogenesis of glaucoma and for developing novel drugs.

MicroRNAs (miRNAs) are a group of non-coding RNAs with 14–20 nucleotides, which are involved in the inhibition of endogenous gene expression through translational cleavage.[6] MiRNAs are implicated in many biological progresses, such as cell proliferation, aging, apoptosis, and tumorigenesis.[7–10] These miRNAs, either directly or indirectly, have been found to play an important role in the pathogenesis of glaucoma in both animal and human visual systems.[11,12] The role of miRNAs in the molecular mechanisms of ECM provides potential for the development of drugs.[13] In their study, Dismuke et al. isolated 10 mature miRNAs from human aqueous humor exosomes, one of which was miR-181a.[14] miR-181a is a family member of miR-181, and has been reported to act as a regulator in cell proliferation, migration and invasion.[15] Interestingly, miR-181a has different functions in different types of cells. For instance, miR-181a improved colorectal carcinoma cells and cartilage cell proliferation, while it inhibited the proliferation of glioma.[16–18] The levels of miR-181a were most decreased with aging.[19] The exact underlying mechanism of miRNAs regulate retinal apoptosis or degeneration is largely unknown. In a study by Parikh et al., miR-181a was found to promote transdifferentiation towards mesenchymal-like cells.[20] The activation of these pathways is thought to contribute to the dysfunction of normal outflow facility.[21] Also, a study by Kozloski et al. demonstrated that miR-181a negatively regulated NF-κB activity, leading to a significant change in the proliferation and survival phenotype of the B-cell-like diffuse large B-cell lymphoma malignancy.[22] However, the role of miR-181a in the pathogenesis of glaucoma remains elusive.

In this study, we investigated the role of miR-181a in apoptosis in human trabecular meshwork cells induced by H_2O_2 through the NF-κB and JNK pathways.

Material and methods

Cell culture and H_2O_2 treatment

Human primary explant-derived trabecular meshwork (TM) cells (TM cell line) were obtained from ScienCell Research Labs (Catalog No. 6590; Carlsbad, USA). Primary human TM cells were grown in the Fibroblast Medium (Catalog No. 2301; ScienCell Research Labs, Carlsbad, USA) wherein the cells from the 3rd to 6th passage were used. For maintenance, the cells were incubated at 37°C in a 5% CO_2 environment. The TM cells were seeded in a 6-well plate or a 96-well plate and treated with different concentrations of H_2O_2 for 2 h.

Small interfering RNA transfection

Mature miR-181a mimic and si-miR-181a were designed and synthesized by GenePharma (Shanghai, China). The insertion fragment was confirmed by DNA sequencing. Cell transfection and co-transfection were performed using the Lipofectamine 3000 reagent (Invitrogen Life Technologies, Carlsbad, USA) according to the manufacturer's instructions.

MTT assay

The viability of the cells was determined using a 3-(4,5-dimethylthiazol-2-yl)-2 5-diphenyl-2H-tetrazolium bromide (MTT) colorimetric assay according to standard methods described previously. Each experiment was performed 3 times.

Apoptosis assay

Flow cytometry analysis was performed to identify and quantify the apoptotic cells by using an Annexin V-FITC/PI apoptosis detection kit (Beijing Biosea Biotechnology, Beijing, China). The cells (100,000 cells/well) were seeded in a 6-well plate. The treated cells were washed twice with cold PBS and resuspended in buffer solution. The adherent and floating cells were combined and treated according to the manufacturer's instructions and measured with a flow cytometer (Beckman Coulter, Fullerton, USA) to differentiate apoptotic cells (Annexin-V-positive and PI-negative) from necrotic cells (Annexin-V-positive and PI-positive).

Quantitative reverse transcriptase--polymerase chain reaction

Total RNA was isolated from transfected cells by using TRIzol reagent (Invitrogen, Carlsbad, USA) and treated with DNase I (Promega, Southampton, UK). Reverse transcription was performed by using a Multiscribe RT kit (Applied Biosystems, Foster City, USA) and random hexamers or oligo(dT). The reverse transcription conditions were 10 min at 25°C, 30 min at 48°C, and a final step of 5 min at 95°C.

Western blot

The protein used for western blotting was extracted using RIPA lysis buffer (Beyotime Biotechnology, Shanghai, China) supplemented with protease inhibitors (Roche, Guangzhou, China). The proteins were quantified using a BCA™ Protein Assay Kit (Pierce, Appleton, USA). The western blotting system was established using a Bio-Rad Bis-Tris Gel system according to the manufacturer's instructions. Primary antibodies were prepared in 5% blocking buffer at a dilution of 1:1,000. Primary antibodies were incubated with the membrane at 4°C overnight, followed by washing and incubation with secondary antibodies marked by horseradish peroxidase for 1 h at room temperature. After rinsing, the polyvinylidene difluoride (PVDF) membrane carrying blots and antibodies were transferred into the Bio-Rad ChemiDoc™ XRS system, and then 200 µL Immobilon Western Chemiluminescent HRP Substrate (Millipore, Bedford, USA) was added to cover the membrane surface. The signals were captured and the intensity of the bands was quantified using Image Lab™ Software (Bio-Rad, Shanghai, China).

Statistical analysis

All data were shown as mean ±SD. Statistical analyses were performed using SPSS 19.0 software (SPSS Science, Chicago, USA). Differences between groups were analyzed using one-way analysis of variance (ANOVA) and/or Student's t-test. A p-value of <0.05 was considered statistically significant. All experiments were conducted in triplicate.

Results

Different concentrations of H_2O_2 suppressed viability of TM cells in a dose-dependent manner

In our study, we cultured TM cells in a 6-well plate or a 96-well plate and treated them with different concentrations of H_2O_2 (50, 100, 200, and 300 µM) for 2 h. Cell viability was assessed by MTT assay. Our results showed that H_2O_2 at a concentration of 200 µM was significantly suppressed. These results suggested that different concentrations of H_2O_2 suppressed the viability of TM cells in a dose-dependent manner and that H_2O_2 in increasing concentrations (100, 200, and 300 µM) suppressed cell viability significantly (Fig. 1, $p < 0.05$ or $p < 0.01$). For the analyses below 200 µM was selected.

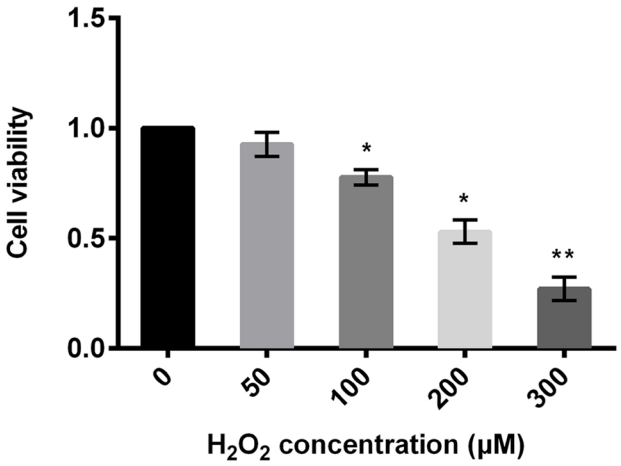

Fig. 1. TM cell viability was significantly suppressed by H_2O_2 in a dose-dependent manner, and 200 µM was selected as a lethal concentration of 50% used in the following analyses

* $p < 0.05$; ** $p < 0.01$.

H_2O_2-treated TM cells revealed a significant fall in miR-181a expression level

The TM cells after treatment with H_2O_2 showed a significant decrease ($p < 0.01$) in the expression level of miR-181a (Fig. 2).

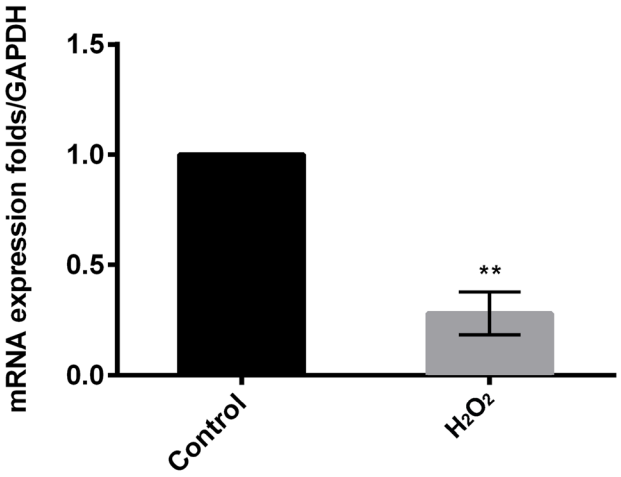

Fig. 2. After H_2O_2 intervention, the miR-181a levels in TM cells were significantly decreased

** $p < 0.01$.

Transfection efficiency of TM cells

TM cells were transfected and then divided into mature miR-181a mimic, si-miR-181a and negative control (siNC) which were then evaluated by qRT-PCR. The results showed a significant decrease ($p < 0.01$) in the mRNA expression level of si-miR-181a compared to the control. Furthermore, they showed a significantly increased ($p < 0.01$) mRNA expression level of miR-181a mimic compared to the control. This suggested that transfection efficiency was observed when miR-181a was overexpressed or suppressed in TM cells (Fig. 3).

H_2O_2 treatment and overexpression of miR-181a increased TM cell viability

Cell viability was measured in the TM cells after treatment with H_2O_2, and the effect of miR-181a on cell viability was measured after transfection. The results showed that cell viability was promoted with increasing time in the miR-181a mimic group compared to si-miR-181a and to control groups. These results suggest that the overexpression of miR-181a enhanced TM cell viability, while the knockdown of miR-181a inhibited cell viability (Fig. 4).

H_2O_2 treatment and overexpression of miR-181a decreased TM cell apoptosis

Cell apoptosis was measured in the TM cells after treatment with H_2O_2, and the effect of miR-181a on cell apoptosis was measured after transfection. The results showed an increased percentage of cell apoptosis ($p < 0.01$) in the si-miR-181a group (mean: 35.7) compared to control groups. Treatment with H_2O_2 caused nuclear condensation, which is an indicator of apoptosis. Also, the miR-181a mimic group (mean: 10.7) showed a significant reduction on cell apoptosis rate ($p < 0.05$), but not as significant as si-miR-181a. These results suggested that the overexpression of miR-181a suppressed TM cell apoptosis, while the knockdown of miR-181a induced apoptosis (Fig. 5).

miR-181a suppressed TM cell apoptosis via blocking the NF-κB and JNK pathways

Generally, H_2O_2 activates the NF-κB and JNK pathways and induces cell apoptosis. The results showed that the si-miR-181a group has a decreased expression of miR-181a and treatment with H_2O_2 suppresses the expression of miR-181a ($p < 0.05$). Thus, in the si-miR-181a + H_2O_2 group, the expression of miR-181a is low and it cannot block the NF-κB and JNK pathways – it will rather produce just the opposite effect (Fig. 6). This suggested that the overexpression of miR-181a could suppress both the pathways, thereby decreasing the rate of cell apoptosis.

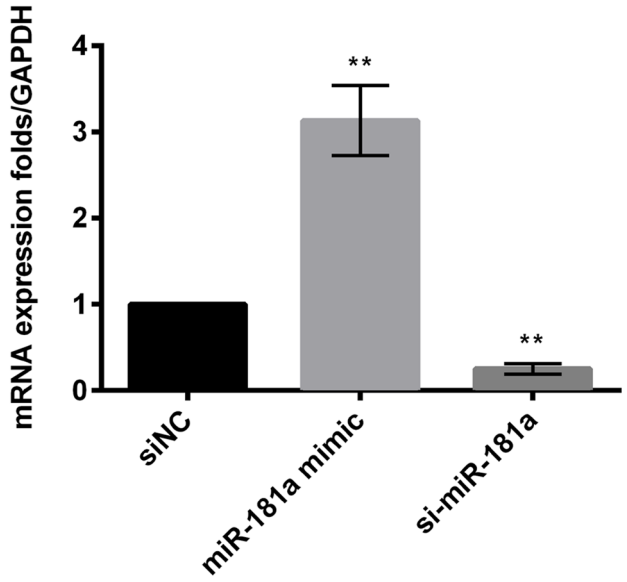

Fig. 3. Overexpressed or suppressed miR-181a in TM cells showed transfection efficiency

** $p < 0.01$.

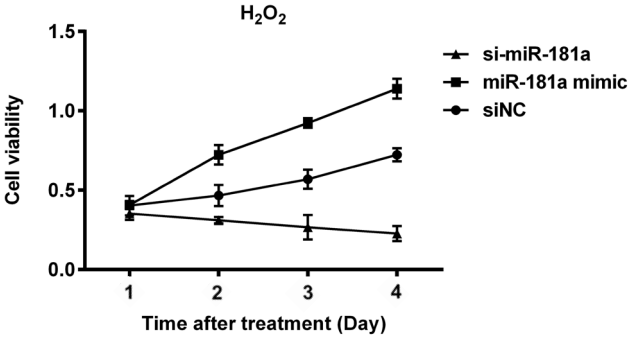

Fig. 4. The overexpression of miR-181a enhanced TM cell viability, while the knockdown of miR-181a inhibited cell viability

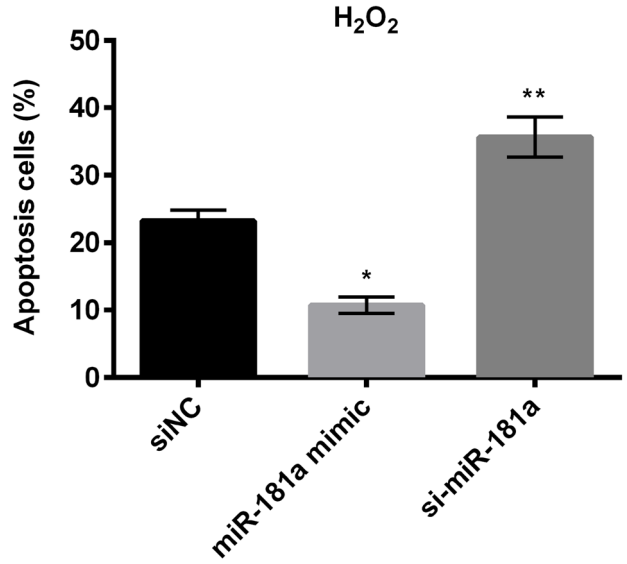

Fig. 5. The overexpression of miR-181a suppressed TM cell apoptosis, while the knockdown of miR-181a induced apoptosis

* $p < 0.05$; ** $p < 0.01$.

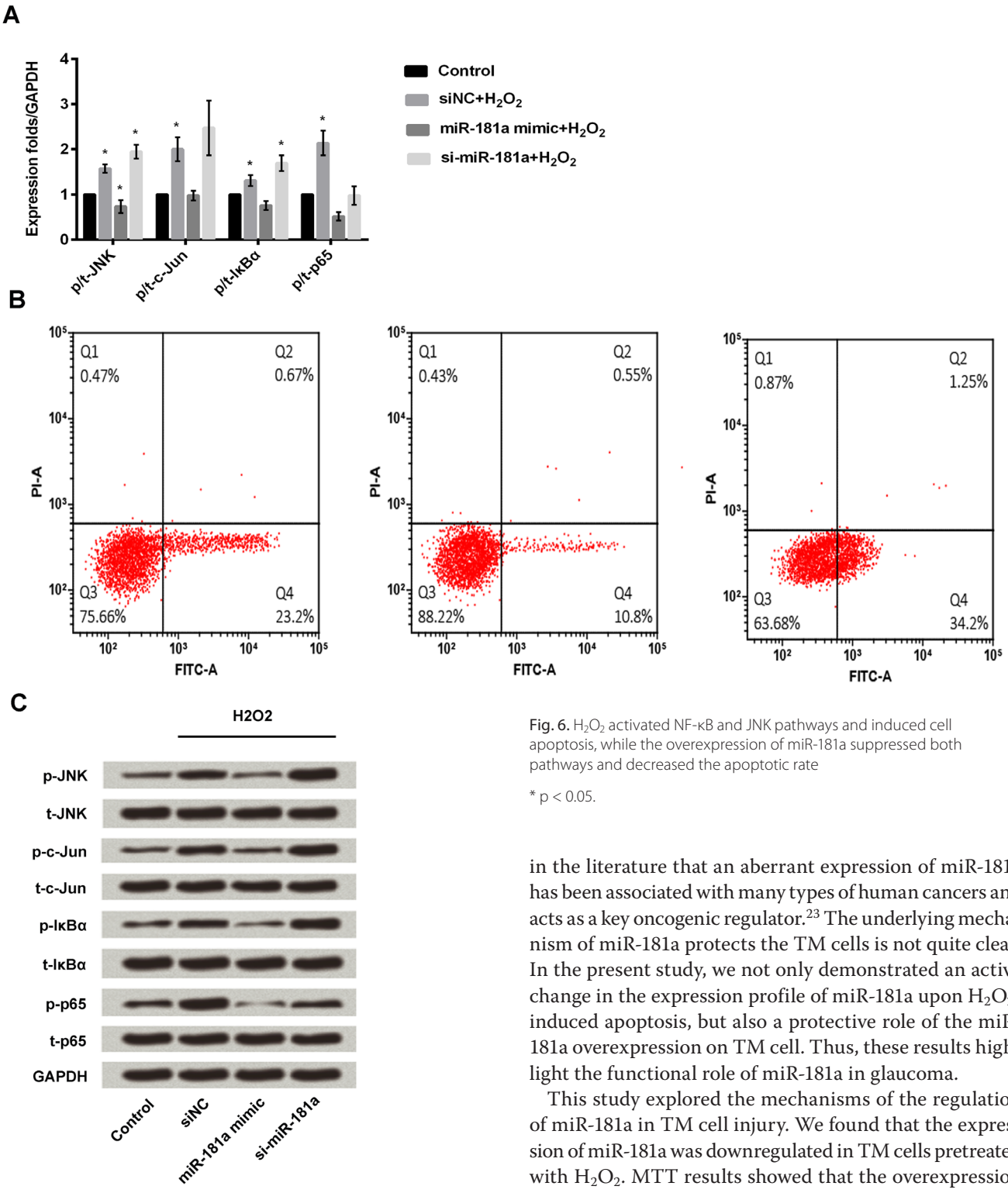

Fig. 6. H_2O_2 activated NF-κB and JNK pathways and induced cell apoptosis, while the overexpression of miR-181a suppressed both pathways and decreased the apoptotic rate

* $p < 0.05$.

Discussion

Oxidative stress has been established as an important contributing factor in TM cell degeneration.[5] The contributory role of H_2O_2 in TM cell degeneration is also known.[23] In the present study, we induced TM cell apoptosis through H_2O_2 and found that miR-181a was downregulated by H_2O_2 in a dose-dependent manner. It has been commonly shown in the literature that an aberrant expression of miR-181a has been associated with many types of human cancers and acts as a key oncogenic regulator.[23] The underlying mechanism of miR-181a protects the TM cells is not quite clear. In the present study, we not only demonstrated an active change in the expression profile of miR-181a upon H_2O_2-induced apoptosis, but also a protective role of the miR-181a overexpression on TM cell. Thus, these results highlight the functional role of miR-181a in glaucoma.

This study explored the mechanisms of the regulation of miR-181a in TM cell injury. We found that the expression of miR-181a was downregulated in TM cells pretreated with H_2O_2. MTT results showed that the overexpression of miR-181a could improve cell viability, while the knockdown of miR-181a suppressed cell viability. Flow cytometry results demonstrated that miR-181a inhibited cell apoptosis, while the knockdown of miR-181a increased apoptosis. Western blotting assay showed a suppression of miR-181a cell apoptosis via blocking the NF-κB and JNK signaling pathways.

In this study, we also showed that during H_2O_2-induced apoptosis downregulating miR-181a blocks the NF-κB and JNK signaling pathways. Our results were similar to one

of the studies conducted by Kozloski et al. in B-cell-like diffuse large B-cell lymphoma.[22] Thus, it is likely that miR-181a upregulation may serve a protective role in glaucoma by exerting a protective effect on H_2O_2-induced apoptosis in TM cells. This hypothesis was further supported by our results, which showed that miR-181a overexpression promoted TM cell apoptosis, which possibly induced the transdifferentiation of mesenchymal-like cells in the aqueous humor of TM cells.[20] NF-κB is considered to be an important nuclear transcription factor that helps in mediating the inflammatory response caused by oxidative stress.[24] In endothelial cells, NF-κB is strongly activated by treatment with H_2O_2 for 4 h.[25] However, to elucidate the exact molecular interaction between miR-181a and the NF-κB and JNK pathways in protecting trabecular meshwork cells, future experiments that require blocking of these pathways or its upstream pathways upon the inhibition of miR-18a would provide solid evidence about the direct targeting of miR-181a on anti-apoptotic pathways in TM cells.

Many miRNAs are involved in the molecular mechanisms of glaucoma; some miRNAs were up-regulated in cells, while others were down-regulated.[12] These miRNAs facilitate the evaluation of specific pathophysiology and offer diagnosis. Further in-depth understanding will help in diagnosing the subtypes of glaucoma, the pathophysiological stages, and the prescription of appropriate drugs.[12] miR-183 was involved in the alteration of integrin-β1 expression, thereby effecting the physiology of TM, resulting in glaucoma.[26] The miR-29 family regulates ECM synthesis in the TM.[27] The changes associated with ECM synthesis result in alterations in the IOP. miR-29b negatively regulates the ECM proteins, and its regulators – under chronic oxidative stress conditions – affect ECM homeostasis in human TM cells. The expression of miR-29b decreased under chronic oxidative stress conditions, resulting in ECM gene upregulation. Similarly, miR-24 plays an important role in the flow pathways.[28] One study identified the involvement of microRNAs in glaucoma with *hsa-let-7b-3p* as the most prevalent factor in the aqueous humor.[13]

In conclusion, this study indicated that miR-181a could improve the survival rate of TM cells after H_2O_2 treatment by blocking the NF-κB and JNK signaling pathways. These findings might provide novel therapeutic oportunities in the treatment of glaucoma.

References

1. Tham YC, Li X, Wong TY, Quigley HA, Aung T, Cheng CY. Global prevalence of glaucoma and projections of glaucoma burden through 2040: A systematic review and meta-analysis: *Ophthalmology*. 2014:121:2081–2090.
2. Cook C, Foster P. Epidemiology of glaucoma: What's new? *Can J Ophthalmol*. 2012:47:223–226.
3. Li A, Chi TL, Peterson-Yantorno K, Stamer WD, Mitchell CH, Civan MM. Mechanisms of ATP release by human trabecular meshwork cells, the enabling step in purinergic regulation of aqueous humor outflow. *J Cell Physiol.* 2012;227:172–182.
4. Luna C, Li G, Huang J, et al. Regulation of trabecular meshwork cell contraction and intraocular pressure by miR-200c. *Plos One*. 2012;7:e51688.
5. Awaikasaoka N, Inoue T, Kameda T, Fujimoto T, Inouemochita M, Tanihara H. Oxidative stress response signaling pathways in trabecular meshwork cells and their effects on cell viability. *Mol Vis*. 2013;19:1332–1340.
6. Pillai RS. MicroRNA function: Multiple mechanisms for a tiny RNA? *RNA*. 2005;11:1753–1761.
7. Ali NM, Boo L, Yeap SK, et al. Probable impact of age and hypoxia on proliferation and microRNA expression profile of bone marrow-derived human mesenchymal stem cells. *Peer J*. 2016;4:e1536
8. Di LG, Croce CM. miRNA profiling of cancer. *Curr Opin Genet Dev*. 2013;23:3–11.
9. Nie Y, Han BM, Liu XB, et al. Identification of microRNAs involved in hypoxia- and serum deprivation-induced apoptosis in mesenchymal stem cells. *Int J Biol Sci*. 2010;7:762–768.
10. Tomé M, López-Romero P, Albo C, et al. miR-335 orchestrates cell proliferation, migration and differentiation in human mesenchymal stem cells. *Cell Death Differ.* 2011;18:985–995.
11. Kong N, Lu X, Li B. Downregulation of microRNA-100 protects apoptosis and promotes neuronal growth in retinal ganglion cells. *BMC Mol Biol*. 2014;15:25–25.
12. Raghunath A, Perumal E. Micro-RNAs and their roles in eye disorders. *Ophthal Res*. 2015;53:169–186.
13. Tanaka Y, Tsuda S, Kunikata H, et al. Profiles of extracellular miRNAs in the aqueous humor of glaucoma patients assessed with a microarray system. *Sci Rep.* 2014;4:633–633.
14. Dismuke WM, Challa P, Navarro I, Stamer WD, Liu Y. Human aqueous humor exosomes. *Exp Eye Res*. 2015;132:73–77.
15. He S, Zeng S, Zhou ZW, He ZX, Zhou SF. Hsa-microRNA-181a is a regulator of a number of cancer genes and a biomarker for endometrial carcinoma in patients: A bioinformatic and clinical study and the therapeutic implication. *Drug Des Devel Ther*. 2015;9:1103–1175.
16. Dragu DL, Necula LG, Bieotu C, et al. Therapies targeting cancer stem cells: Current trends and future challenges. *World J Stem Cells*. 2015;7:1185–1201.
17. Nakamura A, Rampersand YR, Sharma A, et al. Identification of microRNA-181a-5p and microRNA-4454 as mediators of facet cartilage degeneration. *JCI Insight.* 2016;1:e86820.
18. Brodie C, Buchris E, Lee HK. miRNA Expression and Functions in Glioma and Glioma Stem Cells. *MicroRNA Targeted Cancer Therapy*. 2014;112:225–231.
19. Thalyana Smith-Vikos FJS. MicroRNAs and their roles in aging. *J Cell Sci.* 2012;125:7–17.
20. Parikh A, Lee C, Joseph P, et al. MicroRNA-181a has a critical role in ovarian cancer progression through the regulation of the epithelial-mesenchymal transition. *Nat Commun.* 2014;5:149–168.
21. Takahashi E, Inoue T, Fujimoto T, Kojima S, Tanihara H. Epithelial mesenchymal transition-like phenomenon in trabecular meshwork cells. *Exp Eye Res*. 2014;118:72–79.
22. Kozloski GA, Jiang X, Bhatt S, et al. MiR-181a negatively regulates NF-κB signaling and affects activated B-cell like diffuse large B-cell lymphoma pathogenesis. *Blood*. 2016;127(23):2856–2866.
23. Guo LJ, Zhang QY. Decreased serum miR-181a is a potential new tool for breast cancer screening. *Int J Mol Med*. 2012;30:680–687.
24. Bowie A, O'Neill LA. Oxidative stress and nuclear factor-κB activation A reassessment of the evidence in the light of recent discoveries. *Biochem Pharmacol*. 2000;59:13–23.
25. Bowie AG, Moynagh PN, O'Neill LA. Lipid peroxidation is involved in the activation of NF-kappaB by tumor necrosis factor but not interleukin-1 in the human endothelial cell line ECV304. Lack of involvement of H_2O_2 in NF-kappaB activation by either cytokine in both primary and transformed endothelial cells. *J Biol Chem*. 1997;272:25941–25950.
26. Li G, Luna C, Qiu J, Epstein DL, Gonzalez P. Targeting of integrin β1 and kinesin 2α by MicroRNA 183. *J Biol Chem*. 2010;285:5461–5471.
27. Luna C, Li G, Qiu J, Epstein DL, Gonzalez P. Role of miR-29b on the regulation of the extracellular matrix in human trabecular meshwork cells under chronic oxidative stress. *Mol Vis*. 2009;15:2488–2497.
28. Luna C, Guorong LI, Qiu J, Epstein DL, Gonzalez P. MicroRNA-24 regulates the processing of latent TGFβ1 during cyclic mechanical stress in human trabecular meshwork cells through direct targeting of FURIN. *J Cell Physiol*. 2011;226:1407–1414.

Interleukin 21 treatment in a murine model as a novel potential cytokine immunotherapy for colon cancer

Chen Chen[1,A–F], Xiaoning Liu[2,A–C,F], Yi Ren[3,A,B,F]

[1] Clinical School, Hubei University of Chinese Medicine, China
[2] Central Laboratory of Huai'an First People's Hospital, Nanjing Medical University, China
[3] Department of Breast and Thyroid Surgery, Huai'an First People Hospital, Nanjing Medical University, China

A – research concept and design; B – collection and/or assembly of data; C – data analysis and interpretation; D – writing the article; E – critical revision of the article; F – final approval of the article

Advances in Clinical and Experimental Medicine, ISSN 1899-5276 (print), ISSN 2451-2680 (online) *Adv Clin Exp Med*. 2018;27(5):583–589

Address for correspondence
Chen Chen
E-mail: 44736881@qq.com

Funding sources
None declared

Conflict of interest
None declared

Received on January 7, 2016
Reviewed on November 15, 2016
Accepted on January 28, 2017

Abstract

Background. Interleukin 21 (IL-21), which belongs to the common γ-chain (γc) family, is a novel tumor suppressor that has been shown to affect T-cell proliferation, survival and function. However, the role of IL-21 in colon cancer remains unclear.

Objectives. We sought to determine whether IL-21 could inhibit the progression of colon cancer in mice; we also explored the mechanisms underlying the immunological effects of IL-21 in colon cancer.

Material and methods. Exogenous IL-21 protein was expressed to treat tumor-bearing mice and the production of cytokine interleukin 4, interferon gamma and lambda from $CD4^+$ T, $CD8^+$ T, and NK cells were measured, along with the survival times of these tumor-bearing mice.

Results. Interleukin 21 promoted the secretion of interferon gamma from the $CD4^+$ T, $CD8^+$ T and NK cells and it enhanced the production of interferon lambda by the NK cells. More importantly, IL-21 treatment significantly enhanced antitumor effects in favor of tumor eradication. We also found that $CD8^+$ T and NK cells are necessary for the antitumor immune responses elicited by IL-21.

Conclusions. Interleukin 21 is a powerful tool for activating $CD8^+$ T cells and NK cells which exhibit potent cytolytic effector functions and should therefore be exploited for anticancer immunotherapy. Our findings support the development of a novel cytokine immunotherapy against colon cancer.

Key words: colon cancer, immunotherapy, interleukin 21, interferon γ

DOI
10.17219/acem/68703

Copyright
© 2018 by Wroclaw Medical University
This is an article distributed under the terms of the Creative Commons Attribution Non-Commercial License (http://creativecommons.org/licenses/by-nc-nd/4.0/)

Introduction

Colorectal cancer is the 6th leading cause of tumor-related death in China.[1–3] Although the treatment of colorectal cancer has significantly improved over the past few years, the results of the current treatment modalities are unsatisfactory, especially for patients in the advanced stages of colon cancer.[4,5] Therefore, the development of effective therapeutic approaches for colon cancer is necessary. Tumor immunotherapy brings new hope for cancer treatment.

Effective tumor immunotherapy depends on the presence of large numbers of tumor-infiltrating T lymphocytes with effector functions, appropriate phenotypic characteristics, self-renewal potential, and homing capacity.[6–9] In addition to T lymphocytes, $CD8^+$ T cells and natural killer (NK) cells also play an important role in antitumor immune therapy by eliminating tumor cells through the actions of perforin and granzyme.[10,11] Thus, the ability to elicit the cytotoxicity of NK cells and $CD8^+$ T would benefit cancer immunotherapy.

Interleukin 21 (*IL-21*) belongs to the common-gamma chain family, which includes *IL-15*, *IL-9*, *IL-7*, *IL-4*, and *IL-2*.[12,13] These cytokines display a similar 4-helix bundle structure and functional redundancy in their regulation and homeostasis of the lymphoid system, but each family member also performs distinct functions.[13,14] IL-21 is produced by activated $CD4^+$ T cells, NK T cells and follicular T-helper cells (Th).[6] Recently, IL-21 has been revealed to exhibit antitumor function in different tumor models and its mechanism of action has been reported to involve the stimulation of T- or B-cell responses and NK cells.[6,10,11,15] Moreover, the antitumor activity of IL-21 can be potentiated when it is used in combination with other immunostimulants, chemotherapy, or monoclonal antibodies that recognize tumor antigens.[8,13,16] For example, the combined use of IL-21 and peptide-loaded dendritic cells increases the number of human Melan-A/MART-1-specific $CD8^+$ T cells that display high affinity and a $CD45RO^+CD28^{high}$ phenotype upon in vitro stimulation.[13] These results indicate that IL-21 has antitumor activity in vitro.

IL-21 can also enhance the antitumor activity of dendritic-cell vaccines or antibodies. However, for immune-competent murine models of colon cancer, the immunological consequences of IL-21 stimulation have not been addressed so far. Therefore, in this study, we investigated whether IL-21 could suppress the growth of colon cancer in mice; we also tried to elucidate the mechanisms underlying the antitumor immune effects of IL-21. Our findings provide data essential for the development of effective tumor immunotherapies in the future.

Material and methods

Cell lines and mice

Mouse colon cancer cells (CT-26 cells) were obtained from the American Type Culture Collection (ATCC) and maintained in Dulbecco's Modification of Eagle's Medium (DMEM) supplemented with 10% heat-inactivated fetal bovine serum (FBS), 100 μg/mL streptomycin, 100 U/mL penicillin, and 2 mM L-glutamine (Thermo Fisher Scientific, Shanghai, China). Eight-week-old male BALB/c mice were purchased from the Center of Animal Experiment of Wuhan University, China. The mice used in the experiments were fed under specific pathogen-free conditions in the animal facility of Wuhan University and treated in accordance with the guidelines of the Institutional Animal Care and Use Committee (IACUC) of Wuhan University.

Generation of IL-21-His and GST-His fusion protein

To generate an IL-21-His fusion protein, total RNA was extracted from the BALB/c mouse splenocytes, using TRIzol (Invitrogen, Shanghai, China), and comolementary DNA (cDNA) was synthesized using an RT-PCR kit (Fermentas, Shenzhen, China). The sequences encoding IL-21 were then amplified using selected primers (Table 1), and the polymerase chain reaction (PCR) product was sequenced and then cloned in-frame between the *Sal*I and *Hin*dIII (New England Biolabs, Beijing, China) restriction sites of a pET-20b(+) vector to ensure that the His-tag was fused with IL-21. The pET-20b(+) construct was then transfected into BL21(DE3)pLySs (Merckmillipore, Shanghai, China) cells, which were then induced with 0.1 mM isopropyl β-D-1-thiogalactopyranoside (IPTG) (Thermo Scientific, Shanghai, China). Next, the fusion proteins were purified using His-Select Nickel Affinity Gel (Sigma-Aldrich, Shanghai, China) or Glutathione Sepharose 4B (GE Healthcare Life Science, Beijing, China), and lipopolysaccharide contamination was removed using DetoxiGelTM Endotoxin Removing Columns (Thermo Scientific, Shanghai, China). The proteins were then dialyzed in phosphate buffer saline (PBS) and analyzed by sodium dodecyl sulfate-polyacrylamide gel electrophoresis (SDS-PAGE) and western blotting. The endotoxin level was <0.5 EU/mg, as measured using the Limulus Amebocyte Lysate (LAL) assay (BioWhittaker Limulus Amebocyte Assay; Lonza, Basel, Switzerland). We also transfected the pET-32a(+) vector into BL21(DE3)pLySs cells to generate glutathione *S*-transferase (GST)-His fusion protein for use as a negative control.

Western blot analysis

The purified IL-21-His and GST-His proteins were identified by western blot using rabbit anti-mouse-IL-21 monoclonal antibodies (dilution 1:1000) (Abcam, Shanghai,

China). HRP-anti-rabbit IgG (dilution 1:5000) (Abcam, Shanghai, China) was used as a secondary antibody. Commercial IL-21 (eBioscience, San Diego, USA) was used as a positive control.

Isolation of NK cells, CD8+ T cells and CD4+ T cells

NK cells, CD8+ T cells and CD4+ T cells were isolated from the spleens of the BALB/c mice, using the BD™ IMag mouse NK cells, CD8+ T and CD4+ T lymphocytes, and enrichment set-DM and the BD™ IMagnet (BD Pharmingen, Beijing, China) by negative selection.

Cytokine-specific ELISA

The serum interferon gamma (IFN-γ) and IL-4 concentrations from the IL-21-immunized mice were measured by ELISA. In brief, 8 BALB/c mice per group were immunized with IL-21 (50 μg/mouse) through intravenous injection on days 0, 7 and 14. The group of mice immunized with GST (n = 8) or PBS (n = 8) was used as the controls. Peripheral blood from the medial canthus of the eye was drawn on days 0, 7, 14, 21, and 28. Sera were harvested to analyze the cytokine levels via ELISA test using cytokine-specific kits (eBioscience, San Diego, USA), according to the protocol recommended by the manufacturer.

CD4+ T, CD8+ T and NK cells from the mice were treated with IL-21 and the IFN-γ production was analyzed using ELISA. In brief, CD4+ and CD8+ T cells (1×10^6 cells/well) were purified and stimulated with CD3 antibodies (20 ng/mL) and CD28 antibodies (10 ng/mL) (BioLegend, Beijing, China) plus either IL-21 (20 μg/mL) or GST (20 μg/mL) for 3 days. NK cells (1×10^6 cells/well) were purified and stimulated with IL-2 protein (10 ng/mL) (BioLegend, Beijing, China) plus either IL-21 (20 μg/mL) or GST (20 μg/mL) for 3 days, and the supernatants (200 μL/well) were then collected for the IFN-γ assay using cytokine-specific kits (eBioscience, San Diego, USA).

Intracellular IFN-γ assay

For intracellular cytokine staining of the CD8+T, CD4+T and NK cells, the mouse splenocytes (2×10^6 cells/well) were treated using concanavalin A (ConA; 3 μg/mL) plus IL-21 (20 μg/mL) or GST (20 μg/mL) for 3 days, after which the cells were restimulated with 100 ng/mL ionomycin (Sigma-Aldrich, St. Louis, USA), 4 μg/mL GolgiPlug (BD Pharmingen, Beijing, China) and 50 ng/mL phorbol 12-myristate 13-acetate (PMA) for 4 h. After 4 h, the cells were incubated with anti-CD8, anti-CD4, or anti-NK1.1 monoclonal antibodies, then fixed, permeabilized, stained with anti-IFN-γ (BioLegend, Beijing, China), washed, and analyzed by flow cytometry (BD Immunocytometry Systems, San Jose, USA).

Quantitative real-time polymerase chain reaction

The CD4+ T, CD8+ T and NK cells were purified, and total RNA from these cells was extracted using TRIzol (Invitrogen, Shanghai, China). Next, 250 ng of each extracted RNA sample was used to synthesize cDNA, using the RevertAid First-Strand real-time polymerase chain reaction (RT-PCR) kit (Fermentas, Shenzhen, China). Complementary DNA (cDNA) was amplified using primers listed in Table 1 in a 25-μL reaction mixture containing 100 ng of the cDNA template and 12.5 μL of SYBR Green PCR Supermix (Bio-Rad, Hercules, USA) in the recommended cycling conditions.[17] Each transcript was normalized to the amplification levels of glyceraldehyde 3-phosphate dehydrogenase (GAPDH). IFN-λ mRNA levels were quantified using the MyiQ single-color RT-PCR detection system (Bio-Rad, Hercules, USA).

T-cell proliferation assay

To examine in vitro proliferation, [3H]-thymidine-incorporation assays were performed. Briefly, splenocytes from wild-type BALB/c mice were cultured in 96-well plates (5×10^5 cells/well) and treated with PBS, GST, or IL-21 (20 μg/mL) for 72 h. [3H]-Thymidine (HTA Co. Ltd, Beijing, China) was then added 16 h before a 3-day culture, and proliferation was measured using a scintillation counter (Beckman, California,USA). A stimulation index was used to reveal the fold-increase in proliferation. The stimulation index was calculated as $cpm_{exp}/cpm_{control}$.

Mouse immunization and tumor challenge

The BALB/c male mice were challenged with 3×10^5 CT-26 tumor cells subcutaneously and randomly divided into 3 groups (n = 8 mice/group). After 7 days, the mice were immunized with GST-IL-21 by intravenous injection (50 μg/mouse) when palpable tumors formed (3–5 mm in diameter). Two additional GST-IL-21 protein immunizations

Table 1. Primer sequences

Gene name	Forward (5′-3′)	Reverse (5′-3′)
IL-21	TCGTCGACATGGAGAGGACCCTTGTCTGT	CGAAGCTTTGAGTCACTGGGCACAGG
IFN-λ	CTTCCAAGCCCACCCCAACT	GGCCTCCAGGACCTTCAGC
GAPDH	ACCACAGTCCATGCCATCAC	TCCACCACCCTGTTGCTGTA

IL-21 – interleukin 21; *IFN-λ* – interferon λ; *GAPDH* – glyceraldehyde 3-phosphate dehydrogenase.

were performed in the tumor-bearing mice every 7 days after CT26 inoculation. The mice treated with GST or PBS were used as controls. Tumor volumes were surveyed every 2–3 days and calculated using the following formula: $L1^2 \times L2/2$, where L1 is the shortest diameter and L2 is the longest diameter. The mice were euthanized when the tumors grew to 12 mm in diameter. In some experiments, the mice were treated intraperitoneally with CD4 monoclonal antibodies (clone GK1.5; 250 μg/mouse), CD8 monoclonal antibodies (clone 2.43; 500 μg/mouse), anti-NK1.1 monoclonal antibodies (clone PK136; 200 μg/mouse), or isotype control antibodies (250 μg/mouse) 3 times after tumor inoculation (on days 3, 10 and 17).

Statistical analysis

The data were analyzed by Tukey's multiple comparison test for more than 2 study groups (GraphPad Prism, 5.01). A 2-way ANOVA and a Kaplan-Meier survival analysis were performed in order to determine statistical significance for in vivo tumor therapy. Probability value $p < 0.05$ was considered statistically significant.

Results

Expression of recombinant fusion proteins IL-21-His and GST-His

The molecular weight of mouse IL-21 protein is about 20 kDa.[13] As indicated in Fig. 1A and Fig. 1B, the recombinant

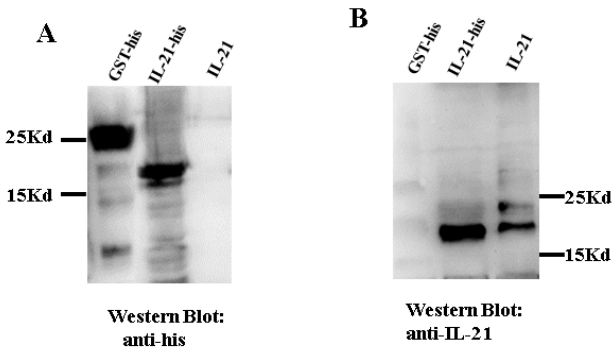

Fig. 1. Identification of the recombinant IL-24-His protein

The proteins IL-21-His and GST-His were purified and then western blotted with mAbs against His-tag (A) and IL-21 (B); commercial IL-21 protein was used as the positive control.

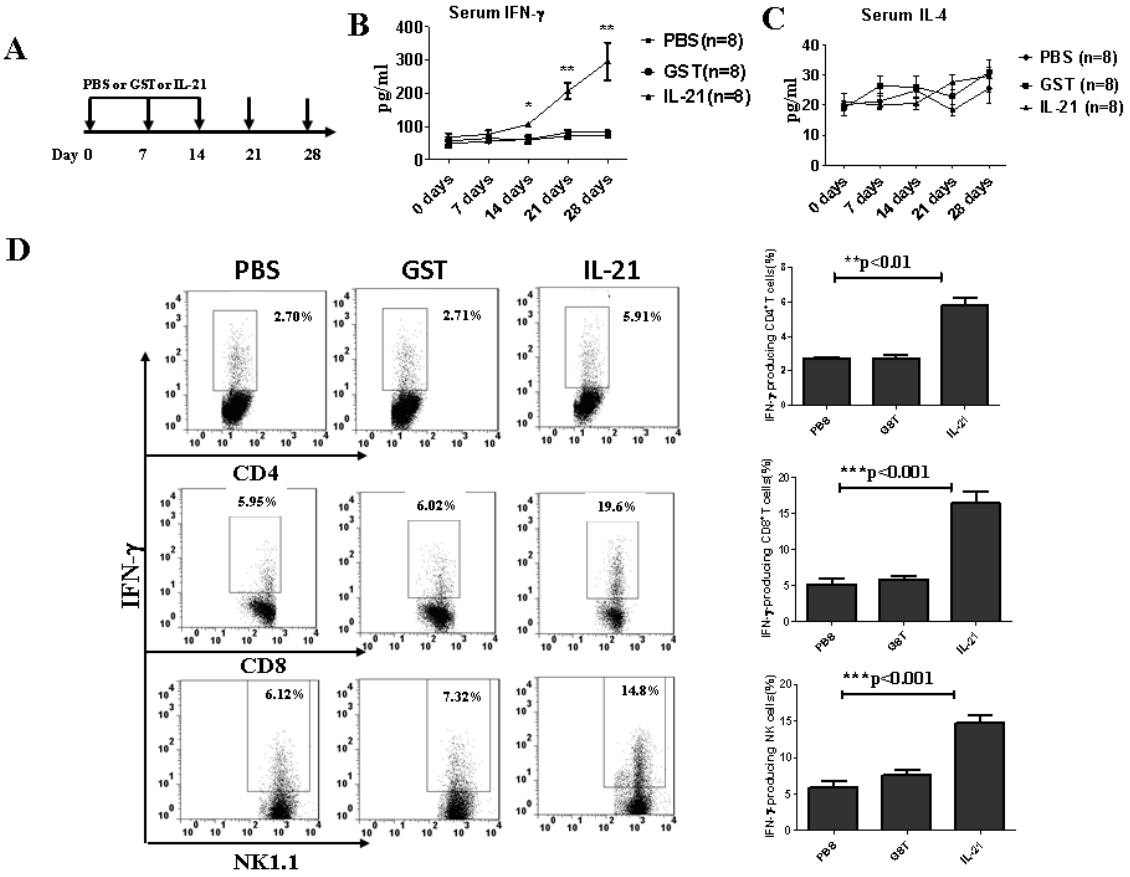

Fig. 2. IL-21-mediated increase in the levels of IFN-γ in the serum and splenic IFN-γ-producing CD8+ T and NK cells

A – BALB/c mice (n = 8 mice/group) were injected 3 times at 1-week intervals with IL-21, GST, or PBS. The sera were then harvested on different days for ELISA analysis of (B) IFN-γ and (C) IL-4 cytokine levels. D – splenocytes obtained from the BALB/c mice were stimulated with ConA plus IL-21 for 3 days. The viable splenocytes were then selected, and the CD4+ T, CD8+ T, or NK cells were gated. The percentage (left) and mean fluorescence intensity (MFI) (right) of the IFN-γ-producing CD4+ T, CD8+ T and NK cells were then analyzed by flow cytometry. Data are representative of 3 experiments. Error bars represent the standard error of the mean; * $p < 0.05$; ** $p < 0.01$; *** $p < 0.001$.

IL-21-His fusion protein was blotted positively using His-Tag (Sigma, Shanghai, China) and IL-21 (Abcam, Shanghai, China) monoclonal antibodies. Commercial IL-21 and GST proteins were used as positive and negative controls, respectively.

Interleukin 21 enhances the activation of CD8⁺ T cells and NK cells

IFN-γ production serves as a marker of effector CD4⁺ and CD8⁺ T cells. To determine whether exogenous IL-21 promotes cytokine production in mice, the serum levels of cytokines IFN-γ and IL-4 from the mice treated with IL-21 were measured on different days (Fig. 2A). The data revealed that the IFN-γ levels were significantly higher in the IL-21-treated mice on days 14, 21 and 28 ($p < 0.01$; Fig. 2B) than in the control-treated mice, but the IL-4 levels showed no significant difference at any of the time points in any group (Fig. 2C).

To examine the types of immune cells producing IFN-γ, we harvested splenocytes from BALB/c mice and analyzed the kinds of IFN-γ-producing cells by flow cytometry (Fig. 2D). The data suggested that IL-21 injection significantly promoted the production of IFN-γ-producing CD8⁺ T cells and NK cells ($p < 0.01$; Fig. 2D).

Interleukin 21 directly induces IFN-γ production in CD4⁺ and CD8⁺ T cells and IFN-γ production in NK cells

We next aimed to further explore whether exogenous IL-21 can directly stimulate these cells to produce IFN-γ and found that IL-21 significantly promoted IFN-γ secretion in the T cells and NK cells ($p < 0.01$; Fig. 3A). Since IFN-γ from NK cells possesses antitumor activity, our next step was to determine whether IL-21 could promote IFN-γ production from NK cells.[21] As shown in Fig. 3B, IL-21 significantly enhanced IFN-γ production in the NK cells. Furthermore, the IL-21 protein, but not PBS or GST, triggered enhanced splenocyte proliferation, as measured by means of [³H]-thymidine incorporation ($p < 0.05$, Fig. 3C).

Vaccination with interleukin 21 fusion protein produces potent antitumor effects

CD8⁺ T cells and NK cells play crucial roles in antitumor immune responses.[22] Therefore, we aimed to determine whether IL-21 administration could establish antitumor immunity. As shown in Fig. 4B, IL-21 treatment could significantly suppress tumor growth as compared to PBS or GST treatment in the tumor-bearing mice ($p < 0.05$). Furthermore, we found that IL-21 treatment significantly prolonged the life of the tumor-bearing mice ($p < 0.05$; Fig. 4C).

To further explore the cellular mechanisms associated with IL-21, CD8⁺ cell, CD4⁺ T cell, and/or NK cell, depletions were carried out during the treatment of the mice. The data showed that mice depleted of NK or CD8⁺ T cells lost the antitumor functions elicited by IL-21 ($p < 0.05$; Fig. 4D and 4E). However, the tumor size and survival time of the tumor-bearing mice depleted of CD4⁺ T cells remained unchanged in the IL-21-treated mice (Fig. 4D and 4E). These results revealed that CD8⁺ T cells and NK cells are essential for the antitumor immune responses induced by IL-21.

Discussion

In our study, the results showed that the cytokine IL-21 has antitumor effects in murine colon cancer models. IL-21 administration enhanced serum IFN-γ levels and

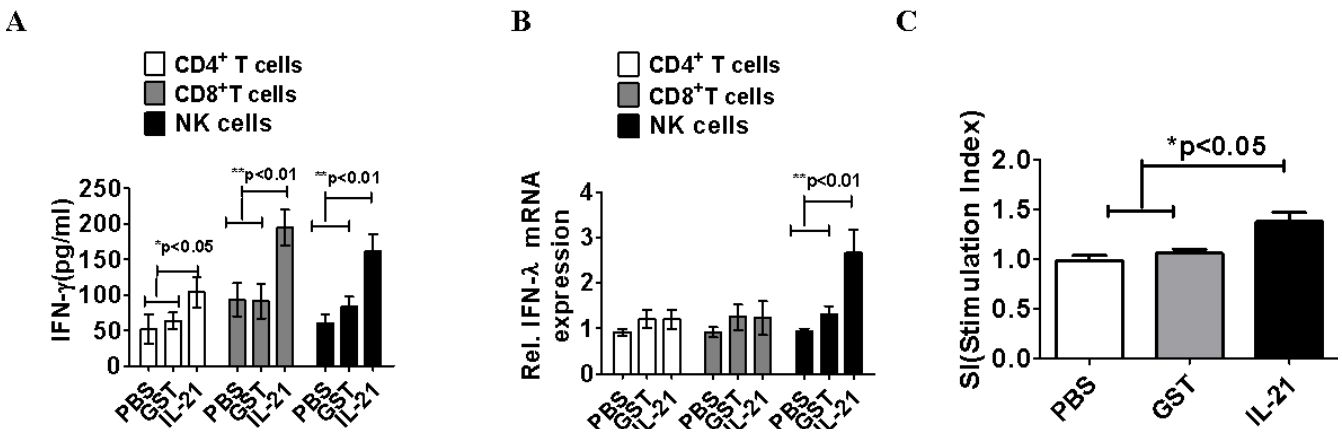

Fig. 3. IL-21 promotes CD8+ T cell and NK cell functions

Purified CD4+ T, CD8+ T and NK cells were stimulated with CD3 and CD28 antibodies or IL-2 plus IL-21 or GST for 3 days, and then the supernatants were collected for IFN-γ assays (A); B – quantitative analysis of IFN-lambda mRNA-expression levels in the CD4+ T, CD8+ T, or NK cells; C – splenocytes from BALB/c mice were cultured in 96-well plates and stimulated with PBS, GST, or IL-21 for 72 h. [3H]-thymidine was added and proliferation was measured using a scintillation counter; the fold-increase in proliferation is shown using a stimulation index. Data are representative of 3 experiments. Error bars represent the standard error of the mean; * $p < 0.05$; ** $p < 0.01$; *** $p < 0.001$.

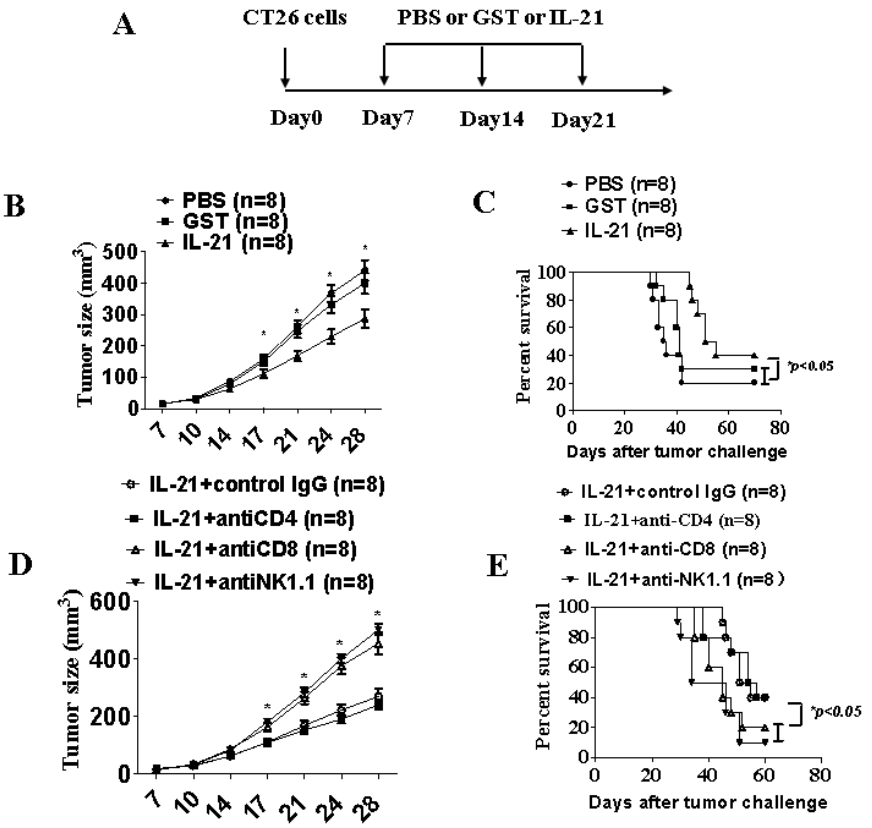

Fig. 4. Reduced tumor burden and enhanced survival rate in tumor-bearing mice following treatment with IL-21

A – schematic of tumor challenge and IL-21 immunization. BALB/c mice were injected subcutaneously with CT-26 tumor cells. After 7 days, the tumor diameter reached 3–4 mm; the mice were then treated 3 times at 1-week intervals with IL-21, GST, or PBS. Tumor growth (B) and survival rate (C) were recorded. D, E – BALB/c mice were challenged subcutaneously with tumor cells and then injected intraperitoneally with anti-CD4 mAb, anti-CD8 mAb, anti-NK1.1 mAb, or isotype control mAb on day 3. The mice were then injected with different proteins. The depleting mAb or isotype control mAb was injected 3 days before protein injection. After 3 protein injections, the tumor size and survival rate of the tumor-bearing mice were recorded. Data are representative of 3 experiments. Error bars represent standard error of the mean; * $p < 0.05$; ** $p < 0.01$; *** $p < 0.001$.

IFN-γ secretion in the $CD8^+$ T, $CD4^+$ T and NK cells. We also established that IL-21 promotes IFN-γ secretion from NK cells as well as the proliferation of splenocytes. Moreover, we found that the antitumor function of IL-21 relied on $CD8^+$ T cells and NK cells.

Previous studies have shown that IL-21 markedly suppresses tumor growth in some cancers, including colon cancer,[18] breast cancer,[19] melanoma,[20] and renal cancer.[21] In these studies, the mechanism underlying the antitumor effect of IL-21 in different tumor models was found to involve the activation of T cells and NK cell responses. Moreover, it was found that the antitumor function of IL-21 could be potentiated when it was used in combination with other immunostimulants, chemotherapy, or monoclonal antibodies that recognize tumor antigens.[22–24] However, the mechanism by which IL-21 affects T cells and NK cells and exerts antitumor effects has not been previously researched in colon cancer models.

Our data revealed that recombinant IL-21 could directly promote the secretion of IFN-γ in $CD8^+$ T, $CD4^+$ T and NK cells. Previously, Zeng and colleagues reported that IL-21 exerts limited effects on the secretion of IFN-γ in $CD8^+$ T cells.[24] However, this does not contradict our data, because IL-21 produces highly limited effects on naïve T cells; in our experiment, we added CD3 and CD28 monoclonal antibodies to activate the T cells. Zeng et al. also reported that IL-21 produces extremely weak effects on the proliferation of $CD8^+$ T cells, $CD4^+$ T cells and NK cells.[24] In contrast, our results indicated that IL-21 markedly enhanced the proliferation of splenocytes. We speculate that IL-21 promotes B-cell proliferation because the spleen contains numerous B cells and because the IL-21 receptor (IL-21R) is expressed on B cells.[14] Thus, our data revealed that the recombinant protein IL-21-His exerted its biological function, but we could not clarify the underlying mechanism. Li et al. previously reported that IL-21R is expressed on the surface of B cells, $CD8^+$T cells, $CD4^+$T cells, and NK cells.[14] We speculate that IL-21 could ligate the IL-21R expressed on the surface of $CD4^+$ and $CD8^+$ T cells, and could thereby activate T cells.

Further, IFN-γ plays very important roles in NK cell-mediated tumor destruction pathways.[25] We therefore measured the changes in the levels of IFN-γ in T and NK cells after treatment with IL-21. Our results revealed that IL-21 could not only enhance IFN-γ production but could also promote IFN-γ production. The data also showed that IL-21 could enhance antitumor immunity in the mice by increasing IFN-γ production and activating NK cells.

Thus, we revealed an important role for NK cells and $CD8^+$ T cells in IL-21-mediated antitumor immune responses. Moreover, we found that the antitumor function of IL-21 was lost in the mice depleted of NK cells or $CD8^+$ T cells, but not in those depleted of $CD4^+$ T cells. Our data also revealed that IL-21 could enhance the secretion of INF-γ in $CD4^+$ and $CD8^+$ T cells. However, because of the expression of CD4 molecules on Treg cells, it is possible that injection of the CD4 antibody in mice depleted Treg cells.

The blockade of immune checkpoints in tumor immunotherapy, such as programmed cell death protein 1 (PD1),

rely on the enhancement of spontaneous antitumor immunity. However, these immunotherapies are limited by the requirement for existing tumor-specific immune responses.[26–28] Therefore, breaking immune tolerance to the tumor and enhancing the immune response to tumor antigens should increase tumor immunogenicity. Our results strongly suggested that IL-21, serving as a cytokine, promotes tumor-specific immune responses. The findings of some other studies provide further in vivo evidence for the tumor-suppressive function of IL-21.[6,12,13,29]

In summary, our study shows that IL-21 can not only directly enhance the secretion of IFN-γ in $CD8^+$ T cells and $CD4^+$ T cells, but can also promote the secretion of IFN-γ and IFN-λ in NK cells and suppress the growth of CT-26 tumor cells. Thus, IL-21 is a powerful tool for activating $CD8^+$ T cells and NK cells which exhibit potent cytolytic effector functions, and should therefore be considered for tumor immunotherapy in the future.

References

1. Zheng ZX, Zheng RS, Zhang SW, Chen WQ. Colorectal cancer incidence and mortality in China, 2010. *Asian Pac J Cancer Prev*. 2014;15: 8455–8460.
2. Liu S, Zheng R, Zhang M, Zhang S, Sun X, Chen W. Incidence and mortality of colorectal cancer in China, 2011. *Chin J Cancer Res*. 2015;27: 22–28.
3. Chen W, Zheng R, Zeng H, Zhang S. The updated incidences and mortalities of major cancers in China, 2011. *Chin J Cancer*. 2015;34:53.
4. Guend H, Patel S, Nash GM. Abdominal metastases from colorectal cancer: Intraperitoneal therapy. *J Gastrointest Oncol*. 2015;6:693–698.
5. Chibaudel B, Tournigand C, Bonnetain F, et al. Therapeutic strategy in unresectable metastatic colorectal cancer: An up-dated review. *Ther Adv Med Oncol*. 2015;7:153–169.
6. Santegoets SJ, Turksma AW, Powell JDJ, Hooijberg E, de Gruijl TD. IL-21 in cancer immunotherapy: At the right place at the right time. *Oncoimmunology*. 2013;2:e24522.
7. Leung J, Suh WK. The CD28-B7 family in anti-tumor immunity: Emerging concepts in cancer immunotherapy. *Immune Netw*. 2014;14: 265–276.
8. Phan GQ, Rosenberg SA. Adoptive cell transfer for patients with metastatic melanoma: The potential and promise of cancer immunotherapy. *Cancer Control*. 2013;20:289–297.
9. Kalos M, June CH. Adoptive T cell transfer for cancer immunotherapy in the era of synthetic biology. *Immunity*. 2013;39:49–60.
10. Moroz A, Eppolito C, Li Q, Tao J, Clegg CH, Shrikant PA. IL-21 enhances and sustains $CD8^+$ T cell responses to achieve durable tumor immunity: Comparative evaluation of IL-2, IL-15, and IL-21. *J Immunol*. 2004; 173:900–909.
11. Kumano M, Hara I, Furukawa J, et al. Interleukin-21 activates cytotoxic T lymphocytes and natural killer cells to generate antitumor response in mouse renal cell carcinoma. *J Urol*. 2007;178:1504–1509.
12. Ozaki K, Spolski R, Feng CG, et al. A critical role for IL-21 in regulating immunoglobulin production. *Science*. 2002;298:1630–1634.
13. Croce M, Rigo V, Ferrini S. IL-21: A pleiotropic cytokine with potential applications in oncology. *J Immunol Res*. 2015;2015:696578.
14. Li J, Shen W, Kong K, Liu Z. Interleukin-21 induces T-cell activation and proinflammatory cytokine secretion in rheumatoid arthritis. *Scand J Immunol*. 2006;64:515–522.
15. Santegoets SJ, Turksma AW, Suhoski MM, et al. IL-21 promotes the expansion of $CD27^+$ $CD28^+$ tumor infiltrating lymphocytes with high cytotoxic potential and low collateral expansion of regulatory T cells. *J Transl Med*. 2013;11:37.
16. Spolski R, Leonard WJ. Interleukin-21: A double-edged sword with therapeutic potential. *Nat Rev Drug Discov*. 2014;13:379–395.
17. Zhou L, Li JL, Zhou Y, et al. Induction of interferon-λ contributes to TLR3 and RIG-I activation-mediated inhibition of herpes simplex virus type 2 replication in human cervical epithelial cells. *Mol Hum Reprod*. 2015;21:917–929.
18. Ugai S, Shimozato O, Kawamura K, et al. Expression of the interleukin-21 gene in murine colon carcinoma cells generates systemic immunity in the inoculated hosts. *Cancer Gene Ther*. 2003;10:187–192.
19. Park YK, Shin DJ, Cho D, et al. Interleukin-21 increases direct cytotoxicity and IFN-gamma production of ex vivo expanded NK cells towards breast cancer cells. *Anticancer Res*. 2012;32:839–846.
20. Green J, Ariyan C. Update on immunotherapy in melanoma. *Surg Oncol Clin N Am*. 2015;24:337–346.
21. Curti BD. Immunomodulatory and antitumor effects of interleukin-21 in patients with renal cell carcinoma. *Expert Rev Anticancer Ther*. 2006;6:905–909.
22. Roda JM, Parihar R, Lehman A, Mani A, Tridandapani S, Carson WE 3rd. Interleukin-21 enhances NK cell activation in response to antibody-coated targets. *J Immunol*. 2006;177:120–129.
23. White L, Krishnan S, Strbo N, et al. Differential effects of IL-21 and IL-15 on perforin expression, lysosomal degranulation, and proliferation in CD8 T cells of patients with human immunodeficiency virus-1 (HIV). *Blood*. 2007;109:3873–3880.
24. Zeng R, Spolski R, Finkelstein SE, et al. Synergy of IL-21 and IL-15 in regulating $CD8^+$ T cell expansion and function. *J Exp Med*. 2005;201: 139–148.
25. Sato A, Ohtsuki M, Hata M, Kobayashi E, Murakami T. Antitumor activity of IFN-lambda in murine tumor models. *J Immunol*. 2006;176:7686–7694.
26. Brahmer JR, Tykodi SS, Chow L, et al. Safety and activity of anti-PD-L1 antibody in patients with advanced cancer. *N Engl J Med*. 2012;366: 2455–2465.
27. Eroglu Z, Kim DW, Wang X, et al. Long term survival with cytotoxic T lymphocyte-associated antigen 4 blockade using tremelimumab. *Eur J Cancer*. 2015;51:2689–2697.
28. Fourcade J, Sun Z, Benallaoua M, et al. Upregulation of Tim-3 and PD-1 expression is as-sociated with tumor antigen-specific $CD8^+$ T cell dysfunction in melanoma patients. *J Exp Med*. 2010;207:2175–2186.
29. Tangye SG. Advances in IL-21 biology – enhancing our understanding of human disease. *Curr Opin Immunol*. 2015;34:107–115.

The protective effect of *Gingko biloba* in a rat model of ovarian ischemia/reperfusion injury: Improvement in histological and biochemical parameters

Nuri Yildirim[1,A,D,F], Deniz Simsek[1,C,D], Semir Kose[2,C,E], Alkim Gulsah Sahingoz Yildirim[3,B,E], Cagri Guven[1,C,E], Gurkan Yigitturk[4,B,E], Oytun Erbas[5,A,E,F]

[1] Department of Obstetrics and Gynecology, Ege University, Izmir, Turkey
[2] Department of Obstetrics and Gynecology, Dokuz Eylul University, Izmir, Turkey
[3] Department of Obstetrics and Gynecology, Tepecik Maternity and Research Hospital, Izmir, Turkey
[4] Department of Histology and Embryology, Ege University, Izmir, Turkey
[5] Department of Physiology, Bilim University, Istanbul, Turkey

A – research concept and design; B – collection and/or assembly of data; C – data analysis and interpretation; D – writing the article; E – critical revision of the article; F – final approval of the article

Advances in Clinical and Experimental Medicine, ISSN 1899-5276 (print), ISSN 2451-2680 (online) *Adv Clin Exp Med*. 2018;27(5):591–597

Address for correspondence
Nuri Yildirim
E-mail: nuri-yildirim@hotmail.com

Funding sources
None declared

Conflict of interest
None declared

Received on June 5, 2016
Reviewed on August 24, 2016
Accepted on February 9, 2017

Abstract

Background. Ovarian torsion is one of the most common gynecological emergencies, which especially affects women of reproductive age.

Objectives. We aimed to evaluate the effect of *Ginkgo biloba* (GB) supplementation in ovarian ischemia/reperfusion injury in an experimental torsion/de-torsion rat model.

Material and methods. This study was carried out in the Ege University Faculty of Medicine in Izmir, Turkey. Thirty mature female Sprague-Dawley albino rats were randomly divided into 5 groups: in Group 1 (control), the abdominal wall was only opened and closed; in the torsion group (Group 2), ischemia was induced for 3 h, using atraumatic vascular clips to create a torsion model; in the torsion/GB group (Group 3), the rats were given 80 mg/kg (oral gavage) of GB 30 min before torsion was induced and the torsion model was formed; in the torsion/de-torsion group (Group 4), the rats underwent 3 h of ischemia and then the vascular clips were removed and reperfusion took place for 3 h; in the torsion/de-torsion/GB group (Group 5), the rats underwent 3 h of ischemia followed by GB (oral gavage) 30 min prior to a 3-h reperfusion period. Ovarian tissue damage was evaluated by a histopathological scoring system. Ovarian tissue malondialdehyde (MDA) and plasma pentraxin-3 were measured.

Results. In comparison with the sham group, both the torsion and torsion/de-torsion groups had significantly higher scores for follicular degeneration, vascular congestion, edema, hemorrhage, and leukocyte infiltration. *Ginkgo biloba* significantly decreased these scores in both groups. Ovarian malondialdehyde and plasma pentraxin 3 were significantly higher both in the torsion and torsion/de-torsion groups compared with the sham group. *Ginkgo biloba* decreased these levels significantly both in the torsion/GB and torsion/de-torsion/GB groups.

Conclusions. Supplementing GB during a surgical procedure decreases ischemia/reperfusion injury to an ovary in an experimental rat model based on histopathological parameters, tissue malondialdehyde, and plasma pentraxin-3 levels.

Key words: malondialdehyde, ischemia/reperfusion injury, ovarian torsion, *Ginkgo biloba*, pentraxin-3

DOI
10.17219/acem/68896

Copyright
© 2018 by Wroclaw Medical University
This is an article distributed under the terms of the Creative Commons Attribution Non-Commercial License (http://creativecommons.org/licenses/by-nc-nd/4.0/)

Introduction

Ovarian torsion is defined as a partial or total rotation of the ovary, the fallopian tube, or both around its vascular axis. The compression of the ovarian vessel obstructs lymphatic and venous outflow first, and subsequently arterial inflow. The blockage of the lymphatic and venous systems leads to ovarian edema, resulting in enlargement of the ovary. Increased ovarian stromal pressure blocks the arterial blood supply, which leads to ovarian ischemia and results in necrosis of the ovarian tissue, infarction, and local hemorrhage. It is the 5th-leading cause of surgical emergencies with a prevalence of 2.7–3%.[1] However, increased infertility treatment tends to raise the incidence rate iatrogenically. The incidence rate rises dramatically to 6% after ovarian stimulation and reaches as high as 16% in cases of ovarian hyperstimulation syndrome.[2]

The majority of ovarian torsion cases occur at reproductive age.[3] The diagnosis is often challenging because of the non-specific signs, symptoms, and limited benefits of imaging techniques and laboratory markers. The classic presentation of ovarian torsion is acute abdominal pain along with nausea, vomiting, and positive peritoneal signs. Additionally, adnexal masses or the impairment of ovarian blood flow would provide support for a diagnosis. Nevertheless, suspicion of ovarian torsion should be kept in mind in order to reduce adverse outcomes, especially the loss of ovarian function. Immediate surgical intervention is necessary as soon as ovarian torsion is diagnosed. In the past, fear of thromboembolic phenomena or a suspected malignant mass led physicians to perform an oophorectomy. However, there are no reported cases of embolic incidents after de-torsion in the literature. Thus, the current recommendation is to salvage the twisted ovary with de-torsion even if the tissues are cyanotic.[4]

De-torsion of the twisted ovary replenishes the blood supply and initiates the recovery process. Paradoxically, the return of blood flow can also result in additional ovarian damage and complications, referred to as reperfusion injury. Ischemia injury occurs because of an imbalance between energy requirements and production.[5] Aerobic energy cannot be utilized in an ischemic patient; the required energy is obtained through the anaerobic pathway. Remnants of this process can damage the cell. These processes are reversible only if reperfusion is instituted. However, reperfusion can be also hazardous because of neutrophil infiltration and excessive production of reactive oxygen species (ROS), called ischemia/reperfusion (I/R) injury. Membrane lipids are the most sensitive structures affected by ROS. Several substances are produced during the lipid oxidation process. Malondialdehyde is one of the most important end-products of lipid peroxidation and is used to indicate the level of oxidative damage. Pentraxin-3 (PTX3) is an acute-phase reactant produced predominantly by macrophages, dendritic cells, and endothelial cells. It functions as a central immune mediator, which is a novel marker for I/R injury, especially in myocardial cells.[6,7]

Ovarian viability and function is related not only to the period of ischemia, but also to reperfusion injury. Recently, many agents like edaravone, oxytocin, and octreotide have been reported to improve the side effects of I/R injury in animal models because of the their anti-inflammatory and antioxidant effects.[8–10]

Ginkgo biloba is one of the world's oldest living tree species. It contains dozens of active substances, including flavonoids, terpene lactones, ginkgo flavone glycosides, and bilobetin. Several investigators have used GB to treat dementia, tinnitus, cerebral insufficiency, sexual dysfunction, vertigo, vitiligo, macular degeneration, and peripheral vascular disease. The mechanism has not yet been defined exactly, but it has neuromodulator effects in the central and peripheral nervous system: it is an antioxidant and a vasodilator. As an antioxidant, GB reduces superoxide release in polymorphonuclear cells, acts as a scavenger for free radicals,and also acts as a mediator of lipid peroxidation and cell damage.[11–13] Recently, GB extracts were screened by ultra-high performance liquid chromatography. Sixty-one compounds were identified, 25 of which showed considerable radical scavenging capacity. This means that GB could have an important protector role not only in ischemic injury, but also in ischemic/reperfusion injury.[14]

To date, there have been several studies investigating the beneficial role of GB on various systems of the body; however, there is limited data on the effect of on ovarian ischemia/reperfusion injury. Therefore, the aim of the present study was to investigate the effect of GB on I/R injury in a rat ovary torsion/de-torsion model using a histopathological score, ovarian tissue MDA, and plasma PTX3 as tissue and systemic I/R injury markers.

Material and methods

Animals

We used 30 mature (12-week-old) female Sprague–Dawley albino rats that weighed 200–220 g each. The animals were fed ad libitum and housed in pairs in steel cages in a temperature-controlled environment (22 ±2°C) with 12-h light/dark cycles.

The local Animal Ethics Committee approved the experimental procedures employed in the present study. All experiments were carried out according to the Guide for the Care and Use of Laboratory Animals, as confirmed by the National Institute of Health (USA).

The estrus stage of each rat was determined by taking a vaginal smear at an interval of 6–12 h. Cells types in the smear were subsequently examined under a microscope according to the Papanicolaou stain procedure. Only the 30 rats, which were confirmed to be in the estrus stage by the smear, were included in the experiment.

Experimental protocol

Rats were anesthetized by an intraperitoneal injection of a combination of 50 mg/kg ketamine hydrochloride and 7 mg/kg xylazine hydrochloride (Alfazyne; Alfasan International BV, Woerden, Holland). After shaving and disinfection, a lower midline laparotomy was performed by making a 2-cm longitudinal incision, and the uterine horns and adnexa were located.

In Group 1 (n = 6, sham-operated control group), only a laparotomy was performed and then closed with 3/0 silk sutures (12). In Group 2 (n = 6, torsion group), ischemia was induced for 3 h by applying atraumatic vascular clips to the vascular pedicle 1 cm above and below the ovary. In Group 3 (n = 6, torsion and GB group), torsion was induced 30 min after the administration (oral gavage) of 80 mg/kg of GB (Tebokan, Abdi Ibrahim, Turkey). In Group 4 (n = 6 torsion/de-torsion group), 3 h of ischemia and 3 h of reperfusion were performed. In Group 5 (n = 6, torsion/de-torsion and GB group), torsion was induced for 3 h, followed by the administration of 80 mg/kg of GB (oral gavage) 30 min prior to de-torsion/reperfusion, which lasted 3 h. Tablets containing 80 mg GB (Tebokan, Abdi Ibrahim, Turkey) were crushed and suspended in tap water to yield a concentration of 10 mg/mL. According to the weight of each rat, the suspended drug solution was topped up to 4 mL with tap water. The medications were given via orogastric tubes. Immediately after the reperfusion period, both ovaries were excised for histological and biochemical evaluation.

Histopathological examination

The specimens were fixed in 10% buffered formalin for 48 h, cleared in xylene, and embedded in paraffin. Tissue sections of 4-µm were stained with hematoxylin and eosin for morphologic analysis. All sections were photographed with an Olympus C-5050 digital camera located on an Olympus BX51 microscope (Olympus Corp., Tokyo, Japan). All primordial and developing follicles were examined histologically.

Follicular degeneration, vascular congestion, hemorrhaging, edema, and infiltration by inflammatory cells were scored from 0 to 3 according to the severity of injury, with 0 indicating no pathological findings and 1, 2, and 3 representing pathological findings of <33%, 33–66%, and >66% of the ovarian section, respectively.[15]

The measurement of tissue lipid peroxidation

Ovarian tissues were homogenized in 150 mM of ice-cold KCl and centrifuged at 5000 g for 10 min. The supernatants were analyzed for lipid peroxidation. Lipid peroxidation was evaluated in each tissue sample by measuring the malondialdehyde level as thiobarbituric acid-reactive substances (TBARS). Briefly, trichloroacetic acid, TBARS reagent, and the tissue samples were mixed and incubated at 100°C for 60 min. After cooling, the samples were centrifuged at 3000 rpm for 20 min and the absorbance of the supernatant was read at 535 nm. The MDA level was calculated from a standard calibration curve using tetraethoxypropane and expressed as nmol/µg of protein.[16]

Measurement of the tissue protein levels

The total protein levels of the tissue samples were analyzed according to Bradford's method using bovine serum albumin as a standard.[17]

Evaluation of plasma pentraxin-3 levels

Plasma pentraxin-3 (PTX3) levels were assessed in each 100-µL sample by the standard ELISA method at 450 nm using a PTX3 kit (USCN Life Science Inc., Wuhan, China). PTX3 levels were determined in duplicate according to the manufacturer's guide. The detection range for PTX3 assay was 0.078–5 ng/mL.

Statistical analysis

Non-parametric variables were analyzed using the Kruskal-Wallis test. Parametric variables were evaluated with one-way ANOVA, followed by Tukey's HSD test with $p < 0.05$ accepted as statistically significant. SPSS v. 15.0 for Windows was used for analysis.

Results

The histopathological findings are shown in Fig. 1. The ovaries of the torsion group (Group 2) were compared with Group 1 according to the histopathological findings. All of the histopathological parameters were significantly higher in Group 2 ($p < 0.01$ and $p < 0.0001$). In the torsion/GB group (Group 3), all these parameters except edema were significantly decreased ($p < 0.05$) compared with Group 2. Decreased edema was detected in Group 3, but this difference did not reach statistically significant levels ($p > 0.05$). Comparison of the torsion/de-torsion group (Group 4) and the torsion/de-torsion + GB group (Group 5) revealed that all histopathological parameters were significantly lower in Group 5 ($p < 0.05$, $p < 0.01$). The histopathological scores are listed in Table 1 and Fig. 2.

Tissue MDA and plasma PTX3 were evaluated as cell injury markers. Group 3 had lower values than Group 2 and these differences were statistically significant ($p < 0.05$). Comparing Groups 4 and 5, Group 4 had higher values than Group 5 and this difference was statistically significant ($p < 0.001$). Tissue MDA and plasma PTX3 are shown in Table 2 and Fig. 3.

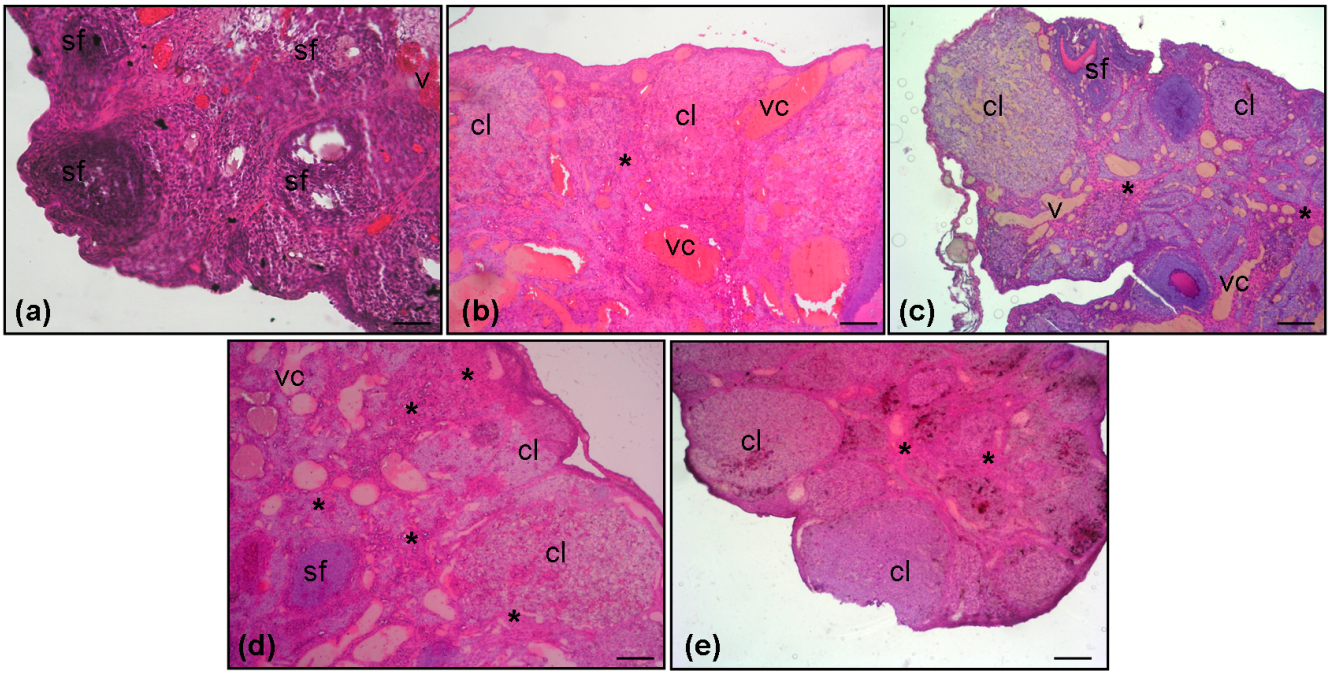

Fig. 1. Ovarian tissue sections of rats in Groups 1–5 are represented in pictures A–E, respectively. Hematoxylin and eosin staining was performed. Scale bars represent 250 µm

a – no pathological changes were detected in the sham group. (v) vessel, (sf) secondary follicle; b – edema (*), vascular congestion (vc) in the 3-h torsion group; c – decreased edema and vascular congestion in the torsion + GB group; d – vascular congestion (vc), edema (*) in the torsion/detorsion group; e – decreased edema (*) in the torsion/de-torsion + GB group.

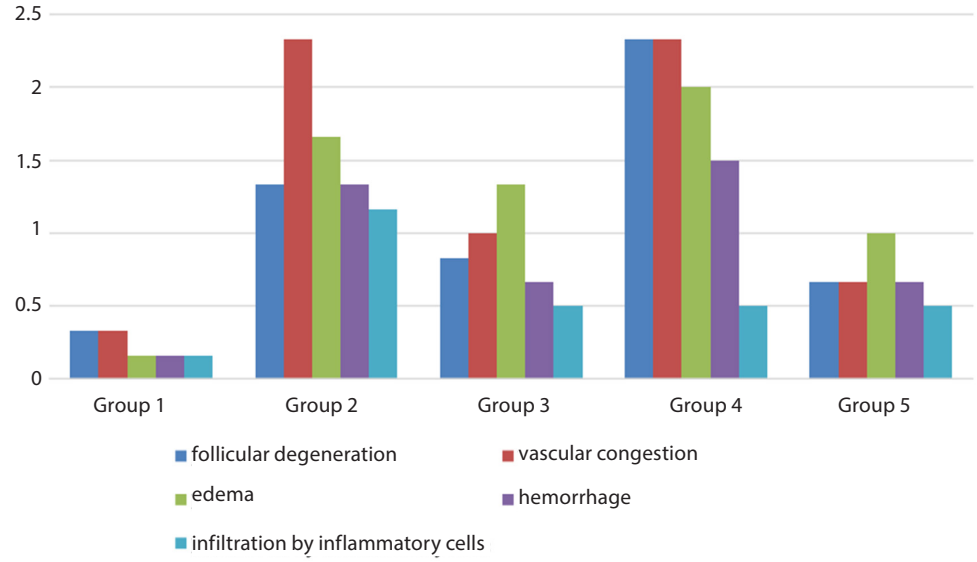

Fig. 2. Scores of histopathological parameters by group

Discussion

Ovarian torsion is a true gynecological emergency. Its prevalence is about 3% and this is rising due to the use of infertility treatments.[1,2] Difficulties in diagnosis prolong the time between the onset of symptoms and treatment. Once a diagnosis of ovarian torsion is confirmed, immediate intervention is necessary. Conservative treatment of the ovary should be the first choice regardless of the tissue color.

After de-torsion of the twisted ovary, the tissue will again receive blood supply and this could trigger further damage, known as ischemia/reperfusion injury. Once the blood flow is disrupted, a series of events lead to tissue injury and cell death. These processes are largely related to energy production and utilization. Reduced energy decreases intracellular ATP levels. Ischemia induces anaerobic energy utilization, which causes an accumulation of the products of anaerobic metabolism and reduces intracellular pH.[5] These processes are reversible if the blood supply is reestablished. However, reperfusion of the tissue is not a situation one should ignore. The reintroduction of oxygen and energy into an ischemic cellular environment

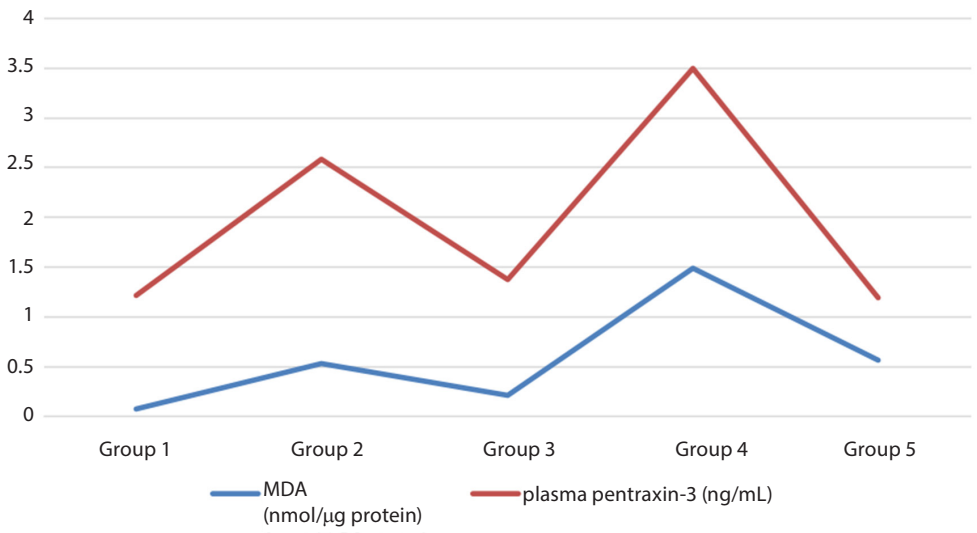

Fig. 3. Tissue MDA and plasma pentraxin-3 levels by group

Table 1. Histopathological parameters by group

Histopathological parameters	Group 1 – control (sham-operated)	Group 2 – torsion group	Group 3 – torsion + GB group	Group 4 – torsion/de-torsion group	Group 5 – torsion/de-torsion + GB group
Follicular degeneration	0.33 ±0.21	1.33 ±0.21*	0.83 ±0.16$^{\#}$	2.33 ±0.33	0.66 ±0.21††
Vascular congestion	0.33 ±0.21	2.33 ±0.21**	1.0 ±0.25$^{\#}$	2.33 ±0.33	0.66 ±0.21††
Edema	0.16 ±0.16	1.66 ±0.33*	1.33 ±0.42^{a}	2.0 ±0.36	1.0 ±0.25†
Hemorrhage	0.16 ±0.16	1.33 ±0.21*	0.66 ±0.21$^{\#}$	1.5 ±0.22	0.66 ±0.21†
Infiltration by inflammatory cells	0.16 ±0.16	1.16 ± 0.16*	0.5 ±0.22$^{\#}$	1.33 ±0.33	0.5 ±0.22†

* $p < 0.01$, Group 2 vs Group 1; ** $p < 0.0001$, Group 2 vs Group 1; $^{\#}$ $p < 0.05$, Group 3 vs Group 2; ^{a} $p > 0.05$, Group 3 vs Group 2; † $p < 0.05$, Group 5 vs Group 4; †† $p < 0.01$, Group 5 vs Group 4.

Table 2. Tissue MDA and plasma pentraxin-3 levels by group

Tissue levels	Group 1 control (sham-operated)	Group 2 – torsion group	Group 3 torsion + GB group	Group 4 torsion/de-torsion group	Group 5 torsion/de-torsion + GB group
MDA [nmol/µg protein]	0.07 ±0.009	0.53 ±0.16*	0.21 ±0.04$^{\#}$	1.49 ±0.18	0.56 ±0.10†
Plasma pentraxin-3 [ng/mL]	1.21 ±0.20	2.58 ±0.14*	1.38 ±0.29$^{\#}$	3.5 ±0.36	1.19 ±0.18†

MDA – malondialdehyde; * $p < 0.05$, Group 2 vs Group 1; $^{\#}$ $p < 0.05$, Group 3 vs Group 2; † $p < 0.001$, Group 5 vs Group 4.

can trigger cell injury by damaging cellular and organelle membranes, including the mitochondria, by free radical formation, by the aggregation of leukocytes and inflammatory mediators, and by the activation of the pro-apoptotic signaling cascade, and complement systems.[5,18,19] All these processes are called ischemia/reperfusion injury.

The primary treatment of ovarian torsion is de-torsion of the twisted ovary. However, due to the aforementioned reperfusion damage, concomitant treatment modalities with surgery are obviously required to reduce injury to the ovarian tissue. In our study, we investigated the effects of GB in I/R injury. Over 400 clinical trials have been performed, looking at a variety of medicinal properties and clinical uses to prevent or contribute beneficial effects for the regression of several diseases.[20] *Ginkgo biloba* extracts, such as terpene lactones and ginkgo flavone glycosides, are purported to be responsible for the beneficial effects.[21] Terpene lactones not only inhibit the platelet-activating factor due to selective antagonism, but also act as selective use-dependent blockers of glycine-activated chloride channels in the central nervous system.[22] In another study, the authors studied GB leaves with high-performance liquid chromatography and indicated that flavonoids in GB had powerful antioxidant attributes.[23]

Gingko biloba bilobalide plays a crucial role in mitochondrial protection during ischemia. Bilobalide allows the mitochondria to maintain respiratory activity at decreased oxygen levels, which delays ischemia-induced injury.[24] In our study, we also aimed to investigate GB's protector role for ischemic injury. We found that the GB torsion group had lower histopathological scores than the torsion-only group. Flavonoids also have antioxidative and

radical scavenger effects. They decrease reactive oxygen species and inhibit membrane lipid oxidation due to the scavenging of superoxide anions, hydroxyl radicals, and peroxyl radicals, and they prevent lipid peroxidation.[25] Flavonoids also act as suppressors of the immune system and reduce inflammatory cytokine production, especially TNF-α, IL-1β, and prostaglandin E2.[26] Our study is the only one in the literature that has investigated the effect of GB in I/R injury in ovarian tissue. We have reported that GB certainly decreased I/R as well as ischemic injury with improved histopathological parameters and tissue and plasma oxidative stress markers in a rat model. The rats which were administered GB had less follicular degeneration, vascular congestion, edema, hemorrhage, and infiltration by inflammatory cells compared with the rats which were not administered GB.

Ginkgo biloba has been widely used in several studies. The proper dosage of GB to initiate I/R injury protection has not been described in the literature. In one study, no significant adverse effects occurred in patients taking 600 mg of leaf extracts in single doses.[27] In experimental animal studies, the dosage of GB has varied between 15 mg/kg and 400 mg/kg.[27–29] We administered 80 mg/kg of GB for each rat in order to evaluate its effects on I/R injury. Although no significant adverse effects occurred in patients taking 600 mg of leaf extracts in single doses, GB is not definitely a safe herbal medicine, as mentioned in one review, because it was reported that it could cause epileptic seizures, unconsciousness, or paralysis of the legs, and may even cause death because of ginkgotoxin, which can be found especially in the GB seeds.[30]

Tissue and plasma oxidative stress markers were also compared between groups. There are several oxidative stress markers, such as total antioxidant status, malondialdehyde, myeloperoxidase, and 8-hydroxy dehydrogenase, which can be investigated in tissue samples to evaluate the tissue I/R injury. Malondialdehyde is one of the most investigated markers in I/R injury. In several recent studies, MDA was used to evaluate tissue injury induced by I/R oxidative stress.[8–10] In our study, the elevated MDA levels in the torsion and torsion/de-torsion groups were consistent with the literature. Furthermore, the GB rats had significantly lower MDA levels. These results demonstrate that GB could be a beneficial supplementary medicine for the prevention of I/R injury if our study is supported by further clinical studies carried out on human beings.

In our study we used pentraxin-3 to evaluate the inflammatory process in rats. PTX3 is a glycoprotein that belongs to the PTX family of acute-phase proteins, such as C-reactive protein (CRP) and serum amyloid P component (SAP). It has been widely studied in the diagnosis of ischemic heart disease.[7,31,32] In a recent experimental rat study, Akman et al. stated that PTX3 could be a specific acute-phase reactant detected in ovarian injuries such as ovarian torsion, and that it could be used as a diagnostic marker.[33] In this study, plasma PTX3 was significantly increased in the torsion and torsion/de-torsion groups. To our knowledge, PTX3 could be a good marker for ovarian injury. We also found that GB relieved I/R injury because of the lower values in the GB groups in comparison with the non-GB groups.

In conclusion, our study is the first and only study that investigates GB on ovarian I/R injury in a rat model. At present, GB is already being used as a dietary supplement, but could become a treatment modality for ischemia/reperfusion injury along with de-torsion surgery if our results are also supported by further clinical studies. It could be a useful dietary supplement or may become a new medicine in the future which can also relieve ischemic injury. Clinical studies with larger sample sizes are needed for more valuable decisions.

References

1. Hibbard LT. Adnexal torsion. *Am J Obstet Gynecol*. 1985;152(4):456–461.
2. Mashiach S, Bider D, Moran O, Goldenberg M, Ben-Rafael Z. Adnexal torsion of hyperstimulated ovaries in pregnancies after gonadotropin therapy. *Fertil Steril*. 1990;53(1):76–80.
3. Houry D, Abbott JT. Ovarian torsion: A fifteen-year review. *Ann Emerg Med*. 2001;38(2):156–159.
4. Huchon C, Fauconnier A. Adnexal torsion: A literature review. *Eur J Obstet Gynecol Reprod Biol*. 2010;150(1):8–12.
5. Jennings RB, Murry CE, Steenbergen C Jr, Reimer KA. Development of cell injury in sustained acute ischemia. *Circulation*. 1990;82(3):II2–12.
6. Diamond JM, Wigfield CH. Role of innate immunity in primary graft dysfunction after lung transplantation. *Curr Opin Organ Transplant*. 2013;18(5):518–523.
7. Zhu H, Cui D, Liu K, et al. Long pentraxin PTX3 attenuates ischemia reperfusion injury in a cardiac transplantation model. *Transpl Int*. 2014;27(1):87–95.
8. Ergenoglu M, Erbaş O, Akdemir A, et al. Attenuation of ischemia/reperfusion-induced ovarian damage in rats: Does edaravone offer protection? *Eur Surg Res*. 2013;51(1–2):21–32.
9. Yildirim N, Yigitturk G, Sahingoz Yildirim AG, et al. Octreotide protects ovary against ischemia-reperfusion injury in rats: Evaluation of histological and biochemical parameters. *J Obstet Gynaecol Res*. 2015;41(10):1591–1597.
10. Akdemir A, Erbas O, Gode F, et al. Protective effect of oxytocin on ovarian ischemia-reperfusion injury in rats. *Peptides*. 2014;55:126–130.
11. Wada K, Ishigaki S, Ueda K, et al. Studies on the constitution of edible and medicinal plants. I. Isolation and identification of 4-O-methylpyridoxine, toxic principle from the seed of *Ginkgo biloba* L. *Chem Pharm Bull*. 1988;36(5):1779–1782.
12. Oyama Y, Fuchs PA, Katayama N, Noda K. Myricetin and quercetin, the flavonoid constituents of *Ginkgo biloba* extract, greatly reduce oxidative metabolism in both resting and Ca(2+)-loaded brain neurons. *Brain Res*. 1994;635(1–2):125–129.
13. Benzi G, Moretti A. Are reactive oxygen species involved in Alzheimer's disease? *Neurobiol Aging*. 1995;16(4):661–674.
14. Guo RZ, Liu XG, Gao W, et al. A strategy for screening antioxidants in Ginkgo biloba extract by comprehensive two-dimensional ultra high performance liquid chromatography. *J Chromatogr A*. 2015; 27(1422):147–154.
15. Guven S, Muci E, Unsal MA, et al. The effects of carbon dioxide pneumoperitoneum on ovarian blood flow, oxidative stress markers, and morphology during laparoscopy: A rabbit model. *Fertil Steril*. 2010;93(4):1327–1332.
16. Tukozkan N, Erdamar H, Seven I. Measurement of total malondialdehyde in plasma and tissues by high-performance liquid chromatography and thiobarbituric acid assay. *Firat Medical Journal*. 2006;11(2): 88–92.
17. Bradford MM. A rapid and sensitive method for the quantitation of microgram quantities of protein utilizing the principle of protein-dye binding. *Anal Biochem*. 1976;72:248–254.

18. Saraste A, Pulkki K, Kallajoki M, et al. Apoptosis in human acute myocardial infarction. *Circulation*. 1997;95(2):320–323.
19. Cannon RO 3rd. Mechanisms, management and future directions for reperfusion injury after acute myocardial infarction. *Nat Clin Pract Cardiovasc Med*. 2005;2(2):88–94.
20. Ude C, Schubert-Zsilavecz M, Wurglics M. *Ginkgo biloba* extracts: A review of the pharmacokinetics of the active ingredients. *Clin Pharmacokinet*. 2013;52(9):727–749.
21. Isah T. Rethinking *Ginkgo biloba* L. Medicinal uses and conservation. *Pharmacogn Rev*. 2015;9(18):140–148.
22. Nakanishi K. Terpene trilactones from *Ginkgo biloba*: From ancient times to the 21st century. *Bioorg Med Chem*. 2005;13(17):4987–5000.
23. Ding XP, Qi J, Chang YX, et al. Quality control of flavonoids in *Ginkgo biloba* leaves by high-performance liquid chromatography with diode array detection and on-line radical scavenging activity detection. *J Chromatogr A*. 2009;1216(11):2204–2210.
24. Janssens D, Michiels C, Delaive E, et al. Protection of hypoxiainduced ATP decrease in endothelial cells by *Ginkgo biloba* extract and bilobalide. *Biochem Pharmacol*. 1995;50(7):991–999.
25. Smith JV, Luo Y. Studies on molecular mechanisms of *Ginkgo biloba* extract. *Appl Microbiol Biotechnol*. 2004;64(4):465–472.
26. Zheng LT, Ock J, Kwon B, Suk K. Suppressive effects of flavonoid fisetin on lipopolysaccharide-induced microglial activation and neurotoxicity. *Int Immunopharmacol*. 2008;8(3):484–494.
27. Pizzorno JE, Murray MT. *A Textbook of Natural Medicine* . Seattle, WA: John Bastyr College Publications; 1985.
28. Das A, Shanker G, Nath C, et al. A comparative study in rodents of standardized extracts of *Bacopa monniera* and *Ginkgo biloba*: Anticholinesterase and cognitive enhancing activities. *Pharmacol Biochem Behav*. 2002;73(4):893–900.
29. Yallapragada PR, Velaga MK. Effect of *Ginkgo biloba* extract on lead-induced oxidative stress in different regions of rat brain. *J Environ Pathol Toxicol Oncol*. 2015;34(2):161–173.
30. Leistner E, Drewke C. *Ginkgo biloba* and ginkgotoxin. *J Nat Prod*. 2010;73(1):86–92.
31. Shimizu T, Suzuki S, Sato A, et al. Cardio-protective effects of pentraxin-3 produced from bone marrow-derived cells against ischemia/reperfusion injury. *J Mol Cell Cardiol*. 2015;2828(15):30084–30085.
32. Hansson GK, Libby P. The immune response in atherosclerosis: A double-edged sword. *Nat Rev Immunol*. 2006;6(7):508–519.
33. Akman L, Erbas O, Terek MC, et al. The long pentraxin-3 is a useful marker for diagnosis of ovarian torsion: An experimental rat model. *J Obstet Gynaecol*. 2015;15:1–4.

Comparison of two models of inflammatory bowel disease in rats

Cristina S. Catana*[1,A,B,D], Cristian Magdas*[2,A,B,D], Flaviu A. Tabaran[3,B–D], Elena C. Crăciun[4,B,C], Georgiana Deak[2,B], Virginia A. Magdaş[2,B], Vasile Cozma[2,E], Călin M. Gherman[2,C], Ioana Berindan-Neagoe[5–7,E], Dan L. Dumitraşcu[8,A,F]

[1] Department of Medical Biochemistry, "Iuliu Haţieganu" University of Medicine and Pharmacy, Cluj-Napoca, Romania
[2] Department of Parasitology and Parasitic Diseases, University of Agricultural Sciences and Veterinary Medicine, Cluj-Napoca, Romania
[3] Department of Anatomic Pathology, Necropsy and Forensic Medicine, University of Agricultural Sciences and Veterinary Medicine, Cluj-Napoca, Romania
[4] Department of Pharmaceutical Biochemistry and Clinical Laboratory, "Iuliu Haţieganu" University of Medicine and Pharmacy, Cluj-Napoca, Romania
[5] Research Center for Functional Genomics, Biomedicine and Translational Medicine, "Iuliu Haţieganu" University of Medicine and Pharmacy, Cluj-Napoca, Romania
[6] Medfuture Research Center for Advanced Medicine, Cluj-Napoca, Romania
[7] Department of Functional Genomics and Experimental Pathology, The Oncology Institute "Prof. Dr. Ion Chiricuta", Cluj-Napoca, Romania
[8] 2nd Medical Department, "Iuliu Haţieganu" University of Medicine and Pharmacy, Cluj-Napoca, Romania

A – research concept and design; B – collection and/or assembly of data; C – data analysis and interpretation;
D – writing the article; E – critical revision of the article; F – final approval of the article

Advances in Clinical and Experimental Medicine, ISSN 1899-5276 (print), ISSN 2451-2680 (online) *Adv Clin Exp Med*. 2018;27(5):599–607

Address for correspondence
Flaviu Alexandru Tabaran
E-mail: alexandru.tabaran@usamvcluj.ro

Funding sources
None declared

Conflict of interest
None declared

* The first 2 authors contributed equally to the work.

Received on September 26, 2016
Reviewed on January 9, 2017
Accepted on February 23, 2017

Abstract

Background. There is a need for experimental animal models for inflammatory bowel diseases (IBD), but no proposed model has been unanimously accepted.

Objectives. The aim of this study was to develop 2 affordable models of IBD in rats and to compare them.

Material and methods. We produced IBD in rats using either dextran sodium sulfate (DSS) or 2, 4, 6-trinitrobenzene sulfonic acid (TNBS). The requirements for experimental models were: a predictable clinical course, histopathology and inflammation similar to human ulcerative colitis (UC) and Crohn's disease (CD). The effect of acute administration of DSS and TNBS on oxidative stress (as measured by the assessment of glutathione peroxidase – GPx) was verified. The activity of whole blood GPx was measured using a commercially available Randox kit (Crumlin, UK).

Results. The administration of DSS increased GPx activity compared to the control and TNBS-treated groups, but not to a statistically significant degree. Histological examination of the colonic mucosa following the administration of DSS showed multifocal erosions with minimal to mild inflammatory infiltrate, mainly by polymorphonuclear cells (PMN), lymphocytes and plasma cells. For TNBS-induced colitis, the histological changes manifested as multifocal areas of ulcerative colitis with mild to severe inflammatory infiltrate. Whole blood GPx values displayed a direct dependence on the chemical agent used. Our results show a correlation between histopathology, proinflammatory state and oxidative stress.

Conclusions. The experimental DSS- or TNBS-induced bowel inflammation used in this study corresponds to human IBD and is reproducible with characteristics indicative of acute inflammation in the case of the protocols mentioned.

Key words: animal model, colitis, dextran sodium sulfate, 2, 4, 6-trinitrobenzene sulfonic acid, inflammatory bowel disease

DOI
10.17219/acem/69134

Copyright
© 2018 by Wroclaw Medical University
This is an article distributed under the terms of the Creative Commons Attribution Non-Commercial License (http://creativecommons.org/licenses/by-nc-nd/4.0/)

Introduction

Animal models can be a valuable tool in understanding complex diseases such as ulcerative colitis (UC) and Crohn's disease (CD). Progress in the research for understanding the mucosal inflammation-immune balance of inflammatory bowel disease (IBD) has been delayed by a lack of adequate experimental models. No single IBD model captures the diversity of this human disease, but each of them provides valuable insight into one main feature of IBD or another, and together they contribute to the foundation of a largely accepted set of pathogenetic principles which enhance the current therapeutic approaches to CD and UC.[1] An "IBD integrom" concept offers a solution for a better understanding of the 4 components of pathogenesis, namely, genetic information (the genome); the surrounding environment (the exposome); the gut microbiota variations (the microbiome); and the intestinal immune reactivity (the immunome).[2] Although the immunome is the primary effector arm of inflammation in CD and UC, having been well characterized through the IL-17/IL-23 axis, other pathogenic processes could be implicated in the first stage of the disease.[3,4] Intestinal cells die by necrosis and release many molecules which are collectively named damage-associated molecular patterns (DAMPs) – independent of pathogen-associated molecular patterns (PAMPs) – leading to traditional microbial inflammation.[2] The release of DAMPs is intrinsic to IBD; these biological products trigger sterile inflammation in IBD mucosa affected by bleeding or ulcer formation.[5] Moreover, there is a hypothesis that chronic inflammation due to IBD could be a combination of traditional and sterile inflammations which is known as unresolving inflammation.[5] In addition, another process with contrasting results in IBD animal models is the inflammasome pathway mediated by caspase-1 in 2,4,6-trinitrobenzene sulfonic acid-induced colitis.[6,7]

A variety of agents could be used as inducers of colitis: acetic acid, formalin, indomethacin, carrageenan, or immune complexes.[8,9] The 2 most widely used IBD inducers in rodents are 2, 4, 6-trinitrobenzene sulfonic acid (TNBS) – ethanol administered as an enema – and dextran sulfate sodium (DSS) – often administered orally (although it can also be administered rectally) – which evoke colitis and immune inflammatory responses.[10–12]

The sulfated polysaccharide of DSS is directly toxic to the colonic epithelium. Thus, the short-term addition of DSS to drinking water leads to a very reproducible acute colonic inflammation as well as to a useful model for a better understanding of UC innate immune mechanisms.[1,13]

Intrarectal administration of a TNBS haptenating agent allows the initiation of a transmural colitis which mimics human CD and is useful for cytokine release patterns, effective immunotherapy and for the exploration of mucosal homeostasis.[1,14] Ample debate still exists as to whether reactive oxygen species (ROS) are involved in the pathogenesis of tissue lesions or are endogenously produced as a consequence of damaged cells. Moreover, in contrast with normal mucosa, significantly elevated concentrations of ROS are found in the actively inflamed mucosa of patients.[15] Extracellular glutathione peroxidase (E-GPx) is a selenoenzyme that reduces organic peroxides, and hydrogen peroxide.[16] GPx activity in humans is attributable to E-GPx. The gastrointestinal (GI) tract also produces and secretes E-GPx into the extracellular environment.

Animal models of IBD remain essential to the proper understanding of the histopathological shift in the GI tract and also play a key role in the development of novel antidotes for IBD.[1,17,18]

The aim of the study was to reproduce 2 models of IBD in rats in order to evaluate GPx activity during GI tract inflammation and to characterize the morphological changes occurring in the colonic wall. The DSS model could be valuable for the study of human UC, while the TNBS model is important for human CD.

Material and methods

In this experiment, 15 male Wistar rats weighing 200––290 g were used, in accordance with Directive 2010/63/EU of the European Parliament and the Council on the Protection of Animals used for Scientific Purposes. The animals were obtained from the Laboratory Animals Biobase of the University of Agricultural Sciences and Veterinary Medicine from Cluj-Napoca, Romania. They were maintained in a restricted access room and were housed in plastic cages under standard laboratory conditions (room temperature of 22°C, humidity of 50–60%, with a controlled 12-h light/dark cycle). They had free access to standard laboratory rodent formula pellets.

The rats were randomized into 3 groups, with 5 rats in each one. Group 1 received tap water; Group 2 received 5% DSS (MW 5000 Da, Sigma, St. Louis, USA) in their drinking water for 7 days; Group 3 intrarectally received a single dose of 100 mg/kg of TNBS (1 M, 293.17 mg/mL, product No. 92822, Fluka, Buchs, Switzerland) diluted in 50% ethanol to a concentration of 31.25 mg/mL, and had free access to tap water. The total volume instilled varied between 0.64–0.8 mL according to the rats' weight. Under anesthesia (10 mg/kg of xylazine and 100 mg/kg of ketamine, 1 M), the TNBS was instilled into the colon lumen via a polyethylene catheter (3-millimeter outer diameter) fitted onto a 1-milliliter syringe, introduced so that the tip was approx. 10 cm proximal to the anus. After instillation, the rats were held with the head down for 1 min to prevent TNBS from leaking out, and they were maintained in a head-down position at 45° until they recovered from the anesthesia.

The animals were observed daily and checked for fecal consistency. Also, water consumption and weight changes were monitored. On day 8 of the experiment, under deep anesthesia, blood samples were collected by cardiac puncture and all the animals were euthanized. Laparotomy was performed and the colon was removed as a whole and placed in a Petri dish containing a saline solution. The colon length was measured; the total length was calculated from the cecocolic junction to the rectum at the synphisic bone. Then the colon was opened along the mesenteric side and the luminal colonic surface was gently washed with an iso-osmotic saline solution to remove residual luminal content; then it was weighed. It was next immersed in a 10% neutral buffered formalin solution (Chempur, cat. No. 200-001-8, Piekary Śląskie, Poland) for 48 h, then trimmed into 3 equal segments (representing the proximal, middle and distal colon) and processed for routine light microscopy according to standard procedures.

Histopathology

The samples were dehydrated in ethanol baths with ascending concentrations, cleared in xylene and embedded in low-melting-point paraffin wax following routine laboratory protocol.[19] Multiple 4-micron sections were cut from the resulting paraffin blocks and stained with hematoxylin and eosin (H&E). Microscopic images were captured with an Olympus BX41 optical microscope coupled with an Olympus UC30 digital camera (Olympus, Hamburg, Germany). Finally, the images were processed by Stream Basic software (Olympus Soft Imaging Solution GmbH, Münster, Germany).

Histological semiquantitative analysis

The severity of induced colonic inflammation was graded morphologically using a semiquantitative scale by the same histopathologist in a single-blind fashion. We employed the histological scoring system previously described by Rachmilewitz for grading the severity of DSS- and TNBS-induced colitis in rodents.[20] This grading system considers the following 5 structural parameters scored on a scale of 0 to 4: depth and extent of the ulcer, presence of inflammation, extent of inflammation, and location of fibrosis (Table 1).

GPx activity assay

GPx activity was measured using a RANSEL kit (Randox Laboratories LTD., cat. No. RS504, Crumlin, UK) at 37°C on a Cobas Mira Plus (Roche, Basel, Switzerland) analyzer at 340 nm. The assay is based on the previously described method.[21]

Hemoglobin concentration assay

The hemoglobin (Hb) concentration was determined by the Drabkin method.[22]

Statistical methods

Descriptive and inferential statistics were used in our study. For the statistical analysis of data, R v. 3.2.4 (A Language and Environment for Statistical Computing, R Core Team, R Foundation for Statistical Computing, Vienna, Austria) and STATISTICA v. 6 (StatSoft, Tulsa, USA) software was used. Student's t-test was used and the equality of variances was previously tested by Levene's test. Because multiple groups were compared, the significance level (α) chosen for all independent t-tests was equal to 0.02.

To evaluate the differences in repeated measurements of body weight, we used a paired t-test. Because there were 7 occasions, the significance level was adjusted after a Bonferroni correction, and it was equal to 0.01. The results of the paired t-test were considered significant if $p \leq 0.01$.

In order to evaluate the colon length differences in the 3 groups, the Kruskal-Wallis and Mann-Whitney tests were used. Because of the multiple comparisons, the significance level was adjusted after a Bonferroni correction, and it was equal to 0.02. The statistical significance was set at $p \leq 0.02$.

The Pearson correlation coefficient (r) was also used to study the degree of correlation between the 2 quantitative variables.

All animal care and experimental protocols used in this study were approved by the Ethics Committee of "Iuliu Haţieganu" University, Cluj-Napoca, Romania (Ethics Committee approval No. 74/20.02.2014). All applicable international, national and/or institutional guidelines for the care and use of animals were followed.

Table 1. Criteria for scoring the histological lesions

Score	Depth of the ulcer	Extent of the ulcer	Presence of inflammation	Extent of inflammation	Location of fibrosis
0	absence of ulcer	absence of ulcer	absence of inflammation	absence of inflammation	absence of fibrosis
1	mucosal involvement	punctate	minimal	mucosal	mucosa only
2	mucosal and submucosal involvement	minimal	mild	mucosal/submucosal involvement	mucosa submucosa
3	penetration of muscularis propria	moderate	moderate	mucosal/submucosal and muscle involvement	including muscle layer
4	penetration of muscularis propria	widespread	severe	full thickness involvement	full thickness fibrosis

Results

After DSS or TNBS inoculation, the rats showed differences in colon weight/length, Hb concentration and GPx activity (Table 2). In the DSS and TNBS rat models, the whole blood GPx activity was higher compared to the control rats (in accordance with those of other studies), but not statistically significantly higher in the TNBS-inoculated rats (Table 1).[15,23]

Comparisons of clinical parameters among the study groups

The Student's t-test for the global comparison of the control and DSS-treated rats indicated statistically significant differences in Hb levels in the 2 groups (t-test assuming unequal variances, t = –2.86; df = 8; p = 0.02). The mean level of Hb concentration was higher (14.32 g/dL) among the DSS-treated group compared to the controls (12.58 g/dL). The mean level of Hb concentration in the DSS-treated group (14.32 g/dL) was significantly higher (t = 4.846; df = 8; p = 0.001 < 0.02) compared to the TNBS group (11.89 g/dL). Mean Hb levels were lower (11.89 g/dL), but not to a statistically significant degree, in the TNBS-treated group compared with controls (12.58 g/dL).

The mean colon weight was significantly different (t = –5.25; df = 8; p = 0.001 < 0.02) in the control rats (2.38 g) compared to Group 3 (3.87 g). Mean colon weight values were significantly different (t = –4.61; df = 8; p = 0.002 < 0.02) in the TNBS-treated group (3.87 g) compared to the DSS-treated group (2.52 g).

Next, the differences in colon length in the 3 groups were established. The Kruskal-Wallis test indicated statistically significant differences among the 3 studied groups (χ^2 = 10.25; df = 2; p = 0.006 < 0.05). These statistically significant differences between the colon length (cm) values in Groups 1 and 3 were confirmed by a post-test analysis (Mann-Whitney test; p = 0.019 < 0.02). We observed lower mean colon length levels in the TNBS-treated group compared to the controls (mean rank = 3.40 vs 7.60). Other statistically significant differences between the colon length (cm) values in the TNBS-treated group compared to the DSS-treated group (mean rank = 3 vs 8) were identified and validated by the Mann-Whitney test (p = 0.007 < 0.02).

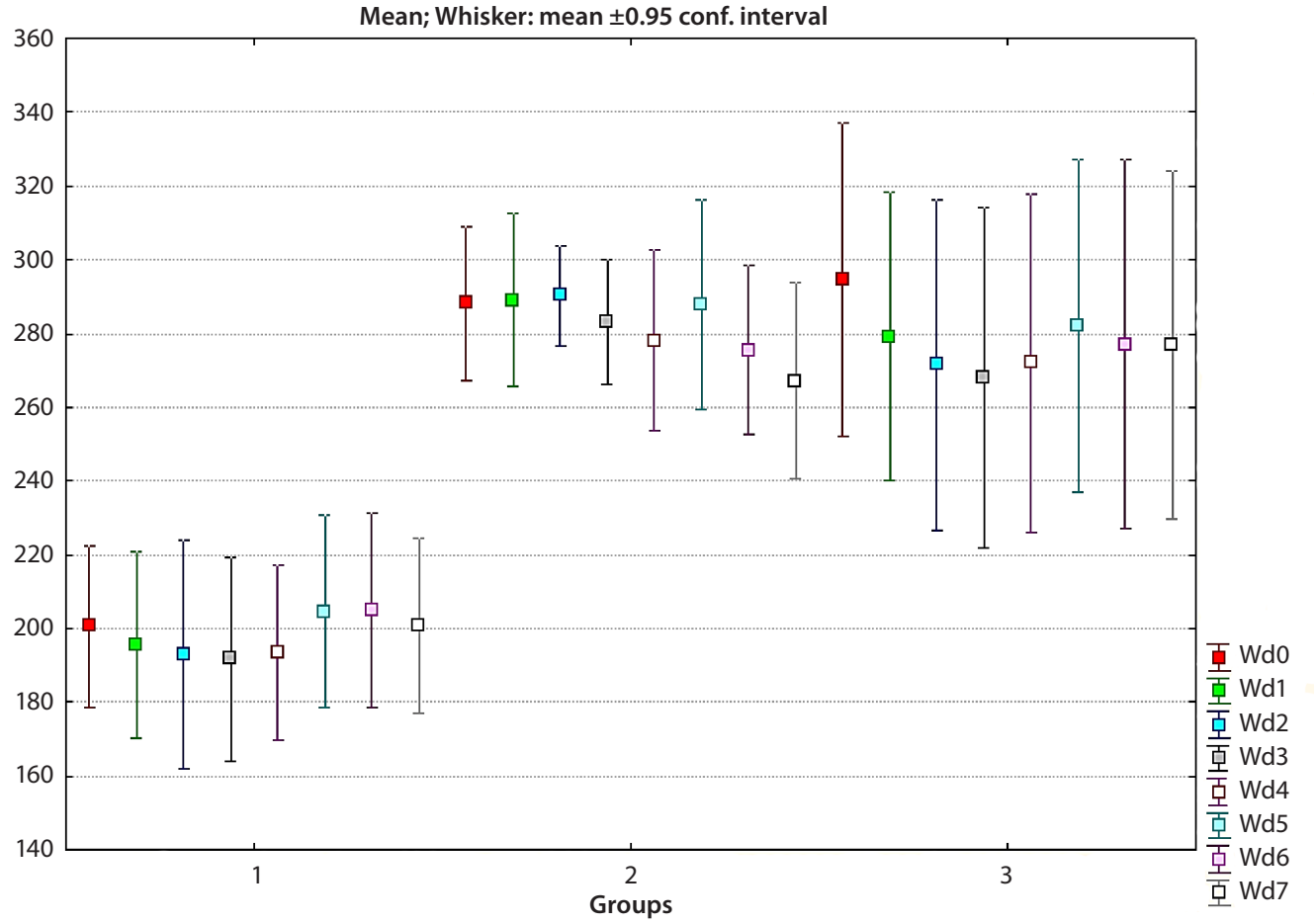

Fig. 1. Total weight evolution in studied groups over 1 week

1 – control group; 2 – DSS-treated group; 3 – TNBS-treated group.

We also established a good negative linear correlation between colon weight and colon length ($r = -0.54$; $p = 0.038 < 0.05$).

There were no statistically significant differences in GPx activity between the control group and the DSS group ($t = -0.53$; $df = 8$; $p = 0.612$), between the controls and the TNBS-treated group ($t = 0.96$; $df = 8$; $p = 0.364$), or between DSS- and TNBS-treated groups ($t = 1.87$; $df = 8$; $p = 0.099$).

In the TNBS-treated group, significant differences in body weight were found between the initial level (Wd0) and day 1 (Wd1) (paired-sample t-test, $t = 7.55$; $df = 4$;

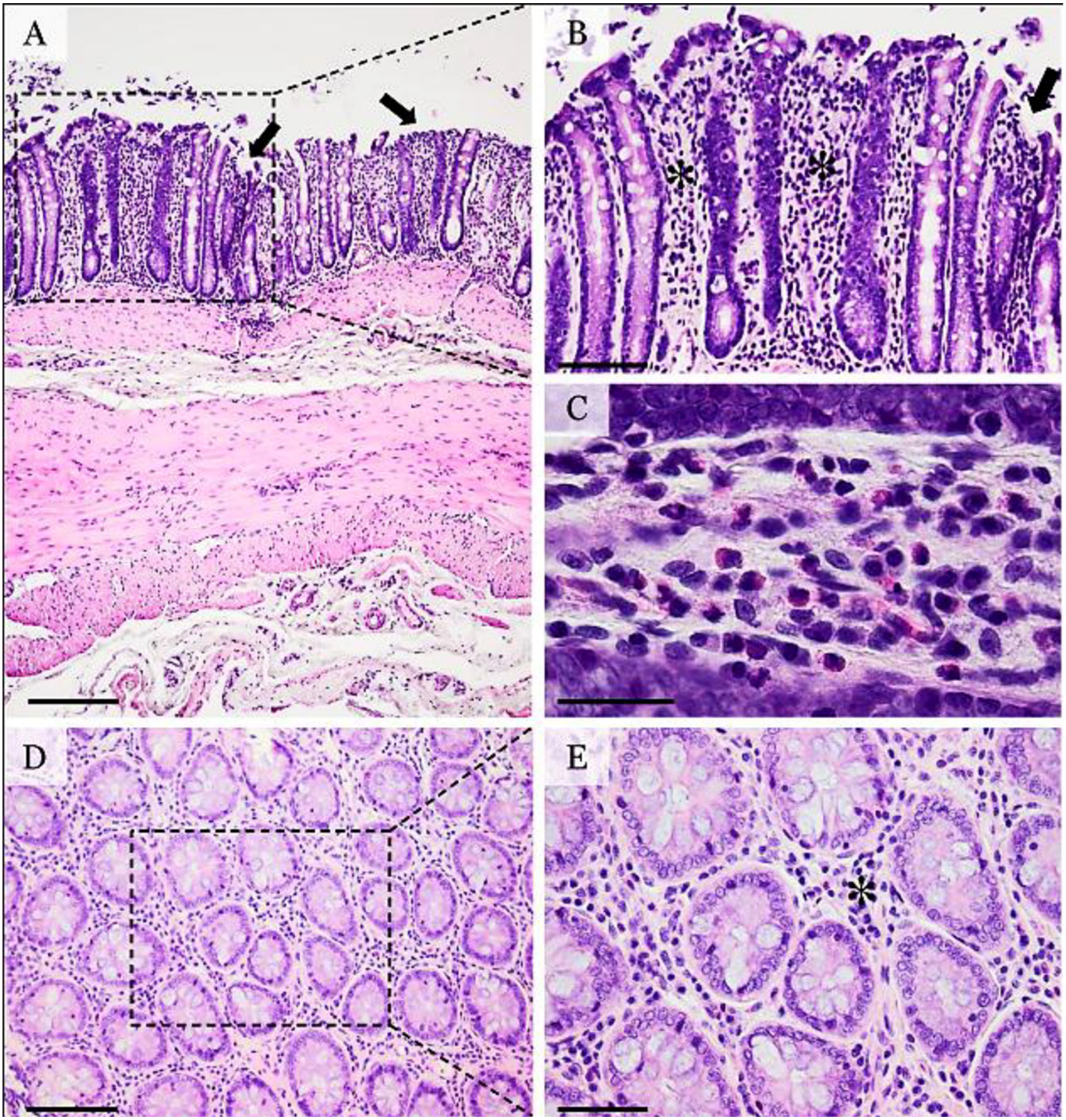

Fig. 2. Histopathological micrographs of DSS-induced colitis

A – general view of the colon, presenting multiple superficial erosions (arrows) and minimal inflammatory infiltrate located in the lamina propria; B – detail of the delineated area from image A, presenting superficial erosions (arrow) and discrete edema accompanied by mixed inflammatory infiltrate in the lamina propria; C – detail of the lamina propria with mixed inflammatory infiltrate represented by polymorphonuclear cells (PMN), lymphocytes and plasma cells; D – horizontal cross-section through intestinal mucosa presenting the interstitial inflammatory infiltrate and minimal fibrosis; E – detail of the delineated area from image D proves discreet interstitial fibrosis and mild inflammatory infiltration with PMN and mononuclear cells; H&E stain, OBX-4 for image A (scale bar = 400 µm), OBX-20 for images B and D (scale bar = 80 µm), OBX-100 for image C (scale bar = 50 µm), and OBX-40 for image E (scale bar = 40 µm).

$p = 0.002 < 0.01$). The mean body weight value was significantly lower in the second evaluation (279.2 g) compared to the initial one (294.6 g).

Furthermore, in the TNBS-treated group there were also significant differences between Wd0 and Wd2 (paired-samples t-test, $t = 14$; $df = 4$; $p = 0.0001 < 0.01$). We observed a lower level of Wd2 (271.60 g) compared to Wd0 (294.60 g). The findings are the same for the 3rd- and 4th-day body weight measurements (Fig. 1).

Macroscopic findings

After the 7-day cycle of DSS administration, the mucosa presented focal congestion and superficial erosions in the middle and distal colon.

At 7 days after TNBS inoculation, we observed diffuse congestion, deep ulcers (single or multiple) – located in the middle and distal colon – multifocal ulcerative colitis, and ulceration areas coated by an adherent fibrinous material. The colon lymph nodes were congested and edematous.

Histological findings

Following the administration of DSS, the colonic mucosa showed multifocal ulcerative colitis-like lesions which tended to occur more in the posterior part of the colon (Fig. 2). The mucosal erosions were superficial, associated with discrete hyperemia and edema of the lamina propria. The inflammatory infiltrate was diffusely distributed in the mucosa, without any apparent connection to the ulcerative foci. The inflammatory population was discreetly present, being composed by a mixture of polymorphonuclear cells, lymphocytes and plasmocytes. Also, discreet interstitial fibrosis and crypt dilatation were observed.

For the TNBS-induced colitis, the histological changes presented as multifocal areas of ulcerative colitis covered by a mixture of cellular debris, fibrin, blood, and polymorphonuclear cells. The ulcerative lesions were deep, involving the mucosa and submucosa of the colon. The ulcers and associated inflammation frequently displayed a transmural pattern, inducing an overall thickening of the colonic wall. Severe villous atrophy with crypt distortion, polymorphonuclear cells and rare mononuclear leukocytes were observed to infiltrate the lamina propria, the muscularis mucosae and the submucosa (Fig. 3). Marked fibrosis of the mucosa, with disruption of the muscularis mucosae and extension through the submucosa, accompany the ulcerative process.

Statistically significant differences in the histological score were found. The mean values of histological scores and also the total score were higher in the TNBS group than in the DSS group (Table 3).

Table 2. Colon weight, colon length, hemoglobin concentration, and GPx activity in study groups

Parameter	Group	Mean ±SD
Colon weight [g]	1	2.38 ±0.44
	2	2.51 ±0.47
	3	3.87 ±0.46
Colon length [cm]	1	22.8 ±1.48
	2	24.8 ±1.48
	3	20.80 ±0.44
Hg [g/dL]	1	12.58 ±1.12
	2	14.32 ±0.76
	3	11.89 ±0.82
GPx [U/gHb]	1	969.38 ±152.06
	2	1013.11 ±105.76
	3	890.78 ±101.25

1 – control; 2 – dextran sodium sulfate; 3 – 2, 4, 6-trinitrobenzene sulfonic acid; SD – standard deviation; GPx – glutathione peroxidase.

Discussion

Using DSS, a polyanionic derivative of dextran, the induced colonic inflammation starts distally after around 5 days and the lesions are confined to the colonic mucosa. DSS has a direct effect on the inner mucus layer and allows bacteria to penetrate it before any signs of inflammation are observed.[18]

DSS colitis is used to explore the role of inflammasome stimulation and Th-17 responses, or dectin receptors and Toll-like-receptor-initiated immune mechanisms.[24–26]

Also, DSS models could serve for the activation of epithelial TLR4 and releasing factors – which have positive effects and reduce the severity of DSS colonic inflammation – as well as for numerous intracellular signaling pathways.[27,28] The DSS-induced colitis in rodents quantifies the process of colonic cancer in relation to IBD.[29,30] Using DSS to induce colitis in Wistar rats, Kishimoto et al. mentioned that it was histologically similar to active

Table 3. Comparison of histological scores between the TNBS- and DSS-treated rat groups

Criterion	Mean ±SD					
	depth of the ulcer	extent of the ulcer	presence of inflammation	extent of inflammation	location of fibrosis	total score
DSS	1	1.6 ±0.89	1.4 ±0.54	1	0.6 ±0.54	5.6 ±1.34
TNBS	2.2 ±0.83	2.6 ±0.54	2.6 ±0.54	3.2 ±0.44	2	12.6 ±0.89
p-value	0.048	0.143	0.048	0.008	0.008	0.008

DSS – dextran sodium sulfate; TNBS – 2, 4, 6-trinitrobenzene sulfonic acid.

human ulcerative colitis.[31] After 6 days of 4% DSS administration in Sprague-Dawley rats, Gaudio et al. reported focal erosions of the epithelium with slight crypt dilatation and lesions similar to the ones found in our study.[29] Chen et al. developed a model of colitis in Sprague-Dawley rats using 2% DSS for 3 days followed by an intracolonic administration of 30% ethanol, which produced severe ulceration and inflammation of the distal part of the rat colon, histologically characterized by increased specific infiltration, the presence of cryptic abscesses, and dysplasia.[32]

TNBS is a nitroaryl oxidizing acid with extreme oxidizing properties; when dissolved in ethanol, it induces severe

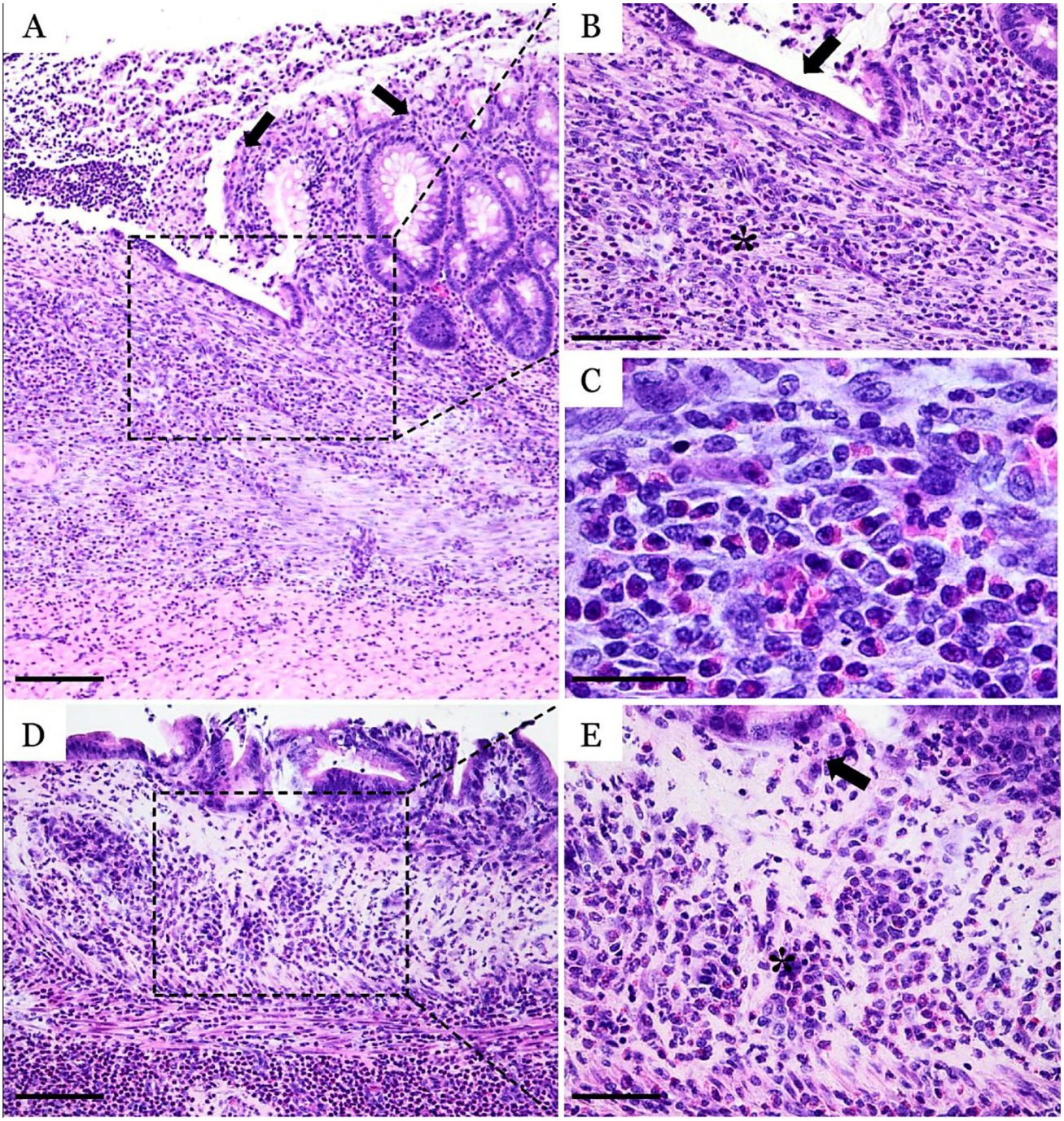

Fig. 3. Histopathological micrographs of TNBS-induced colitis

A – the margin of an ulcerative area involving the mucosa and submucosa of the colon; the massive inflammatory infiltrate extends through the muscularis layer. The adjacent mucosa present crypt dilation and distortion; B – detail of the delineated area from image A presenting the superficial part of the ulcer with epithelial regeneration (arrow), massive infiltration with PMN cells (*) and young, well-oriented granulation tissue; C – a high power view of the deep areas of the ulcer containing many PMN cells and rare mononuclear leukocytes; D – severe atrophy and fibrosis of the mucosa, with crypt distortion. Many polymorphonuclear cells are infiltrating the lamina propria, muscularis mucosa and submucosa; E – detail of the lamina propria from image D presenting severe fibrosis and inflammatory infiltration with PMN cells (*) and rare mononuclear leukocytes (arrow); H&E stain, OBX-10 for images A and D (scale bar = 400 µm), OBX-40 for images B and E (scale bar = 80 µm), OBX-100 for image C (scale bar = 50 µm).

colonic necrosis surrounded by acute inflammation areas. TNBS reduces mucosal hydrophobicity by reacting with the surface-active phospholipids of the colonic mucosa, thus inducing colonic inflammation.[1,33] Ethanol is very commonly used as a "barrier breaker" by increasing mucosal permeability. A failure in this barrier may result in intestinal inflammation, most likely through exposure to fecal antigens.[32] In TNBS-induced colitis in rats, the inflammatory response includes mucosal and submucosal infiltration by lymphocytes, macrophages, polymorphonuclear leukocytes, connective tissue mast cells, and fibroblasts.[34] The TNBS model highlights the fact that the loss of immune tolerance could lead to chronic intestinal inflammation. Moreover, modulation of the regulatory immune cells acts as a potential treatment method for the proper management of inflammatory intestinal disorders.[35] Additionally, this colitis model served as a source of knowledge about the cytokine profile in human IBD and also as a way to treat the disease in humans. Moreover, it continues to be an advantageous platform for studying the fundamental aspects of human IBD in terms of its spontaneous fibrosis and resolution.[1] The activation of the immune system leads to the increased production of proinflammatory cytokines, such as IL-17, TNF-α, IL-1β, IL-6, and IL-21, ROS, and prostaglandins contributing to a chronic inflammatory process.[15]

In our study, the lesions produced by TNBS were characterized by a higher histological score for all criteria than the ones generated by DSS; in 4 of the 5 criteria, the histological scores were statistically significant. In the DSS group, the highest histological score (1.6 ±0.89) was recorded for the criterion which described the extent of the ulcer, in most cases with a punctuate aspect. For the TNBS group, the highest histological score (3.2 ±0.44) was recorded for the extent of inflammation, characterized mostly by mucosal/submucosal and muscle involvement. Significantly reduced colon length as a result of muscular contraction compared to controls was also reported by Gaudio et al. in rat experimental colitis after oral DSS administration.[29]

Conclusions

The experimental DSS- or TNBS-induced bowel inflammation used in this study corresponds to human IBD and is reproducible with characteristics indicative of acute inflammation in the case of the protocols mentioned.

References

1. Kiesler P, Fuss IJ, Strober W. Experimental models of inflammatory bowel diseases. *Cell Mol Gastroenterol Hepatol*. 2015;1(2):154–170.
2. Fiocchi C. Inflammatory bowel disease pathogenesis: Where are we? *J Gastroenterol Hepatol*. 2015;1:12–18.
3. Cătană CS, Berindan-Neagoe I, Cozma V, Magdaş C, Tăbăran F, Dumitraşcu DL. Contri-bution of the IL-17/IL-23 axis to the pathogenesis of inflammatory bowel disease. *World J Gastroenterol*. 2015;21(19):5823–5830.
4. McCracken JM, Jiang L, Deshpande KT, O'Neil MF, Pritchard MT. Differential effects of hyaluronan synthase 3 deficiency after acute vs chronic liver injury in mice. *Fibrogenesis Tissue Repair*. 2016;31(9):4. doi:10.1186/s13069-016-0041-5
5. Sugimoto MA, Vago JP, Teixeira MM, Sousa LP. Annexin A1 and the resolution of in-flammation: Modulation of neutrophil recruitment, apoptosis, and clearance. *J Immunol Res*. 2016;2016:8239258. doi:10.1155/2016/8239258
6. Hao LY, Liu X, Franchi L. Inflammasomes in inflammatory bowel disease pathogenesis. *Curr Opin Gastroenterol*. 2013;29:363–369.
7. Oh SY, Cho KA, Kang JL, Kim KH, Woo SY. Comparison of experimental mouse models of inflammatory bowel disease. *Int J Mol Med*. 2014;33(2):333–340.
8. Elson CO, Sartor RB, Tennyson GS, Riddell RH. Experimental models of inflammatory bowel disease. *Gastroenterology*. 1995;109:1344–1367.
9. Jiminez JA, Uwiera TC, Douglas Inglis G, Uwiera RR. Animal models to study acute and chronic intestinal inflammation in mammals. *Gut Pathog*. 2015;7:29. doi:10.1186/s13099-015-0076-y
10. Yan Y, Kolachala V, Dalmasso G, et al. Temporal and spatial analysis of clinical and molecular parameters in dextran sodium sulfate induced colitis. *PLoS One*. 2009;4(6):e6073.
11. Johansson ME, Gustafsson JK, Sjoberg KE, et al. Bacteria penetrate the inner mucus layer before inflammation in the dextran sulfate colitis model. *PloS One*. 2010;5(8):e12238. doi:10.1371/journal.pone.0012238
12. Laroui H, Ingersoll SA, Liu HC, et al. Dextran sodium sulfate (DSS) induces colitis in mice by forming nano-lipocomplexes with medium-chain-length fatty acids in the colon. *PLoS One*. 2012;7(3):e32084.
13. Chami B, Yeung AW, van Vreden C, King, NJ, Bao, B. The role of CXCR3 in DSS-induced colitis. *PloS One*. 2014;9(7):e101622. doi:10.1371/journal.pone.0101622
14. Alex P, Zachos NC, Nguyen T, et al. Distinct cytokine patterns identified from multiplex profiles of murine DSS and TNBS-induced colitis. *Inflamm Bowel Dis*. 2009;15(3):341–352. doi:10.1002/ibd.20753
15. Pandurangan AK, Ismail S, Saadatdoust Z, Esa NM. Allicin alleviates dextran sodium sulfate- (DSS-) induced ulcerative colitis in BALB/c mice. *Oxid Med Cell Longev*. 2015;2015:605208. doi:10.1155/2015/605208
16. Tham DM, Whitin JC, Cohen HJ. Increased expression of extracellular glutathione perox-idase in mice with dextran sodium sulfate-induced experimental colitis. *Pediatr Res*. 2002;51(5):641–646.
17. Randhawa PK, Singh K, Singh N, Jaggy AS. A review on chemical-induced inflammatory bowel disease models in rodents. *Korean J Physiol Pharmacol*. 2014;18(4):279–288. doi:10.4196/kjpp.2014.18.4.279
18. Barnett M, Fraser A. Animal models of colitis: Lessons learned, and their relevance to the clinic. In: O'Connor M, ed. *Ulcerative Colitis – Treatments, Special Populations and the Future*. Rijeka: InTech; 2011:173–178.
19. Tăbăran AF. Tehnici în histopatologie. In: Cătoi C, Gal A, Taulescu M. *Tehnici de Anatomie Patologică Veterinară*. Cluj-Napoca, Romania: Editura AcademicPres; 2014:136–153.
20. Rachmilewitz D, Karmeli F, Takabayashi K, et al. Immunostimulatory DNA ameliorates experimental and spontaneous murine colitis. *Gastroenterology*. 2002;122(5):1428–1441.
21. Paglia DE, Valentine WN. Studies on the quantitative and qualitative characterization of erythrocyte glutathione peroxidase. *J Lab Clin Med*. 1967;70(1):158–169.
22. Drabkin DL, Austin JH. Spectrophotometric studies: Spectrophotometric constants for common hemoglobin derivatives in human, dog and rabbit blood. *J Biol Chem*. 1932;98:719–733.
23. Balmus IM, Ciobica A, Trifan A, Stanciu C. The implications of oxidative stress and an-tioxidant therapies in inflammatory bowel disease: Clinical aspects and animal models. *Saudi J Gastroenterol*. 2016;22(1):3–17. doi:10.4103/1319-3767.173753
24. Iliev ID, Funari VA, Taylor KD, et al. Interactions between commensal fungi and the C-type lectin receptor Dectin-1 influence colitis. *Science*. 2012;336:1314–1317.
25. Wlodarska M, Thaiss CA, Nowarski R, Henao-Mejia J, Zhang JP, Brown EM. NLRP6 inflammasome orchestrates the colonic host-microbial interface by regulating goblet cell mucus secretion. *Cell*. 2014;156(5):1045–1059.
26. Sokol H, Conway KL, Zhang M, et al. Card9 mediates intestinal epithelial cell restitution, T-helper 17 responses, and control of bacterial infection in mice. *Gastroenterology*. 2013;145:591–601.

27. Ren G, Sun A, Deng C, et al. The anti-inflammatory effect and potential mechanism of cardamonin in DSS- induced colitis. *Am J Physiol Gastrointest Liver Physiol*. 2015;309(7):G517–527. doi:10.1152/ajpgi.00133.2015
28. Chae WJ, Ehrlich AK, Chan PY, et al. The Wnt antagonist Dickkopf-1 promotes pathological type 2 cell-mediated inflammation. *Immunity*. 2016;44(2):246–258. doi:10.1016/j.immuni.2016.01.008
29. Gaudio E, Taddei G, Vetuschi A, et al. Dextran sulfate sodium (DSS) colitis in rats: Clinical, structural, and ultrastructural aspects. *Dig Dis Sci*. 1999;44:1458–1475.
30. Rayudu V, Raju AB. Effect of Triphala on dextran sulphate sodium-induced colitis in rats. *Ayu*. 2014;35(3):333–338.
31. Kishimoto S, Kobayashi H, Shimizu S, et al. Changes of colonic vasoactive intestinal peptide and cholinergic activity in rats with chemical colitis. *Dig Dis Sci*. 1992;37:1729–1737.
32. Chen Y, Si JM, Liu WL, et al. Induction of experimental acute ulcerative colitis in rats by administration of dextran sulfate sodium at low concentration followed by intracolonic ad-ministration of 30% ethanol. *J Zhejiang Univ Sci B*. 2007;8(9):632–637.
33. Tatsumi Y, Lichtenberger LM. Molecular association of trinitrobenzenesulfonic acid and surface phospholipids in the development of colitis in rats. *Gastroenterology*. 1996;110(3):780–789.
34. Coskun ZK, Kerem M, Gurbuz N, et al. The study of biochemical and histopathological effects of spirulina in rats with TNBS-induced colitis. *Bratisl Lek Listy*. 2011;112(5):235–243.
35. Sun M, He C, Cong Y, Liu Z. Regulatory immune cells in regulation of intestinal inflammatory response to microbiota. *Mucosal Immunol*. 2015;8(5):969–978.

Comparison of the anticonvulsant potency of various diuretic drugs in the maximal electroshock-induced seizure threshold test in mice

Katarzyna Załuska[1,B–D], Maria W. Kondrat-Wróbel[1,B–D], Jarogniew J. Łuszczki[1,2,A,C–F]

[1] Department of Pathophysiology, Medical University of Lublin, Poland
[2] Isobolographic Analysis Laboratory, Institute of Rural Health, Lublin, Poland

A – research concept and design; B – collection and/or assembly of data; C – data analysis and interpretation; D – writing the article; E – critical revision of the article; F – final approval of the article

Advances in Clinical and Experimental Medicine, ISSN 1899-5276 (print), ISSN 2451-2680 (online) *Adv Clin Exp Med*. 2018;27(5):609–613

Address for correspondence
Jarogniew J. Łuszczki
E-mail: jarogniew.luszczki@umlub.pl

Funding sources
None declared

Conflict of interest
Prof. J.J. Łuszczki has been involved in the design and development of new antiepileptics and CNS drugs. He has received, within the last 5 years, an unrestricted research grant from GlaxoSmith-Kline (Brentford, UK). The remaining authors have no conflict of interest to disclose.

Acknowledgements
This study was supported by grants from the Medical University of Lublin (DS 474/2012-2014 and DS 474/2015-2016).

Received on June 14, 2016
Reviewed on October 1, 2016
Accepted on January 27, 2017

Abstract

Background. The coexistence of seizures and arterial hypertension requires an adequate and efficacious treatment involving both protection from seizures and reduction of high arterial blood pressure. Accumulating evidence indicates that some diuretic drugs (with a well-established position in the treatment of arterial hypertension) also possess anticonvulsant properties in various experimental models of epilepsy.

Objectives. The aim of this study was to assess the anticonvulsant potency of 6 commonly used diuretic drugs (i.e., amiloride, ethacrynic acid, furosemide, hydrochlorothiazide, indapamide, and spironolactone) in the maximal electroshock-induced seizure threshold (MEST) test in mice.

Material and methods. Doses of the studied diuretics and their corresponding threshold increases were linearly related, allowing for the determination of doses which increase the threshold for electroconvulsions in drug-treated animals by 20% (TID_{20} values) over the threshold in control animals.

Results. Amiloride, hydrochlorothiazide and indapamide administered systemically (intraperitoneally – i.p.) increased the threshold for maximal electroconvulsions in mice, and the experimentally-derived TID_{20} values in the maximal electroshock seizure threshold test were 30.2 mg/kg for amiloride, 68.2 mg/kg for hydrochlorothiazide and 3.9 mg/kg for indapamide. In contrast, ethacrynic acid (up to 100 mg/kg), furosemide (up to 100 mg/kg) and spironolactone (up to 50 mg/kg) administered i.p. had no significant impact on the threshold for electroconvulsions in mice.

Conclusions. The studied diuretics can be arranged with respect to their anticonvulsant potency in the MEST test as follows: indapamide > amiloride > hydrochlorothiazide. No anticonvulsant effects were observed for ethacrynic acid, furosemide or spironolactone in the MEST test in mice.

Key words: diuretic drugs, threshold for electroconvulsions, TID_{20} values

DOI
10.17219/acem/68694

Copyright
© 2018 by Wroclaw Medical University
This is an article distributed under the terms of the Creative Commons Attribution Non-Commercial License (http://creativecommons.org/licenses/by-nc-nd/4.0/)

Introduction

Arterial hypertension is the most common cardiovascular disease affecting approx. 26% of the worldwide population, and thus, it is a major public health problem in both developed and developing countries.[1] In contrast, epilepsy is a serious neurological disorder affecting approx. 1% of the population in every country throughout the world.[2] The coexistence of both diseases (seizures and hypertension) requires adequate and efficacious treatment which simultaneously protects against seizures and reduces arterial blood pressure. In such cases, a combined treatment of antihypertensive and antiepileptic drugs is prescribed for these patients. However, any combined pharmacotherapy is associated with the appearance of interactions, whose nature may be pharmacodynamic, pharmacokinetic, or mixed.[3] The most notable group of drugs with a well-established position in the treatment of arterial hypertension are diuretics.[4]

Accumulating experimental evidence indicates that some diuretic drugs also possess anticonvulsant properties in various experimental models of epilepsy.[5–8] Previously, it was discovered that amiloride, hydrochlorothiazide and indapamide (3 classical diuretics) elevated the threshold for maximal electroconvulsions in experimental animals.[9–11] Unfortunately, the anticonvulsant properties of the diuretics were not directly compared to each other. However, to unequivocally assess the anticonvulsant potential of agents or drugs that increase the threshold for electroconvulsions, Swinyard et al. recommended determining doses of the compounds that increase the electroconvulsive threshold in drug-treated animals 20% over the threshold in control animals (i.e., TID_{20} values).[12] Thus, the TID_{20} values allow researchers to precisely assess the anticonvulsant potency of drugs or agents in preclinical studies.[12,13]

Considering the abovementioned facts, it was of pivotal importance to determine the TID_{20} values for 6 commonly prescribed diuretics (i.e., furosemide, spironolactone, amiloride, ethacrynic acid, hydrochlorothiazide, and indapamide) in the maximal electroshock-induced seizure threshold (MEST) test in mice in order to assess their anticonvulsant potency in this seizure model. There is no doubt that diuretic drugs with anticonvulsant properties can be preferentially recommended for patients with both high arterial blood pressure and seizures.

Material and methods

Animals and experimental conditions

Experiments were performed on adult male albino Swiss mice weighing 22–26 g. The experimental protocol described in this study conformed to the "Guide for the Care and Use of Laboratory Animals" and was approved by the Local Ethics Committee.[14]

Drugs

Ethacrynic acid, indapamide and spironolactone (all 3 drugs from Sigma-Aldrich, Poznań, Poland) as well as hydrochlorothiazide (Polpharma S.A., Starogard Gdański, Poland) were suspended in a 1% solution of Tween 80 (Sigma-Aldrich) in distilled water. Amiloride hydrochloride hydrate (Sigma-Aldrich) and furosemide (for injection 10 mg/mL; Polpharma S.A.) were dissolved in distilled water. All diuretic drugs were administered intraperitoneally (i.p.) in a volume of 0.005 mL/g body weight as follows: ethacrynic acid and furosemide at 30 min before the MEST-induced seizures, amiloride at 60 min before, and hydrochlorothiazide, indapamide and spironolactone at 120 min before.

Maximal electroshock seizure threshold test and the calculation of threshold increasing doses by 20% (TID_{20}) values

Seizure activity (electroconvulsions) was evoked by a current (sine-wave, 0.2 s stimulus duration, 50 Hz, 500 V) delivered via auricular electrodes by a Rodent Shocker generator (Hugo Sachs Elektronik, Freiburg, Germany).[15] To assess the threshold for maximal electroconvulsions, 4 groups of mice (8 mice per group) were subjected to electroshocks of varying intensities (ranging from 4 to 10 mA) to yield seizures in 10–30%, 30–50%, 50–70%, and 70–90% of animals. The log-probit method was used to calculate the median current strength (CS_{50} [mA]), representing the current intensity necessary to induce tonic hind limb extension in 50% of the mice challenged.[16] The threshold (CS_{50} values) for maximal electroconvulsions in mice receiving amiloride, ethacrynic acid, furosemide, hydrochlorothiazide, indapamide, and spironolactone (all diuretics in increasing doses), were experimentally determined as described in detail previously.[17,18] Subsequently, the percentage of increase in CS_{50} values for animals injected with increasing doses of diuretics over the control CS_{50} value was calculated. The doses of diuretics and their resultant percentage of threshold increase over the control were graphically plotted in rectangular coordinates of the Cartesian plot system and examined with the least-squares linear regression analysis. From linear regression equations, the TID_{20} values were calculated as recommended earlier.[12,13]

Statistics

The CS_{50} values with their standard error of mean (SEM) were statistically analyzed with one-way analysis of variance (ANOVA) followed by the Tukey-Kramer post-hoc test. Differences among values were considered statistically significant if $p < 0.05$.

Results

Effects of various diuretic drugs on the threshold for maximal electroshock-induced seizures

Amiloride administered systemically (i.p.) at doses of 5, 10, 50, 75, and 100 mg/kg elevated the threshold for MEST-induced seizures over the controls by 11.2%, 12.7%, 24.2%, 37.2%, and 51.2%, respectively (Table 1). With one-way ANOVA and the Tukey-Kramer post-hoc test, only amiloride (100 mg/kg) significantly raised ($p < 0.05$) the threshold for electroconvulsions in mice ($f (5; 90) = 2.889$; $p = 0.0182$) (Table 1). Similarly, hydrochlorothiazide administered i.p. at doses of 25, 50 and 100 mg/kg increased the threshold for maximal electroconvulsions by 11.5%, 15.4% and 26.9%, respectively (Table 1). Statistical analysis of data with one-way ANOVA revealed that hydrochlorothiazide (100 mg/kg) significantly elevated ($p < 0.05$) the electroconvulsive threshold in mice ($f (3; 76) = 2.535$; $p = 0.0631$) (Table 1). Moreover, indapamide administered i.p. at doses of 1.5, 3 and 6 mg/kg raised the threshold for MEST-induced seizures by 2.2%, 12.1% and 37.4%, respectively (Table 1). In this case, indapamide (6 mg/kg) significantly increased ($p < 0.05$) the threshold for electroconvulsions in mice ($f (3; 60) = 3.718$; $p = 0.0161$) (Table 1). In the case of ethacrynic acid, the drug at a maximally tested dose of 100 mg/kg elevated the threshold only by 5.9%, which was not statistically significant (Table 1). In contrast, furosemide and spironolactone (both at a maximally tested dose of 100 mg/kg) decreased the threshold for electroconvulsions in experimental animals in the MEST test. The observed changes, however, were not statistically significant (Table 1).

Subsequently, the doses of amiloride, hydrochlorothiazide and indapamide were linearly related to the threshold increases, and the respective equations describing these relations are illustrated in Fig. 1. The experimentally-derived TID_{20} values in the MEST test in mice were 30.2 mg/kg

Table 1. Influence of 6 diuretic drugs in the maximal electroshock seizure threshold test in mice

Drug [mg/kg]	CS_{50} [mA]	n	TI [%]	One-way ANOVA
Control	5.92 ±0.77	16	–	f (5; 90) = 2.889; p = 0.0182
Amiloride (5)	6.58 ±0.59	16	11.2	
Amiloride (10)	6.67 ±0.61	24	12.7	
Amiloride (50)	7.35 ±0.45	8	24.2	
Amiloride (75)	8.12 ±0.72	16	37.2	
Amiloride (100)	8.95 ±0.53*	16	51.2	
Control	6.8 ±0.61	24	–	f (2; 53) = 0.0976; p = 0.9072
Ethacrynic acid (50)	7.0 ±0.72	16	2.9	
Ethacrynic acid (100)	7.2 ±0.62	16	5.9	
Control	4.89 ±0.40	16	–	f (2; 45) = 0.0168; p = 0.9833
Furosemide (50)	4.76 ±0.45	8	2.7	
Furosemide (100)	4.84 ±0.36	24	1.0	
Control	5.2 ±0.37	16	–	f (3; 76) = 2.535; p = 0.0631
Hydrochlorothiazide (25)	5.8 ±0.29	24	11.5	
Hydrochlorothiazide (50)	6.0 ±0.35	16	15.4	
Hydrochlorothiazide (100)	6.6 ±0.40*	24	26.9	
Control	5.54 ±0.42	16	–	f (3; 60) = 3.718; p = 0.0161
Indapamide (1.5)	5.66 ±0.51	16	2.2	
Indapamide (3.0)	6.21 ±0.48	16	12.1	
Indapamide (6.0)	7.61 ±0.55*	16	37.4	
Control	5.5 ±0.47	16	–	f (5; 74) = 0.2891; p = 0.9176
Spironolactone (12.5)	5.4 ±0.42	8	–1.8	
Spironolactone (25)	5.2 ±0.35	24	–5.5	
Spironolactone (37.5)	5.1 ±0.45	8	–7.3	
Spironolactone (50)	5.0 ±0.40	16	–9.1	
Spironolactone (100)	4.8 ±0.46	8	–12.7	

Results are median current strengths (CS_{50} [mA] ±SEM) necessary to produce tonic convulsions in 50% of the animals tested; control groups of animals received a vehicle (1% of solution of Tween 80 in distilled water); n – number of animals tested at those current strength intensities whose seizure effects ranged between 16% and 84%; TI – threshold increasing values are presented as percentage of increase in CS_{50} values for animals injected with increasing doses of diuretics over the control (vehicle-treated) animals; statistical analysis of data was performed with one-way ANOVA followed by the Tukey-Kramer post-hoc test;* $p < 0.05$ vs the control (vehicle-treated) animals.

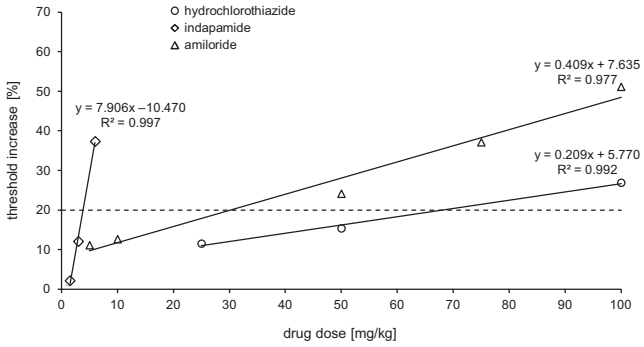

Fig. 1. Linear regression analysis of doses of various diuretic drugs and their corresponding threshold increases in the MEST test in mice

y – threshold increase [%]; x – dose of the diuretic; R2 – coefficient of determination. The dashed line reflects the TID20 values (threshold increasing doses by 20%) in the MEST test.

for amiloride, 68.2 mg/kg for hydrochlorothiazide and 3.9 mg/kg for indapamide, respectively.

Discussion

Results indicate that there was a close correlation between the doses of 3 diuretic drugs (i.e., amiloride, hydrochlorothiazide and indapamide) and their anticonvulsant properties in mice subjected to the MEST test. In this study, linear regression analysis allowed for the determination of the TID_{20} values for amiloride, hydrochlorothiazide and indapamide. In the case of ethacrynic acid, the drug had no impact on the threshold for electroconvulsions. In contrast, furosemide and spironolactone diminished the threshold for electroconvulsions in mice, although the data did not reach the level of statistical significance.

Of note, the TID_{20} values presented in this study for diuretic drugs can be readily compared to those reported earlier for some second-generation antiepileptic drugs (AEDs). The TID_{20} values for some AEDs were as follows: 70 mg/kg for gabapentin,[18] 44 mg/kg for levetiracetam,[19] 103.2 mg/kg for stiripentol,[20] 4.4 mg/kg for tiagabine,[17] and 226.2 mg/kg for vigabatrin.[17,18] A direct comparison of TID_{20} values of the second-generation AEDs with those calculated for the 3 diuretics revealed that indapamide has the lowest TID_{20} value (3.9 mg/kg). In contrast, gabapentin, levetiracetam, stiripentol, and vigabatrin have higher TID_{20} values than those calculated for amiloride (30.2 mg/kg). In the case of hydrochlorothiazide, its TID_{20} value (68.2 mg/kg) is lower than that of gabapentin, stiripentol and vigabatrin in the MEST test. Thus, considering the anticonvulsant potency of the studied diuretics, the drugs can be arranged from the lowest to the highest TID_{20} values as follows: indapamide > amiloride > hydrochlorothiazide. This comparative study allowed for the assessment of the most favorable diuretic drug with the lowest TID_{20} value (indapamide), which is effective in suppressing MEST-induced tonic seizures in experimental animals.

There is another fact worth keeping in mind while translating the results from this study to a clinical setting. Since the TID_{20} value for indapamide in mice was 3.9 mg/kg, it can be readily converted to a dose of indapamide used in humans, according to the method presented by Reagan-Shaw et al.[21] The converted dose of indapamide for a 60 kg human should be 18.72 mg (i.e., 0.312 mg/kg of body weight). The recommended maximum daily dose of indapamide in humans is 5 mg.[22] Thus, it seems that the anticonvulsant effects of indapamide would appear if the daily dose of indapamide exceeded ~4 times the recommended maximum. Similarly, the TID_{20} values for amiloride and hydrochlorothiazide were 30.2 mg/kg and 68.2 mg/kg, respectively. Thus, the corresponding doses of the diuretics in a 60 kg human should amount to 145 mg for amiloride and 327.4 mg for hydrochlorothiazide. The recommended maximum daily dose of amiloride is 20 mg,[23] and for hydrochlorothiazide it is 100 mg,[24] so the anticonvulsant effects of amiloride would be expected if the daily dose exceeded ~7 times the recommended maximum, and that of hydrochlorothiazide ~3 times. We are fully aware of such limitations in translational studies. However, it has to be noted that diuretic drugs cannot be used alone as anticonvulsant agents in patients with epilepsy, but always in combination with classical and novel AEDs in order to provide epilepsy patients with the most effective treatment against both arterial hypertension and seizures. Obviously, combinations of diuretics and AEDs always produce interactions of a pharmacodynamic, pharmacokinetic, or mixed nature.[3] However, preclinical studies on animals allowed us to characterize the interactions between diuretics and AEDs. For instance, it has been reported that indapamide significantly potentiated the anticonvulsant action of carbamazepine, phenobarbital and valproate, although the effects observed for phenobarbital in the mouse maximal electroshock seizure (MES) model were of a pharmacokinetic nature.[11] Only the interactions between indapamide and carbamazepine and valproate were pharmacodynamic in the mouse MES model, suggesting their clinical applicability in epilepsy patients.[11] In the case of hydrochlorothiazide, the diuretic drug exclusively enhanced the anticonvulsant activity of carbamazepine in the mouse MES model.[10] As regards amiloride, the drug potentiated the anticonvulsant activity of carbamazepine, oxcarbazepine, phenobarbital, topiramate, and valproate in the mouse MES model.[9] Unfortunately, amiloride pharmacokinetically potentiated the effects of carbamazepine, oxcarbazepine and phenobarbital in mice challenged with the MEST test. Only the pharmacodynamic interactions between amiloride and topiramate, and valproate deserve recommendation for their clinical use in epilepsy patients.

In conclusion, indapamide – with the lowest TID_{20} value in the mouse MEST test – deserves recommendation for clinical use as an add-on therapy in epilepsy patients who additionally require the application of diuretic drugs.

References

1. Kearney PM, Whelton M, Reynolds K, Muntner P, Whelton PK, He J. Global burden of hypertension: Analysis of worldwide data. *Lancet*. 2005;365:217–223.
2. Kwan P, Schachter SC, Brodie MJ. Drug-resistant epilepsy. *N Engl J Med*. 2011;365:919–926.
3. Patsalos PN, Froscher W, Pisani F, van Rijn CM. The importance of drug interactions in epilepsy therapy. *Epilepsia*. 2002;43:365–385.
4. Doroszko A, Janus A, Szahidewicz-Krupska E, Mazur G, Derkacz A. Resistant hypertension. *Adv Clin Exp Med*. 2016;25:173–183.
5. Ali A, Ahmad FJ, Dua Y, Pillai KK, Vohora D. Seizures and sodium hydrogen exchangers: Potential of sodium hydrogen exchanger inhibitors as novel anticonvulsants. *CNS Neurol Disord Drug Targets*. 2008;7:343–347.
6. Kahle KT, Staley KJ. The bumetanide-sensitive Na-K-2Cl cotransporter NKCC1 as a potential target of a novel mechanism-based treatment strategy for neonatal seizures. *Neurosurg Focus*. 2008;25:E22. doi:10.3171/FOC/2008/25/9/E22
7. Löscher W, Puskarjov M, Kaila K. Cation-chloride cotransporters NKCC1 and KCC2 as potential targets for novel antiepileptic and antiepileptogenic treatments. *Neuropharmacology*. 2013;69:62–74.
8. Xiong ZG, Pignataro G, Li M, Chang SY, Simon RP. Acid-sensing ion channels (ASICs) as pharmacological targets for neurodegenerative diseases. *Curr Opin Pharmacol*. 2008;8:25–32.
9. Luszczki JJ, Sawicka KM, Kozinska J, Dudra-Jastrzebska M, Czuczwar SJ. Amiloride enhances the anticonvulsant action of various antiepileptic drugs in the mouse maximal electroshock seizure model. *J Neural Transm*. 2009;116:57–66.
10. Lukawski K, Swiderska G, Czuczwar SJ. Effect of hydrochlorothiazide on the anticonvulsant action of antiepileptic drugs against maximal electroshock-induced seizures in mice. *Pharmacol Rep*. 2012;64:315–320.
11. Kozinska J, Sawicka KM, Zadrozniak A, et al. Indapamide enhances the protective action of carbamazepine, phenobarbital, and valproate against maximal electroshock-induced seizures in mice. *Adv Med Sci*. 2009;54:66–74.
12. Swinyard EA, Brown WC, Goodman LS. Comparative assays of antiepileptic drugs in mice and rats. *J Pharmacol Exp Ther*. 1952;106:319–330.
13. Löscher W, Fassbender CP, Nolting B. The role of technical, biological and pharmacological factors in the laboratory evaluation of anticonvulsant drugs. II. Maximal electroshock seizure models. *Epilepsy Res*. 1991;8:79–94.
14. National Research Council (US) Committee for the Update of the Guide for the Care and Use of Laboratory Animals. *Guide for the Care and Use of Laboratory Animals*. 8th ed. Washington, DC: National Academies Press US; 2011.
15. Kondrat-Wróbel MW, Luszczki JJ. Interaction of three-drug combination of lacosamide, carbamazepine and phenobarbital in the mouse maximal electroshock-induced seizure model: An isobolographic analysis. *Health Probl Civiliz*. 2016;10:55–61.
16. Litchfield JT Jr, Wilcoxon F. A simplified method of evaluating dose-effect experiments. *J Pharmacol Exp Ther*. 1949;96:99–113.
17. Luszczki JJ, Czuczwar SJ. Isobolographic characterization of interactions between vigabatrin and tiagabine in two experimental models of epilepsy. *Prog Neuropsychopharmacol Biol Psychiatry*. 2007;31:529–538.
18. Luszczki JJ, Ratnaraj N, Patsalos PN, Czuczwar SJ. Isobolographic and behavioral characterizations of interactions between vigabatrin and gabapentin in two experimental models of epilepsy. *Eur J Pharmacol*. 2008;595:13–21.
19. Luszczki JJ, Czuczwar SJ. How significant is the difference between drug doses influencing the threshold for electroconvulsions? *Pharmacol Rep*. 2005;57:782–786.
20. Luszczki JJ, Dudra-Jastrzebska M, Andres-Mach M, et al. Stiripentol in a dose-dependent manner elevates the threshold for maximal electroshock-induced seizures in mice. *JPCCR*. 2007;1:155–157.
21. Reagan-Shaw S, Nihal M, Ahmad N. Dose translation from animal to human studies revisited. *FASEB J*. 2008;22:659–661.
22. Drugs.com. Indapamide dosage. http://www.drugs.com/dosage/indapamide.html. Updated August 5, 2016. Accessed March 6, 2018.
23. Drugs.com. Amiloride dosage. http://www.drugs.com/dosage/amiloride.html. Updated March 8, 2016. Accessed March 6, 2018.
24. Drugs.com. Hydrochlorothiazide dosage. http://www.drugs.com/dosage/hydrochlorothiazide.html. Updated August 9, 2016. Accessed March 6, 2018.

The effect of music on the cardiac activity of a fetus in a cardiotocographic examination

Grażyna Gebuza[1,A,C–F], Marta Zaleska[2,B,C,E,F], Marzena Kaźmierczak[2,C,E,F], Estera Mieczkowska[2,C,E,F], Małgorzata Gierszewska[2,C,E,F]

[1] Department of Obstetric Care Basics, Faculty of Health Sciences, Nicolaus Copernicus University in Toruń, Poland
[2] Faculty of Health Sciences, Nicolaus Copernicus University in Toruń, Poland

A – research concept and design; B – collection and/or assembly of data; C – data analysis and interpretation;
D – writing the article; E – critical revision of the article; F – final approval of the article

Advances in Clinical and Experimental Medicine, ISSN 1899-5276 (print), ISSN 2451-2680 (online) *Adv Clin Exp Med*. 2018;27(5):615–621

Address for correspondence
Grażyna Gebuza
E-mail: grazyna.gebuza@cm.umk.pl

Funding sources
None declared

Conflict of interest
None declared

Acknowledgements
We express our gratitude to the mothers and to the infants involved in this study.

Received on February 7, 2016
Reviewed on May 25, 2016
Accepted on January 27, 2017

Abstract

Background. Music therapy as an adjunct to treatment is rarely used in perinatology and obstetrics, despite the proven therapeutic effect. Auditory stimulation through music positively impacts the health of adults and infants, its special role being observed in the development of prematurely born neonates. It is equally interesting how music impacts fetuses.

Objectives. The aim of this study is to assess the parameters of fetuses through cardiotocographic recording in women in the 3rd trimester of pregnancy while listening to Pyotr Tchaikovsky's "Sleeping Beauty" and "Swan Lake."

Material and methods. The study was conducted in 2015 at Dr. Jan Biziel 2nd University Hospital in Bydgoszcz, on 48 women in the 3rd trimester of pregnancy. The cardiotocographic parameters of the fetus were examined by means of a Sonicaid Team Standard Oxford apparatus (Huntleigh Healthcare, Cardiff, United Kingdom).

Results. Significant changes were observed in the number of uterine contractions, accelerations, episodes of higher variability, and fetal movements after listening to the music.

Conclusions. Listening to classical music can serve as a successful method of prophylaxis against premature deliveries, indicated by the lower number of uterine contractions, and in stimulating fetal movement in the case of a non-reactive non-stress test (NST). Music therapy, as a therapeutic method which is inexpensive and soothing, should be used more frequently in obstetrics wards, indicated by pathological pregnancies, isolation from the natural environment, and distress resulting from diagnostics and from being in an unfamiliar environment.

Key words: music therapy, uterine contractions, cardiotocography, short-term versatility, fetal movements

DOI
10.17219/acem/68693

Copyright
© 2018 by Wroclaw Medical University
This is an article distributed under the terms of the Creative Commons Attribution Non-Commercial License (http://creativecommons.org/licenses/by-nc-nd/4.0/)

Introduction

The extrauterine surroundings of a fetus are dominated by sounds coming from the mother's body, but the fetus also experiences sounds from outside the womb, which impact its development. Scientists suggest that experiencing sounds in the mother's womb is connected with the baby's preferences directly post-delivery and with the infant's health; therefore, wards hosting neonates should be designed in a way that allows infants the same type of experiences as in their fetal lives.[1] Scientists agree that in the prenatal period the fetus is capable of learning and discerning sounds; they point to a possible role of perinatal auditory experiences in the future development of speech and attachment. One of the studies revealed that infants who had listened to pop music from a television drama in their fetal lives showed changes in the rhythm of their heartbeats and more movement, and that they significantly changed their behavior while listening to it, up to 4 days post-delivery.[2] Musical stimulation significantly impacts human physiology and psychology; consequently, it should be carefully selected according to the aim of a particular therapy. Individual preferences and needs – and most of all, the health condition – should also be taken into account.[3] Several reactions of the body were observed, depending on the type of music being played. Fast-paced music leads to an increase in blood pressure and to faster breath.[4,5] Slow-paced music leads to a lower heart rate and breath rate in comparison to their baseline values.[6] The soft sounds of a regular and low rhythm (lullabies) are perfect for fetuses and infants.[3,6] Auditory stimulation through music positively impacts the health of adults and infants, its special role being observed in the development of prematurely born neonates. Numerous studies have proven that the mother's voice and the sound of her heartbeat have a tranquilizing effect and they show short-term clinical gains for prematurely delivered neonates. In Doheny's study, increased circulatory stability in neonates and less frequent apnea in prematurely born infants were observed after listening to the recording of the mother's voice and heartbeat, in comparison to listening to the sounds of medical apparatus. Even more beneficial effects were observed when combining the above-mentioned methods with kangaroo care.[7–9] A normalization in temperature, breathing, heart rate, and body mass were observed in neonates. Using such a therapy also led to an increase in saturation value and growth rate, fewer feeding intolerance instances, and shorter hospitalization periods.[10–15] The mother's voice is one of the crucial sensual stimuli. In a study by Arnon et al., parents sang and played musical instruments in the intensive care unit; after the musical stimulation, heart rates were observed to decrease, and 30 min of deep sleep ensued.[16] In a study by Keith et al., a decrease in the frequency and length of crying episodes was observed in neonates. The outcomes of the research also pointed to an improvement in physiological parameters, such as heart rate, respiratory rate, saturation, and mean arterial pressure.[17] In the intensive care unit, the children who listened to lullabies cried less and slept more. Changes were also observed in mothers, who became significantly more tranquil during kangaroo care.[9,18]

Although the impact of music on the mothers' health is not the subject of our research, we do cite several examples of the impact of music on women in the pre-delivery period below. Childbirth may be a stressful experience in a woman's life, and assuming this new role may result in a decrease in quality of life, or it may reveal anxiety or depression.[19,20] Having women listen to specially selected music is a significant element of care in such cases. Music shows many positive impacts on a pregnant female body, be it under normal physiological conditions or in a high-risk pregnancy. In a study by Sidorenko, music proved to be an effective therapy leading to the prevention of premature deliveries, and it successfully treated hypertension during pregnancy. Music has also been used as a perfect method of pre-operational preparation for caesarean delivery. A powerful stress-reducing effect was observed, leading to a lower dosage of anesthetics.[21] Music is successful under many circumstances and it may be used as an effective method to treat different conditions. In pregnant women, it significantly reduced anxiety and, following delivery, it proved to be a successful therapy in mitigating the symptoms of worsened temper, as well as facilitating breast-feeding.[20,22–24] Following therapy of rhythmical music and lullabies in a neonatal intensive care unit, lower stress was also observed in the parents.[18] Based on the cited literature, it can be shown that many beneficial effects can be achieved through music therapy in infants and mothers. Fetal parameters under classical music have hardly been studied so far. In our research, only a single Polish study was found, and a handful of others in English on a similar subject. Since the experiences of hospitalized women and fetuses are important to us, this research subject was embraced.

The aim of the study was to assess the cardiac activity parameters of fetuses through cardiotocographic recording in women in the 3rd trimester of pregnancy while listening to classical music by Pyotr Tchaikovsky, namely, "Swan Lake" and "Sleeping Beauty."

Material and methods

The study was conducted in 2015 at the Obstetrics Department of the University Hospital in Bydgoszcz, having received authorization from the Committee for Bioethics (No. 777/2014). The study included 48 women in the 3rd trimester of pregnancy. The women gave their informed consent to participate in the study. The stage of pregnancy was between the 27th week and the 41st week (35th week on average).

The studied women were not at risk of premature delivery. In the initial stage of the study, non-stress tests (NST) were performed on 15 pregnant women without music and with "Swan Lake." On 15 other pregnant women, NST was

performed without music and with "Sleeping Beauty," and on another 18 women, with both of previously mentioned compositions. Among the 18 women, 2 were carrying twins. The 1st stage of the study consisted of cardiotocography of the fetus's cardiac activity with no (musical) stimuli to the fetus, and in analyzing the cardiocotographic parameters by means of a Sonicaid Team Standard Oxford apparatus. The 2nd stage consisted of performing a 15-min music therapy session, where the women listened to "Swan Lake" and "Sleeping Beauty" from a tape recorder, followed by an analysis of cardiotocographic parameters by means of a Sonicaid Team Standard Oxford apparatus.

All cardiotocographic parameters were analyzed by means of the statistics pack, PQStat v. 1.6 (PQStat Software, Poznań, Poland). Owing to the fact that the studied parameters significantly diverged from the theoretical normal distribution (which was determined by a Shapiro-Wilk test), analyses were conducted with the non-parametrical approach. The levels of the studied parameters before and after musical stimulation were compared by a Wilcoxon signed-rank test. A testing probability of $p < 0.05$ was assumed to be significant, while $p < 0.01$ was assumed to be highly significant.

Results

According to the assumptions of the study, the values of cardiotocographic parameters from the 2 sessions were compared: with no music and with Pyotr Tchaikovsky's "Swan Lake" or "Sleeping Beauty." The studied parameters are presented in the tables below.

In the above analysis, after listening to Pyotr Tchaikovsky's "Swan Lake," a significant decrease in the values of cardiotocographic parameters was observed regarding the number of uterine contractions, >10 and >15 accelerations, and higher variability and lower variability. After listening to this musical piece, the fetuses' movements were observed to increase in number. The parameters of short-term variability slightly increased.

In this analysis, after listening to Pyotr Tchaikovsky's "Sleeping Beauty", a significant decrease in the values of cardiotocographic parameters was observed regarding the number of accelerations >10 and higher variability. After listening to this composition, a statistically insignificant decrease in the number of fetal movements and uterine contractions was observed (0.06). The short-term variability parameters increased insignificantly.

The analysis did not reveal a statistically significant difference between the musical compositions used, as to which showed a larger influence on fetal parameters.

Discussion

The aim of the study was to assess fetal cardiac activity through cardiotocographic recording in women in the 3rd trimester of pregnancy, with and without listening to classical music compositions by Pyotr Tchaikovsky. "Swan Lake" is characterized by a rhythmical tempo, while "Sleeping Beauty" can be classified as a lullaby. Music is rarely used as a form of therapy in perinatology. In fact, single studies on this topic exist, mostly regarding neonatal care in an intensive care unit, distress suffered by pregnant

Table 1. Values of cardiotocographic parameters under the stimulation of Pyotr Tchaikovsky's "Swan Lake"

Parameters	Exposure to music	Mean	Standard deviation	Min	Lower quartile	Median	Upper quartile	Max	Wilcoxon's test
Fetal movements	before	45.34	30.03	3	23.5	39	58	117	Z = 2.38 p = 0.0175
	during	64.46	44.29	0	30	60	83.5	174	
Baseline fetal heart rate	before	140.30	11.70	120	134	138	145.5	168	Z = 1.49 p = 0.1355
	during	137.40	11.50	103	131.5	137	141.5	167	
Contractions	before	0.94	1.30	0	0	1	1	6	Z = 3.05 p = 0.0023
	during	0.20	0.76	0	0	0	0	4	
Accelerations >10	before	7.34	4.39	0	4.5	8	10	18	Z = 3.93 p = 0.0001
	during	3.94	3.01	0	2	3	5	14	
Accelerations >15	before	4.23	3.75	0	1	3	7	15	Z = 2.71 p = 0.0068
	during	2.29	2.15	0	1	1	4	8	
High variability	before	13.23	8.95	0	7	14	21	31	Z = 2.74 p = 0.0062
	during	7.46	6.68	0	5	6	10	27	
Low variability	before	3.39	5.06	0	0	0	6.5	18	Z = 2.41 p = 0.0159
	during	0.86	2.52	0	0	0	0	10	
Short-term variability	before	9.27	2.52	4.3	7.65	9.1	11	14.5	Z = 1.65 p = 0.0997
	during	10.38	4.56	3.6	7.45	10	12.25	28.6	

Table 2. Values of cardiotocographic parameters under stimulation of Pyotr Tchaikovsky's "Sleeping Beauty"

Parameters	Exposure to music	Mean	Standard deviation	Min	Lower quartile	Median	Upper quartile	Max	Wilcoxon's test
Fetal movements	before	62.17	52.59	6	26.5	50	92.5	276	Z = 1.08 p = 0.2794
	during	54.17	47.00	0	15	46	82.5	182	
Baseline fetal heart rate	before	139.20	10.65	120	134.5	137	144	168	Z = 1.50 p = 0.1331
	during	137.70	12.89	108	131.5	136	142.5	169	
Contractions	before	0.71	1.18	0	0	0	1	6	Z = 1.82 p = 0.0685
	during	0.29	0.62	0	0	0	0	2	
Accelerations >10	before	6.31	4.28	0	2.5	6	9	17	Z = 2.80 p = 0.0050
	during	3.94	4.10	0	1	3	5.5	19	
Accelerations >15	before	3.46	3.41	0	1	3	5.5	14	Z = 0.69 p = 0.4914
	during	2.89	3.43	0	0.5	2	4	15	
High variability	before	12.57	8.88	0	7	11	19	31	Z = 3.46 p = 0.0005
	during	6.34	6.79	0	0	6	10	29	
Low variability	before	2.79	4.89	0	0	0	5.35	17	Z = 0.75 p = 0.4501
	during	2.26	4.42	0	0	0	2	16	
Short-term variability	before	9.40	2.31	4.3	7.75	9.7	11.1	14	Z = 0.25 p = 0.8059
	during	9.57	3.86	3.6	6.8	9.1	11.7	19.6	

women, and the use of vibroacoustic stimulation testing (VAS) to stimulate the fetus. Only 1 study has been conducted, by Poręba et al. in 2000.[25]

Comparing the number of fetal movements in the 2 sessions – with no music and with classical music – a significant increase in the number of fetal movements was observed after listening to "Swan Lake", from an average of 45 movements to 64. Poręba et al. presented their results on the impact of musical sounds on the performance of selected cardiotocographic parameters in full-term pregnancy (39.5 weeks of pregnancy on average). An increase of 8 movements was achieved under relaxing music.[25] In our study of the relationship with the increased number of fetal movements, it should be considered whether such music could be used in a situation when it is necessary to cause the fetus to react as a result of a non-reactive NST recording. An acoustic test with Pyotr Tchaikovsky's "Swan Lake" could serve in such cases as an alternative to VAS. In the study, no statistically significant changes were observed while listening to "Sleeping Beauty" in the number of fetal movements, which reduced from 62 movements to 54. Such behavior of fetuses likely stemmed from the peaceful rhythm of the lullaby-like composition. Some researchers claim that VAS with an excessively non-physiological pitch and intense sound, performed to provoke a reaction in the fetus, may even be dangerous for hearing development and health, and that it should be used with the utmost care.[26–28] In another study, listening to music during NST showed a positive impact on maternal and fetal parameters and an increase in the number of fetal movements was observed.[29]

In a study by Annunziata et al., fetal movements, the number of accelerations, and short-term variability (STV) made a significant increase in VAS. For a low-risk pregnancy, an improvement in the values of accelerations and movements was found, while STV did not improve. The results indicate that only in high-risk pregnancy was the increase in STV, the number of movements, and accelerations following VAS significantly connected with the well-being of neonates.[30]

Another analyzed parameter was baseline fetal heart rate (BPM). In this study, no difference was found between the BPM in cardiocotographic recording preceding

Table 3. Comparing cardiotocographic parameters under stimulation of Pyotr Tchaikovsky's "Swan Lake" and "Sleeping Beauty" (by Mann-Whitney's U test)

Parameters	Exposure to music	Z	p-value
Fetal movements	before	1.257503	0.208572
Fetal movements	during	1.175247	0.239896
Baseline fetal heart rate	before	0.411816	0.680474
Baseline fetal heart rate	during	0.023516	0.981239
Contractions	before	0.832026	0.405394
Contractions	during	1.265204	0.205798
Accelerations >10	before	0.925018	0.354956
Accelerations >10	during	0.662857	0.507422
Accelerations >15	before	0.901178	0.367494
Accelerations >15	during	0.274505	0.783697
Higher variability	before	0.330056	0.741357
Higher variability	during	0.836228	0.403026
Lower variability	before	0.640739	0.521692
Lower variability	during	1.550059	0.121127
Short-term variability	before	0.381992	0.702467
Short-term variability	during	0.787126	0.431208

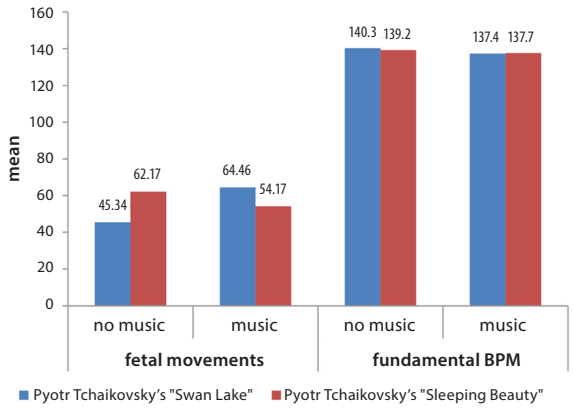

Fig. 1. Comparison of fetal movements and baseline fetal heart rate (BPM) under stimulation of Pyotr Tchaikovsky's "Swan Lake" and "Sleeping Beauty"

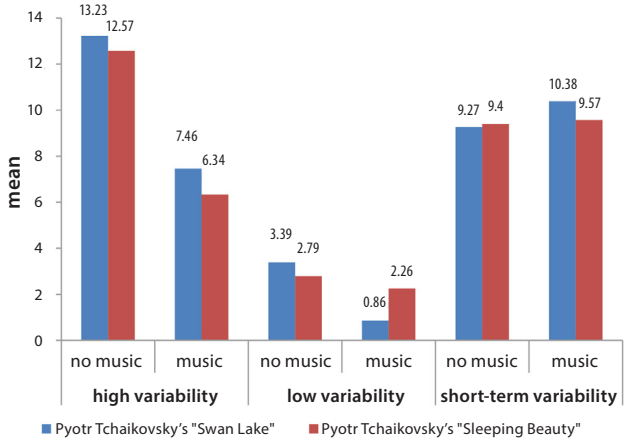

Fig. 2. Comparison of high variability, low variability, and short-term variability under stimulation of Pyotr Tchaikovsky's "Swan Lake" and "Sleeping Beauty"

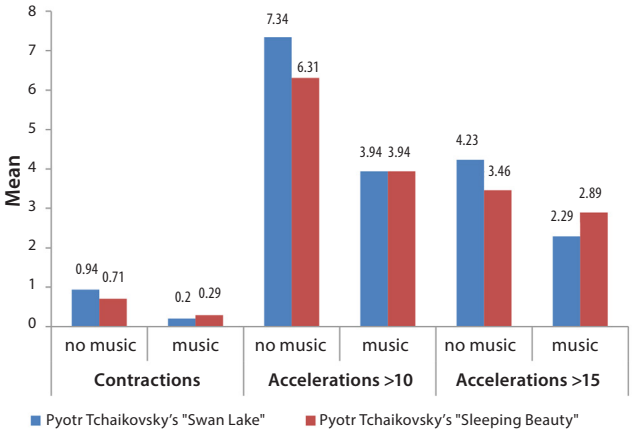

Fig. 3. Comparison of contractions, accelerations >10 and accelerations >15 under stimulation of Pyotr Tchaikovsky's "Swan Lake" and "Sleeping Beauty"

the musical session and the BPM following the music therapy session. In the case of the study by Poręba et al., listening to music also had no influence on the baseline cardiac activity of the fetus.[25] Stemming from this situation, the received result is a beneficial and welcome phenomenon. Of key importance is the fact that the fetal cardiac activity parameters remain within the norms of 110–160 beats per min.[31] Al-Qahtani studied whether pre-natal exposure to music and to a human voice changes the fetus's behavior. It was found that the behavior of the fetus changed, indeed: fetal heart rate was observed to increase in response to music and to a human voice.[32] Similar observations were discovered by other researchers during ultrasound examination. Stimulation of the fetus with familiar music, frequently listened to by the mother, or with the voice of the father, caused an increase in the heart rate, opening of the eyes, bodily movements, and turning of the head and the entire body toward the source of the acoustic stimulus.[33]

In other studies – as in ours – classical music caused a lower heart rate in prematurely born infants. In a study by Loewy et al., a decrease in heart rate and breath rate was observed while listening to a lullaby and to rhythmic music. Rhythmic music also contributed to effective suction and better sleep in infants.[18,34]

In the current study, a difference was observed between the number of uterine contractions in cardiotocographic recording without the use of music and the number of uterine contractions after listening to compositions by Pyotr Tchaikovsky. The number of uterine contractions decreased significantly under the influence of "Swan Lake" and non-significantly after "Sleeping Beauty." In studies by Poręba et al., an increase in the number of uterine contractions was observed in pregnant women. The discrepancy between the results by Poręba et al. and our results may stem from the selection of classical music as well as from the difference in the length of pregnancy.[25] In Poręba's study, all women were in full-term pregnancy, and predictory contractions may have occurred.[25] Meanwhile, in our study, not all women were in full-term pregnancy (35th week of pregnancy on average), so a lack of contractions in their case was welcome. In proprietary studies, decreasing the number of uterine contractions under the impact of music is important and it can be used in the prevention of premature delivery, when an intensified uterine tension and contractions occur, causing a shortening and dilating of the cervix uteri. In contemporary perinatology, preventing premature deliveries is crucial. Pregnant women at risk of premature delivery suffer anxiety about the premature birth of their infants, which may further aggravate fear and lead to uterine contraction, and in effect, to preterm delivery. Therefore, relaxation with music is of key importance. In such a case, it may be argued that classical music, as used in this study, may serve as an additional therapeutic support in preventing premature deliveries, since a decrease in the number of uterine contractions was observed. In obstetric wards, it is often observed that women passively listen to and watch stressful television broadcasts. In such circumstances, therapy with classical music may be indicated as a method of supporting treatment.

In studies by Poręba et al., musical sounds played to pregnant women significantly increased the number of accelerations of the heart of the fetus, in comparison to NST without music. The accelerations increased on average from 12 to 17.[25] In proprietary studies, 2 types of accelerations were analyzed: >10 BPM and >15 BPM for a duration of 15 s. In every observation, the number of accelerations was decreased. According to the criteria of biophysical variable point allocation for NST, in a 30-min recording, 2 or more accelerations of fetal heartbeats – by at least 15 BPM – should appear, lasting at least 15 s, associated with fetal movements.[31] A decrease in the number of accelerations is not a good indicator of a fetus's well-being. The number of accelerations of >10 BPM lasting 15 s in cardiotocographic recording performed without the use of music was significantly higher in comparison to the values recorded during cardiotocographic examination with the music of Pyotr Tchaikovsky. Only during the music therapy with "Sleeping Beauty" no significant difference was observed in cardiotocographic recording in the number of accelerations of >15 BPM, lasting 15 s. However, the number of accelerations did not change to an extent which could endanger the health of the examined fetuses. The cause for the decreased number of accelerations might be the type of music played (lullaby), with fetuses becoming pacified during the music therapy session and falling asleep. According to the Recommendations of the Polish Gynecological Society, a lack of accelerations in cardiotocographic recording may indicate a period of fetal sleep or it may pose an alarming risk of in-utero hypoxia.[31] An increase in the number of accelerations was noted by Annunziata et al., when they analyzed fetal parameters following VAS.[30] In another study, listening to music during NST showed a positive influence on maternal and fetal parameters: researchers observed an increase in the number of accelerations.[29]

In this study, the number of higher variability episodes was also analyzed. The analysis reveals that all parameters significantly differ from the results achieved through cardiotocographic examination while listening to Pyotr Tchaikovsky's compositions. Their number decreased, but not to an extent which could endanger the health of the fetuses. Using Tchaikovsky's music therapy in instances of tachycardia caused by the mother's anxiety can be appropriate and may result in beneficial effects.

In our study, the analysis also included short-term variability, the parameters of which are useful in identifying fetal hypoxia and the metabolic acidosis associated with it. An STV of less than 3 ms indicates a high risk of acidosis occurrence and/or in-utero fetal death, and it is the basis for quick decisions.[35,36] In the presented research material, short-term variability values increased following each musical track, but they did not undergo statistically significant changes. This serves as proof of the beneficial effect of the selected music. The above-mentioned parameters were not included in the study by Poręba et al., so they cannot be compared.[25] In another study, STVs increased following VAS in high-risk pregnancies and they were significantly associated with the well-being of the fetus. However, in low-risk pregnancies, following VAS the STV parameters did not undergo any improvement.[30]

In conclusion, the primary aim of this study was to evaluate the impact of classical music on fetuses in the womb. In spite of many publications dealing with music therapy in medicine, the number of papers on music therapy in obstetrics and perinatology is insufficient.[25,29,31,37] In our study assessing the cardiotocographic recordings of a fetal heart in the 3rd trimester of pregnancy while listening to Pyotr Tchaikovsky's "Swan Lake" and "Sleeping Beauty", a beneficial impact of music on fetal parameters was found. Music therapy, as a therapeutic method which is inexpensive and soothing, should be used more frequently in obstetrics wards, indicated by pathological pregnancies, isolation from the natural environment, and distress resulting from diagnostics and from being in an unfamiliar environment.

Conclusions

Music therapy is an effective method and it can serve as an alternative in medicine. In this study, it was revealed that music therapy may reduce the tension of the uterine muscle and intensify fetal movements. Therefore, this study serves as initial proof of the effectiveness of listening to classical music as a method of preventing premature delivery, as indicated by the decreased number of uterine contractions and fetal stimulation in cases of non-reactive NST.

References

1. Ullal-Gupta S, Vanden Bosch der Nederlanden Ch, Tichko P, Lahav A, Hannon EE. Linking prenatal experience to the emerging musical mind. *Front Syst Neurosci.* 2013;7:48. doi: 10.3389/fnsys.2013.00048
2. Hepper PG, Scott D, Shahidullah S. Newborn and fetal response to maternal voice. *J Reprod Infant Psychol.* 1993;11(3):147–153.
3. Trappe HJ. Role of music in intensive care medicine. *Int J Crit Illn Inj Sci.* 2012;2(1):27–31.
4. Altenmüller E, Schüermann K, Lim VK, Parlitz D. Hits to the left, flops to the right: Different emotions during listening to music are reflected in cortical lateralisation patterns. *Neuropsychologia.* 2002;40:2242–2256.
5. Bernardi L, Porta C, Sleight P. Cardiovascular, cerebrovascular, and respiratory changes induced by different types of music in musicians and non-musicians: The importance of silence. *Heart.* 2006;92:445–452.
6. Trappe HJ. Music and health – what kind of music is helpful for whom? What music is not? [in German]. *Dtsch Med WSchr.* 2009;134:2601–2606.
7. Doheny L, Hurwitz S, Insoft R, Ringer S, Lahav A. Exposure to biological maternal sounds improves cardiorespiratory regulation in extremely preterm infants. *J Matern Fetal Neonatal Med.* 2012;25(9):1591–1594.
8. Doheny L, Morey JA, Ringer SA, Lahav A. Reduced frequency of apnea and bradycardia episodes caused by exposure to biological maternal sounds. *Pediatr Int.* 2012;54(2):1–3.
9. Lai HL, Chen CJ, Peng TC, et al. Randomized controlled trial of music during kangaroo care on maternal state anxiety and preterm infants' responses. *Int J Nurs Stud.* 2006;43(2):139–146.
10. Ludington-Hoe SM, Lewis T, Morgan K, Cong X, Anderson L, Reese S. Breast and infant temperatures with twins during shared kangaroo care. *J Obstet Gynecol Neonatal Nurs.* 2006;35(2):223–231.

11. Charpak N, Ruiz J, Zupan J, et al. Kangaroo mother care: 25 years after. *Acta Paediatr.* 2005;94:514–522.
12. Standley JM, Moore RS. Therapeutic effects of music and mother's voice on premature infants. *Pediatr Nurs*. 1995;21(6):509–512.
13. Zimmerman E, Keunen K, Norton M, Lahav A. Weight gain velocity in very low-birth-weight infants: Effects of exposure to biological maternal sounds. *Am J Perinatol*. 2013;30(10):863–870. doi: 10.1055/s-0033–1333669
14. Krueger C, Parker L, Chiu SH, Theriague D. Maternal voice and short-term outcomes in preterm infants. *Dev Psychobiol.* 2010;52(2):205–212. doi: 10.1002/dev.20426
15. Cevasco AM. The effects of mothers' singing on full-term and preterm infants and maternal emotional responses. *J Music Ther*. 2008;45:273–306.
16. Arnon S, Shapsa A, Forman L, et al. Live music is beneficial to preterm infants in the neonatal intensive care unit environment. *Birth.* 2006;33(2):131–136.
17. Keith DR, Russell K, Weaver BS. The effects of music listening on inconso-lable crying in premature infants. *J Music Ther.* 2009;46(3):191–203.
18. Loewy J, Stewart K, Dassler A, Telsey A, Homel P. The effects of music therapy on vital signs, feeding, and sleep in premature infants. *Pediatrics*. 2013;131:902–918.
19. Rowlands I, Redshaw M. Mode of birth and women's psychological and physical wellbeing in the postnatal period. *BMC Pregnancy Childbirth*. 2012;12:138–156.
20. Yang M, Li L, Zhu H, et al. Music therapy to relieve anxiety in pregnant women on bedrest: A randomized, controlled trial. *MCN Am J Matern Child Nurs*. 2009;34(5):316–323.
21. Sidorenko VN. Clinical application of medical resonance therapy music in high-risk pregnancies. *Integr Physiol Behav Sci.* 2000;35(3):199–207.
22. Shin HS, Kim FH. Music therapy on anxiety, stress and maternal-fetal attachment in pregnant women during transvaginal ultrasound. *Asian Nurs Reaserch.* 2011;5(1):19–27.
23. Lee SM. The effects of music therapy on postpartum blues and maternal attachment of puerperal women. *J Korean Acad Nurs.* 2010;40:60–68.
24. Vianna MN, Barbosa AP, Carvalhaes AS, Cunha AJ. Music therapy may increase breastfeeding rates among mothers of premature newborns: A randomized controlled trial. *J Pediatr (Rio J).* 2011;87(3):206–212.
25. Poręba A, Dutkiewicz D, Drygalski M. Wpływ dźwięków muzycznych na zachowanie się wybranych parametrów kardiotokograficznych u kobiet w ciąży donoszonej. *Ginekol Pol.* 2000;71(8):915–920.
26. Romero R, Mazor M, Hobbins HJ. A critical appraisal of fetal acoustic stimulations as an antenatal test for fetal well-being. *Obstet Gynecol.* 1988;71:781–786.
27. Arabin B, Becker R, Mohnhaupt A, Entezami M, Weitzel HK. Prediction of fetal distress and poor outcome in intrauterine growth retardation – a comparison of FHR-monitoring combined with stress tests and Doppler ultrasound. *Fetal Diagn Ther.* 1993;8:234–240.
28. Arabin B. Music during pregnancy. *Ultrasound Obstet Gynecol.* 2002;20:435–430.
29. Simavli S, Gumus I, Kaygusuz I, Yildirim M, Usluogullarii B, Kafali H. Effect of music on labor pain relief, anxiety level and postpartum analgesic requirement: A randomized controlled clinical trial. *Gynecol Obstet Invest.* 2014;78(4):244–250. doi: 10.1159/000365085
30. Annunziata ML, Scala M, Giuliano N, et al. Fetal vibroacoustic stimulation in computerized cardiotocographic analysis: The role of short-term variability and approximate entropy. *J Pregnancy* 2012. http://dx.doi.org/10.1155/2012/814987
31. Polish Gynecological Society. Recommendations of the Polish Gynecological Society concerning application of cardiotocography in obstetrics [in Polish]. *Ginekol Pol.* 2014;85:713–716.
32. Al-Qahtani NH. Fetal response to music and voice. *Aust NZJ Obstet Gynaecol.* 2005;45(5):414–417.
33. Federico G. Fetal responses to a musical stimulation. Music therapy and pregnancy. X World Congress of Music Therapy, Oxford, England; 2002. http://www.gabrielfederico.com/articles/oxford2002.pdf. Accessed May 31, 2016.
34. Amini E, Rafiei P, Zarei K, Gohari M, Hamidi M. Effect of lullaby and classical music on physiologic stability of hospitalized preterm infants: A randomized trial. *J Neonatal Perinatal Med.* 2013;6(4):295–301.
35. Słomko Z, Malewski. Mianownictwo kardiotokograficzne. In: Słomko Z, Drews K, Malewski Z, eds. *Kardiotokografia kliniczna*. Warszawa: Wydawnictwo Lekarskie PZWL; 2010;109–110.
36. Gonçalves H, Costa A, Ayres-de-Campos D, Costa-Santos C, Rocha AP, Bernardes J. Comparison of real beat-to-beat signals with commercially available 4 Hz sampling on the evaluation of fetal heart rate variability. *Med Biol Eng Comput.* 2013;51:665–676.
37. Wakim JH, Smith S, Guinn C. The efficacy of music therapy. *J Perianesth Nurs*. 2010;25(4):226–232.

The structure of the vascular system of the septomarginal trabecula in the heart of an adult

Miłosz Zajączkowski[1,A–F], Adam Kosiński[1,A–F], Marek Grzybiak[1,A,E,F], Rafał Kamiński[1,B,C], Agata Kaczyńska[1,B,C,E], Stanisław Zajączkowski[2,C,D,E], Ewa Nowicka[1,B,C]

[1] Department of Clinical Anatomy, Medical University of Gdansk, Poland
[2] Department of Physiology, Medical University of Gdansk, Poland

A – research concept and design; B – collection and/or assembly of data; C – data analysis and interpretation; D – writing the article; E – critical revision of the article; F – final approval of the article

Advances in Clinical and Experimental Medicine, ISSN 1899-5276 (print), ISSN 2451-2680 (online) *Adv Clin Exp Med*. 2018;27(5):623–631

Address for correspondence
Miłosz Zajączkowski
E-mail: milosz@gumed.edu.pl

Funding sources
None declared

Conflict of interest
None declared

Received on January 15, 2016
Reviewed on November 14, 2016
Accepted on January 27, 2017

Abstract

Background. In cardiology, the paths of the arteries penetrating the septomarginal trabecula (SMT) are especially important. They provide blood supply to the apparatus of the right atrioventricular orifice and often form anastomoses with the system of the right coronary artery. Despite this, only a few publications discuss the morphological aspect of the septomarginal trabecula, and available histological analyses seldom deal with its blood supply.

Objectives. The aim of this study was to analyze the vessel structure of the septomarginal trabecula in terms of the variability of the area of the cross-section of the lumen and the muscular layer of the artery.

Material and methods. The study was carried out on the material of 50 human hearts from adults of both sexes. The material was divided into 4 morphological types. Histological examinations were conducted by means of classic staining methods.

Results. At the initial cross-section of the septomarginal trabecula, the area of the cross-section increased to half of the length of the trabecula, and then it started to decrease. This is connected with the thickening of the inner muscular layer of the artery, which proportionally takes up more area of the cross-section of the whole artery of the SMT. The total area of the cross-section of all vessels in both types examined was also the largest in the middle part of the SMT. Furthermore, the results of this study confirm the presence of a connection between both systems of coronary arteries.

Conclusions. As the septomarginal trabecula passes through the lumen of the right ventricle, its arteries become exposed to the influence of the factors which may evoke a biological response from the walls of this vessel, causing the thickening of the muscular layer and, as a result, of the section of the whole artery, in particular its middle part.

Key words: morphology, human heart, coronary arteries, heart ventricle, septomarginal trabecula

DOI
10.17219/acem/68692

Copyright
© 2018 by Wroclaw Medical University
This is an article distributed under the terms of the Creative Commons Attribution Non-Commercial License (http://creativecommons.org/licenses/by-nc-nd/4.0/)

Introduction

Among the wide network of the trabeculae of the right ventricle of the human heart, the septomarginal trabecula (SMT) plays a particularly important role. Its structure contains vessels supplying the valve apparatus of the right ventricle, which often form anastomoses with the right coronary artery. Moreover, within the trabecula there are often branches of the right offshoot of the bundle of His.

Despite this, only a few publications present the morphological aspect of the SMT. Available histological analyses are devoted to the issues of the ratio of muscle tissue to connective tissue, as well as the presence of fibers of the conduction system, so they seldom discuss its blood supply. Therefore, a detailed analysis of the arterial blood supply of this structure seems to have a clinical significance. The dynamic development of cardiac surgery and invasive diagnostic and treatment methods reveal the need for more detailed knowledge of the positions of vessels in various structures inside the heart cavities. Such knowledge may lead to procedures with optimal saving of the heart structures and to the prevention of potential complications.

The aim of this study was to analyze the vessel structure of the septomarginal trabecula in terms of the variability of the area of the cross-section of the lumen and the muscular layer.

Material and methods

The study was carried out on the material of 50 human hearts fixed in a solution of formalin and ethanol. The hearts, in which no lesions or developmental defects were found macroscopically during the section, came from adults (18–76 years old) of both sexes. The material was divided into 4 morphological types according to the classification suggested by Kosiński et al.[1] The analysis was performed on the basis of the observation of the cross-sections of the SMT divided into 10 equal sections (levels) (Fig. 1). The histological examination was conducted by means of classic staining methods (hematoxylin eosin, van Gieson's stain with Goldner's modification) under a stereo-microscope (MN 800 Series; Opta-Tech, Warszawa, Poland) with Moticam 2000 2.0M camera (Motic Incorporation Ltd., Hong Kong) and the use of the Motic Images Plus v. 2.0 2006 (Motic China Group Co., Ltd., Xiamen, China) computer program.

The majority of variables did not have a normal distribution and were analyzed by means of non-parametric tests. The 1st tested hypothesis which stated that the probability distributions were the same in all examined groups was rejected (the Friedman test; $p < 0.001$). Taking the natural structure of the examined material into consideration, the results of this test were not included in the paper, and post hoc procedures were performed. When performing these procedures, the Mann–Whitney test for paired samples was used (which is, of course, equivalent to the Wilcoxon test for paired samples in this case). A p-value <0.05 was considered to be statistically significant. The statistical analyses were performed using R v. 2.15.1.[2]

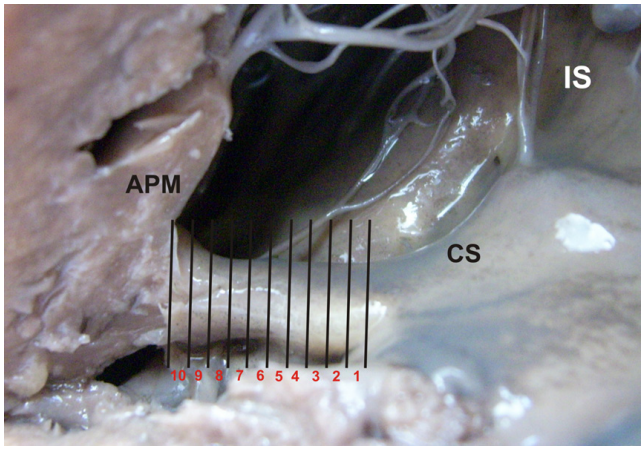

Fig. 1. The division of the SMT into 10 levels. The view of the right ventricle

AMP – anterior papillary muscle; CS – supraventricular crest; IS – intraventricular septum.

Results

During the study, 4 morphological types of the SMT were confirmed. The division into these types regards the paths of the SMT penetrating through the lumen of the right ventricle and the relation of SMT to the anterior papillary muscle. In type I, the SMT, which varied with respect to thickness, constituted a homogenous structure not directly connected with the anterior papillary muscle. In types II and III, the SMT constituted a homogenous structure undivided by the anterior papillary muscle. The difference from type I lies in a close connection of the base of the anterior papillary muscle with the anterior wall of the ventricle, as well as its direct connection with the trabecula. Type II is a tangent connection of the trabecula and the anterior papillary muscle or their permanent integration to some degree. However, in type III, the base of the muscle attached to the anterior wall was closely connected with the peripheral end of the SMT. Type IV included cases in which 2 parts of the SMT could be distinguished. The first is septal-papillary part that connects the intraventricular septum and the anterior papillary muscle. The second one is the papillary-marginal part located between the anterior papillary muscle and the anterior wall of the right ventricle.

The frequency of the occurrence of particular types of SMT is presented in Table 1.

The results presented in this study include the 2 most numerous morphological types: type III and IV.

The main vascularization of the SMT is formed by its main artery, which offshoots from one of the septal

Table 1. Frequency of occurrence of particular types of SMT

Type	Number	%
I	3	6
II	6	12
III	24	48
IV	17	34
Total	50	100

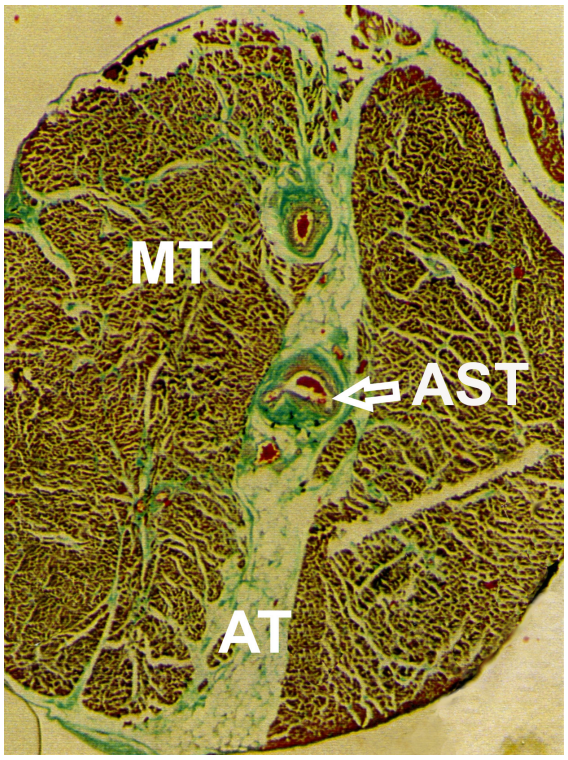

Fig. 2. The cross-section of the SMT

Masson–Goldner staining; magnification ×2; AST – the artery of the SMT; AT – adipose tissue; MT – muscle tissue.

arteries. On the cross-section of the trabecula, its main artery is most often found in a central location (Fig. 2).

The artery takes the peripheral position when it approaches the anterior papillary muscle (Fig. 3).

The main artery of the SMT is always significantly larger than other SMT arteries (Fig. 4).

In some cases, the artery may comprise a substantial part of the whole cross-section of the SMT (Fig. 5).

The area of the cross-section of the artery of the septomarginal trabecula

Our results indicate that in type III, the area of the cross-section of the artery of the SMT increases only on 4 levels. On the next levels, it slightly decreases or remains at the same value. On the 4th level, the examined artery assumes the highest median and max values. The artery of the SMT is found to first widen successively until it reaches its peak value at level 4, and then its area is getting smaller (Table 2).

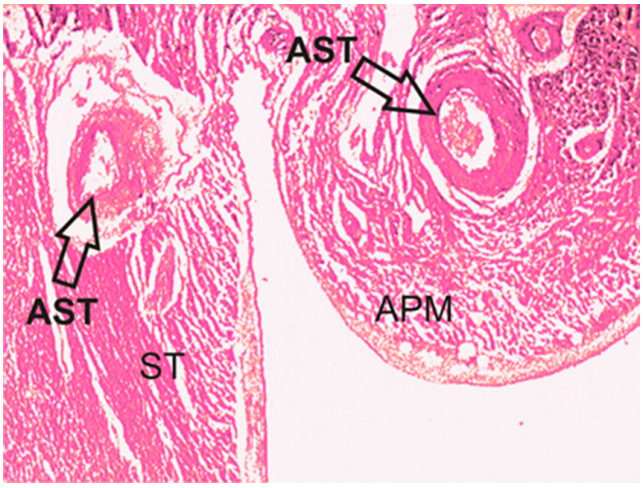

Fig. 3. The cross-section of the SMT and the anterior papillary muscle

Hematoxylin and eosin stain; magnification ×4; APM – anterior papillary muscle; AST – the artery of the SMT.

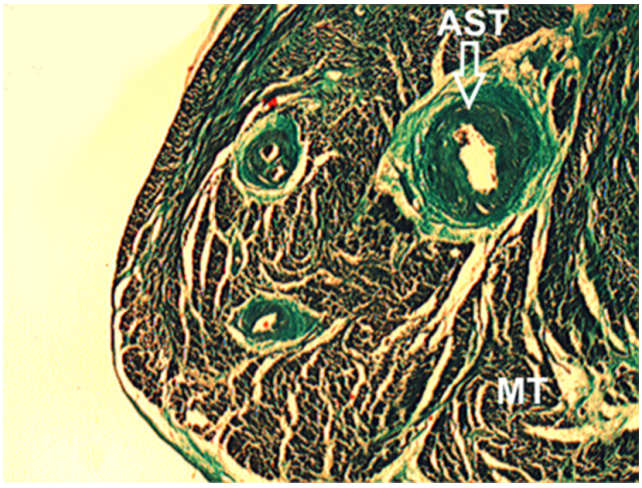

Fig. 4. The cross-section of the SMT

Masson-Goldner staining; magnification ×4; MT – muscle tissue; AST – the artery of the SMT.

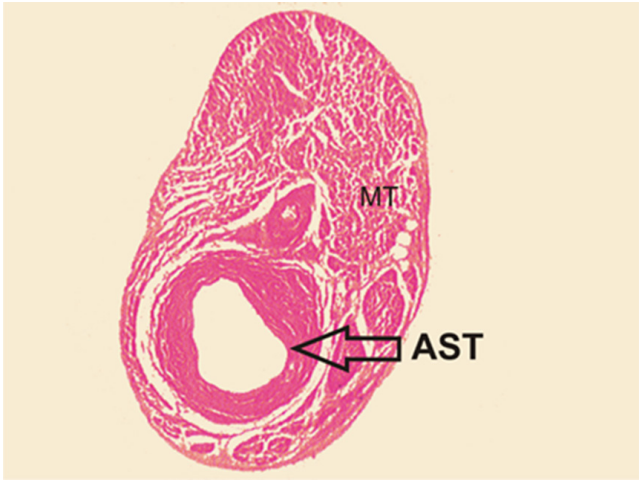

Fig. 5. The cross-section of the SMT

Hematoxylin and eosin stain; magnification ×4; AST – the artery of the SMT; MT – muscle tissue.

Table 2. Type III: The values of statistical characteristics of the area of the cross-section of the artery of the SMT on 10 levels of the trabecula

Level	Median [mm²]	Min [mm²]	Max [mm²]
1	0.241[a]	0.04	0.57
2	0.238[b,c]	0.047	0.584
3	0.272[d]	0.057	0.667
4	0.278[e,f]	0.045	0.732
5	0.25	0.044	0.594
6	0.27	0.056	0.536
7	0.252	0.066	0.555
8	0.263	0.047	0.591
9	0.249	0.052	0.587
10	0.255	0.062	0.637

[a] 1 vs 4, p = 0.03; [b] 2 vs 3, p = 0.04; [c] 2 vs 4, p = 0.01; [d] 3 vs 4, p = 0.04; [e] 4 vs 7, p = 0.04; [f] 4 vs 9, p = 0.04.

Table 3. Type IV: The values of statistical characteristics of the area of the cross-section of the artery of the SMT on 10 levels of the trabecula

Level	Median [mm²]	Min [mm²]	Max [mm²]
1	0.204	0.045	0.732
2	0.21[a,b,c]	0.043	0.502
3	0.206	0.047	0.5
4	0.19	0.049	0.63
5	0.216	0.047	0.62
6	0.218[d]	0.043	0.772
7	0.215[e]	0.051	0.653
8	0.227	0.068	0.592
9	0.216	0.065	0.608
10	0.214	0.059	0.474

[a] 2 vs 3, p = 0.04; [b] 2 vs 5, p = 0.04; [c] 2 vs 6, p = 0.04; [d] 6 vs 9, p = 0.04; [e] 7 vs 9, p = 0.04.

The results indicate that the area of the cross-section of the artery of the SMT in type IV is subject to fluctuations over the whole length, with a distinct gradual decrease in the area from level 6 to level 9. The median value of the area of the artery of the trabecula increases statistically significantly between level 2 and levels 3, 5 and 6 (Table 3).

Total area of the cross-section of all arteries of the septomarginal trabecula

The results indicate that in type III, the total area of the cross-section of all arteries of the trabecula increases statistically significantly on the first 5 levels. From that point, certain fluctuations occur: the area slightly decreases or slightly increases. Statistical analyses have also revealed a significant decrease of the studied value from level 4 to level 9 (Table 4).

Table 4. Type III: The values of statistical characteristics of the total area of the cross-section of all arteries of the SMT on 10 levels of the trabecula

Level	Median [mm²]	Min [mm²]	Max [mm²]
1	0.259[a,b,c,d,]	0.066	1.085
2	0.293[e]	0.071	1.052
3	0.318	0.082	1.034
4	0.33[f]	0.067	1.031
5	0.339	0.068	1.022
6	0.343	0.081	1.035
7	0.29	0.092	1.088
8	0.3	0.062	1.13
9	0.284	0.058	1.139
10	0.289	0.077	1.095

[a] 1 vs 2, p = 0.05; [b] 1 vs 3, p = 0.05; [c] 1 vs 4, p = 0.04; [d] 1 vs 5, p = 0.03; [e] 2 vs 4, p = 0.04; [f] 4 vs 9, p = 0.03.

Table 5. Type IV: The values of statistical characteristics of the total area of the cross-section of all arteries of the SMT on 10 levels of the trabecula

Level	Median [mm²]	Min [mm²]	Max [mm²]
1	0.246[a]	0.045	0.748
2	0.239[b,c,d,e,f,g]	0.043	0.678
3	0.229[h]	0.05	0.66
4	0.231[i]	0.053	0.82
5	0.225	0.048	0.804
6	0.232	0.043	0.839
7	0.241[j]	0.053	0.699
8	0.249	0.07	0.616
9	0.233	0.075	0.668
10	0.248	0.073	0.601

[a] 1 vs 5, p = 0.04; [b] 2 vs 3, p = 0.03; [c] 2 vs 4, p = 0.02; [d] 2 vs 5, p = 0.03; [e] 2 vs 6, p = 0.03; [f] 2 vs 7, p = 0.02; [g] 2 vs 8, p = 0.04; [h] 3 vs 7, p = 0.03; [i] 4 vs 7, p = 0.03; [j] 7 vs 9, p = 0.02.

Our results indicate that in type IV, the total area of the cross-section of all arteries of the trabecula increases statistically significantly between level 2 and level 8. A gradual increase in the median value of this area from level 5 to level 8 of the trabecula may be observed (Table 5).

The number of arteries on the cross-section of the septomarginal trabecula

When particular levels are grouped into sections corresponding to the beginning, middle and end of the trabecula, statistical differences among all groups can be seen in type III. The number of arteries increases successively from the beginning to the end of the trabecula (Fig. 6 A). However, in type IV, statistically significant differences occurred between group 1 and groups 2 and 3. The number

of arteries increases from the beginning to the end of the trabecula (Fig. 6 B).

Type III – statistically significant differences, on the level of $p < 0.05$ (the Wilcoxon test), between levels 1–3 and 4–7; 4–7 and 8–10; 1–3 and 8–10.

Type IV – statistically significant differences, on the level of $p < 0.05$ (the Wilcoxon test), between levels 1–3 and 4–7; 1–3 and 8–10.

The ratio of the area of the cross-section of all the arteries of the septomarginal trabecula to their number

When particular levels are grouped into sections corresponding to the beginning, middle and end of the trabecula, then statistical differences among all 3 groups can be noticed in type III (F ig. 7 A). However, in type IV, statistically significant differences occurred between the end and the beginning, and the middle parts of the trabecula (Fig. 7 B).

Type III – statistically significant differences, on the level of $p < 0.05$ (the Wilcoxon test), between levels 1–3 and 4–7; 1–3 and 8–10; 4–7 and 8–10.

Type IV – statistically significant differences, on the level of $p < 0.05$ (the Wilcoxon test), between levels 1–3 and 8–10; 4–7 and 8–10.

The area of the cross-section of the muscular layer of the septomarginal trabecula

The results indicate that in type III, the area of the cross-section of the muscular layer of the SMT shows certain dynamics of behavior. Although it is not statistically significant, the median value increases up to the middle of the trabecula (Table 6).

The results of this study show the following tendency: in type IV, the median value of the area of the cross-section of the muscular layer gradually increases up to level 7, and then decreases up to the end of the trabecula (Table 7).

The ratio of the area of the cross-section of the muscular layer of the SMT to the area of the cross-section of the artery of the SMT

Our results revealed an increase in the median value of the ratio of the area of the cross-section of the muscular layer to the area of the cross-section of the artery in type III from level 2 to level 6. The median is smaller at the beginning than at the end of the trabecula (Table 8).

The results indicate that in type IV, the median value of the ratio of the area of the cross-section of the muscular layer to the area of the cross-section of the artery increases from level 3 to level 6 of the trabecula. The median is smaller at the beginning than at the end of the trabecula (Table 9).

When particular levels are grouped into sections corresponding to the beginning, middle and end of the trabecula, in type III, statistically significant differences can be found between the end and the beginning, and the middle of the trabecula (Fig. 8 A). However, in type IV there is a statistically significant difference between the end and the beginning of the trabecula (Fig. 8 B).

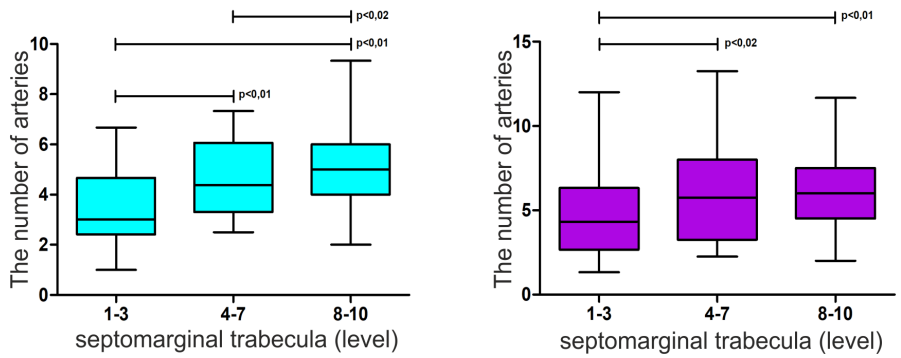

Fig. 6. The number of arteries on the cross-section of the SMT in 3 groups of different distance from the trabecula (the results are presented as a median and an interquartile range)

A – type III; B – type IV.

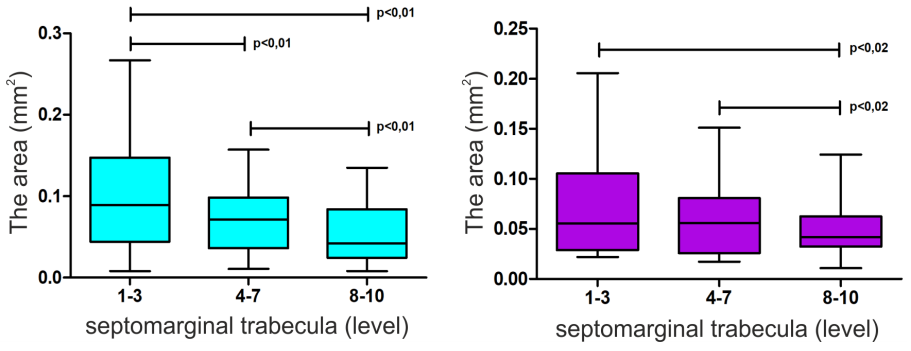

Fig. 7. The ratio of the area of the cross-section of all arteries of the SMT to their number in 3 groups of different distance from the trabecula (the results are presented as a median and an interquartile range)

A – type III; B – type IV.

Table 6. Type III: The values of statistical characteristics of the area of the cross-section of the muscular layer of the artery of the SMT on 10 levels of the trabecula

Level	Median [mm²]	Min [mm²]	Max [mm²]
1	0.127	0.028	0.374
2	0.146	0.035	0.362
3	0.152	0.044	0.409
4	0.16	0.035	0.413
5	0.159	0.03	0.403
6	0.14	0.039	0.366
7	0.138	0.04	0.419
8	0.167	0.03	0.418
9	0.14	0.04	0.432
10	0.172	0.037	0.499

Table 7. Type IV: The values of statistical characteristics of the area of the cross-section of the muscular layer of the artery of the SMT on 10 levels of the trabecula

Level	Median [mm²]	Min [mm²]	Max [mm²]
1	0.103	0.025	0.411
2	0.113	0.024	0.37
3	0.119	0.024	0.379
4	0.113	0.024	0.452
5	0.121	0.022	0.463
6	0.136	0.022	0.612
7	0.152	0.023	0.519
8	0.148	0.031	0.467
9	0.125	0.032	0.464
10	0.15	0.028	0.392

Table 8. Type III: The statistical values of the ratio of the area of the cross-section of the muscular layer of the artery of the SMT to the area of the cross-section of its artery

Level	Median [mm²]	Min [mm²]	Max [mm²]
1	0.637	0.322	0.929
2	0.608[a]	0.333	0.918
3	0.623[b,c,d]	0.388	0.915
4	0.626[e,f,g]	0.346	0.93
5	0.641[h]	0.351	0.924
6	0.646	0.417	0.927
7	0.635	0.363	0.935
8	0.662	0.406	0.929
9	0.643	0.44	0.926
10	0.652	0.359	0.934

[a] 2 vs 8, p = 0.04; [b] 3 vs 8, p = 0.02; [c] 3 vs 9, p = 0.05; [d] 3 vs 10, p = 0.05; [e] 4 vs 8, p < 0.01; [f] 4 vs 9, p = 0.01; [g] 4 vs 10, p = 0.03; [h] 5 vs 8, p = 0.04.

Table 9. Type IV: The statistical values of the ratio of the area of the cross-section of the muscular layer of the artery of the SMT to the area of the cross-section of its artery

Level	Median [mm²]	Min [mm²]	Max [mm²]
1	0.621	0.407	0.894
2	0.614	0.391	0.88
3	0.594	0.306	0.871
4	0.621[a]	0.322	0.84
5	0.644[b]	0.348	0.855
6	0.651	0.47	0.89
7	0.65	0.44	0.888
8	0.635	0.409	0.882
9	0.675	0.481	0.904
10	0.633	0.478	0.895

[a] 4 vs 10, p = 0.04; [b] 5 vs 10, p = 0.05.

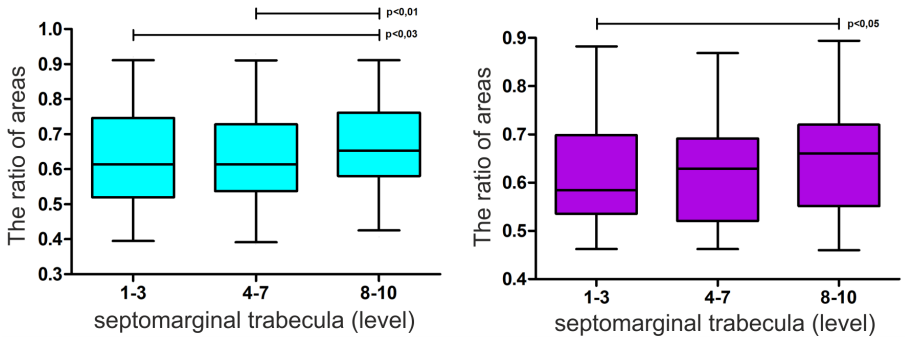

Fig. 8. The ratio of the area of the cross-section of the muscular layer of the SMT to the area of the cross-section of the artery of the SMT in 3 groups of different distance from the trabecula (the results are presented as a median and an interquartile range)

A – type III; B – type IV.

Type III – statistically significant differences, on the level of p < 0.05 (the Wilcoxon test), between levels 1–3 and 8–10; 4–7 and 8–10.

Type IV – statistically significant differences, on the level of p < 0.05 (the Wilcoxon test), between levels 1–3 and 8–10.

Discussion

There is hardly a substantial body of knowledge on the blood supply of the septomarginal trabecula. Gross was the first researcher to observe the constant occurrence of the artery of the SMT (ramus limbi dextri) in 1921, and other

researchers have confirmed its presence.[3–12] It is often described as a branch of one of the septal arteries, which branches off from the anterior descending artery. While studying the position of the artery of the trabecula, Reig et al. noticed that in 20 cases (71%) this artery originated in the 2nd anterior septal artery, in 5 cases (18%) in the 1st anterior septal artery, and in 2 cases (7%) in the 3rd one.[6] However, in 1 case (4%) they confirmed the presence of 2 arteries in the trabecula and both of them originated in the 2nd and 3rd anterior septal artery. They described 2 possible paths of the arteries which mark the beginning of the artery of the SMT (in relation to a short heart axis). In 19 out of 28 examined cases, there was a horizontal path. This type included arteries that originated from the 1st anterior septal artery and the majority of vessels originating from the 2nd anterior septal artery.

They proceeded through the site of the septal papillary muscle in a subendocardial position and branched off to it, as well as toward the apex of the heart. Then, they passed through the muscle accompanying and providing blood supply to the right branch of the bundle of His. Both of these structures followed the paths through the whole length of the SMT, and the SMT artery was positioned deeper until it reached the base of the anterior papillary muscle.[6] The same location of the artery of the SMT was observed in our study; it ran mainly in the central part of the cross-section of the trabecula (Fig. 2). Nevertheless, it took a peripheral position when it approached the anterior papillary muscle (Fig. 3). However, according to Melo et al., this artery is located in the lower part.[4]

Reig et al. state that the 2nd path which arteries may follow to the SMT is an oblique path. It extends from the right side of the SMT toward the apex of the heart until it reaches the place where the SMT separates from the septum. From that point on, it displays the same topography and relations as in the case of the horizontal path. The arteries following this path may also branch off to the septal papillary muscle and the initial part of the right branch of the bundle of His. This type of path was found in the arteries of the SMT originating mainly from the 3rd and sometimes from the the 2nd septal artery.[6]

Melo et al., after examining 30 human hearts, characterized the number and trajectory of the major septal arteries which serve as the origin of the SMT artery. They confirmed the presence of 210 septal arteries, which means on average 7 arteries per heart. One major septal artery was found in 90% (27) of hearts, 2 were found in 7% (2) of hearts and 3% (1) of the hearts had 3 arteries, from which 1 would always enter the SMT in its lower part.[4]

The knowledge of the topography of the arteries of the SMT, as well as of the paths of the vessels leading to it, is very important for every cardiac surgeon. Procedures can be carried out with a maximum saving rate of the structures of the right ventricle and with the prevention of possible complications (e.g., during the application of a surgical method requiring incisions in the area of the septum, such as the correction of the Tetralogy of Fallot – TOF). The topography of the abovementioned arteries may also be assessed with the use of angiographic techniques. Therefore, in vivo diagnostics deserves special attention.[11,13,14]

In angiographical analyses, Bowles and Daves noticed that the minor artery branches off directly from the main septal artery. It directs its course through the whole length of the trabecula and the anterior papillary muscle, and is anchored in the anterior leaflet of the tricuspid valve.[11]

While describing the visualization of all arteries with a diameter over 200 μm in coronarography, Pawlak stated that the artery of the SMT was often visible.[14] Bowles and Daves confirmed its presence in 34 out of 36 septomarginal trabeculae in children's hearts and in 26 out of 36 adult hearts.[11]

Our research indicates that the artery of the SMT is the most developed among all the arteries passing through the SMT. At times, there are several major vessels present, but it is always larger than the rest (Fig. 4, 5). However, Kosiński and Grzybiak observed 2 arterioles of different size in 5 out of the 10 examined trabeculae.[15]

In our material, in the most numerously represented morphological types of the SMT, an initial increase in the area of the cross-section of both the artery of the trabecula and all arterial vessels altogether was noticed. In the case of the artery of the trabecula, this parameter increased up to half of the length of the SMT, and then decreased toward its end. In type III, the vessel was characterized on average by the same section as at the beginning of the trabecula; however, it was smaller in type IV at the end of the artery (Tables 2, 3). The total area of the section of all vessels in both types was also larger in the middle part of the trabecula; at the same time, it turned out to be larger at the end rather than at the beginning of the trabecula (Tables 4, 5).

It may be concluded that the reduction of the area of the cross-section of the artery toward the end of the SMT is compensated by an increase in the area of the section of smaller vessels, which one by one branch off from the main trunk as it follows its path through the trabecula. This is proved by a statistically significant increase in the number of the arterial vessels observed in subsequent sections through the trabecula (Fig. 6 A, B), parallel to a reduction of the ratio of the area of the section of all vessels to their number (Fig. 7 A, B).

In conclusion, the artery of the trabecula is reduced in favor of other arteries branching off. In the middle sections, the total area of the sections of the vessels increases, and in the final sections, it is higher than in the initial sections. It may show the role which is performed by the vessels of the trabecula in the blood supply of the anterior papillary muscle. In the discussed morphological types, it is strictly connected with the SMT and the branches of the left coronary artery, which passes through the trabecula and provides the majority of the blood supply for the muscle.

Another subject of the assessment was the thickness of the muscular layer of the SMT. In each of the morphological types of the SMT, there was an initial increase in the thickness of the muscular layer and a gradual decrease toward the end of the trabecula (Tables 6, 7). Statistical analyses confirmed an increase in the thickness of the muscular layer in the middle levels in types III and IV. Moreover, it was noticeable that the thickness of particular layers of the wall of the artery on the section was variable, but it did not affect the dimensions of the lumen of the vessel. This was similarly described by Lorenz, who noticed that the changes in the thickness of the inner and middle layer did not affect the size of the lumen on the section. This variability seems to be one of the mechanisms of adaptation to exposure to deforming forces.[16,17] It must be assumed that the middle part of the SMT is more susceptible to deformation. Both the tensing up of muscle fibers and blood ejection during systole of the right ventricle, as well as the relaxation of its muscles during diastole, along with the influence of blood flow, may be the mechanical factors causing a biological response from the walls of the blood vessels in the trabecula.

The ratio of the area of the cross-section of the muscular layer of the trabecula to the area of the cross-section of the whole SMT artery was similar in all types: it increased on the whole length of the trabecula (Tables 8, 9). Statistical grouping analyses confirm the importance of this tendency (Fig. 8 A, B). Taking into consideration that both the areas of the cross-section of the artery of the trabecula and its muscular layer decrease from the middle levels toward the end of the trabecula, it can be assumed that the muscular layer takes relatively more area of the cross-section of the whole artery toward the anterior papillary muscle. This may be related to the fact that in the area where the trabecula and the anterior papillary muscle are connected with the anterior wall of the right ventricle there are particularly intensive tensions during systole, which determine the thickness of the muscles of the blood vessels.

This study shows that the arteries of the SMT, which are in close connection with the anterior papillary muscle, supply it with blood when they reach it. Furthermore, the structure of the vessels of the trabecula may also form a crucial component of the blood supply of the free part of the anterior-lateral wall of the right ventricle. Similar data can be found in the literature.[3,7,9] According to many authors, properly-shaped vessels of the trabecula may create anastomoses between the system of the left and right coronary artery.

The analyses of Reig-Vilallonga et al. confirmed the presence of anastomoses in 96% of the examined cases, including the anastomoses within the supraventricular crest, where the SMT was created in 76% of the cases. Moreover, they distinguished 4 types.[18] In their previous study, they confirmed the existence of anastomoses in 68.1% of cases.[19] The results of the study we conducted also confirm the presence of such arterial connections – on the anterior wall of the right ventricle and on the base of the anterior papillary muscle.

The authors of numerous works show the protective role of the blood flow to the muscle of the right ventricle through the arteries of the SMT.[3,20–26] The research suggests that myocardial infarction of the right ventricle is caused by the narrowing of the proximal section of the right coronary artery, especially of the abovementioned artery of the trabecula.[22] When the vessel is unobstructed in the anterior-lateral part of the free wall of the right ventricle, ischemic damages occur less frequently.[3,27] Haupt et al. described 19 cases of acute myocardial infarction of the anterior-lateral wall of the right ventricle as a result of the closure of the lumen of the section proximal to the right coronary artery. In 5 patients who had an extensive (>25%) myocardial infarction of the right ventricle, 4 had a significant (>75%) narrowing of the anterior left descending artery (proximal to the beginning of the artery of the SMT), 2 had a closure of the 1st septal branch of this artery, and 1 had coronary thrombosis in the initial part of the right coronary artery. The authors observed a positive correlation between the extension of myocardial infarction of the ventricle and some degree of impairment of a potential collateral flow from the anterior left descending artery to the right coronary artery.[22]

Other researchers have described a clinical situation in which myocardial infarction affected the left ventricle of the heart and until the moment of total closure of the lumen of the left coronary artery, the collateral circulation path was provided by the arteries of the SMT, but in the opposite direction. In the postmortem coronography, they noticed a well-developed artery in the SMT.[5]

In conclusion, the passing of the septomarginal trabecula through the lumen of the right ventricle exposes its arteries to the influence of factors which may evoke a biological response from the walls of this vessel, causing the thickening of the muscular layer and, as a result, of the cross-section of the whole artery, in the middle sections. Moreover, in the final sections of the SMT, the muscular layer of its artery gradually takes up more and more area of the cross-section of the whole vessel.

References

1. Kosiński A, Kozłowski D, Nowiński J, Lewicka E, Dąbrowska-Kugacka A. Morphogenetic aspects of the septomarginal trabecula in the human heart. *Arch Med Sci*. 2010;6:733–743.
2. The R Core Team. *R: A Language and Environment for Statistical Computing*. Vienna: R Foundation for Statistical Computing; 2012.
3. Farrer-Brown G. Vascular pattern of myocardium of right ventricle of human heart. *Br Heart J*. 1968;30:679–686.
4. Melo JQ, Abecassis M, Neves J, et al. Can the location of the large septal artery be predicted? *Eur J Cardio-Thoracic Surg*. 1995;9:628–630.
5. Pyda M, Grajek S. Ramus limbi dextri or 'moderator band' artery. *Kardiol Pol*. 1991;34:26–29.
6. Reig J, Alberti N, Petit M. Arterial vascularization of the human moderator band: An analysis of this structure's role as a collateral. *Clin Anat*. 2000;13:244–250.
7. Dobyns BM. Note on an artery of the moderator band. *Anat Rec*. 1936;66:397–400.

8. Minne I, Depreux R, Mestdagh H, Houcke M. Arterial vascularization of the moderator band (septomarginal trabecula). *Lille Med*. 1975;20:478–480.
9. Fitzgerald D, Lazzara R. Functional anatomy of the conduction system. *Hosp Pract*. 1988;23:81–92.
10. Jacobs JE. Computed tomographic evaluation of the normal cardiac anatomy. *Radiol Clin North Am*. 2010;48:701–710.
11. Bowles CR, Daves ML. Ramus limbi dextri: Demonstration by coronary angiography. *Radiology*. 1985;155:574.
12. Gross L. *The Blood Supply to the Heart in its Anatomical and Clinical Aspects*. New York, NY: Paul B. Hoeber; 1921.
13. Miller SW, ed. *Cardiac Angiography*. Boston: Little Brown and Company; 1984.
14. Pawlak B. Krążenie oboczne w miażdżycy tętnic wieńcowych. *Pol J Radiol*. 1979;43:161–164.
15. Kosiński A, Grzybiak M. The blood supply of the septomarginal trabecula in the hearts of elder people. *Geriatria*. 2010;4:237–241.
16. Lorenz G, Guski H. Histotopographic and morphometric studies of the intramural coronary arteries in the trabecula septomarginalis of swine and pigmy goats. *Z Allg Pathol und Pathol Anat*. 1990;136:87–95 [in German].
17. Lorenz G. Histotopographical studies of the intramural coronary arteries into the trabecula septomarginalis of the right cardiac ventricle in pig (Sus scrofa domesticus) and pygmy goat (Capra aegagrus f. domestica). *Z Mikrosk Anat Forsch*. 1990;104:607–616 [in German].
18. Reig-Vilallonga J, Loncan-Vidal MP, Domenech-Mateu JM. Coronary arterial anastomoses study of their distribution in adult hearts specially emphasizing the crista supraventricularis area. *Anat Anz*. 1987;164:1–12 [in German].
19. Reig-Vilallonga J, Loncan-Vidal MP, Domenech-Mateu JM. Study of the coronary artery branches to the crista supraventricularis. *Bull Assoc Anat*. 1983;67:337–345.
20. Cohn JN, Guiha NH, Broder MI, Limas CJ. Right ventricular infarction: Clinical and hemodynamic features. *Am J Cardiol*. 1974;33:209–214.
21. Dwyer EM, Coquia S, Greenberg H, Pinkernell BH. Inferior myocardial infarction and right coronary artery occlusive disease: A correlative study. *Br Heart J*. 1975;37:464–470.
22. Haupt HM, Hutchins GM, Moore GW. Right ventricular infarction: Role of the moderator band artery in determining infarct size. *Circulation*. 1983;67:1268–1272.
23. Laurie W, Woods JD. Infarction (ischaemic fibrosis) in the right ventricle of the heart. *Acta Cardiol*. 1963;399–411.
24. Ratliff NB, Hackel DB. Combined right and left ventricular infarction: Pathogenesis and clinicopathologic correlations. *Am J Cardiol*. 1980:45:217–221.
25. Rotman M, Ratliff NB, Hawley J. Right ventricular infarction: A haemodynamic diagnosis. *Br Heart J*. 1974;36:941–944.
26. Wade WG. The pathogenesis of infarction of the right ventricle. *Br Heart J*. 1959;21:545–54.
27. Luciano DS, Vander AI, Sherman JH. *Human Function and Structure*. New York, NY: McGraw-Hill Companies; 1978.

Effect of physical activity on the sequelae of osteoporosis in female residents of residential care facilities

Agnieszka J. Nawrat-Szołtysik[1,2,A–D,F], Anna Polak[3,B,C], Andrzej Małecki[4,C,E], Laura Piejko[5,B], Dominika Grzybowska-Ganszczyk[5,B], Michał Kręcichwost[6,B,C], Józef Opara[4,A,E,F]

[1] Department of Health Promotion and Methodology of Research, The Jerzy Kukuczka Academy of Physical Education in Katowice, Poland
[2] St. Elizabeth Center, Ruda Śląska, Poland
[3] Department of Basic Physical Therapy, The Jerzy Kukuczka Academy of Physical Education in Katowice, Poland
[4] Department of Nervous System and Musculoskeletal System, The Jerzy Kukuczka Academy of Physical Education in Katowice, Poland
[5] The Jerzy Kukuczka Academy of Physical Education in Katowice, Poland
[6] Department of Biomedical Engineering, Silesian University of Technology, Zabrze, Poland

A – research concept and design; B – collection and/or assembly of data; C – data analysis and interpretation;
D – writing the article; E – critical revision of the article; F – final approval of the article

Advances in Clinical and Experimental Medicine, ISSN 1899-5276 (print), ISSN 2451-2680 (online) *Adv Clin Exp Med*. 2018;27(5):633–642

Address for correspondence
Aleksandra Nawrat-Szołtysik
E-mail: a.nawrat-szoltysik@awf.katowice.pl

Funding sources
None declared

Conflict of interest
None declared

Received on February 17, 2016
Reviewed on August 18, 2016
Accepted on January 10, 2017

Abstract

Background. Osteoporosis is one of the most common diseases that develop with age and cause high morbidity and mortality among elderly people.

Objectives. This study was set out to evaluate the influence of a program of modified Sinaki exercises, Nordic walking (NW) and a combination of these physical activities on people with osteoporosis.

Material and methods. A sample consisting of 91 women aged 65–98 years living in residential care facilities was randomized into 4 groups. The control group (group 1) received only pharmacological treatment. In the other 3 groups, the same drug therapy was enhanced by a program of modified Sinaki exercises (group 2), Nordic walking (group 3), and Sinaki exercises and Nordic walking applied together (group 4). At baseline and after 12 months of intervention, the participants were assessed for bone density, rib cage mobility, motor abilities, risk of falling (Timed Up and Go Test – TUG, Functional Reach Test – FRT), and locomotor activity (based on pedometer readings). The intervention was completed by 83 participants.

Results. Bone density (T-score) was higher in all intervention groups and in the control group ($p < 0.003$). The improvement in rib cage mobility was statistically significant in groups 2 ($p < 0.001$) and 4 ($p < 0.002$). Locomotor activity significantly improved in groups 3 ($p < 0.000$) and 4 ($p < 0.000$). The post-intervention results of the TUG and FRT tests showed a significantly lower risk of falling in group 4. In groups 1 and 2, the risk was higher, but not statistically significantly, and in group 3, it did not change.

Conclusions. Modified Sinaki exercises and Nordic walking significantly improved the mobility of the rib cage, locomotor activity and motor abilities in the women comprising groups 2 and 3, but the best results of the intervention were noted in the group treated with both forms of physical activity.

Key words: physical activity, osteoporosis, Nordic walking, elderly people

DOI
10.17219/acem/68381

Copyright
© 2018 by Wroclaw Medical University
This is an article distributed under the terms of the Creative Commons Attribution Non-Commercial License (http://creativecommons.org/licenses/by-nc-nd/4.0/)

Introduction

Osteoporosis is one of the most common diseases which develop with age and contribute to high morbidity and mortality rates among the elderly. Its symptoms include postural deformities, pain and disorders of the alimentary canal and breathing function. Falls resulting in low-energy fractures are as much a symptom as a consequence. It is estimated that up to 10–25% of falls reported by residents of residential care facilities (RCFs) and hospitals lead to fractures, triple the rate of that for people living in the home environment.[1]

Osteoporosis is easier to prevent and diagnose than to treat, particularly when advanced. Using drugs alone is not an effective therapy, unlike a comprehensive approach consisting of pharmacological treatment, appropriate dietary intervention and physical activity.[2] One of the most useful physical activities in the case of osteoporotic patients is walking, during which the musculoskeletal system counteracts gravitational forces. The alternate contraction and relaxation of the muscles strengthens them and improves the bone resorption-to-formation ratio.[3] One type of walking activity that is becoming increasingly popular is Nordic walking (NW), i.e., walking with a pair of sticks similar to those used in cross-country skiing. How exactly Nordic walking benefits people with osteoporosis is yet to be established, but it is already known to be an effective means of rehabilitation and recreation for elderly people.[4,5] The survey of 100 students of the Third Age University conducted by Morgulec-Adamowicz et al. has indicated that an increasing number of elderly people are taking an interest in pole-assisted walking.[6] There is evidence that doing carefully selected physical exercises on a regular basis can increase bone mass density (BMD) in young people and prevent its reduction in the elderly.[7] Physical exercises have also been found to improve osteoporotic patients' mobility and to alleviate their pain, thus raising their quality of life. The range of physical exercises that can be effectively used to manage osteoporosis includes atypical movements that stretch, flex and twist the musculoskeletal system, and combinations thereof. A good example would be isometric and resistance exercises that make the bones cope with loads different from those related to regular daily activities.[8–10]

One of the first programs of physical exercises addressing the needs of people with osteoporosis was created at the Mayo Clinic, USA, by Mehrsheed Sinaki in 1982. Three years later, similar programs were compiled by Goodman, and by Simkin and Aylon. In 1987, the existing exercises were modified and standardized by Steinberg.[8,9] The Sinaki exercises are performed in a prone or supine position, a hands-and-knees position, while sitting in a chair, or on the floor with legs extended forward. The whole set of exercises can be completed in around 40 min.[11]

In this study, the exercise positions proposed by Sinaki were modified by reducing their number to 1 sitting position that was easy and safe for elderly females.[12]

The purpose of the study was to evaluate the effect of programs containing modified Sinaki exercises, Nordic walking and a combination of these 2 activities on people with osteoporosis.

The specific research goals of the study were the following:

– to assess the effect of modified Sinaki exercises on bone density, rib cage mobility, locomotor activity, motor abilities, and the risk of a fall in elderly women with reduced bone mass;

– to assess the influence of Nordic walking on these variables;

– and to assess the joint effect of modified Sinaki exercises and Nordic walking on these variables.

Material and methods

The study protocol was approved by the Bioethics Commission at the Academy of Physical Education in Katowice (decision No. 7/2009).

The selection of the study participants was performed based on a set of inclusion and exclusion criteria. The qualifying females had to submit written consent to participate in the study.

Selection of the sample

The study participants were women staying in 4 residential care facilities: 2 in Ruda Śląska, 1 in Katowice and 1 in Tychy.

The inclusion criteria were as follows:

– osteoporosis and osteopenia confirmed by densitometry (T-score ≤–1.0);

– age ≥65 years;

– the ability to understand the purpose of the study;

– pharmacological treatment for osteoporosis or osteopenia.

The exclusion criteria included:

– unconfirmed osteoporosis or osteopenia (T-score >–1.0);

– age <65 years;

– reluctance to cooperate;

– problems with understanding the purpose of the study;

– not receiving pharmacological treatment for osteoporosis or osteopenia.

Of the 131 women aged 65–98 years who were initially screened, 91 were enrolled in the study. They were randomized into 3 intervention groups and a control group, all receiving the same pharmacological therapy. Group 1 (n = 24) was a control, "drugs-only" group (C). The other 3 groups were additionally administered the following types of physical activity:

– group 2 (n = 23) (EX) – modified Sinaki exercises (sessions on Mondays and Thursdays);

– group 3 (n = 21) (NW) – Nordic walking (sessions on Tuesdays and Fridays);

– group 4 (n = 23) (EX + NW) – a combination of the above activities (modified Sinaki exercises on Mondays and Thursdays and Nordic walking on Tuesdays and Fridays).

The study spanned a period of 12 months. By the end of that period, the group had diminished to 83 women (20 in group 1 and 21 in each of the other 3 groups) for reasons such as death (n = 4), major health problems (n = 2) and voluntary withdrawal (n = 2) (Fig. 1).

Research methods

The participants were examined at baseline, and then after 12 months of physical exercises. The following methods were used for measurement:

– bone densitometry – forearm bone density was measured with a peripheral DXA scanner (PIXI, GE Medical Systems Lunar, Madison, USA); the Least Significant Change (LSC) was 2.9;

– measurement of the circumferences of the participants' chests at max inhalation and max exhalation to determine rib cage mobility (with a measuring tape [cm]);

– the Timed Up and Go Test (TUG) evaluating the participants' mobility and risk of falling by measuring the time needed to rise from sitting in a chair, walk 3 m along a line, return to the chair, and sit down. In this study, the height of the chair (46 cm) was the same as that used by Siggeirsdóttir et al.[13] The measure of a participant's performance was the average time obtained from 2 trials. According to Żak, an elderly person capable of completing the test in 20 s has good motor abilities and can get up and sit down unaided.[14] Times longer than 20 s indicate an increased risk of falling;

– the Functional Reach Test (FRT) evaluating postural balance and the risk of falling. In the test, a person stands sideways to the wall with the pelvis and 1 arm touching it, and raises that arm to 90°. The tip of the middle finger having been marked on the wall, the person leans forward as far as possible without moving their feet and pelvis, and the tip of the same finger is marked on the wall again. The distance between the 2 marks determines a patient's performance on the test. In this study, the average of 2 trials was used to evaluate the participants. As in other

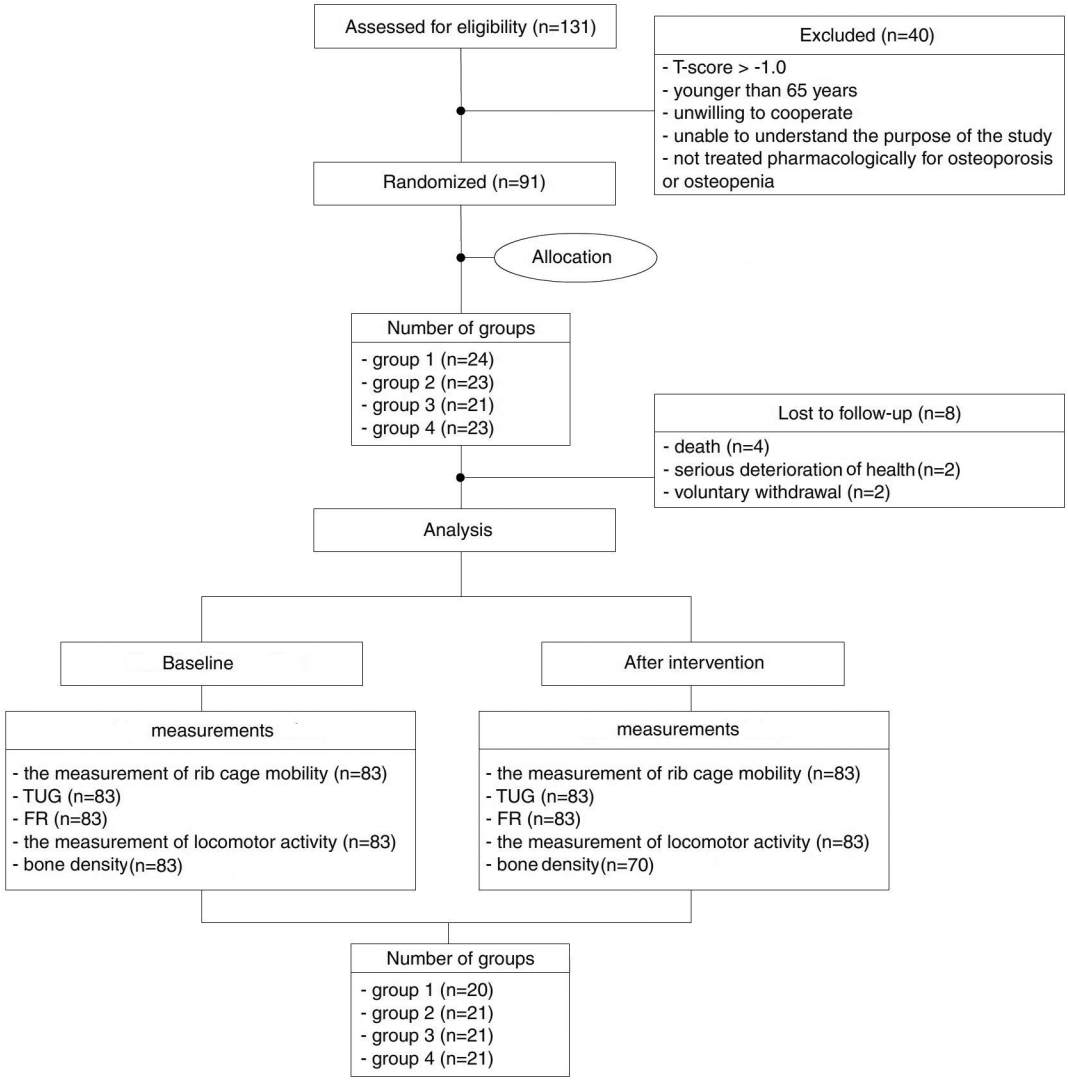

Fig. 1. Flow diagram of the study

studies, it was assumed that a distance smaller than 25 cm was indicative of a higher risk of falling;

– the measurement of the participants' locomotor activity with Yamax Digi-Walker pedometers (Yamax Health & Sport Inc., San Antonio, USA). The pedometers were clipped to the participants upon leaving bed in the morning and were removed before night rest. The participants wore the pedometers for a total of 14 days, i.e., 7 days before the study and 7 days after it ended. According to Tudor-Locke, chronically ill and disabled people aged 65 and older should take 3,500–5,500 steps a day.[15]

Modified Sinaki exercises

Sessions of modified Sinaki exercises started with a warm-up followed by stretching, isometric and body resistance exercises, resistance exercises involving the use of a flexible band, abdomen and back strengthening exercises, and relaxation exercises.

The participants exercised in a sitting position twice a week for 12 months. Exercises were done to music, and various accessories were used to make them more interesting. On warm days, participants exercised outdoors. Researchers stress that the exercises need to be done on a regular basis, because each time they are discontinued or done with lower intensity, bone mass density returns to its baseline values.[16]

Nordic walking

Nordic walking is a brisk walk during which specially designed sticks engaging the shoulder girdle muscles are used. In the study, the NW group exercised, weather permitting, twice a week on flat terrain for a period of 12 months. Exercise intensity was set to 70% of the participants' max heart rate, and walking speed was 2–3 km/h. During Nordic walking, pedometers were not used.

A single NW session consisted of:

– a 5–10 min warm-up including stretching and breathing exercises to enable the participants to exercise at higher intensity and to reduce the risk of injuries;

– a 30 min walk, the duration of which was increased by 5 min (16%) every 3 months, finally amounting to 45 min;

– a relaxation phase for restoring and stabilizing normal cardiorespiratory function in the participants.

Statistical analysis

The statistical analysis started with the calculation of basic descriptive statistics, such as arithmetic averages, medians, standard deviations (SD), and kurtosis (Ku) and skewness (Sk) of the distributions. Their values were tested for normal distribution using the Kolmogorov-Smirnov test. Those found to have normal distributions were analyzed with parametric tests.

In order to determine if modified Sinaki exercises and/or Nordic walking caused changes in the participants' bone density, rib cage mobility, motor abilities, locomotor activity, or risk of falling, the repeated factor (the results of pre- and post-intervention measurements) and the grouping factor (the type of therapy) were analyzed with 2-way repeated-measure ANOVA. When the effect of the order of examination (the difference between the results of pre- and post-intervention measurements), the effect of a therapy, or the effect of interaction between therapies were statistically significant, the intergroup differences were tested with Bonferroni's post-hoc test to find out which therapy was statistically significant.

Statistical analysis was performed using STATISTICA v. 10 software (StatSoft, Tulsa, USA). The level of statistical significance was accepted at $p < 0.05$.

Results

The equivalence of the groups

ANOVA showed that the study groups were not significantly different at baseline in mean age ($f = 0.123$; $p = 0.95$), BMI ($f = 2.09$; $p = 0.11$), T-score ($f = 1.56$; $p = 0.2$), or the length of residence at an RCF ($f = 0.39$; $p = 0.76$).

The participants ranged in age from 65 to 98 years (the mean age was 81 years). Their mean BMI and mean bone density were 26.9 and –3.3, respectively. The average length of residence at an RCF was 4.7 years.

The effect of intervention on bone density

Bone density measurements were made post-intervention in 60 participants (16 in group 1, 19 in group 2, 11 in group 3, and 14 in group 4). Because of health problems, 23 females did not appear for examination (Fig. 1). Bone densitometry showed that bone mass density had increased in all exercise groups, as well as in the control group (T-score) (Fig. 2).

ANOVA indicated that the effect of the order of examination was statistically significant ($p < 0.003$) (Table 1).

The effect of intervention on rib cage mobility

Rib cage mobility improved from baseline in all exercise groups, but in the control group it deteriorated (Fig. 3). ANOVA showed that both the effect of the order of examination ($p < 0.000$) and the effect of interaction ($p < 0.004$) were statistically significant (Table 1).

The results of Bonferroni's post-hoc test pointed to statistically significantly better rib cage mobility in groups 2 ($p < 0.001$) and 4 ($p < 0.002$) (Fig. 3).

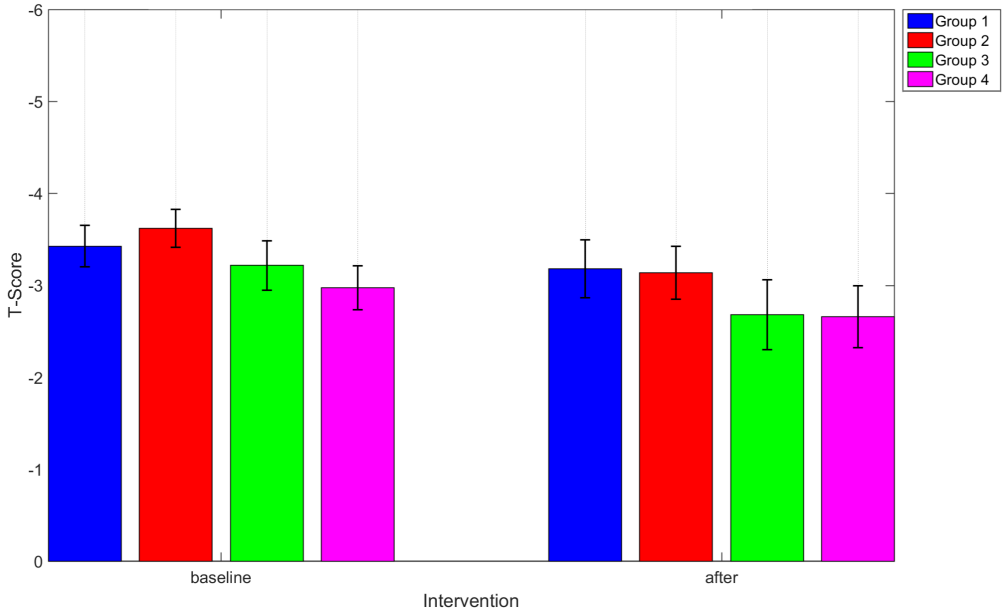

Fig. 2. Bone density at baseline and after intervention, by group

The length of the whiskers represents the standard error (SE) of the group's mean.

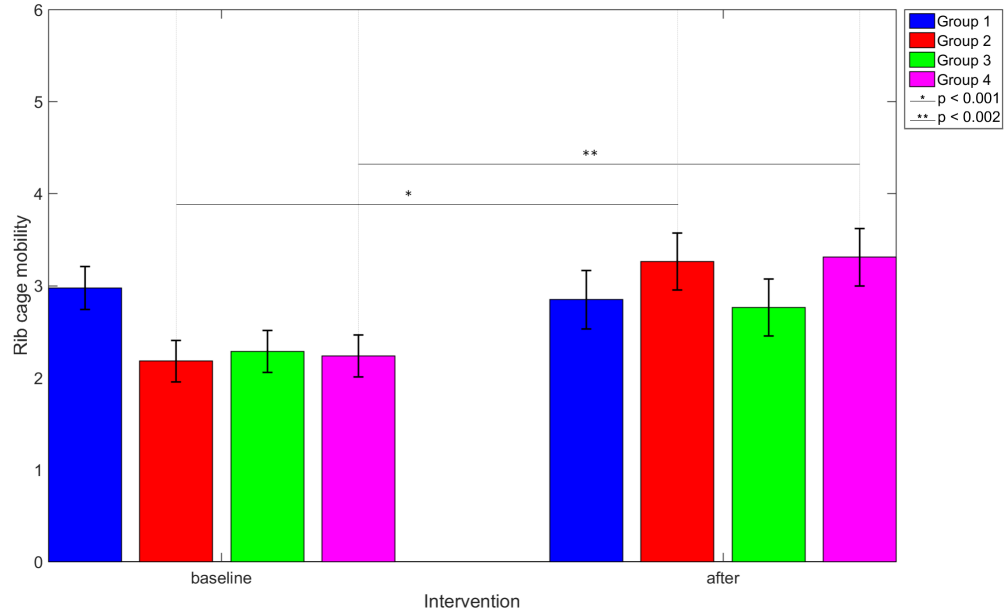

Fig. 3. Rib cage mobility at baseline and after intervention, by group

The length of the whiskers represents the standard error (SE) of the group's mean.

The effect of intervention on locomotor activity

Twelve months of physical exercises proved insufficient for the study participants to reach 3,500–5,500 steps per day, which is recommended for chronically ill people aged ≥65 years (Fig. 4).[15]

ANOVA showed that the effect of the type of therapy ($p < 0.029$), of the order of examination ($p < 0.000$) and of the interaction between them ($p < 0.000$) were significant (Table 1).

Bonferroni's post-hoc test revealed that locomotor activity (i.e., the daily number of steps) improved statistically significantly after intervention in groups 3 ($p < 0.000$) and 4 ($p < 0.000$). In the control group, it was statistically significantly worse ($p < 0.005$) (Fig. 4).

Table 1. ANOVA results

Effect	Bone density		Rib cage mobility		Locomotor activities		Motor abilities	
	f	p-value	f	p-value	f	p-value	f	p-value
Therapy	1.165	0.331	0.444	0.722	3.155	0.029	4.716	0.004
Order of examination	9.957	0.003	23.475	0.000	25.618	0.000	0.582	0.448
Interaction	0.300	0.825	4.878	0.004	29.103	0.000	9.984	0.000

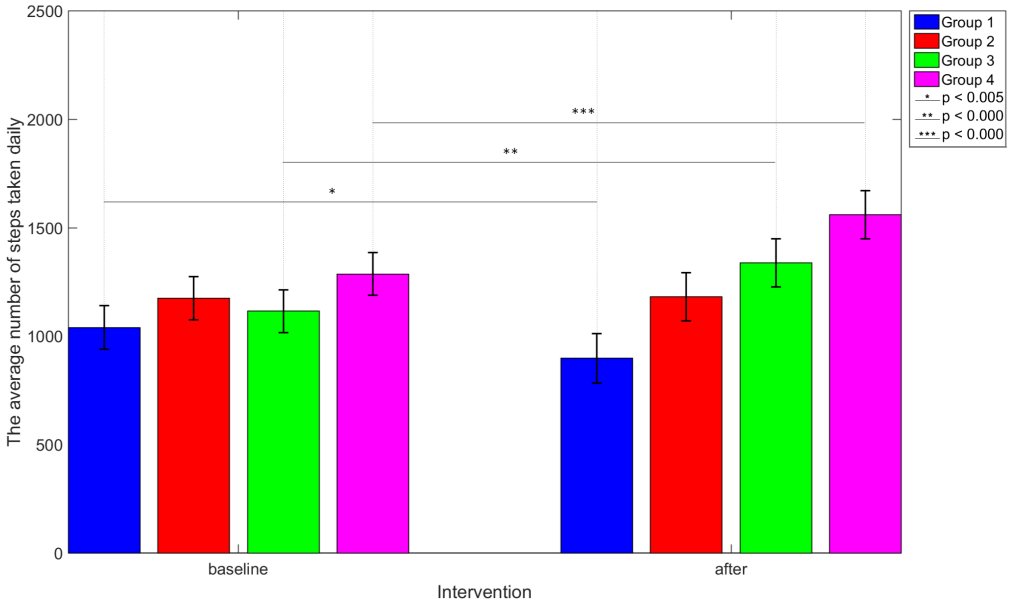

Fig. 4. Average number of steps taken daily by the participants at baseline and after intervention, by group

The length of the whiskers represents the standard error (SE) of the group's mean.

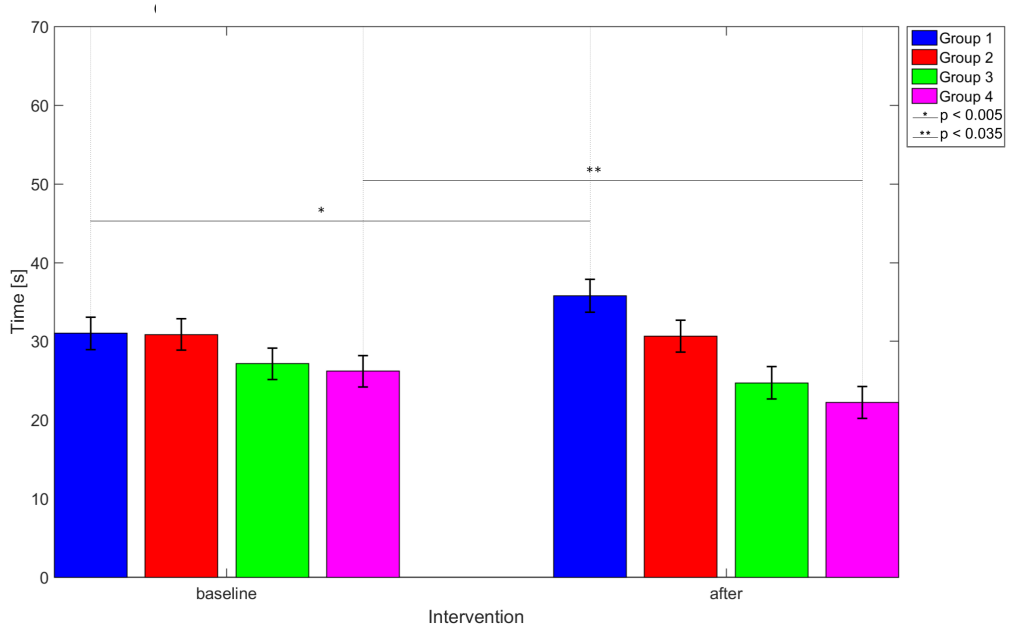

Fig. 5. Groups' scores on the Timed Up & Go Test at baseline and after intervention

The length of the whiskers represents the standard error (SE) of the group's mean.

The effect of intervention on motor abilities

After 12 months of intervention, all exercise groups scored higher on the Timed Up and Go Test, but the control group's scores were worse than at baseline (Fig. 5).

ANOVA showed that the effect of the type of therapy and interaction were statistically significant ($p < 0.004$ and $p < 0.000$, respectively) (Table 1).

The results of Bonferroni's post-hoc test revealed significant improvement in group 4, who completed the TUG test in significantly less time ($p < 0.035$). However, the scores of group 1 (controls) were significantly worse than at baseline ($p < 0.005$) (Fig. 5).

The effect of intervention on the risk of falls

Participants' scores on the post-intervention TUG test showed a considerably lower risk of falls in group 4, a slightly higher risk in groups 1 and 2 and the same risk in group 3 (maximum likelihood χ^2 (ML χ^2) of 9.473; $p = 0.148$) (Fig. 6).

Participants' scores obtained on the FRT were consistent with their scores on the TUG test (ML χ^2 of 8.42; $p = 0.20$) (Fig. 7).

Participants' scores on the post-intervention TUG test showed that 90% of women in group 1, 90.5% in group 2, 61.9% in group 3, and 52.4% in group 4 were at risk of falls. The ML χ^2 value revealed that the differences between

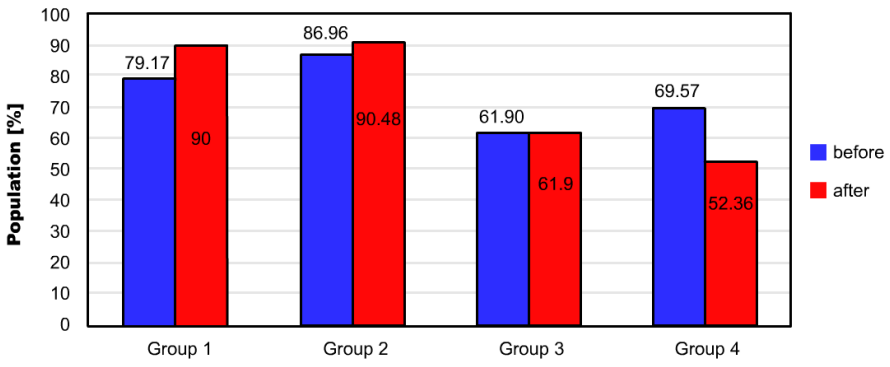

Fig. 6. Risk of falls at baseline and after intervention according to the Timed Up & Go Test scores

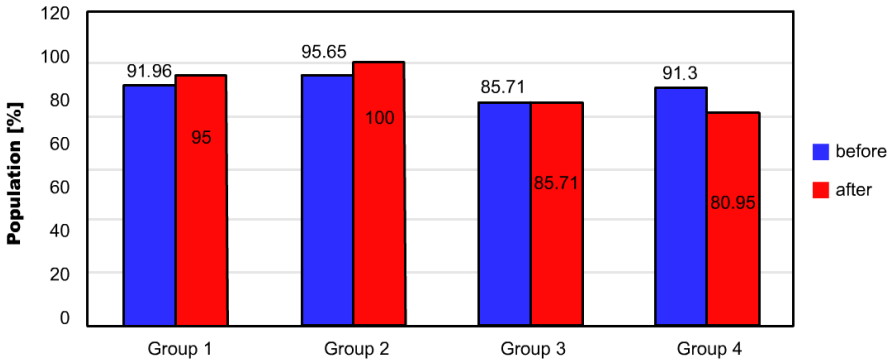

Fig. 7. Risk of falls at baseline and after intervention according to the Functional Reach Test scores

these rates were statistically significantly different (χ^2 value of 12.80; p = 0.00), in contrast with those calculated at baseline (χ^2 value of 4.33; p = 0.22).

The FRT scores obtained post-intervention were similar, but the ML χ^2 test did not show the risk of falls to be statistically significantly different between the groups (χ^2 value of 7.012; p = 0.07).

Discussion

Many studies provide evidence that anti-osteoporotic therapy is more effective in groups that also do physical exercises than in groups where physical activity is not increased.[17,18] In the study by Simkin and Ayalon, 14 women aged 53–54 years participated in a 5-month program of bone strengthening exercises. The bone density measurements performed at month 6 showed that in the exercise group, bone density level was greater by almost 4%, while in the control group it had decreased by 2%.[11] Dalsky et al. studied 2 groups of post-climacteric women, 1 of which exercised for 22 months while the other (controls) abstained from exercise. In the exercise group, bone mass increased by 6.1%, but in the control group no changes in BMD were noted.[19] According to Ishimi's recent article, secondary prevention of osteoporosis must be accompanied by an essential change in lifestyle, including a new approach to nutrition, physical activity, smoking, and alcohol intake.[20] In the review article on Nordic walking that Opara has published recently, the health benefits that the activity offers include improved gait efficiency, coordination and postural stability. Most importantly, however, Nordic walking reduces the risk of falls which in the case of osteoporotic patients can have extremely painful consequences.[21]

Weber-Rajek et al. indicated in their review report that while the whole-body vibration exercise could be recommended for the management of postmenopausal osteoporosis, it could not replace pharmacological and dietary therapies.[22] Hakestad et al., working for the OsteoACTIVE program, reported that exercises with weight vests and a patient education program were effective in the case of women with osteopenia and a healed wrist fracture.[23]

Most studies on osteoporosis recommend walking in addition to other physical exercises. Dawson-Hughes et al. established that post-climacteric women walking approx. 1 mile per day had higher bone density than those walking shorter distances.[24] This observation was supported by Shangold, who found bone density to be higher and more stable in people walking several kilometers per day.[25] In the Pindel and Pluskiewicz study, the only effective exercise was a brisk walk with an additional load applied to the spine.[26] Bonaiuti et al. reported that in participants who walked 20–25 min every day covering a distance of 1–2 km, mineral bone density improved.[27]

One of the aims of this study was to establish whether Nordic walking and modified Sinaki exercises would have an effect on the participants' BMD. The results are less optimistic than those presented above. Bone density improved

not only in the 3 exercise groups but also in the control group. Intervention was most effective in groups 2 and 3 (T-score higher by 0.5) and group 4 (0.3). In the control group, T-score improved by as little as 0.2. The intergroup differences were not statistically significant, probably because of bone density being measured at the distal radial bone and not at the lumbar spine, which is more suitable for monitoring the course of treatment. In none of the 4 groups did bone density change statistically significantly. Smidt also failed to find statistically significant differences between women doing resistance exercises 3 times a week over a period of 12 months and those who did not exercise (bone mass decreased in both groups).[28] The higher post-intervention BMD values in this study's exercise groups and control group imply that bone density was mainly determined by pharmacological treatment, which was the same in all groups. Cukras and Jegier reported that although regular physical activity could slow down skeletal demineralization in people over 50 years of age, it was less effective than anti-osteoporotic drugs. They concluded that physical activity should be used as an enhancement of nutritional therapy and pharmacotherapy rather than as primary treatment for people with low BMD.[29]

According to many researchers, regular physical activity offers elderly people with osteoporosis more health benefits than a moderate increase in bone density alone. These benefits include better respiratory function, greater independence in everyday activities and improved physical and mental function. Of equal importance is the fact that physical activity increases muscle strength, endurance, balance, and motor control, thus reducing the risk of falls and fractures.[3,30]

In this study, 12 months of regular physical exercises significantly improved rib cage mobility in groups 2 and 4 (by 1.1 cm). The 0.5 cm increase noted in group 3 was not statistically significant, and in group 1 (controls), rib cage mobility decreased by 0.1 cm. According to Roczniak et al., respiratory exercises and exercises stretching the intercostal muscles can help preserve or increase rib cage mobility in osteoporotic patients.[31] The results of this study lead to the same conclusion, because rib cage mobility improved only in groups 2 and 4, the ones who did modified Sinaki exercises including the abovementioned exercises.

Elderly people are assessed for the risk of a fall by means of the Timed Up and Go Test and the Functional Reach Test measuring their motor abilities and postural balance. A review of studies provided conflicting information on whether physical exercises can improve performance in these tests. In the study that Żak et al. carried out with 28 residents of a Chorzów RFC, after 12 months of a fall prevention program, 29% of the participants had less difficulty rising from a chair, 67% performed as before and 4% reported that the TUG test was more difficult for them. The results were statistically significant.[32] In the study by Kozak-Szkopek and Galus, 22 females (aged 72–88 years) living in a care facility for retired health care personnel in Warszawa participated in a 2-month rehabilitation program made up of individual and group exercises (general fitness and breathing exercises, also stretching exercises with the Tri-Gym™ device; KOO Medical, Shanghai, China) that were done for 30 min, 3 times a week. The program reduced the average time the participants took to complete the TUG test from 12.41 s to 11.27 s. However, the difference was not statistically significant ($p = 0.06$).[33] The results that Ballad et al. obtained in a study with 2 groups of 20 women aged >65 years (the intervention group and the control group) were not statistically significant, either. The first of them exercised for 1 h, 3 times a week over a period of 15 months. The average results each group achieved in the FRT performed at baseline and after intervention were not statistically significantly different from each other (10.5 cm).[34] In the Mętel et al.'s study, the exercise group that did sensorimotor exercises twice a week did not perform significantly better than controls on the FRT and TUG tests. The authors concluded that the most likely reason why the tests failed to show the expected positive changes was the physical fitness of the participants in the exercise group.[35]

In our study, after 12 months of modified Sinaki exercises and Nordic walking, all 3 exercise groups took less time to complete the TUG test. Group 4 was statistically significantly faster than at baseline (by 4 s; $p < 0.035$), and groups 2 and 3 were slightly faster (by 0.2 s and 2.5 s, respectively), but the differences were not statistically significant. Group 1 (controls) performed significantly worse than at baseline (by 4.8 s; $p < 0.005$). The FRT performed post-intervention showed that postural balance improved statistically insignificantly in groups 4 and 3 (as indicated by functional reach increasing by 7.8 cm and 0.9 cm, respectively). It is likely that the results would have been better had the modified Sinaki exercises and Nordic walking programs been enhanced by static and dynamic balance exercises, exercises with balance discs and training in getting up after a fall. The same conclusion was reached by Żak et al., who conducted a study with 46 persons aged 78–86 years suffering from gait disorders and impaired mobility. At baseline, it took them from 21 to 30 s to complete the TUG test (as in our study). The intervention consisted of rehabilitation exercises (the same as we used), postural balance exercises and training in walking safely. Participants exercised at home for 45 min, 3 times a week for a period of 12 months. After intervention, 62.5% of them completed the TUG test in 11–20 s ($p < 0.004$).[36] Wnuk et al. studied 30 osteoporotic patients aged 60–80 years with impaired physical fitness and balance disorders. In addition to doing exercises used in the earlier studies (stretching and strengthening exercises, resistance exercises with flexible bands, circulation, breathing and relaxation exercises, etc.), they also exercised while sitting on balance discs and walked backwards on a treadmill.[37] The intervention significantly improved their performance on the FRT and TUG tests.

There are studies according to which the postural balance of people with reduced bone mass can also be improved by Tai Chi training. Evidence of this has been provided by Maciaszek et al., who studied the effect of 18 weeks of Tai Chi training on postural balance and risk of falling. The study involved 49 males aged 60–82 years of age diagnosed with osteopenia or osteoporosis. They were divided into an exercise group (n = 25) that did Tai Chi twice a week for 45 min and a control group (n = 24). Body balance measurements were made with the Computer Posturographic System PE 90 (Natus Medical Inc., Pleasanton, USA). The measurements were also an opportunity to analyze the participants' ability to perform specific balance tasks (by measuring deflections in the set scope and direction). Intervention increased the effectiveness of balance task performance ($p \leq 0.01$) in the Tai Chi group from 80.95% to 84.45%, while in the control group, a statistically significant improvement in the level of body balance was not noted.[38]

This study also sought to establish the effect of 12 months of Sinaki exercises and Nordic walking on the number of steps the study participants took per day. Bonferroni's post-hoc test showed a statistically significant increase in the number of steps in groups 3 ($p < 0.000$) and 4 ($p < 0.000$), and a significant reduction in the control group ($p = 0.005$). Not a single participant reached the level of 3,500–5,500 steps per day, which is recommended for chronically ill persons aged ≥65 years.[13] The highest statistically significant increase in the number of steps was observed in group 4 (272.3 steps). In the Fitzpatrick et al.'s study with 418 elderly persons (mean age of 75 years), 4 months of chair exercises and walking increased the daily number of steps by 29% ($p \leq 0.0001$) and extended the duration of physical activity by 26% ($p \leq 0.001$). The authors also noted that with the increased locomotor activity of the study participants, their physical fitness improved.[39]

Conclusions

The results of the study allow the following conclusions to be drawn:

– the program of modified Sinaki exercises performed twice a week for 12 months statistically significantly increased rib cage mobility and insignificantly improved motor abilities and bone density in the elderly women with reduced bone mass participating in the study;

– the Nordic walking program, during which participants exercised with the same frequency as above, statistically significantly increased their locomotor activity, while the improvement in motor abilities, bone density and rib cage mobility was not statistically significant;

– the program combining modified Sinaki exercises and Nordic walking that the study participants performed 4 times a week for a period of 12 months proved the most effective therapeutically; it statistically significantly increased their motor abilities, rib cage mobility and locomotor activity, and it improved bone density and reduced the risk of falls, though not significantly;

– in the control group, measurements performed after 12 months of intervention revealed statistically insignificantly higher bone density, significantly lower locomotor activity and insignificantly decreased rib cage mobility and motor abilities, while the risk of falls was higher than at baseline.

References

1. Badurski J, Czerwiński E, Marcinowska-Suchowierska E. Osteoporoza – ocena ryzyka złamania. Status Quo Arte Anno 2007/2008: Przegląd stanowisk Światowej Organizacji Zdrowia (WHO), Europejskiej Agencji Medycznej (EMEA), Europejskiego Towarzystwa Klinicznych i Ekonomicznych Aspektów Osteoporozy (ESEAO), Międzynarodowej Fundacji Osteoporozy (IOF), Polskiej Fundacji Osteoporozy (PFO) i Polskiego Towarzystwa Osteoartrologii (PTOA). *Post Nauk Med*. 2008;21(6):335–359.
2. Sran MM, Karim M, Khan KM. Physiotherapy and osteoporosis: Practice behaviors and clinicians' perceptions – A survey. *Manual Therapy*. 2005;10:21–27.
3. Yamazaki S, Ichimura S, Iwamoto J, et al. Effect of walking exercise on bone metabolizm in postmenopausal women with osteopenia/osteoporosis. *J Bone Miner Metab*. 2004;22:500–508.
4. Hansen L. Nordic walking does not reduce the loading of knee joint. *Skan J Med Sci Sports*. 2008;18:436–441.
5. Suija K. Physical activity of depressed patients and their motivation to exercise: Nordic walking in family practice. *Int J Rehabil Res*. 2009;32(2):132–138.
6. Morgulec-Adamowicz N, Rutkowska I, Rekowski W, et al. Aktywność fizyczna osób starszych w Uniwersytecie Trzeciego Wieku w Polsce. *Post Rehab*. 2010;24(2):73–80.
7. Bello M, Cirilo Cousa M, Neto G, et al. The effect of a long-term, community-based exercise program on bone mineral density in postmenopausal women with pre-diabetes and type 2 diabetes. *J Human Kinetics*. 2014;43:43–48.
8. Sinaki M. Exercise and osteoporosis. *Arch Phys Med Rehab*. 1989,70(3): 220–229.
9. Sinaki M, Khosia S, Limburg PJ. Muscle strength in osteoporotic versus normal women. *Osteoporosis Int*. 1993;3:8–12.
10. Izquierdo M, Gonzalez-Badillo JJ, Häkkinen K, et al. Effect of loading on unintentional lifting velocity declines during singles sets of repetitions to failure during upper and lower extremity muscle actions. *Int J Sports Med*. 2006;27:718–724.
11. Simkin E, Ayalon J. *Osteoporoza, zapobieganie i zwalczanie ruchem*. Warszawa: SIC; 1996.
12. Nawrat-Szołtysik A, Opara J, Kucio C. Własna modyfikacja ćwiczeń według Mehrsheed Sinaki w osteoporozie u osób starszych. *Rehabil Prakt*. 2011;5:27–32.
13. Siggeirsdóttir K, Jónsson BY, Jónsson H Jr, Iwarsson S.The timed 'Up & Go' is dependent on chair type. *Clin Rehabil*. 2002;16(6):609–616.
14. Żak M. Physical rehabilitation of geriatric patients with gait and functional disorders. *Adv Rehabil*. 2005;1:37–40.
15. Tudor-Locke C. Taking steps toward increased physical activity: Using pedometers to measure and motivate. *Res Digest*. 2002;3(7):1–8.
16. Wolff I, Croonenborg I, Temper HCG, et al. The effect of exercise training programs on bone mass: A meta-analysis of published controlled trials in pre-and postmenopausal women. *Osteoporosis Int*. 1999;9:1–2.
17. Tan AM, Lamontage AD, Sarmugan R, et al. A cluster-randomised, controlled trial to assess the impact of a workplace osteoporosis prevention intervention on the dietary and physical activity behaviours of working women: Study protocol. *BMC Public Health*. 2013;29(1): 405–416.
18. Bravo G, Gauthier P, Roy P, et al. Impact of 12-month exercise program on the physical and psychological health of osteoporosis women. *J Am Geriatr Soc*. 1996;44(7):756–762.

19. Dalsky GP, Stocke KS, Ehsani AA, Slatopolsky E, Lee WC, Birge SJ Jr. Weight-bearing exercise training and lumbar bone mineral content in postmenopausal women. *Ann Intern Med*. 1998;108: 824–828.
20. Ishimi Y. Osteoporosis and lifestyle. *J Nutr Sci Vitaminol* (*Tokyo*). 2015; 61(S):139–141.
21. Opara J. Nordic walking w zapobieganiu upadkom. In: Czerwiński E, ed. *Osteoporoza. Problem interdyscyplinarny*. Warszawa: PZWL; 2015:229–235.
22. Weber-Rajek M, Mieszkowski J, Niespodziński B, Ciechanowska K. Whole-body vibration exercise in postmenopausal osteoporosis. *Prz Menopauz*. 2015;14:41–47.
23. Hakestad KA, Torstveit MK, Nordsletten L, Risberg MA. Effect of exercises with weight vests and a patient education programme for women with osteopenia and a healed wrist fracture: A randomized, controlled trial of the OsteoACTIVE programme. *BMC Musculoskelet Disord*. 2015;16(1):352–360.
24. Dawson-Hughes B, Jacques P, Shipp C. Bone density of the radius, spine and hip inrelation to percent ideal body weight in postmenopausal women. *Calcif Tissue Int*. 1987;40:310–314.
25. Shangold MM. Exercise and menopause. *Phys Sports Med*. 1998;26(12): 45–59.
26. Pindel B, Pluskiewicz W. Rola wysiłku fizycznego w zapobieganiu i leczeniu osteoporozy. *Pol Tyg Lek*. 1993;48(37/49):780–781.
27. Bonaiuti D, Shea B, Lovine R, et al. Exercise for preventing and treating osteoporosis in postmenopausal women. *Cochrane Database Sys Rev*. 2002;3:333–339.
28. Smidt GL. The effects of high-intensity trunk exercise on bone mineral density of postmenopausal women. *Spine*. 1992;17(3): 280–285.
29. Cukras Z, Jegier A. Aktywność fizyczna a gęstość mineralna kości – aktualny stan wiedzy. *Pol Arch Med Wew*. 2005;113(2):164–171.
30. Kemmler W. Exercise effects on bone mineral density, falls, coronary risk factors, and health care costs in older women: The randomized controlled senior fitness and prevention (SEFIP) study. *Arch Int Med*. 2010;70(2):179–185.
31. Roczniak W, Babińska-Roczniak M, Roczniak A, et al. Zalecenia rehabilitacyjne dla pacjentów z osteoporozą. *Probl Med Rodz*. 2011;13(3): 35–42.
32. Żak M, Melcher U. Rehabilitacja jako element programu zapobiegania upadkom osób starszych. *Przegl Lek*. 2002;59:4–5.
33. Kozak-Szkopek E, Galus K. Wpływ rehabilitacji ruchowej na sprawność psychofizyczną osób w podeszłym wieku. *Gerontol Pol*. 2009; 17(2):79–94.
34. Ballad JE, McFarland C, Wallace LS, Holiday DB, Roberson G. The effect of 15 weeks of exercise on balance, leg strength, and reduction in falls in 40 women aged 65–89 years. *J Am Med Womens Assoc*. 2004;59:255–261.
35. Mętel S, Milert A, Szczygieł A, et al. Wpływ 6-miesięcznego treningu sensomotorycznego na sprawność funkcjonalną osób starszych z przewlekłym bólem krzyża. *Post Rehab*. 2010;24(3):51–65.
36. Żak M, Skalska A, Szczerbańska K. Programy nauki samodzielnego podnoszenia się po upadku dla osób starszych – badanie randomizowane. *Ortop Traumatol Rehabil*. 2008;10(5):491–502.
37. Wnuk B, Walusiak M, Durmała J, et al. Wpływ fizjoterapii rozszerzonej o różne formy treningu chodu na bieżni ruchomej na sprawność funkcjonalną osób starszych zagrożonych upadkiem. *Fizjoterapia*. 2010;18(2):3–9.
38. Maciaszek J, Osiński W, Szeklicki R. Effect of Tai Chi on body balance: Randomized controlled trial in men with osteopenia or osteoporosis. *Am J Chin Med*. 2007;35(1):1–9.
39. Fitzpatrick SE, Reddy S, Lommel TS, et al. Physical activity and physical function improved following a community-based intervention in older adults in Georgia senior centers. *J Nutr Elder*. 2008;27:1–2.

Detection of *Brucella abortus* by immunofluorescence assay using anti outer membrane protein of 19 kDa antibody

Elham Mohammadi[1,A,C,D], Mehdi Golchin[2,A,D–F]

[1] Division of Microbiology, Department of Pathobiology, Faculty of Veterinary Medicine, Shahid Bahonar University of Kerman, Iran
[2] Department of Pathobiology, Faculty of Veterinary Medicine, Shahid Bahonar University of Kerman, Iran

A – research concept and design; B – collection and/or assembly of data; C – data analysis and interpretation;
D – writing the article; E – critical revision of the article; F – final approval of the article

Advances in Clinical and Experimental Medicine, ISSN 1899-5276 (print), ISSN 2451-2680 (online) *Adv Clin Exp Med*. 2018;27(5):643–648

Address for correspondence
Elham Mohammadi
E-mail: elham_mohammadidamaneh@yahoo.com

Funding sources
This investigation was supported by grant No. 96003341 from Iran National Science Foundation (INSF).

Conflict of interest
None declared

Received on December 25, 2016
Reviewed on January 18, 2017
Accepted on February 6, 2018

Abstract

Background. Brucellosis in humans is one of the most prevalent zoonotic diseases around the world with more than 500,000 new cases per year. It is a weakening disease that requires long-term antibiotic treatment, often resulting in permanent and disabling consequences. Outer membrane proteins (OMPs) of *Brucella*, which are non-lipopolysaccharide (LPS) antigens, have been used for the diagnostic kits of brucellosis and vaccine design.

Objectives. The aim of this study was to identify *Brucella abortus* with an immunofluorescence (IF) test using an antibody against recombinant outer membrane protein (OMP) of 19 kDa of this bacterium.

Material and methods. The OMP19 gene of *Brucella* spp. was synthesized, cloned and expressed in *Escherichia coli* cells. The OMP19 protein was purified by metal chelate affinity chromatography and subsequently used for the immunization of rabbits to produce a polyclonal antibody. Then, this antibody was conjugated to fluorescein isothiocyanate (FITC) and used for the detection of *Brucella* by an IF test. Also, the sensitivity and specificity of this antibody for the diagnosis of clinical isolates was calculated.

Results. Outer membrane protein 19 was expressed well and reacted with a commercial antiserum against His-tag in an immunoblot assay. Polyclonal antibodies obtained from the serum of rabbits immunized with the purified protein showed strong reactivity in the enzyme-linked immunosorbent assay (ELISA). Moreover, the polyclonal antibody conjugated to FITC was able to properly identify *Brucella abortus*. Sensitivity and specificity of this IF test in comparison with a polymerase chain reaction (PCR) assay was 84.2% and 50%, respectively.

Conclusions. This high-titer antibody could potentially be valuable for the specific diagnostic test of brucellosis.

Key words: antibody, immunofluorescence assay, OMP19, *Brucella abortus*

DOI
10.17219/acem/85081

Copyright
© 2018 by Wroclaw Medical University
This is an article distributed under the terms of the Creative Commons Attribution Non-Commercial License (http://creativecommons.org/licenses/by-nc-nd/4.0/)

Introduction

Brucella spp. are intracellular Gram-negative bacteria that cause human disease and significant economic losses worldwide due to livestock infection.[1] Lipopolysaccharide (LPS) of *Brucella* spp. elicits long-term serological reactions in vaccinated and infected animals.[1–4] In serologic tests, LPS of the bacterial cell membrane has been mainly used to identify particular antibodies. For these reasons, it is difficult to differentiate between infected and vaccinated animals using LPS-based serological tests.[5–8] Moreover, serological examinations on the basis of the detection of LPS, due to a cross-reaction with other Gram-negative microorganisms, for example *Salmonella* spp., *Escherichia coli* and *Yersinia enterocolitica* O:9, cause false-positive reactions.[9–12] Outer membrane proteins (OMPs) of *Brucella*, which are non-LPS antigens, have been used for the diagnostic kits of brucellosis and vaccine design.[13–18] The *Brucella* cell wall consists of a peptidoglycan (PG) layer firmly connected with the external layer consisting of at least 75 proteins with several OMPs.[19] These include the major OMPs of group 2 (porin, 34–40 kDa), group 3 (25–30 kDa) that was described initially by Dubray and Bezard[20] and Verstreate et al.,[21] the lipoprotein covalently bound to PG,[22,23] and the minor OMPs of group 1 (88–94 kDa). The OMPs of *Brucella* spp. have been widely considered as potentially defensive and immunogenic antigens.[24,25] Monoclonal antibodies (mAbs) against group 1, 2 and 3 OMPs, as well as mAbs to minor surface-exposed OMPs with molecular masses (MMs) of 10, 16, 19, and 31–34 kDa (the latter is a major OMP in *B. melitensis* strains but is less abundant in *B. abortus*), have been produced.[26] Physicochemical and practical examination has recently confirmed that OMP10, OMP16 and OMP19 are lipoproteins that are uncovered at the cell surface.[27] It has been proven that these lipoproteins are present in several *Brucella* strains. These strains represent all 6 *Brucella* species and all their biovars. According to published data, OMP19 is an immunoreactive outer membrane lipoprotein.[28–33] The appearance of OMP19 has been proven to be necessary for the acceptance of a defensive reaction by the vaccine strain *B. abortus* S19, since the abrogation of its gene in this strain leads to the destruction of its protective ability in heifers,[34] showing that OMP19 should be a key component of a subunit vaccine against brucellosis. Furthermore, we have previously reported that recombinant OMP19, when injected with the mucosal adjuvant cholera poison, is a protective mucosal antigen that confers protection against an oral challenge with virulent *Brucella*.[30] For this reason, in this research, we expressed OMP19 for the creation of a polyclonal antibody to use it in an immunofluorescence assay (IFA).

The study was endorsed by Animal Experimentation Ethics Committee of Kerman University of Medical Sciences, Iran.

Material and methods

Cloning and expression

The OMP19 gene was synthesized based on the existing gene sequence of *B. abortus* (accession No. U35742) and cloned into the pET-28a expression vector by Genray Biotechnology Company (Shanghai, China). The pET-28a vector allowed the expression of the cloned gene as a fusion protein with a 6-histidine residue at the amino terminus. The recombinant plasmid was transformed into an *E. coli* strain BL21 (DE3) competent cell by the heat shock method (42°C for 90 s), according to standard protocols.[35] The transformant bacterium was chosen from Luria Bertani (LB) agar medium containing 30 µg/mL of kanamycin. The transformant was grown in 10 mL LB containing 50 mg/mL kanamycin at 37°C, shaken at 200 rpm overnight. Then, 1 mL of the medium was supplemented to 100 mL of fresh LB. The transformant was grown at 37°C until the optical density (OD) at 600 nm achieved 0.6, and after being prompted by including Isopropyl-β-D-1-thiogalactopyranoside (IPTG) at a final concentration of 1 mM and incubation at 25°C overnight with shaking. The transformant was amassed by centrifugation at 5000 × g for 10 min, then the cell was resuspended in the (5-pellet volume) lysis buffer pH 8.0 (300 mM NaCl, 10 mM Imidazole, 50 mM NaH_2PO_4) and incubated at 4°C for 30 min. The lysate was also sonicated (10 s pulse on followed by 10 s pulse off, total time: 4 min). The resulting lysate was centrifuged at 5000 × g for 30 min at 4°C. The supernatant including the recombinant protein was examined by sodium dodecyl sulfate-polyacrylamide gel electrophoresis (SDS-PAGE), using 5% stacking and 15% resolving gels, dot blot and western blot analyses. The recombinant OMP19 was purified using metal chelate affinity chromatography by Ni–NTA column (Qiagen, Hilden, Germany).

Immunization

A New Zealand white female rabbit was immunized intramuscularly with the purified recombinant OMP19 protein (0.5 mg/mL) mixed with Freund's complete adjuvant (Sigma-Aldrich, St. Louis, USA) (1:1) administered into the back legs of the rabbit, followed by 2 injections emulsified with Freund's incomplete adjuvant and without adjuvant, respectively, at 2-week intervals.

Antiserum collection

The rabbit was bled 4 times (before each injection and 2 weeks after the 3rd injection). Blood was obtained from the marginal vein of the ear and kept at 4°C overnight. Serum was isolated by centrifugation at 3000 × g for 10 min and put away at –20°C until utilized.

To evaluate the serum titer, 2 enzyme-linked immunosorbent assay (ELISA) tests were carried out. In the

1st ELISA test, the reaction of serum during immunization against the purified recombinant protein was tested. In the 2nd ELISA test, final serum was diluted from 1/100 until 1/100000 to determine the serum titer.

Enzyme-linked immunosorbent assay

Sera were assessed by ELISA for antibody reactivity vs the recombinant OMP19 as follows: 96-well polystyrene microtiter plates (Nunc, Roskilde, Denmark) were covered with the recombinant OMP19 (100 µL per well) in phosphate-buffered saline (PBS) (Sigma-Aldrich, St. Louis, USA) at a density of 25 µg/mL and incubated overnight at 4°C. The wells were washed 3 times with PBS and blocked with 200 µL of blocking buffer PBS containing 3% bovine serum albumin (BSA) (Sigma-Aldrich) for 2 h at 37°C. After 3 washes, the diluted sera were added and the plates were incubated for 1 h at 37°C. The plates were then washed 3 times with 0.1% (v/v) Tween-20 in PBS (PBST). Antibodies attaching to OMP19 were visualized using 100 µL polyclonal goat peroxidase-conjugated anti-rabbit IgG (Bio-Rad Laboratories, Inc., Hercules, USA) diluted 15,000-fold in blocking buffer. After 1-h incubation at 37°C, the plates were washed with PBST and developed with 100 µL of 3,3',5,5'-tetramethylbenzidine (TMB) substrate (1 mL TMB, 9 mL of citrate-phosphate buffer, pH 5, and 3 µL of 30% H_2O_2). The reaction was stopped after 15 min by the addition of 50 µL 1.0 M H_2SO_4 to each well and read at 450 nm by the ELISA plate reader.

Immunofluorescence test

The polyclonal antibody was purified using the Proteus Protein Mini Purification Spin Column Pack (Bio-Rad Laboratories, Inc., Hercules, USA). The antibody was conjugated to fluorescein isothiocyanate (FITC) using standard protocols. Briefly, 40 µL of antibody (100 µg/mL) was mixed with 80 µL of borate buffer (0.1 M). Then, 4 µL of FITC (1 mg/mL) was added to 120 µL of the mixture and incubated at 37°C for 30 min. The conjugated antibody was stored at 4°C until use.

The detection of *B. abortus* by IFA: The amount of 500 µL of culture medium, which included *B. abortus, E. coli, Salmonella*, and *Klebsiella* (negative controls), was centrifuged at 4000 × g for 10 min. The resulting pellets were washed 3 times with PBS and suspended in 200 µL of PBS. Then, 20 µL of the conjugated antibody was added and the suspensions were incubated at room temperature overnight with shaking. Subsequently, the suspensions were centrifuged, washed 3 times with PBS, and then 10 µL of the samples were examined under a fluorescence microscope.

In this study, 29 bacterial isolates including 19 *Brucella* isolates, confirmed with specific primers in the polymerase chain reaction (PCR), and 10 non-*Brucella* isolates without a specific amplicon in the PCR, were used to determine the sensitivity and specificity of the above-mentioned immunofluorescence (IF) test, using the anti-OMP19 antibody.

The results of variables, including truly positive (TP), truly negative (TN), false positive (FP), and false negative (FN) ones, were analyzed using the following formulas:

$$\text{Sensitivity} = [TP/(TP + FN)] \times 100$$
$$\text{Specificity} = [TN/(TN + FP)] \times 100$$

Results

Expression and purification

The induced transformant was examined using SDS-PAGE and immunoblotting. The SDS-PAGE examination of extracted total proteins indicated that OMP19 was expressed successfully with an estimated molecular weight of 19 kDa (Fig. 1, 2). The protein was transferred to the nitrocellulose membrane and the specificity of the expressed 6×His-tagged recombinant OMP19 protein was determined using a commercial anti-His-tag antibody (Sigma-Aldrich, St. Louis, USA) by an immunoblot assay (Fig. 3, 4). The recombinant protein was purified with an affinity chromatography and subsequently used for the immunization of the rabbit.

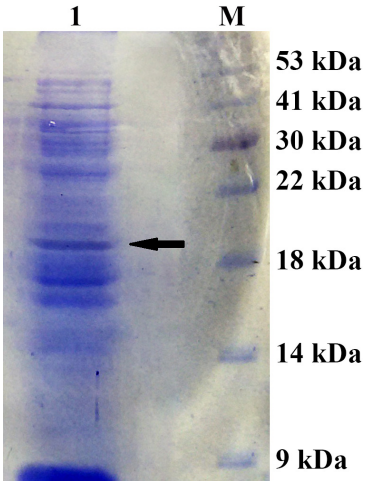

Fig. 1. SDS-PAGE analysis of total cell lysate of *E. coli* producing the OMP19 protein

OMP19 – the recombinant outer membrane protein 19 kDa; lane 1 – OMP19; lane M – protein prestained ladder; the arrowhead shows the location of the *Brucella* recombinant protein.

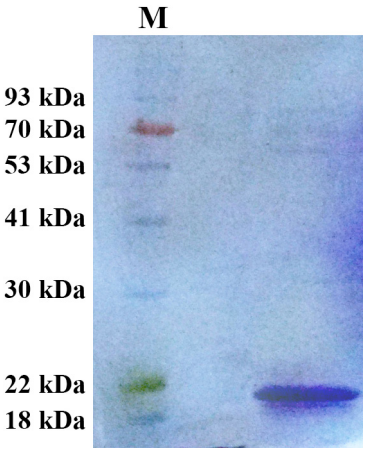

Fig. 2. SDS-PAGE analysis of the purified recombinant *Brucella* OMP19 protein

OMP19 – the recombinant outer membrane protein 19 kDa; lane M – protein prestained ladder.

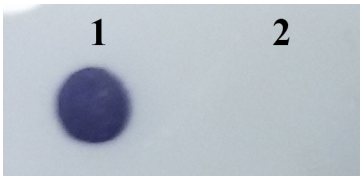

Fig. 3. Dot blot analysis of the expressed His-tagged OMP19 protein, using a commercial anti-His-tag peroxidase-conjugated antibody

OMP19 – the recombinant outer membrane protein 19 kDa; lane 1 – OMP19; lane 2 – negative control.

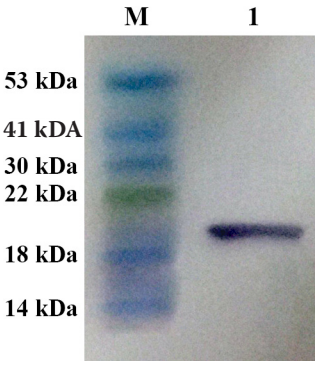

Fig. 4. Western blot analysis of the expressed His-tagged OMP19 protein, using a commercial anti-His-tag peroxidase-conjugated antibody

OMP19 – the recombinant outer membrane protein 19 kDa; lane 1 – OMP19; lane M – protein prestained ladder.

Production of a polyclonal antibody

The immunization of a New Zealand white female rabbit led to the production of a specific polyclonal antibody against the OMP19 protein. As Fig. 5 shows, during the immunization procedure the titer of the antibody against this protein rose gradually. Figure 6 indicates that a high affinity antibody with a strong reaction was achieved after the last immunization.

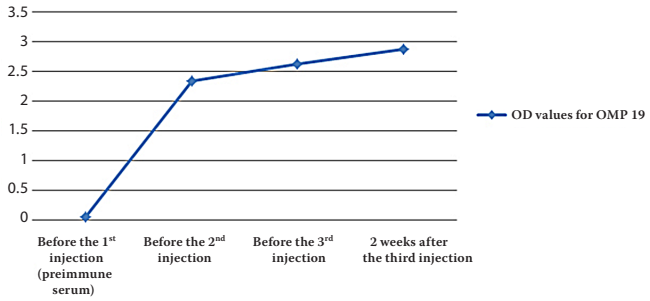

Fig. 5. The production of the polyclonal antibody against the recombinant outer protein 19 kDa (OMP19) of *Brucella* spp. during the immunization of a rabbit by the enzyme-linked immunosorbent assay (ELISA)

OD – optical density.

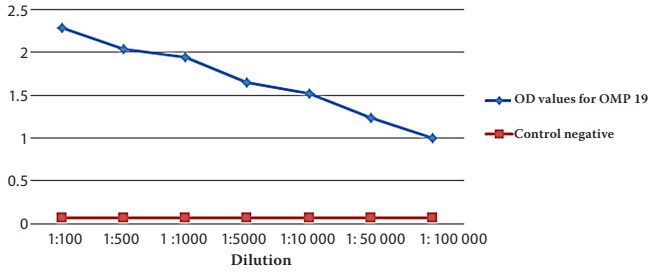

Fig. 6. Determination of the titer of the polyclonal antibody by the enzyme-linked immunosorbent assay (ELISA)

OD – optical density.

Recognition of *Brucella* with a fluorescence microscope

The anti-OMP19 polyclonal antibody conjugated to FITC was able to properly identify *B. abortus*, while the negative controls were not identified (Fig. 7). In evaluating sensitivity and specificity, 16 of 19 *Brucella* isolates and 5 of 10 non-*Brucella* isolates were IF-positive in the test. Therefore, the sensitivity and specificity of this test were 84.2% and 50%, respectively.

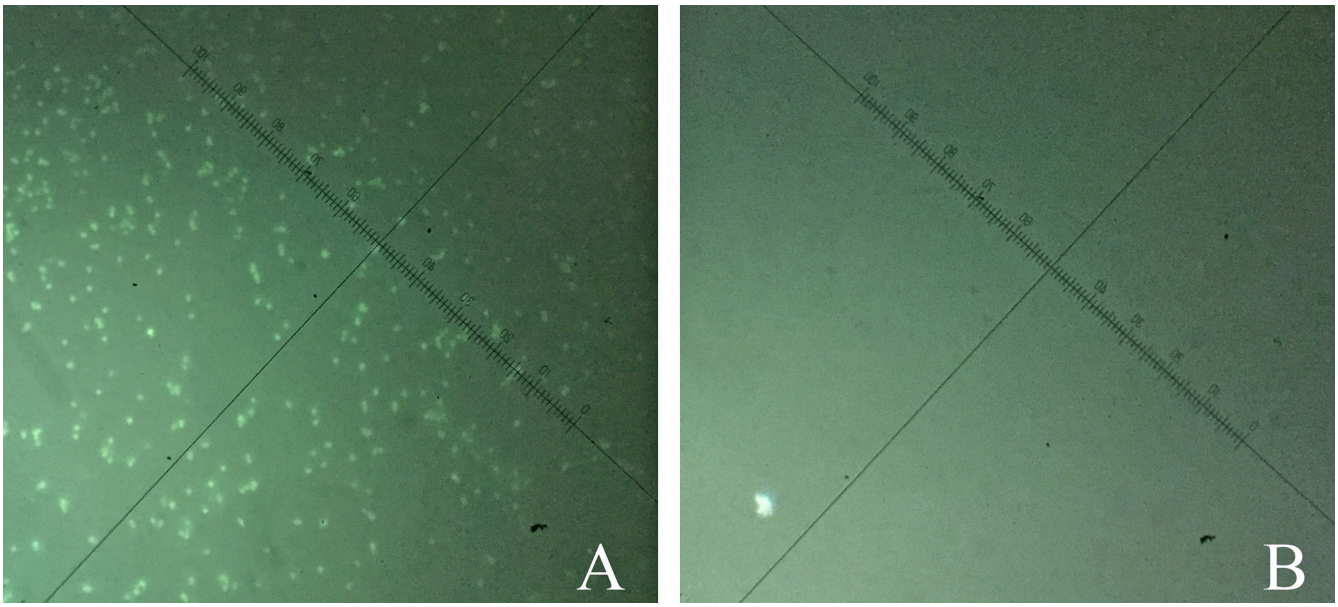

Fig. 7. Recognition of *Brucella* with a fluorescence microscope

A – *B. abortus*; B – negative controls.

Discussion

The diagnosis of brucellosis by serological examinations on the basis of the detection of antibodies against LPS of bacterial cell membranes causes false positive results in some cases because of cross-reactivity with other Gram-negative microorganisms. The OMPs of *Brucella* spp. have been widely considered as potential immunogenic and protective antigens.

In this research, 1 OMP of *Brucella*, a non-LPS group of immunogens, was used. The OMP19 was expressed as a fusion protein containing 6×His-tag. The recombinant OMP19 reacted positively with the antibody against His-tag in blotting assays. The immunization of a New Zealand white female rabbit by the recombinant OMP19 led to a high-titer polyclonal antibody, as showed in ELISA. The high-titer polyclonal antibody can be utilized for experimental biology, medicine, biomedical research, the development of a vaccine and improved diagnostic tests. Some other investigators have previously produced particular antibodies vs several OMPs of *Brucella*. For example, several mAbs to 7 *Brucella* outer membrane proteins were considered by Cloeckaert.[14] These antibodies were achieved by vaccinating mice with sodium dodecyl sulfate-insoluble (SDS-I) portions, cell walls, or whole bacterial cells of *B. melitensis* or *B. abortus*. The OMPs detected by these antibodies were the proteins with a molecular weight of 25–27 kDa and 36–38 kDa (porin) (major proteins), and the proteins with a molecular weight of 10, 16.5, 19, 31–34, and 89 kDa (minor proteins).[26]

The production of an mAb against OMPs with a molecular mass of 25–27 kDa (Ba-4, Ba-5), 36–38 kDa (Ba-6) of *B. abortus* S99 and rOMP31 of goat *Brucella* was performed by Farshad et al. and Zheng et al.[36,37] It was proven by Ghasemi et al. that the immunized serum was achieved from a rabbit that was inoculated with attenuated *B. melitensis.* This serum contained antibodies against recombinant OMP31 (rOMP31).[38] The production of antibodies against OMPs of *B. ovis* in rams was performed by Riezu-Boj et al.[39] The production of immunoglobulins was investigated by Sung et al. in BALB/c immunized with Cu/Zn superoxide dismutase (SOD1) and OMP2b porin of *B. abortus*.[40] The production of an antibody against the minor 89-kDa OMP of *Brucella* in cattle was performed by Limet et al.[41] Western immunoblot analysis using antisera raised against 3 strains of *B. abortus*, i.e., RB 51, S19 and a local field isolate of biotype 1 in buffaloes, indicated the production of antibodies against OMPs in a study by Munir et al.[42] On the basis of previous studies, it can be stated that OMPs of *Brucella* are capable of inducing an immune response and antibody production. These antibodies can be utilized for the improvement of vaccine candidates and diagnostic tests of brucellosis.

The antibody produced against the recombinant OMP19 had a high titer. Therefore, it could be utilized for diagnostic tests of brucellosis and the improvement of vaccine candidates for humans and animals. Moreover, this antibody conjugated to FITC was able to properly identify *B. abortus*. Therefore, it could be used for diagnostic tests of brucellosis in humans and animals. Although the sensitivity of antibodies was high, their specificity was moderate in an IF test. This could be due to some cross-reactions of the polyclonal antibody.

References

1. Baldi PC, Giambartolomei GH, Goldbaum FA, et al. Humoral immune response against lipopolysaccharide and cytoplasmic proteins of *Brucella abortus* in cattle vaccinated with *B. abortus* S19 or experimentally infected with *Yersinia enterocolitica* serotype 0:9. *Clin Diagn Lab Immunol*. 1996;3:472–476.
2. De Bagüés MJ, Marin C, Blasco J, Moriyon I, Gamazo C. An ELISA with *Brucella* lipopolysaccharide antigen for the diagnosis of *B. melitensis* infection in sheep and for the evaluation of serological responses following subcutaneous or conjunctival *B. melitensis* strain Rev 1 vaccination. *Vet Microbiol*. 1992;30:233–241.
3. Raybould T. Antigens of diagnostic significance in *Brucella abortus*. *Can J Microbiol*. 1982;28:557–566.
4. Watarai M, Kim S, Yamamoto J, et al. A rapid agglutination assay for canine brucellosis using antigen coated beads. *J Vet Med Sci*. 2007;69:477–480.
5. Corbel M. Recent advances in brucellosis. *J Med Microbiol*. 1997;46:101–103.
6. Delpino MV, Estein SM, Fossati CA, Baldi PC, Cassataro J. Vaccination with *Brucella* recombinant DnaK and SurA proteins induces protection against *Brucella abortus* infection in BALB/c mice. *Vaccine*. 2007;25:6721–6729.
7. Morgan W, MacKinnon D, Lawson J, Cullen G. The rose bengal plate agglutination test in the diagnosis of brucellosis. *Vet Rec*. 1969;85:636–641.
8. Ruiz-Mesa J, Sánchez-Gonzalez J, Reguera J, Martin L, Lopez-Palmero S, Colmenero J. Rose Bengal test: Diagnostic yield and use for the rapid diagnosis of human brucellosis in emergency departments in endemic areas. *Clin Microbiol Infect*. 2005;11:221–225.
9. Christopher S, Umapathy B, Ravikumar K. Brucellosis: Review on the recent trends in pathogenicity and laboratory diagnosis. *J Lab Physicians*. 2010;2:55.
10. Eskra L, Canavessi A, Carey M, Splitter G. *Brucella abortus* genes identified following constitutive growth and macrophage infection. *Infect Immun*. 2001;69:7736–7742.
11. Lindler LE, Hadfield TL, Tall BD, et al. Cloning of a *Brucella melitensis* group 3 antigen gene encoding Omp28, a protein recognized by the humoral immune response during human brucellosis. *Infect Immun*. 1996;64:2490–2499.
12. Smirnova EA, Vasin AV, Sandybaev NT, et al. Current methods of human and animal brucellosis diagnostics. *Adv Infect Dis*. 2013;3:177–184.
13. Cloeckaert A, Baucheron S, Vizcaino N, Zygmunt MS. Use of recombinant BP26 protein in serological diagnosis of *Brucella melitensis* infection in sheep. *Clin Diagn Lab Immunol*. 2001;8:772–775.
14. Cloeckaert A, Jacques I, Bosseray N, et al. Protection conferred on mice by monoclonal antibodies directed against outer-membrane-protein antigens of *Brucella*. *J Med Microbiol*. 1991;34:175–180.
15. de Bagüés MJ, Elzer P, Blasco J, Marin C, Gamazo C, Winter A. Protective immunity to *Brucella ovis* in BALB/c mice following recovery from primary infection or immunization with subcellular vaccines. *Infect Immun*. 1994;62:632–638.
16. Ficht TA, Bearden S, Sowa B, Adams L. A 36-kilodalton *Brucella abortus* cell envelope protein is encoded by repeated sequences closely linked in the genomic DNA. *Infect Immun*. 1988;56:2036–2046.
17. Gupta V, Kumari R, Vohra J, Singh S, Vihan V. Comparative evaluation of recombinant BP26 protein for serological diagnosis of *Brucella melitensis* infection in goats. *Small Rumin Res*. 2010;93:119–125.
18. Ko KY, Kim JW, Her M et al. Immunogenic proteins of *Brucella abortus* to minimize cross reactions in brucellosis diagnosis. *Vet Microbiol*. 2012;156:374–380.
19. Sowa B, Kelly K, Ficht T, Frey M, Adams L. SDS-soluble and peptidoglycan-bound proteins in the outer membrane-peptidoglycan complex of *Brucella abortus*. *Vet Microbiol*. 1991;27:351–369.

20. Dubray G, Bezard G. Isolation of three *Brucella abortus* cell-wall antigens protective in murine experimental brucellosis. *Ann Rech Vet*. 1980;11:367–373.
21. Verstreate D, Creasy M, Caveney N, Baldwin C, Blab M, Winter A. Outer membrane proteins of *Brucella abortus*: Isolation and characterization. *Infect Immune*. 1982;35:979–989.
22. Gomez-Miguel MJ, Moriyon I. Demonstration of a peptidoglycan-linked lipoprotein and characterization of its trypsin fragment in the outer membrane of *Brucella* spp. *Infect Immune*. 1986;53:678–684.
23. Gomez-Miguel MJ, Moriyon I, Lopez J. *Brucella* outer membrane lipoprotein shares antigenic determinants with *Escherichia coli* Braun lipoprotein and is exposed on the cell surface. *Infect Immune*. 1987;55:258–262.
24. Cassataro J, Pasquevich KA, Estein SM, et al. A DNA vaccine coding for the chimera BLSOmp31 induced a better degree of protection against *B. ovis* and a similar degree of protection against *B. melitensis* than Rev. 1 vaccination. *Vaccine*. 2007;25:5958–5967.
25. Cloeckaert C, Jacques I, Limet J, Dubray G. Immunogenic properties of *Brucella melitensis* cell-wall fractions in BALB/c mice. *J Med Microbiol*. 1995;42:200–208.
26. Cloeckaert A, De Wergifosse P, Dubray G, Limet J. Identification of seven surface-exposed *Brucella* outer membrane proteins by use of monoclonal antibodies: Immunogold labeling for electron microscopy and enzyme-linked immunosorbent assay. *Infect Immune*. 1990;58:3980–3987.
27. Tibor A, Decelle B, Letesson J-J. Outer membrane proteins Omp10, Omp16, and Omp19 of *Brucella* spp. are lipoproteins. *Infect Immune*. 1999;67:4960–4962.
28. Farahi F, Asli E, Mobarez AM, Khoramabadi N, Bakhtiari A. Recombinant *Brucella abortus* outer membrane protein 19 (rOmp19) significantly stimulates splenic lymphocytes of immunized BALB/c mice. *Afr J Microbiol Res*. 2012;6:4128–4131.
29. Giambartolomei GH, Zwerdling A, Cassataro J, Bruno L, Fossati CA, Philipp MT. Lipoproteins, not lipopolysaccharide, are the key mediators of the proinflammatory response elicited by heat-killed *Brucella abortus*. *J Immunol*. 2004;173:4635–4642.
30. Pasquevich KA, Estein SM, Samartino CG, et al. Immunization with recombinant *Brucella* species outer membrane protein Omp16 or Omp19 in adjuvant induces specific CD4+ and CD8+ T cells as well as systemic and oral protection against *Brucella abortus* infection. *Infect Immune*. 2009;77:436–445.
31. Pasquevich KA, IbañezAE, Coria LM, et al. An oral vaccine based on U-Omp19 induces protection against *B. abortus* mucosal challenge by inducing an adaptive IL-17 immune response in mice. *PLoS One*. 2011;6:e16203.
32. Sidhu-Munoz RS, Sancho P, Vizcaino N. *Brucella ovis* PA mutants for outer membrane proteins Omp10, Omp19, SP41, and BepC are not altered in their virulence and outer membrane properties. *Vet Microbiol*. 2016;186:59–66.
33. Tibor A, Saman E, de Wergifosse P, Cloeckaert A, Limet JN, Letesson JJ. Molecular characterization, occurrence, and immunogenicity in infected sheep and cattle of two minor outer membrane proteins of *Brucella abortus*. *Infect Immun*. 1996;64:100–107.
34. Fiorentino MA, Campos E, Cravero S, et al. Protection levels in vaccinated heifers with experimental vaccines Brucella abortus M1-luc and INTA 2. *Vet Microbiol*. 2008;132:302–311.
35. Sambrook J, Russell DW. *Molecular Cloning: A Laboratory Manual*. 3rd ed. New York, NY: Coldspring-Harbour Laboratory Press; 2001.
36. Farshad S, Mehrabanpour M, Namavari M, Hosseini S, Tavakkoli A, Ghaderi A. Production and characterization of monoclonal antibodies against *Brucella abortus* S (99) surface antigens. *Iran Biomed J*. 2002;6:7–12.
37. Zheng W, Wang Y, Zhang Z, Yan F. Immunological characteristics of outer membrane protein omp31 of goat *Brucella* and its monoclonal antibody. *Genet Mol Res*. 2015;14:11965.
38. Ghasemi A, Salari MH, Zarnani AH, et al. Immune reactivity of *Brucella melitensis*-vaccinated rabbit serum with recombinant Omp31 and DnaK proteins. *Iran J Microbiol*. 2013;5:19–23.
39. Riezu-Boj JI, Moriyon I, Blasco J, Gamazo C, Diaz R. Antibody response to *Brucella ovis* outer membrane proteins in ovine brucellosis. *Infect Immune*. 1990;58:489–494.
40. Sung KY, Jung M, Shin MK, et al. Induction of immune responses by two recombinant proteins of *Brucella abortus*, outer membrane proteins 2b porin and Cu/Zn superoxide dismutase, in mouse model. *J Microbiol Biotechnol*. 2014;24:854–861.
41. Limet J, Cloeckaert A, Bezard G, Van Broeck J, Dubray G. Antibody response to the 89-kDa outer membrane protein of *Brucella* in bovine brucellosis. *J Med Microbiol*. 1993;39:403–407.
42. Munir R, Afzal M, Hussain M, Naqvi S, Khanum A. Outer membrane proteins of *Brucella abortus* vaccinal and field strains and their immune response in buffaloes. *Pak Vet J*. 2010;30:110–114.

Impact of selected magnetic fields on the therapeutic effect in patients with lumbar discopathy: A prospective, randomized, single-blinded, and placebo-controlled clinical trial

Jakub Taradaj[1,2,A–F], Marcin Ozon[3,A–F], Robert Dymarek[4,B–E], Bartosz Bolach[5,C–E], Karolina Walewicz[6,A–E], Joanna Rosińczuk[4,B–E]

[1] Department of Physiotherapy Basics, Academy of Physical Education in Katowice, Poland
[2] College of Rehabilitation Sciences, University of Manitoba in Winnipeg, Canada
[3] Private Physiotherapy Practice "OzonMedica Clinic", Gorlice, Poland
[4] Department of Nervous System Diseases, Wroclaw Medical University, Poland
[5] Department of Sport Didactics, University School of Physical Education in Wroclaw, Poland
[6] Institute of Physiotherapy, Public Higher Medical Professional School in Opole, Poland

A – research concept and design; B – collection and/or assembly of data; C – data analysis and interpretation; D – writing the article; E – critical revision of the article; F – final approval of the article

Advances in Clinical and Experimental Medicine, ISSN 1899-5276 (print), ISSN 2451-2680 (online) *Adv Clin Exp Med*. 2018;27(5):649–666

Address for correspondence
Robert Dymarek
E-mail: r.dymarek@gmail.com

Funding sources
None declared

Conflict of interest
None declared

Received on November 16, 2016
Reviewed on November 29, 2016
Accepted on January 27, 2017

Abstract

Background. Interdisciplinary physical therapy together with pharmacological treatment constitute conservative treatment strategies related to low back pain (LBP). There is still a lack of high quality studies aimed at an objective evaluation of physiotherapeutic procedures according to their effectiveness in LBP.

Objectives. The aim of this study is to carry out a prospective, randomized, single-blinded, and placebo-controlled clinical trial to evaluate the effectiveness of magnetic fields in discopathy-related LBP.

Material and methods. A group of 177 patients was assessed for eligibility based on inclusion and exclusion criteria. In the end, 106 patients were randomly assigned into 5 comparative groups: A ($n = 23$; magnetic therapy: 10 mT, 50 Hz); B ($n = 23$; magnetic therapy: 5 mT, 50 Hz); C ($n = 20$; placebo magnetic therapy); D ($n = 20$; magnetic stimulation: 49.2 μT, 195 Hz); and E ($n = 20$; placebo magnetic stimulation). All patients were assessed using tests for pain intensity, degree of disability and range of motion. Also, postural stability was assessed using a stabilographic platform.

Results. In this study, positive changes in all clinical outcomes were demonstrated in group A ($p < 0.05$). The most effective clinical effect was observed for pain reduction ($p < 0.05$), improvement of the range of motion ($p < 0.05$) and functional ability of the spine ($p < 0.05$). It is also worth noting that the effects in the majority of the measured indicators were mostly short-term ($p > 0.05$).

Conclusions. It was determined that the application of magnetic therapy (10 mT, 50 Hz, 20 min) significantly reduces pain symptoms and leads to an improvement of functional ability in patients with LBP.

Key words: low back pain, clinical assessment, lumbar discopathy, stabilometric platform, magnetic field therapy

DOI
10.17219/acem/68690

Copyright
© 2018 by Wroclaw Medical University
This is an article distributed under the terms of the Creative Commons Attribution Non-Commercial License (http://creativecommons.org/licenses/by-nc-nd/4.0/)

Introduction

Lumbar spinal pain syndrome (LSP), commonly referred to as low back pain (LBP), is defined as pain located between the 12th rib and the inferior gluteal folds, which progresses down the lower extremities with the possibility of peripheralization.[1] LBP affects a majority of the population, irrespective of age, as it often begins in childhood and adolescence, where the frequency of occurrence is similar to that in the adult population.[2]

LBP occurs at least once in a lifetime in 65–80% of adults, and in 15% of patients it occurs more frequently, becoming a chronic condition.[3] In 54–90% of patients, symptoms recur within 1 year from the first episode.[4,5] The chronic form of LBP is a major cause of reduced daily life mobility and activity and the related deteriorated quality of life in persons under the age of 45 years.[6,7] Despite the seriousness of the problem, it is possible that no more than 10% of all patients suffering from LBP will seek the help of a physician or a physical therapist.[8]

The lumbar region of the spine is the area where pain is most frequently located due to the greatest multiplane mobility and the occurrence of forces burdening its stabilizing structures, as well as the constant accumulation of micro-injuries and overloading, which most often result from non-ergonomic habits and movement patterns.[9,10] In the vast majority, i.e., 90% of all cases, lumbosacral pain is nonspecific and depends on the level of physical activity, among other things, which translates into excessive overload of the spine.[8,11]

Among the most frequently indicated causes of LBP are degenerative proliferative changes, ankylosing spondylitis, osteoporotic changes, or secondary post-traumatic deformations. However, the most frequent cause of LBP is definitely a chronic intervertebral disc disorder, falling under the term "discopathy".[12] Long-term persistent changes in the affected spinal segments may provoke chronic structural and degenerative disorders in the muscles of the lumbar region.[13]

In addition to pharmacological treatment, interdisciplinary physical therapy is the superior conservative treatment method for ailments related to LBP.[14–17] The methods used for therapeutic purposes include standard kinesiotherapeutic exercises, various massage and neuromobilization methods, proprioception training, and manual mobilization and manipulation techniques in individual therapy with the patient, as well as a wide range of physical methods, including magnetic therapy and magnetic stimulation.[18–22]

Even though many various physical therapy methods are used on a daily basis to combat LBP, few of them are based on substantiated and reliable scientific grounds supported by reliable clinical research of high methodological quality. This also refers to the use of magnetic fields, which may often prove to be of little or no help, and are therefore completely pointless.

Undeniably, there is a justified need for the continuous search for the most efficient methods to help an LBP patient in combating the severe and progressive reduction of mobility which results in secondary pathological changes in the form of various asymmetries and destabilization of the postural pattern, as compared to healthy individuals.[23,24]

Observing the center of pressure and asymmetry in the burden placed on feet in patients with LBP using objective tools, such as a stabilometric (posturographic) test, may be a precise method of monitoring the patient's condition and the ongoing progress of therapy. It also offers full control over the complex treatment process and allows the verification of scientific hypotheses during clinical studies.[25,26]

It is worth noting that none of the articles published to date which present the possibilities of therapeutic application of pulsed magnetic fields in LBP have used several comparison groups in 1 experiment (analysis of the potential effect of magnetic induction on clinical effects). Also, no detailed randomization was used, and such studies were often conducted with relatively small groups of patients and were based solely on subjective questionnaires and pain assessment scales, disregarding the available measurement methods which would objectify therapeutic progress. It must also be stressed that the available studies did not include an analysis of long-term follow-up results which would clearly state whether the achieved therapeutic effect was only temporary or whether there was a long-term remission of symptoms.

The purpose of this study was to attempt to carry out a prospective, randomized and controlled clinical trial with a single blind trial and a thorough analysis of the effectiveness of magnetic fields with varying intensity in the treatment of symptoms of discopathy-related LBP, based on reliable and homogeneous research material. The primary goal was to demonstrate the therapeutic efficacy of magnetic fields with different levels of magnetic induction on pain reduction, functional ability improvement, increased range of joint mobility, and a presentation of positive therapeutic effects in terms of postural control. The secondary goal was to identify the most efficient form of magnetic stimulation, considering the values of magnetic induction with regard to the evaluated clinical symptoms and stabilometric parameters.

Material and methods

Patient qualification

The research project was approved by the Bioethics Commission of the Academy of Physical Education in Katowice (Poland) with resolution No. 10/2012 of December 13, 2012. The study recruited patients with lumbosacral discopathy, referred for physical therapy to the OzonMedica Clinic in Gorlice (Poland). The project spanned from September 2, 2013 to May 20, 2016.

The qualification of patients was done by a team composed of an orthopedist, a neurologist, a neurosurgeon, an internist, a radiologist, and a physical therapist. The selection of patients for participation in the study was purposeful. Patients who qualified for the study suffered from L5–S1 discopathy, chronic (lasting over 6 months) radiating pain and pseudoradicular syndrome, and had no previous surgical procedures within the spinal area. The patients had to be at least 18 years old and have recent magnetic resonance imaging (MRI) scans confirming their diagnosis (at least type III° changes in accordance with the Modic classification in the L5–S1 section). The qualified patients were randomly assigned to 6 comparison groups.

Inclusion and exclusion criteria

Exclusion criteria included: acute spinal pain (lasting less than 6 months, as symptoms lasting longer were treated as chronic), radicular syndrome, discopathy of other spine sections (patients with early type I and II° changes were not excluded from the study, only type III° degeneration as per the Modic classification in the MRI image was grounds for exclusion), no pain or reduction of mobility in the lumbosacral section, other disorders of the spine (spondylolisthesis, fractures, tumors, rheumatic diseases, or cauda equina syndrome), pregnancy, pacemakers, symptoms of defects, cardiovascular diseases, metal implants such as an endoprosthesis of the hip and/or knee joint, mental disorders, cancers, psoriasis, scleroderma, and viral or bacterial infections.

Patients who had undergone spinal surgery or were taking painkillers or anti-inflammatory drugs were also excluded from the study. Moreover, the exclusion criteria included damage to the vestibule and/or a part of the vestibulocochlear nerve, Ménière's syndrome, sudden loss of function of the inner ear, and damage to the cerebellum, spinal cord, or brainstem, resulting in balance disorders.

Patient randomization

The study was conducted on the intention-to-treat approach (patients who for various reasons did not qualify for subsequent stages of the research project were provided with basic medical treatment – painkillers, non-steroidal anti-inflammatory drugs, and mobility rehabilitation – per medical recommendations). The randomized assignment of patients to individual groups was continuous during the entire duration of the study, i.e., each newly qualified person was randomized by a computer number generator and assigned to a given comparison group accordingly.

Characteristics of the procedures

Patients in group A were treated with magnetic therapy. The treatment parameters were rectangular flow, a magnetic induction of 10 mT, a frequency of 50 Hz, each treatment lasting 20 min, and the application method was an induction coil 60 cm in diameter.

Patients in group B were also treated with magnetic therapy. The treatment parameters were rectangular flow, a magnetic induction of 5 mT, a frequency of 50 Hz, each treatment lasting 20 min, and the application method was an induction coil 60 cm in diameter.

Patients in group C, however, were treated with pseudo-magnetic therapy (simulated treatment: treatment parameters were set with the device switched on, but no real application took place). This group was meant to constitute the single blind trial (patients had no knowledge of which group they belonged to) and to evaluate the placebo effect during studies of this kind of therapy.

Patients in group D were treated with magnetic stimulation. The treatment parameters were rectangular flow, a magnetic induction of 49.2 μT, a frequency of 195 Hz, each treatment lasting 20 min, and the application method was a pillow 45 cm × 24 cm × 3 cm.

Patients in group E were administered pseudo-magnetic stimulation (treatment parameters were set, but as with group C no application took place). In this case, the group constituted the blind trial and simulated treatment for real magnetic stimulation.

A detailed flow of participants at each stage of the project is shown in Fig. 1. Patients in all of the comparison groups were homogeneous in terms of basic characteristics specific for the studied populations (Table 1). The groups were also homogeneous as regards the initial measurements concerning pain assessment, functional state, mobility range, and body posture.

Apart from physical therapy, patients in all groups underwent a uniform basic therapy through motor improvement in the form of functional training (45 min once a day for 5 days/week). Standard stabilization training comprised the following elements: (1) myofascial release techniques for the erector spinae muscle; (2) activation techniques for the neutral position of the lumbo-pelvic-hip complex and deep-core muscles; (3) activation of proper breathing and exercising the transversus abdominis muscle; (4) coordination of the work of superficial and deep-core muscles; and (5) postural and dynamic training.

Patients in all comparison groups were subjected to a series of 15 physical therapy treatments, 5 times a week (Monday to Friday) for a period of 3 weeks. Magnetic therapy (in groups A, B and C) was performed using the Cyborg Mag generator (Cosmogamma, Cento, Italy). Treatments were performed in a coil applicator with a diameter of 60 cm, mounted on the system of longitudinal drive rails of the treatment bed. During treatment, the patients lay down on their back on the treatment bed, and their lumbosacral region was positioned within the induction coil. Magnetic stimulation was performed using the Viofor JPS device (Med & Life, Komorów, Poland). Treatments were also performed in the lie-back position: the patients lay on the bed so that the lumbosacral section of their spine was directly on a special pillow (applicator), remaining in constant contact.

Table 1. Characteristics of study population in each group after random allocation

Characteristic	Group A	Group B	Group C	Group D	Group E	p-value
Gender (n) female/male	15/8	16/7	12/8	13/7	14/6	>0.05*
Age [years] mean SD	50.45 10.11	55.20 11.40	52.30 8.22	51.80 11.50	55.75 9.28	>0.05**
Hight [cm] mean SD	163.89 5.33	168.20 7.18	167.10 6.88	165.30 6.82	164.95 7.66	>0.05**
Body mass [kg] mean SD	78.30 17.92	72.77 13.10	74.77 14.09	72.20 12.46	79.11 18.11	>0.05**
Obesity (n) BMI > 30 kg/m^2	11	8	6	6	8	>0.05*
Disease duration [years] mean SD	4.12 3.76	3.96 3.12	4.35 3.78	4.77 4.08	4.34 3.89	>0.05**
Osteoarthritis (n) right side/left side	15/8	14/9	12/8	11/9	12/8	>0.05*
Radiological changes in Modic classification (n) III°/IV°	17/6	16/7	15/5	15/5	14/6	>0.05*
Pain intensity in VAS (score) mean SD	5.80 2.56	5.55 1.75	5.70 1.88	5.70 2.49	5.40 1.63	>0.05**
Pain intensity in LPS (score) mean SD	5.90 2.21	6.10 1.89	6.30 3.07	5.85 2.36	6.20 2.83	>0.05**
Disability level in ODI (score) mean SD	16.50 8.27	15.95 8.12	16.15 7.98	15.70 8.41	16.10 8.04	>0.05**
Disability level in RMDQ (score) mean SD	12.05 6.18	13.90 7.12	13.10 6.65	12.95 6.56	13.86 2.16	>0.05**
Body posture in sagittal plane [mm] mean SD	125.12 90.11	125.19 98.45	120.89 104.12	123.17 91.22	124.03 93.82	>0.05**
Body posture in frontal plane [mm] mean SD	101.49 80.23	100.21 82.39	102.88 85.02	102.63 84.12	100.95 80.99	>0.05**

Statistical tests for homogeneity analyses between study groups: * χ^2 test with the highest reliability; ** Friedmann's ANOVA homogeneity test; VAS – Visual Analogue Scale; LPS – Laitinen Pain Scale; ODI – Oswestry Disability Index; RMDQ – Roland-Morris Disability Questionnaire.

Pain questionnaires and functional tests

In order to analyze the therapeutic progress for the subjective assessment of pain, functional capacity and degree of disability, the following tests were performed:

– the Visual Analogue Scale pain assessment scale (VAS) – used to subjectively assess the experienced pain. The patient assesses the experienced pain on a simple scale from 0 to 10, where 0 denotes a lack of pain and 10 denotes the most acute pain;

– the Laitinen Pain Scale (LPS) – in the modified Laitinen Pain Scale, 4 indicators are assessed: pain intensity, frequency of pain occurrence, use of analgesics, and limitations of mobility;

– the Oswestry Questionnaire (The Oswestry Low-Back Pain Disability Questionnaire, Oswestry Disability Index – ODI) – used to evaluate the functional ability of patients; a widely recognized and reliable scale for evaluating patients with low back pain. The questionnaire consists of 10 questions regarding symptoms and everyday activities. When answering the individual questions, the patient can choose 1 of the 6 options scored 0–5: A – 0 points; B – 1 point; C – 2 points; D – 3 points; E – 4 points; and F – 5 points. After summing the scores for all questions, the Oswestry Disability Index is calculated as follows: no disability (0–4 points); minimal disability (5–14 points); moderate disability (15–24 points); severe disability (25–34 points); or full disability (35–50 points);

– The Roland-Morris Disability Questionnaire (RMDQ) – used to assess the degree of disability in patients with low back pain. It reflects the condition of the patient on the day of the examination. The questionnaire contains

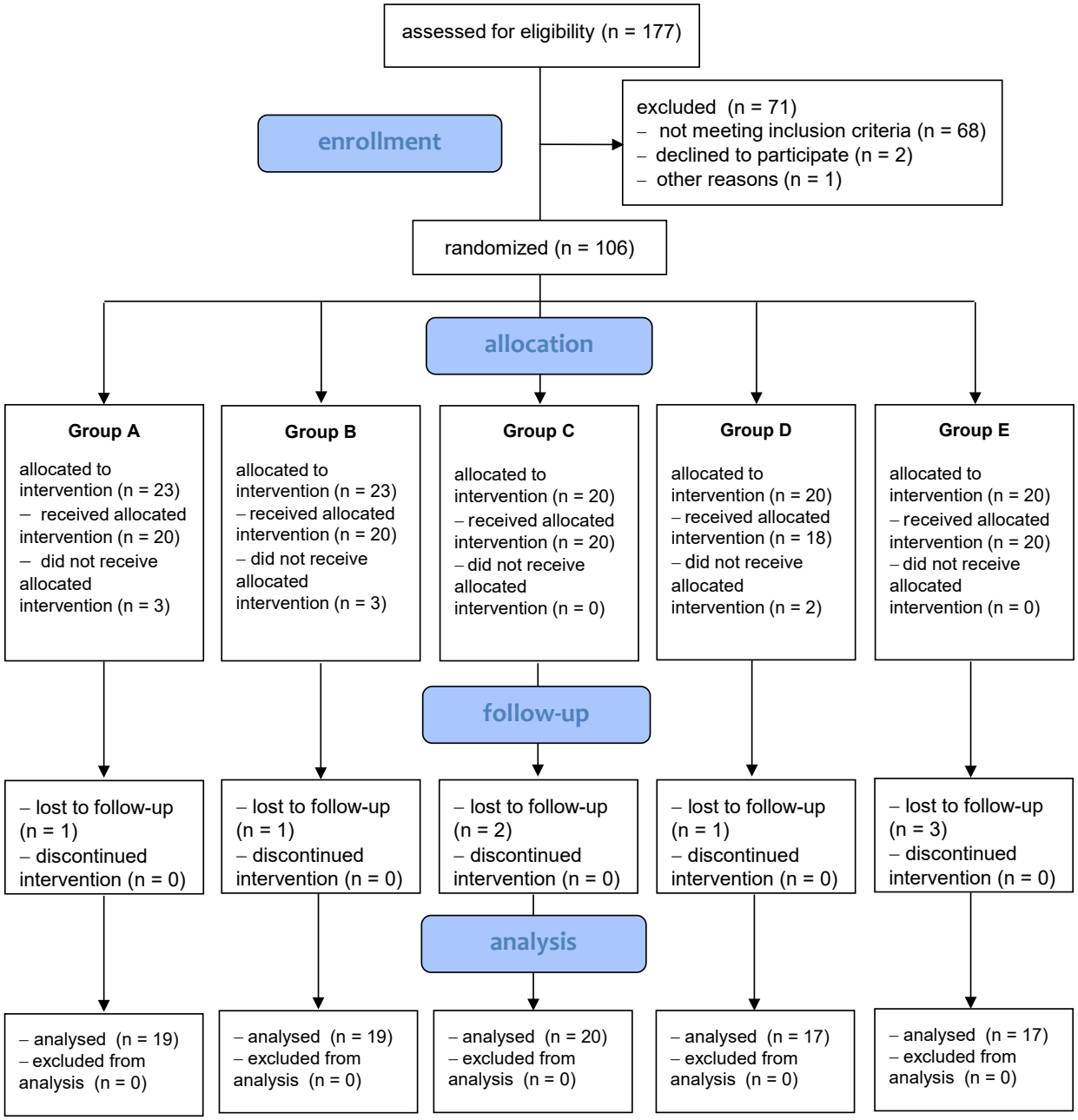

Fig. 1. Flowchart of patients' assessment for eligibility in the study in all stages

24 questions which are answered 'yes' or 'no'. Each 'yes' answer scores 1 point and each 'no' answer scores 0 points. After summing the scores for all questions, the Roland-Morris disability index is given as follows: no disability (0–3 points); minimal disability (4–10 points); moderate disability (11–17 points); or severe disability (18–24 points);

– the Lasègue test (LaT) – may be used to measure the range of motion of the hip joint on the side of the herniated disc in the course of spinal discopathy. The starting position is with the patient lying down on his or her back with both legs straight. The examiner then slowly lifts one of the patient's legs while the knee is straight at the joint until pain is noted. The mobility range is measured in degrees of angle using a goniometer;

– the Schober test (ShT) – used to evaluate the mobility of the lumbosacral spine. While the patient is in a standing position, the examiner marks 2 points on the patient's skin: the first one 10 cm above the line connecting the posterior superior iliac spines, and the other one 5 cm below that line. The patient then slowly bends down as far as possible, while keeping the knees straight. The measurement is made using a tape measure. The obtained result is accurate within 0.5 cm. The range of motion tests were carried out by the same technician and each measurement was an arithmetic mean of 5 trials.

Postural stability assessment

Additionally, an objective measurement tool for evaluating postural stability was used. The evaluation was performed using a double-plate stabilographic platform (SP) equipped with a computer-aided posturographic system, model CQ Stab2P (CQ Electronic System, Czernica, Poland).

The measurement error was 0.86%. For each patient, 2 trials were carried out: the 1st trial with eyes open in full visual control, and the 2nd trial with eyes closed and no visual control. The subjects were in a habitual upright position, standing barefoot on the SP (feet apart in line with their hips, arms down alongside their bodies, head facing forward, and eyes fixed on a designated point at eye level about 1.5 m away).

Statistical analyses of the basic posturographic parameters were conducted in order to compare balance in the tested groups of patients. The following parameters were analyzed: (1) SPAP – anterior/posterior path length in the sagittal plane [mm]; (2) SPML – medio/lateral path length in the frontal plane [mm]; (3) SA – sway area (the total sway area of the center of pressure during the 30-second trial) [mm^2]; (4) MF – mean frequency of sway in all planes [Hz]; and (5) MV – mean velocity of sway in all planes [mm/s].

The abovementioned measurements of posture-related parameters were made before and after the treatment process. In the second stage of the project, the measurements were repeated (along with the subjective research based on questionnaires and functional tests) as long-term results (follow-up) 1 and 3 months after completion of the study (during this period, the patients were not subjected to any treatment).

Statistical analysis

The results were analyzed using STATISTICA v. 10.0 software (StatSoft Inc., Tulsa, USA). The normality of sample distribution was analyzed with the Shapiro-Wilk test. The distribution of the samples in most cases were not consistent with a normal distribution, hence the use of non-parametric tests. Skewness and kurtosis (flatness) were less than 2.5 and they were unimodal distributions, therefore the arithmetic mean and standard deviation were taken as a measure of central tendency and dispersion. The homogeneity of the distribution of patients' characteristics in all groups was analyzed with the most reliable version of the χ^2 test and the Kruskal-Wallis homogeneity test. Statistical significance was set at $p < 0.05$. Friedmann's ANOVA analysis was used for dependent variables, and nonparametric Kruskal-Wallis variance analysis was used for independent variables. Tukey's post hoc multiple comparisons test was used to identify the exact dependencies resulting from the variance analysis between individual groups, and the Bonferroni's post hoc test was used for analysis of multiple intra-group measurements. Statistical significance was set at $p < 0.05$.

Results

Analysis of the Visual Analogue Scale pain intensity scores

All the comparison groups demonstrated a statistically significant reduction in pain, as compared to the initial values, measured according to the VAS scale (Table 2).

In group A (magnetic therapy 10 mT), the value of pain sensations decreased during the 3-week treatment period from 5.80 to 2.15 points on average ($p = 0.0015$ in the post hoc analysis). Interestingly, at the 1-month follow-up evaluation, a further reduction of pain was observed in relation to the condition directly after the treatments from 2.15 to 1.40 points on average ($p = 0.0401$ in the post hoc analysis). However, at 3 months post-therapy, in relation

Table 2. Intragroup comparisons of pain intensity changes in VAS and LPS scores before and after treatment

Characteristic		Before treatment		After treatment		1 month after treatment		3 months after treatment	
		VAS[a]	LPS[b]	VAS[a]	LPS[b]	VAS[a]	LPS[b]	VAS[a]	LPS[b]
Group A	mean	5.80	5.90	2.15	3.10	1.40	3.20	1.55	3.30
	SD	2.56	2.21	1.69	2.45	1.33	2.38	1.29	2.59
Group B	mean	5.55	6.10	3.25	4.15	2.20	4.20	2.45	4.35
	SD	1.75	1.89	1.35	2.53	1.78	2.70	1.56	2.69
Group C	mean	5.70	6.30	3.20	4.35	2.75	4.50	2.90	4.65
	SD	1.88	3.07	1.27	2.71	1.56	2.86	1.86	2.96
Group D	mean	5.70	5.85	3.10	4.10	2.20	4.25	2.30	4.35
	SD	2.49	2.36	1.99	2.15	1.68	2.61	1.74	2.78
Group E	mean	5.40	6.20	3.10	4.30	2.70	4.35	2.85	4.55
	SD	1.63	2.83	1.41	2.11	1.44	2.45	1.74	2.77

[a] Friedmann's ANOVA analysis (a total values of significant levels in each groups without the post hoc Bonferroni's test): group A ($p = 0.0128$); group B ($p = 0.0380$); group C ($p = 0.0372$); group D ($p = 0.0367$); group E ($p = 0.0370$); [b] Friedmann's ANOVA analysis (a total values of significant levels in each groups without the post hoc Bonferroni's test): group A ($p = 0.0358$); group B ($p = 0.0460$); group C ($p = 0.0471$); group D ($p = 0.0466$); group E ($p = 0.0478$); VAS – Visual Analogue Scale; LPS – Laitinen Pain Scale; SD – standard deviation.

to the value recorded at 1 month post-therapy, there was a gradual, albeit statistically insignificant, increase in the pain level (from 1.40 to 1.55 points on average, $p > 0.05$ in the post hoc analysis).

On the other hand, in group B (magnetic therapy 5 mT), during the 3-week treatment period, the recorded values of pain sensations were reduced from 5.55 to 3.25 points on average ($p = 0.0082$ in the post hoc analysis). Again, it was interesting to observe that in the follow-up evaluation at 1 month post-therapy a further reduction of pain was observed in relation to the condition directly post-treatment – from 3.25 to 2.20 points on average ($p = 0.0278$ in the post hoc analysis). However, at 3 months post-therapy, in relation to the value recorded at 1 month post-therapy, there was a gradual, statistically insignificant recurrence of pain sensations (from 2.20 to 2.45 points on average, $p > 0.05$ in the post hoc analysis).

In group C (magnetic therapy, placebo), after 3 weeks of simulated treatments the value of pain sensations was reduced from 5.70 to 3.20 points on average ($p = 0.0061$ in the post hoc analysis). Here again, in the follow-up evaluation at 1 month post-therapy, a further reduction of pain was observed compared to the condition directly post-treatment – from 3.20 to 2.75 points on average ($p = 0.0478$ in the post hoc analysis). Similarly to the previous groups, at 3 months post-therapy a tendency of increased pain sensations was observed as compared to the value at 1-month post-therapy (from 2.75 to 2.90 points on average, $p > 0.05$ in the post hoc analysis).

In group D (magnetic stimulation), during the 3-week treatment period, the index of pain sensations decreased from 5.70 to 3.10 points on average ($p = 0.0052$ in the post hoc analysis). Interestingly, the follow-up evaluation at 1 month post-therapy showed a further reduction of pain in relation to the condition directly post-treatment – from 3.10 to 2.20 points on average ($p = 0.0352$ in the post hoc analysis). However, in the follow-up evaluation at 3 months post-therapy, a slight increase in pain was observed (from 2.20 to 2.30 points on average, $p > 0.05$ in the post hoc analysis).

In group E (magnetic stimulation, placebo), after 3 weeks of simulated treatments the index of pain sensations was reduced from 5.40 to 3.10 points on average ($p = 0.0088$ in the post hoc analysis). Curiously, in the follow-up evaluation at 1 month post-therapy, a further change in the pain sensations was observed, as compared to the condition directly post-treatment – from 3.10 to 2.70 points on average ($p = 0.0488$ in the post hoc analysis). Similarly, at 3 months post-therapy – in relation to the value recorded at 1 month post-therapy – a statistically insignificant recurrence of pain was recorded (from 2.70 to 2.85 points on average, $p > 0.05$ in the post hoc analysis).

In conclusion, it may be observed that the greatest rate of progress of the therapy, as measured according to the VAS scale, occurred in all study groups within the 3-week period when kinesiotherapy and physical treatments were used (this also refers to the simulated placebo treatments). Despite discontinuing the treatment process, the analgesic effect continued and was relatively stable. Moreover, during the 1-month period after cessation of therapy (in the follow-up observation) a further significant decrease in pain sensations was recorded in patients (despite the lack of any medical treatment). Unfortunately, the long-term results at 3-month follow-up showed a tendency, albeit statistically insignificant, of a gradual recurrence of pain in all study groups.

This means that the therapeutic progress was significant, but short-term in nature, which may be confirmed by the signs of deterioration of progress 3 months after completion of the therapeutic process.

Analysis of the Laitinen Pain Scale pain intensity scores

A similarly subjective reduction in pain was recorded using the Laitinen questionnaire (Table 2). The therapy was effective in all study groups because at each stage of the project, improvement was recorded in relation to the pre-treatment condition. However, as in the case of the VAS scale, the effect was rather short-term because the follow-up results showed a negative trend of increasing pain sensations (in this case, an unfavorable statistical trend of deterioration occurred even 1 month post-therapy, which unfortunately continued in the subsequent measurement at 3-month follow-up).

In group A (magnetic therapy 10 mT) during the 3-week treatment period, the value of pain sensations reduced from 5.90 to 3.10 points on average ($p = 0.0014$ in the post hoc analysis). At 1 month post-therapy, a slight increase in pain was observed in relation to the previous state – from 3.10 to 3.20 points on average ($p > 0.05$ in the post hoc analysis). At 3 months post-therapy, in relation to the value recorded at 1 month post-therapy, there was a further, statistically insignificant, increase (from 3.20 to 3.30 points on average, $p > 0.05$ in the post hoc analysis).

On the other hand, in group B (magnetic therapy 5 mT), during the 3-week treatment period, the assessment of pain was reduced from 6.10 to 4.15 points on average ($p = 0.0092$ in the post hoc analysis). One month after the completion of therapy, however, a statistically insignificant increase in symptoms compared to the earlier state was observed – from 4.15 to 4.20 points on average ($p > 0.05$ in the post hoc analysis). At 3 months post-therapy, a further, gradual recurrence of pain sensations was recorded in relation to the value 1 month after the completion of therapy (from 4.20 to 4.35 points on average, $p > 0.05$ in the post hoc analysis).

In group C (magnetic therapy, placebo), after 3 weeks of simulated treatments the value of pain sensations was reduced from 6.30 to 4.35 points on average ($p = 0.0091$ in the post hoc analysis). Follow-up evaluation at 1 month post-therapy revealed an unfavorable, albeit insignificant, increase in pain symptoms as compared to the condition directly post-treatment – from 4.35 to 4.50 points

on average (p > 0.05 in the post hoc analysis). Similarly to the previous groups, at 3 months post-therapy a further, slight increase in pain sensations was recorded in relation to the value at 1 month after the completion of therapy (from 4.50 to 4.65 points on average, p > 0.05 in the post hoc analysis).

In group D (magnetic stimulation) during the 3-week treatment period, the value of pain symptoms decreased from 5.85 to 4.10 points on average (p = 0.0092 in the post hoc analysis). Unfortunately, at 1 month post-therapy an increase (statistically insignificant) in symptoms was observed in relation to the previous state – from 4.10 to 4.25 points on average (p > 0.05 in the post hoc analysis). After 3 months, a further slight increase in pain sensations was observed (from 4.25 to 4.35 points on average, p > 0.05 in the post hoc analysis).

In group E (magnetic stimulation, placebo), after 3 weeks of simulated treatments the value of pain sensations reduced from 6.20 to 4.30 points on average (p = 0.0091 in the post hoc analysis). At 1 month post-therapy, an unfavorable trend was observed in relation to the earlier state – an increase, on average, from 4.30 to 4.35 points (p > 0.05 in the post hoc analysis). Similarly, at 3 months post-therapy, in relation to the value recorded at 1 month post-therapy, a statistically insignificant recurrence of pain was recorded (from 4.30 to 4.55 points on average, p > 0.05 in the post hoc analysis).

The intergroup analysis we conducted demonstrates that the greatest analgesic effect was recorded in group A, where the results were significantly better than in other groups. Results obtained with an application of a magnetic field of 10 mT were statistically significantly better than those obtained with magnetic stimulation or magnetic therapy using lower induction. The advantage of group A over the remaining groups was clearly visible at all stages of treatment. Curiously, no differences were observed between groups B (magnetic therapy 5 mT), C (pseudo-magnetic therapy), D (magnetic stimulation), and E (pseudo-magnetic stimulation), which attests to the fact that the other magnetic fields did not produce positive effects compared to the placebo methods.

This is confirmed by both the results of measurements performed using the VAS scale (Fig. 2) and by the Laitinen questionnaire (Fig. 3).

Analysis of the Oswestry Disability Index functional ability scores

After 3 weeks of therapy, all of the comparison groups demonstrated a statistically significant improvement of functional ability, as measured by the ODI (Table 3).

In group A (magnetic therapy, 10 mT) functional ability improved significantly during the 3 weeks of therapy (p = 0.0041 in the post hoc analysis). The follow-up evaluation (1 month after the end of therapy) showed a statistically insignificant decrease in functional ability (p > 0.05). A similarly unfavorable statistical tendency also occurred in the evaluation 3 months after the end of physical therapy treatments (p > 0.05).The same applied to group B (magnetic therapy, 5 mT), where functional ability measured by the ODI had initially significantly improved after the therapy (p = 0.0225 in the post hoc analysis). Unfortunately,

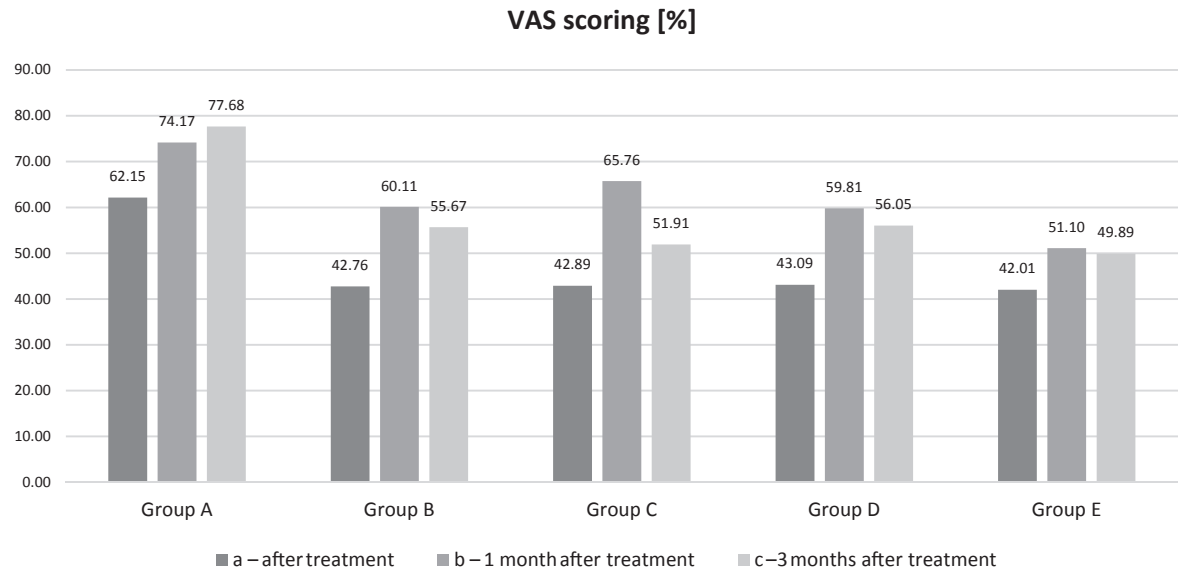

Fig. 2. Intergroup comparisons of the pain intensity reduction in VAS scoring [%] after treatment and in follow-up analyses, 1 and 3 months after treatment

a – Kruskal-Wallis ANOVA analysis (p = 0.0328); T Tukey's post hoc analysis: p(A,B) = 0.0122, p(A,C) = 0.0188, p(A,C) = 0.0224, p(A,E) = 0.0122, p(B,C) > 0.05, p(B,D) > 0.05, p(B,E) > 0.05, p(C,D) > 0.05, p(C,E) > 0.05, p(D,E) > 0.05; b – Kruskal-Wallis ANOVA analysis (p = 0.0466); T Tukey's post hoc analysis: p(A,B) = 0.0380, p(A,C) = 0.0182, p(A,C) = 0.0224, p(A,E) = 0.0122, p(B,C) > 0.05, p(B,D) > 0.05, p(B,E) > 0.05, p(C,D) > 0.05, p(C,E) > 0.05, p(D,E) > 0.05; c – Kruskal-Wallis ANOVA analysis (p = 0.0403); T Tukey's post hoc analysis: p(A,B) = 0.0280, p(A,C) = 0.0166, p(A,C) = 0.0124, p(A,E) = 0.0082, p(B,C) > 0.05, p(B,D) > 0.05, p(B,E) > 0.05, p(C,D) > 0.05, p(C,E) > 0.05, p(D,E) > 0.05.

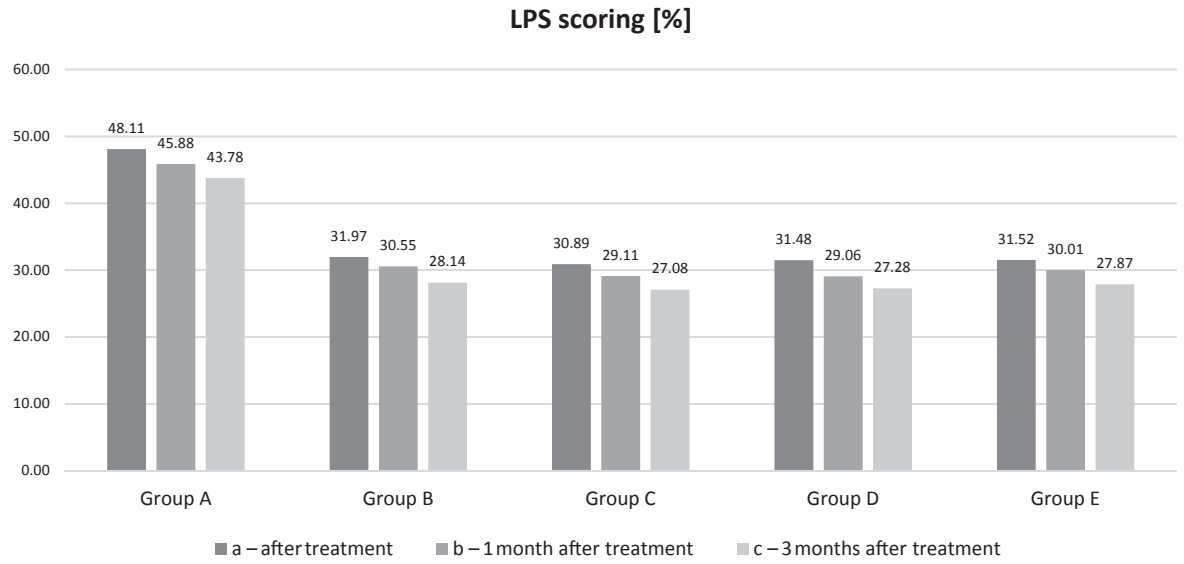

Fig. 3. Intergroup comparisons of the pain intensity reduction in LPS scoring [%] after treatment and in follow-up analyses, 1 and 3 months after treatment

a – Kruskal-Wallis ANOVA analysis (p = 0.0368); T Tukey's post hoc analysis: p(A,B) = 0.0228, p(A,C) = 0.0122, p(A,C) = 0.0260, p(A,E) = 0.0272, p(B,C) > 0.05, p(B,D) > 0.05, p(B,E) > 0.05, p(C,D) > 0.05, p(C,E) > 0.05, p(D,E) > 0.05; b – Kruskal-Wallis ANOVA analysis (p = 0.0388); T Tukey's post hoc analysis: p(A,B) = 0.0208, p(A,C) = 0.0380, p(A,C) = 0.0382, p(A,E) = 0.0182, p(B,C) > 0.05, p(B,D) > 0.05, p(B,E) > 0.05, p(C,D) > 0.05, p(C,E) > 0.05, p(D,E) > 0.05; c – Kruskal-Wallis ANOVA analysis (p = 0,0390); T Tukey's post hoc analysis: p(A,B) = 0.0224, p(A,C) = 0.0240, p(A,C) = 0.0270, p(A,E) = 0.0270, p(B,C) > 0.05, p(B,D) > 0.05, p(B,E) > 0.05, p(C,D) > 0.05, p(C,E) > 0.05, p(D,E) > 0.05.

Table 3. Intragroup comparisons of the disability level changes in ODI and RMDQ scoring before and after treatment

Characteristic		Before treatment		After treatment		1 month after treatment		3 months after treatment	
		ODI[a]	RMDQ[b]	ODI[a]	RMDQ[b]	ODI[a]	RMDQ[b]	ODI[a]	RMDQ[b]
Group A	mean	16.50	12.05	10.10	6.15	10.20	6.30	11.15	6.55
	SD	8.27	6.18	6.58	4.88	6.82	5.28	7.19	5.54
Group B	mean	15.95	13.90	12.25	9.15	13.00	9.30	13.20	9.40
	SD	8.12	7.12	6.44	5.12	6.43	5.48	7.87	6.11
Group C	mean	16.15	13.10	12.75	9.05	12.90	9.15	13.15	9.25
	SD	7.98	6.65	6.78	5.18	7.77	5.55	10.62	6.72
Group D	mean	15.70	12.95	12.10	9.15	12.75	9.25	13.10	9.30
	SD	8.41	6.56	5.72	5.70	7.53	5.83	10.82	7.03
Group E	mean	16.10	13.85	12.50	9.55	13.05	9.65	13.20	9.80
	SD	8.04	2.16	6.63	5.53	7.45	6.05	9.59	7.09

[a] Friedmann's ANOVA analysis (a total values of significant levels in each groups without the post hoc Bonferroni's test): group A (p = 0.0288); group B (p = 0.0473); group C (p = 0.0475); group D (p = 0.0466); group E (p = 0.0478); [b] Friedmann's ANOVA analysis (a total values of significant levels in each groups without the post hoc Bonferroni's test): group A (p = 0.0112); group B (p = 0.0278); group C (p = 0.0291); group D (p = 0.0282); group E (p = 0.0270); ODI – Oswestry Disability Index; RMDQ – Roland-Morris Disability Questionnaire; SD – standard deviation.

in the follow-up observations (at 1 month and 3 months post-therapy) the situation was reversed and a statistical trend was observed towards deterioration of functional ability in the patients (p > 0.05).

Similarly, group C (magnetic therapy, placebo) demonstrated an intense, although short-term, improvement of the patients' ability (p = 0.0242 in the post hoc analysis), but the process did not continue and follow-up observations showed a tendency towards a gradual weakening of the ODI (p > 0.05).

In case of group D (magnetic stimulation), a significant increase in functional ability was detected in short-term observation (p = 0.0317 in the post hoc analysis), but as with the previous groups, after the therapy was stopped a slight deterioration of effects occurred (p > 0.05).

In group E (magnetic stimulation, placebo) the recorded changes were similar, i.e., the patients' ability improved after the 3-week therapy (p = 0.0235 in the post hoc analysis). However, similarly to the previously discussed groups, a statistical trend reflecting a gradual recurrence of adverse symptoms occurred (p > 0.05). Detailed data concerning the Oswestry questionnaire are presented in Fig. 4.

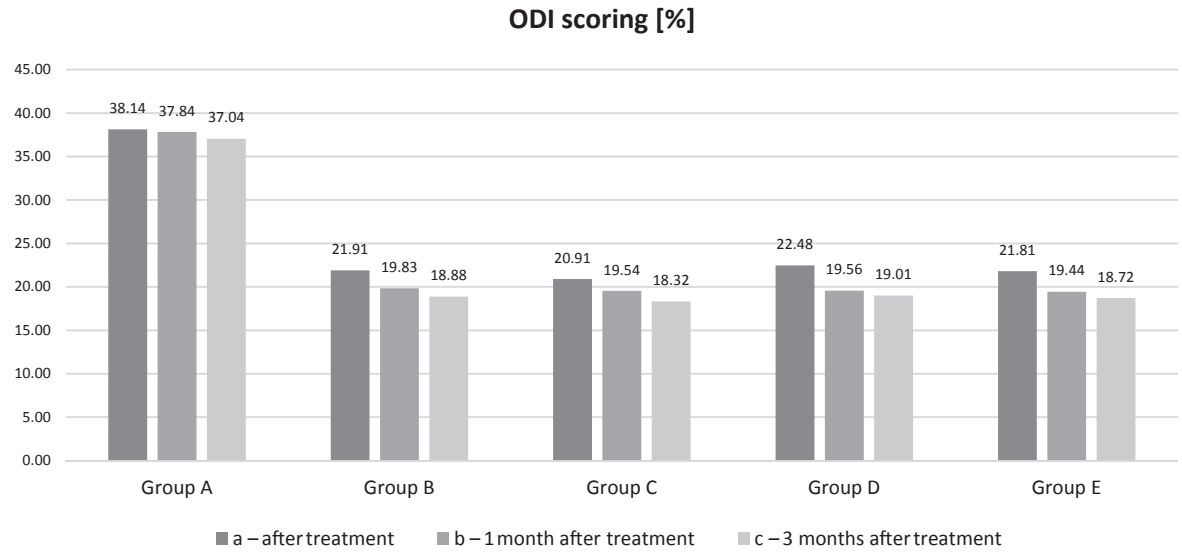

Fig. 4. Intergroup comparisons of the disability level diminishment in ODI scoring [%] after treatment and in follow-up analyses, 1 and 3 months after treatment

a – Kruskal-Wallis ANOVA analysis (p = 0.0408); T Tukey's post hoc analysis: p(A,B) = 0.0288, p(A,C) = 0.0220, p(A,C) = 0.0298, p(A,E) = 0.0292, p(B,C) > 0.05, p(B,D) > 0.05, p(B,E) > 0.05, p(C,D) > 0.05, p(C,E) > 0.05, p(D,E) > 0.05; b – Kruskal-Wallis ANOVA analysis (p = 0.0408); T Tukey's post hoc analysis: p(A,B) = 0.0288, p(A,C) = 0.0220, p(A,C) = 0.0298, p(A,E = 0.0292, p(B,C) > 0.05, p(B,D) > 0.05, p(B,E) > 0.05, p(C,D) > 0.05, p(C,E) > 0.05, p(D,E) > 0.05; c – Kruskal-Wallis ANOVA analysis (p = 0.0455); T Tukey's post hoc analysis: p(A,B) = 0.0305, p(A,C) = 0.0288, p(A,C) = 0.0341, p(A,E) = 0.0312, p(B,C) > 0.05, p(B,D) > 0.05, p(B,E) > 0.05, p(C,D) > 0.05, p(C,E) > 0.05, p(D,E) > 0.05.

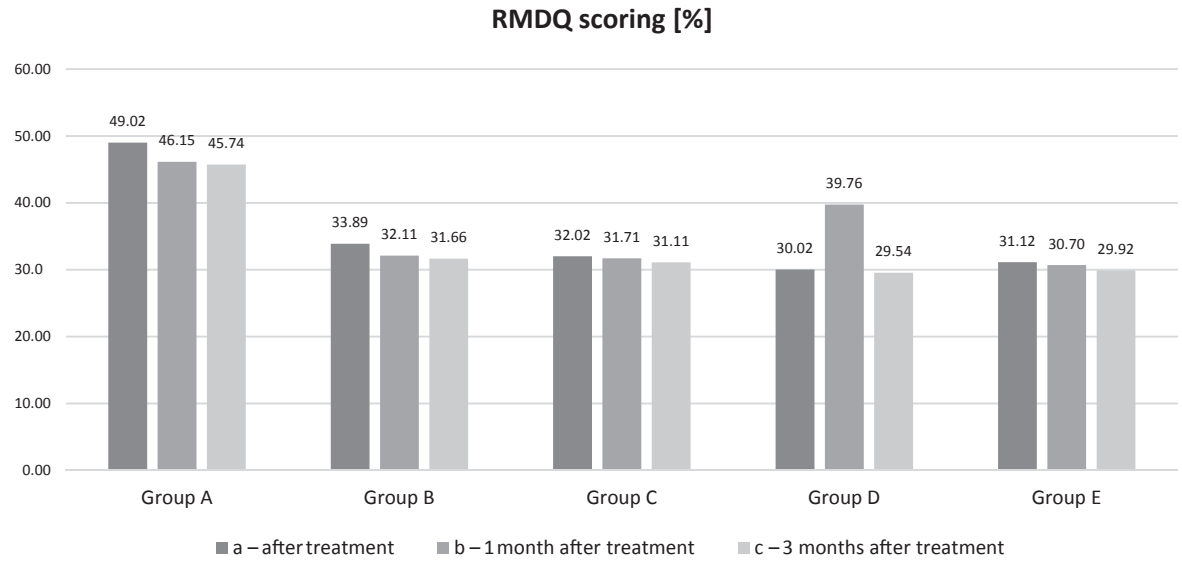

Fig. 5. Intergroup comparisons of the disability level diminishment in RMDQ scoring [%] after treatment and in follow-up analyses, 1 and 3 months after treatment

a – Kruskal-Wallis ANOVA analysis (p = 0.0388); T Tukey's post hoc analysis: p(A,B) = 0.0320, p(A,C) = 0.0212, p(A,C) = 0.0208, p(A,E) = 0.0256, p(B,C) > 0.05, p(B,D) > 0.05, p(B,E) > 0.05, p(C,D) > 0.05, p(C,E) > 0.05, p(D,E) > 0.05; b – Kruskal-Wallis ANOVA analysis (p = 0.0466); T Tukey's post hoc analysis: p(A,B) = 0.0310, p(A,C) = 0.0317, p(A,C) = 0.0268, p(A,E) = 0.0286, p(B,C) > 0.05, p(B,D) > 0.05, p(B,E) > 0.05, p(C,D) > 0.05, p(C,E) > 0.05, p(D,E) > 0.05; c – Kruskal-Wallis ANOVA analysis (p = 0.0443); T Tukey's post hoc analysis: p(A,B) = 0.0330, p(A,C) = 0.0347, p(A,C) = 0.0298, p(A,E) = 0.0306, p(B,C) > 0.05, p(B,D) > 0.05, p(B,E) > 0.05, p(C,D) > 0.05, p(C,E) > 0.05, p(D,E) > 0.05.

Analysis of the Roland-Morris Disability Questionnaire functional ability scores

Similar conclusions may be drawn from the analysis of results concerning the degree of disability assessed by the Roland-Morris questionnaire (Table 3). In all of the studied groups, significant therapeutic progress was recorded in the short-term observation. Values of the significance levels from the post hoc analysis were p = 0.0014 for group A; p = 0.0173 for group B; p = 0.0184 for group C; p = 0.0182 for group D; and p = 0.0174 for group E. However, the long-term follow-up observation unfortunately

showed a statistical tendency towards an increase in disability ($p > 0.05$).

As was the case with pain sensations and with regard to the influence of magnetic fields on physical fitness of patients with lumbosacral discopathy, there was a significant advantage of magnetic therapy with an induction of 10 mT. In the other groups, the results obtained were statistically significantly worse. Also, no differences were observed between groups B, C, D, and E, which suggests that exposure to magnetic stimulation and magnetic therapy with an intensity of 5 mT failed to meet expectations in comparison with the placebo groups.

Detailed data concerning the Roland-Morris questionnaire are presented in Fig. 5.

Analysis of results of the Lasègue hip mobility test

When evaluating changes in the mobility of the hip joint (measured by the Lasègue test) it must be noted that clinical improvement occurred in all study groups (Table 4).

After 15 treatments, Group A (magnetic therapy, 10 mT) demonstrated in the Lasègue test a statistically significant improvement in mobility compared to their pre-therapy results ($p = 0.0102$ in the post hoc analysis). The results were similar in other comparison groups, although the changes occurred with a lower level of significance: $p = 0.0323$ for group B; $p = 0.330$ for group C; $p = 0.0342$ for group D; and $p = 0.0338$ for group E. Consequently, as was the case with the parameters studied before, the long-term follow-up results (at 1 month and 3 months post-therapy) also reflected a statistical tendency attesting to a gradual recurrence of limited mobility in the lumbosacral section of the spine ($p > 0.05$).

Analysis of results of the Schober low back mobility test

In case of mobility measured by the Schober test, it was found that the range of motion improved in all groups, but the observed changes were of no statistical significance. Only in group A (magnetic therapy, 10 mT) did the improvement in spine mobility approach the significance threshold (Table 4). In group A, the post hoc analysis indicated the following findings: an increase of mobility from $p = 0.0588$ (directly post-therapy), a decrease of mobility from $p > 0.05$ (at 1 month post-therapy) and a further decrease of mobility from $p > 0.05$ (at 3 months post-therapy). In the remaining groups, the changes were of similar nature, but in no case did they approach the statistical significance threshold.

After carrying out an intergroup analysis of variance, it was found that the increase in the range of motion was most prominent in group A (magnetic therapy, 10 mT) which achieved an advantage over the other groups. Once again, no statistically significant differences were observed between groups B, C, D, and E. Intergroup comparisons (in %) regarding the Lasègue test and the Schober test are presented in Fig. 6 and 7.

Analysis of results of the stabilographic platform postural stability test

After the completion of the therapy process, tests on the stabilometric platform showed some improvement of balance in all patients compared to their initial state. The parameters were lower in all comparison groups, both with eyes open and eyes closed. However, in the study groups the changes were not significant, so only a certain statistical tendency can be declared here. When evaluating the

Table 4. Intragroup comparisons of hip joint mobility changes in LaT testing [degree] and changes in spine mobility at the lower Th in ShT testing [cm] before and after treatment

Characteristic		Before treatment		After treatment		1 month after treatment		3 months after treatment	
		LaT[a]	ShT[b]	LaT[a]	ShT[b]	LaT[a]	ShT[b]	LaT[a]	ShT[b]
Group A	mean	62.15	2.15	80.10	3.45	77.90	3.30	75.85	3.00
	SD	10.45	1.12	18.33	2.67	17.89	2.84	18.64	2.89
Group B	mean	60.95	2.25	70.15	3.05	68.35	2.75	66.55	2.55
	SD	10.33	1.89	17.73	2.70	18.40	2.05	18.89	2.09
Group C	mean	61.45	2.25	71.15	3.05	68.05	2.65	67.05	2.60
	SD	10.74	1.77	18.44	2.23	19.39	2.33	19.11	2.13
Group D	mean	63.05	2.30	72.05	3.10	69.75	3.05	67.80	2.80
	SD	11.21	1.21	17.70	2.74	16.79	2.45	16.63	2.39
Group E	mean	62.55	2.25	71.65	2.95	69.55	2.85	67.85	2.85
	SD	10.56	1.59	16.44	2.04	16.65	2.11	16.89	2.09

[a] Friedmann's ANOVA analysis (a total values of significant levels in each groups without the post hoc Bonferroni's test): group A ($p = 0.0322$); group B ($p = 0.0488$); group C ($p = 0.0491$); group D ($p = 0.0484$); group E ($p = 0.0485$); [b] Friedmann's ANOVA analysis (a total values of significant levels in each groups without the post hoc Bonferroni's test): group A ($p > 0.05$); group B ($p > 0.05$); group C ($p > 0.05$); group D ($p > 0.05$); group E ($p > 0.05$); LaT – Lasègue testing; ShT – Schober testing; SD – standard deviation.

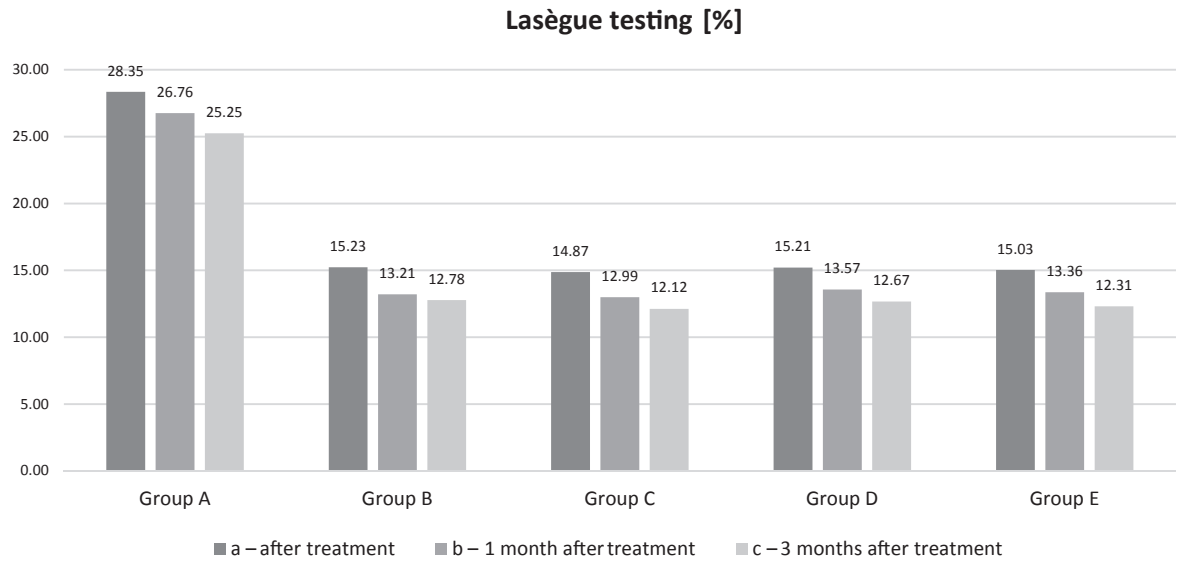

Fig. 6. Intergroup comparisons of hip joint mobility improvement in Lasègue testing [%] after treatment and in follow-up analyses, 1 and 3 months after treatment

a – Kruskal-Wallis ANOVA analysis (p = 0.0313); T Tukey's post hoc analysis: p(A,B) = 0.0269, p(A,C) = 0.0145, p(A,C) = 0.0270, p(A,E) = 0.0188, p(B,C) > 0.05, p(B,D) > 0.05, p(B,E) > 0.05, p(C,D) > 0.05, p(C,E) > 0.05, p(D,E) > 0.05; b – Kruskal-Wallis ANOVA analysis (p = 0.0322); T Tukey's post hoc analysis: p(A,B) = 0.0270, p(A,C) = 0.0166, p(A,C) = 0.0279, p(A,E) = 0.0301, p(B,C) > 0.05, p(B,D) > 0.05, p(B,E) > 0.05, p(C,D) > 0.05, p(C,E) > 0.05, p(D,E) > 0.05; c – Kruskal-Wallis ANOVA analysis (p = 0.0308); T Tukey's post hoc analysis: p(A,B) = 0.0188, p(A,C) = 0.0216, p(A,C) = 0.0209, p(A,E) = 0.0101, p(B,C) > 0.05, p(B,D) > 0.05, p(B,E) > 0.05, p(C,D) > 0.05, p(C,E) > 0.05, p(D,E) > 0.05.

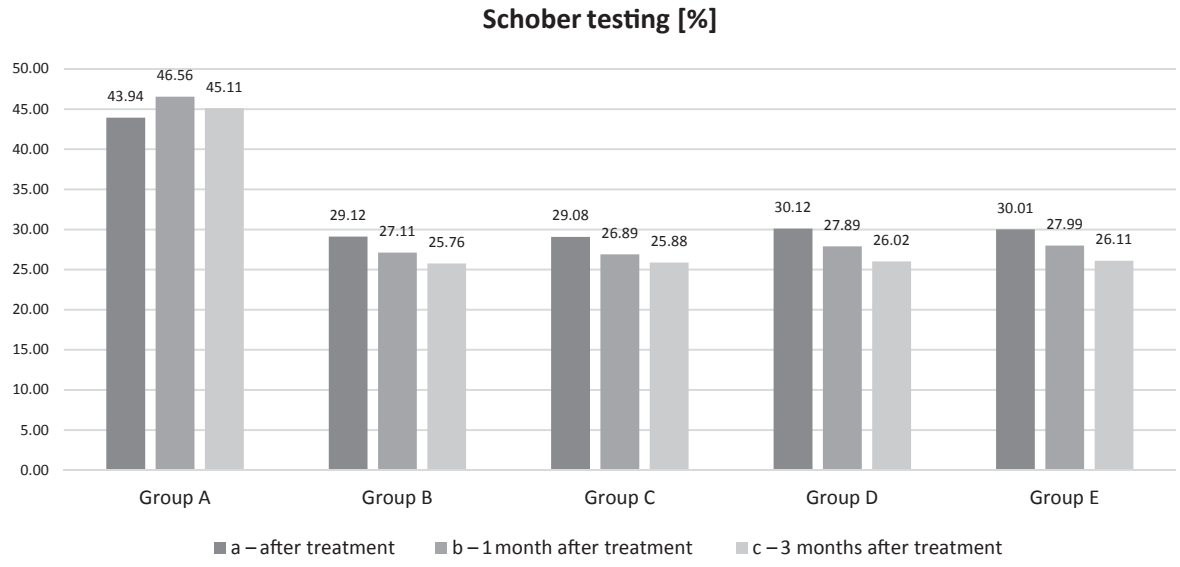

Fig. 7. Intergroup comparisons of spine mobility at the lower Th in Schober testing [%] after treatment and in follow-up analyses, 1 and 3 months after treatment

a – Kruskal-Wallis ANOVA analysis (p = 0.0289); T Tukey's post hoc analysis: p(A,B) = 0.0210, p(A,C) = 0.0122, p(A,C) = 0.0202, p(A,E) = 0.0102, p(B,C) > 0.05, p(B,D) > 0.05, p(B,E) > 0.05, p(C,D) > 0.05, p(C,E) > 0.05, p(D,E) > 0.05; b – Kruskal-Wallis ANOVA analysis (p = 0.0277); T Tukey's post hoc analysis: p(A,B) = 0.0103, p(A,C) = 0.0106, p(A,C) = 0.0280, p(A,E) = 0.0288, p(B,C) > 0.05, p(B,D) > 0.05, p(B,E) > 0.05, p(C,D) > 0.05, p(C,E) > 0.05, p(D,E) > 0.05; c – Kruskal-Wallis ANOVA analysis (p = 0.0318); T Tukey's post hoc analysis: p(A,B) = 0.0177, p(A,C) = 0.0219, p(A,C) = 0.0276, p(A,E) = 0.0110, p(B,C) > 0.05, p(B,D) > 0.05, p(B,E) > 0.05, p(C,D) > 0.05, p(C,E) > 0.05, p(D,E) > 0.05.

results pre- and post-therapy without statistical analysis, it appears that a beneficial reduction of posturographic indicators took place, particularly in group A. Long-term follow-up observations showed tendencies for the deterioration of body posture in all of the studied parameters, although these changes were also statistically insignificant. Some indicators after 3 months nearly returned to the state prior to the therapy. In the Kruskal-Wallis analysis of variance (ANOVA), no intergroup differences were observed ($p > 0.05$). That is why only the results of the analysis of variance for dependent variables are shown below, reflecting certain statistical tendencies in each of the groups (Tables 5–9).

Table 5. Intragroup comparisons of the total path length parameter (SP) changes in stabilometric examination with open and closed eyes before and after treatment [mm]

Characteristic		Before treatment		After treatment		1 month after treatment		3 months after treatment	
		open[a]	closed[b]	open[a]	closed[b]	open[a]	closed[b]	open[a]	closed[b]
Group A	mean	125.12	184.22	117.56	176.43	122.45	180.02	124.67	181.17
	SD	90.11	158.11	110.58	167.22	112.67	170.89	120.34	177.24
Group B	mean	125.19	175.22	123.65	171.66	123.87	173.42	125.02	175.20
	SD	98.45	128.33	100.21	150.19	110.89	162.83	111.02	162.32
Group C	mean	120.89	178.19	118.56	174.42	120.03	176.66	120.15	177.72
	SD	104.12	153.77	116.74	161.32	118.21	160.99	118.54	164.44
Group D	mean	123.17	182.65	120.34	178.11	121.53	180.63	122.90	181.59
	SD	91.22	140.28	100.72	132.34	100.45	150.15	112.03	152.67
Group E	mean	124.03	181.12	121.22	177.89	122.11	179.02	123.83	180.89
	SD	93.82	139.99	98.12	136.02	107.56	150.33	111.63	159.78

[a] Friedmann's ANOVA analysis (a total values of significant levels in each groups without the post hoc Bonferroni's test): group A ($p > 0.05$); group B ($p > 0.05$); group C ($p > 0.05$); group D ($p > 0.05$); group E ($p > 0.05$); [b] Friedmann's ANOVA analysis (a total values of significant levels in each groups without the post hoc Bonferroni's test): group A ($p > 0.05$); group B ($p > 0.05$); group C ($p > 0.05$); group D ($p > 0.05$); group E ($p > 0.05$).

Table 6. Intragroup comparisons of the statokinesiogram path length (SPAP) changes on the frontal plane in stabilometric examination with open and closed eyes before and after treatment [mm]

Characteristic		Before treatment		After treatment		1 month after treatment		3 months after treatment	
		open[a]	closed[b]	open[a]	closed[b]	open[a]	closed[b]	open[a]	closed[b]
Group A	mean	101.49	112.34	94.06	102.46	95.89	106.22	98.22	108.43
	SD	80.23	90.23	86.88	94.34	82.77	100.84	85.66	100.98
Group B	mean	100.21	110.91	97.99	107.99	99.02	110.01	100.60	110.69
	SD	82.39	82.39	83.55	88.46	86.44	100.04	80.01	107.67
Group C	mean	102.88	112.01	99.02	109.41	99.96	110.56	101.21	111.12
	SD	85.02	94.12	83.33	96.45	85.81	102.82	89.16	108.89
Group D	mean	102.63	112.31	99.11	108.99	101.54	111.04	102.09	111.79
	SD	84.12	104.63	83.54	100.45	87.77	100.54	80.87	110.97
Group E	mean	100.95	111.54	97.92	109.92	98.82	110.83	100.09	112.32
	SD	80.95	90.99	82.32	94.02	81.29	94.54	80.84	99.46

[a] Friedmann's ANOVA analysis (a total values of significant levels in each groups without the post hoc Bonferroni's test): group A ($p > 0.05$); group B ($p > 0.05$); group C ($p > 0.05$); group D ($p > 0.05$); group E ($p > 0.05$); [b] Friedmann's ANOVA analysis (a total values of significant levels in each groups without the post hoc Bonferroni's test): group A ($p > 0.05$); group B ($p > 0.05$); group C ($p > 0.05$); group D ($p > 0.05$); group E ($p > 0.05$).

Discussion

The present study is certainly innovative, as it presents an unequivocal evaluation of the efficacy of magnetic therapy (with different induction output values) and magnetic stimulation in the treatment of lumbar discopathy at L5–S1 within a single, prospective, randomized clinical trial based on a strict protocol of inclusion and exclusion criteria, using modern objective and subjective measurements, and accompanied by a uniform statistical analysis and observation of the long-term effects. To date, none of the authors of the available literature has carried out such a wide-ranging research project on the application of magnetic fields in therapy of low back pain in accordance with the guidelines of Evidence Based Medicine and Physiotherapy (EBM&P).

The present study was the first such attempt in the literature. Thus, it has been difficult to refer the results to any published articles, especially with regard to body balance tests using a stabilometric platform. Moreover, no existing study on physical therapy of low back pain has carried out such detailed diagnostics or classification based on the radiological Modic assessment criteria. This allowed for a very representative population to be recruited for the purpose of this project. A crucial element of the study was also the use of simulated treatments and the fact that it was a single blind trial, which has significantly raised the profile of the study and strengthened the reliability of its conclusions. In this study, only one application of magnetic fields demonstrated certain medical efficacy, namely the magnetic therapy with the following parameters: magnetic

Table 7. Intragroup comparisons of the sway area (SA) of the center of pressure changes in stabilometric examination with open and closed eyes before and after treatment [mm^2]

Characteristic		Before treatment		After treatment		1 month after treatment		3 months after treatment	
		open[a]	closed[b]	open[a]	closed[b]	open[a]	closed[b]	open[a]	closed[b]
Group A	mean	124.55	201.34	112.06	187.65	116.11	193.12	118.40	198.55
	SD	75.04	105.33	71.21	106.12	75.41	109.19	75.23	108.35
Group B	mean	120.41	205.16	117.69	197.92	120.33	200.98	120.79	202.29
	SD	70.21	108.14	79.62	105.33	80.94	100.98	80.97	100.02
Group C	mean	122.41	200.66	119.03	194.37	120.38	198.88	120.78	200.02
	SD	64.87	102.33	68.53	103.32	70.82	104.99	70.09	101.32
Group D	mean	123.14	203.67	119.79	198.09	121.01	199.89	121.89	202.33
	SD	64.33	104.11	96.87	102.07	74.94	103.42	74.08	104.83
Group E	mean	122.08	205.01	119.02	199.92	120.39	201.91	121.82	204.04
	SD	80.02	100.23	80.21	106.11	81.41	109.13	81.55	113.88

[a] Friedmann's ANOVA analysis (a total values of significant levels in each groups without the post hoc Bonferroni's test): group A ($p > 0.05$); group B ($p > 0.05$); group C ($p > 0.05$); group D ($p > 0.05$); group E ($p > 0.05$); [b] Friedmann's ANOVA analysis (a total values of significant levels in each groups without the post hoc Bonferroni's test): group A ($p > 0.05$); group B ($p > 0.05$); group C ($p > 0.05$); group D ($p > 0.05$); group E ($p > 0.05$).

Table 8. Intragroup comparisons of the mean frequency (MF) of sway in all planes changes in stabilometric examination with open and closed eyes before and after treatment [Hz]

Characteristic		Before treatment		After treatment		1 month after treatment		3 months after treatment	
		open[a]	closed[b]	open[a]	closed[b]	open[a]	closed[b]	open[a]	closed[b]
Group A	mean	0.34	0.44	0.28	0.40	0.31	0.41	0.36	0.41
	SD	0.23	0.33	0.22	0.33	0.28	0.32	0.35	0.30
Group B	mean	0.33	0.46	0.30	0.45	0.32	0.45	0.32	0.45
	SD	0.18	0.38	0.23	0.37	0.30	0.40	0.30	0.42
Group C	mean	0.36	0.44	0.34	0.42	0.35	0.45	0.36	0.45
	SD	0.23	0.30	0.22	0.31	0.31	0.36	0.33	0.44
Group D	mean	0.34	0.44	0.33	0.43	0.33	0.43	0.33	0.43
	SD	0.21	0.31	0.24	0.32	0.26	0.42	0.26	0.43
Group E	mean	0.31	0.46	0.28	0.42	0.30	0.44	0.34	0.44
	SD	0.20	0.37	0.20	0.39	0.23	0.36	0.24	0.36

[a] Friedmann's ANOVA analysis (a total values of significant levels in each groups without the post hoc Bonferroni's test): group A ($p > 0.05$); group B ($p > 0.05$); group C ($p > 0.05$); group D ($p > 0.05$); group E ($p > 0.05$); [b] Friedmann's ANOVA analysis (a total values of significant levels in each groups without the post hoc Bonferroni's test): group A ($p > 0.05$); group B ($p > 0.05$); group C ($p > 0.05$); group D ($p > 0.05$); group E ($p > 0.05$).

induction of 10 mT, frequency of 50 Hz and a single treatment duration of 20 min. Under the influence of the above physical stimuli, the most prominent analgesic effect was observed in the improvement of mobility and functional ability of the spine, but also to a lesser extent in the improvement of parameters related to the balance of the patients.

It is also worth noting that the effects of the applied therapy were mostly short-term, as recurrent symptoms were observed in the majority of measured indicators at 1 month and 3 months post-therapy. This means that the physical treatment selected for the purposes of the study may only have an acute effect, although it shows a high efficacy in short-term observation.

It is probable that continuation of the stabilization training may have achieved a more sustainable improvement with physical therapy. It is certainly an interesting challenge for future scientific research. Unfortunately, application of magnetic therapy with a low induction value of 5 mT, and of magnetic stimulation, which is immensely popular in clinical practice, proved pointless in the treatment of symptoms of chronic lumbosacral discopathy. The use of these physical treatments contributed nothing to the therapeutic process, and the achieved effects, in comparison with the placebo methods, failed to meet expectations and cast serious doubt on the possibility of using these magnetic fields in the treatment of low back pain in accordance with the principles of modern science and medicine.

When analyzing the available literature regarding the application of magnetic fields in the treatment of patients with L5–S1 discopathy, one may notice that a majority

Table 9. Intragroup comparisons of the mean velocity (MV) of sway in all planes changes in stabilometric examination with open and closed eyes before and after treatment [mm/s]

Characteristic		Before treatment		After treatment		1 month after treatment		3 months after treatment	
		open[a]	closed[b]	open[a]	closed[b]	open[a]	closed[b]	open[a]	closed[b]
Group A	mean	3.43	4.37	3.29	4.19	3.31	4.21	3.41	4.31
	SD	2.37	2.78	2.31	2.76	2.42	2.88	2.43	2.94
Group B	mean	3.49	4.36	3.40	4.28	3.42	4.32	3.43	4.33
	SD	2.68	2.32	2.77	2.04	2.88	2.31	2.92	2.39
Group C	mean	3.44	4.40	3.36	4.35	3.40	4.35	3.45	4.40
	SD	2.49	2.77	2.41	2.56	2.46	2.78	2.54	2.79
Group D	mean	3.47	4.33	3.40	4.28	3.40	4.30	3.43	4.32
	SD	2.25	2.51	3.22	2.23	3.34	2.50	3.37	2.57
Group E	mean	3.51	4.31	3.45	4.25	3.44	4.26	3.50	4.30
	SD	3.07	2.77	3.19	2.55	3.36	2.76	3.35	2.76

[a] Friedmann's ANOVA analysis (a total values of significant levels in each groups without the post hoc Bonferroni's test): group A ($p > 0.05$); group B ($p > 0.05$); group C ($p > 0.05$); group D ($p > 0.05$); group E ($p > 0.05$); [b] Friedmann's ANOVA analysis (a total values of significant levels in each groups without the post hoc Bonferroni's test): group A ($p > 0.05$); group B ($p > 0.05$); group C ($p > 0.05$); group D ($p > 0.05$); group E ($p > 0.05$).

of studies fail to meet the criteria of the EBM&P, which makes it extremely difficult to carry out a clear and objective analysis of the clinical efficacy of the treatments that are widely used in everyday practice.

Omar et al. studied the efficacy of magnetic therapy (4 mT, 50 Hz, 20 min, 5 treatments/week) in 40 patients presenting with pain in the lumbosacral spine.[27] The patients were randomly assigned to 2 comparison groups (a group treated with a magnetic field, n = 20; and a placebo group with simulated treatments, n = 20). Before the commencement of the study and after its completion (3 weeks), a measurement was taken of the surface electromyography of selected groups of back muscles, and an assessment was made of the pain symptoms in accordance with the Visual Analogue Scale and the Oswestry questionnaire. A statistically significant reduction in pain was recorded under the influence of the magnetic field compared to the placebo group ($p = 0.024$ in the VAS and $p < 0.001$ in the Oswestry questionnaire). In the case of the electromyography parameters as well, significantly more beneficial effects were observed in the exposed group ($p = 0.022$ for the parameter of relative latency of the erector spinae muscles). A weakness of the study, however, was a lack of strictly defined inclusion and exclusion criteria and no follow-up analysis.

Thuile and Walzl studied the effects of magnetic field therapy on patients presenting with lumbar radiculopathy and neck pain after sustaining a whiplash-type injury.[28] The experiment involved 100 patients suffering from low back pain, 92% of whom had additionally sustained a whiplash injury of the neck section of the spine. Therapeutic progress was evaluated with the Lasègue test in the case of the lower section of the spine, and with the subjective visual analogue pain scale in examining the neck section. After a 2-week therapy, in the group subjected to physical treatments (8 mT, 50 Hz, 20 min), the Lasègue test was negative in 68% of patients (as compared to only 36% before the therapy). In the control group (placebo), no changes in this respect were recorded. With regard to the neck section of the spine, the magnetic field therapy also brought about a positive effect, as the pain symptoms decreased on average by 2.2 points on the VAS. In the control group, this parameter did not improve. Limitations of the study included a lack of objective measurement tools, the heterogeneity of the population and an evaluation of only the early effects of the therapy.

Oke and Umebese used magnetic therapy in 16 patients, randomly assigned to 2 comparison groups.[29] All patients took oral non-steroidal anti-inflammatory medication, and 8 patients were additionally exposed to magnetic field therapy (10 mT, 50 Hz, 30 min) for 9 days. After completion of the therapy, a significantly greater improvement was observed in patients subjected to physical treatments. Two serious limitations of the study were its small population and methodological errors – statistical inference based on Student's t-test for 8 cases (in addition, the study does not indicate whether the distributions were normal). Moreover, the application of analgesics was also misguided, as it was difficult to evaluate the analgesic effect of physical therapy or of pharmacotherapy, because they had been combined.

Ratajczak et al. evaluated the influence of laser therapy and magnetotherapy in conjunction with kinesiotherapy used in patients with degenerative lumbosacral spine disease.[30] The study involved 30 patients aged from 41 to 62 years. The patients were ordered to undergo a series of 10 treatments using laser light, magnetic therapy and kinesiotherapy. All subjects were examined pre- and post-therapy by using the Lasègue test and by measuring pain intensity with the VAS test. Also, the mobility of their lumbosacral spine was measured with a Saunders digital inclinometer (Pearson Surgical,

Sylmar, USA). An analysis of the mean values of the studied parameters, reflecting the range of spinal mobility, showed higher values in the post-therapy examination. The mobility range was found to have improved in all planes. After the VAS test, a statistically significant difference was observed between the pre- and post-therapy results. Before therapy, the Lasègue sign was positive in 43.4% of the patients, while after the therapy 20% of the patients had a positive sign. A methodological error in the above study was the fact that instead of using monotherapy in the comparison groups, the study used a combination of all the physical methods and motor improvement within a single group. Without comparing individual treatments to each other, it is impossible to draw any conclusions on the efficacy of the magnetic field – one may only state that the combination therapy was effective.

On the other hand, Janiszewski conducted a clinical trial involving 53 patients with osteoarthritis of the lower back and found that in the study group (magnetic stimulation 30 μT, 190 Hz, 20 min) a significant reduction in pain symptoms occurred and the duration of morning stiffness was shorter.[31] Patients were administered treatments for a period of 4–6 weeks. The weakness of this study, however, was a lack of objective measurement tools and an evaluation limited only to the early effects.

A study by Pasek et al. analyzed the therapeutic efficacy of magnetic stimulation on various nosological units.[32] The study was based on gathering information through anonymous questionnaires. In total, 1,874 patients participated in the study and were divided into sub-groups, depending on the diagnosis. The authors proved that after a series of treatments the patients experienced a reduction or clearance of pain symptoms, as well as an increased range of mobility in their joints, spin and paretic extremities. Shortcomings of the study included a significant dispersion of the population and a lack of reliable examination of the participants (assessment through a questionnaire).

In another study, Pasek et al. studied the influence of a treatment using a magnetic field and polarized light on back pain syndromes, and on sciatic neuralgia in particular.[33] The study involved a group of 47 patients, 30 women and 17 men, diagnosed with sciatic neuralgia caused by degenerative intervertebral disc disease. The diagnosis was confirmed with a preliminary medical examination, a radiological examination and a CT scan of the lumbar spine. The patients were divided into 3 study groups. The 1st group was treated with magnetic therapy with the following parameters: a frequency of 40 Hz, magnetic induction of 10 mT with a triangular magnetic field, and a duration of 12 min. The 2nd group was subjected to magnetic stimulation with the Viofor JPS apparatus (Med & Life, Komorów, Poland) using the M2P2 program, field intensity of 8, and treatment duration of 12 min. The 3rd group was treated with magnetoledotherapy, also using the Viofor JPS apparatus, M2P2 program and optical IR radiation (wavelength 830 mm) with a treatment duration of 12 min. Each patient underwent the Lasègue test both before and after the therapy, and was examined with the subjective assessment of experienced pain using VAS. In addition, a questionnaire was used to assess the frequency of taking analgesic medication and quality of life was evaluated using the EuroQoL scale. The authors demonstrated that in each of the study groups the treatment resulted in a significant reduction of pain, a reduced demand for analgesic medication, and improved quality of life. The study did not state a significant advantage of any of the analyzed methods in relation to the results obtained. Unfortunately, the study did not incorporate any verification of therapeutic effects based on objective measurement tools.

Nowadays, application of magnetic stimulation is widely used, not only in the therapy of persons suffering from pain in the motor system, but also in stomatology, neurology, and in the treatment of internal organ dysfunction.

In the period of 2003–2004, Kapłun et al. at the rehabilitation ward in Hrubieszów (Poland) attempted to evaluate the usefulness of magnetic stimulation treatments in patients after a stroke with low back discopathy as a concomitant disease.[34] The rehabilitation program covered 318 patients, but the analysis was carried out with respect to 53 patients after brain stroke of different etiology, which included 17 women (32%) and 36 men (68%). Electromagnetic therapy using the Viofor JPS apparatus (Med & Life, Komorów, Poland) was recommended in order to reduce spasticity, normalize the emotional sphere, normalize the functions of the circulatory system, and obtain an analgesic effect. These treatments were an addition to pharmacological therapy and kinesiotherapy. The patients received treatments twice a day for 12 min using the M2P2 program, for 5 days/week, i.e., about 20–30 treatments were administered. The effects of the therapy were assessed through a general medical examination, evaluation of the functional status using the Brunnström scale and evaluation of muscle tension using the Ashworth scale. The results were compared with a group of patients treated without the application of a magnetic field. Irrespective of the etiology of the stroke, the time elapsed from the onset of the disease and the concomitant diseases, in the study group a significant improvement was obtained in 28 patients (52.8%), an improvement in 20 patients (37.8%), a lack of improvement in 3 patients (5.7%), and a deterioration in 2 patients (3.7%). The therapeutic effects concerned functional ability and spastic reaction. The study did, however, lack an analysis of the long-term results and a unification of the rehabilitation program for all the patients studied. Another weakness was the incorporation of pharmacotherapy, which additionally impeded verification of the obtained results and made it more difficult to draw unequivocal conclusions.

One can see from the above and from the review of literature presented in the introduction, there is a shortage of well-planned, methodologically impeccable, randomized clinical studies regarding the discussed subject.

It is not possible to refer the results obtained in our study to any data in the available literature, as this was the first such clinical trial among publications worldwide.

Despite the innovative character of this study and its novel elements, it also contains a number of limitations. It would certainly be worthwhile to supplement the project in the future with other modern and objective measurement tools, such as muscle electromyography or systems for movement and balance analysis.

Unfortunately, balance measurements taken with the use of stabilometric platforms are characterized by a certain lability and a relatively low (despite their immense referentiality in biomedical sciences) measurement repeatability (even though all measurements were performed by the same person in compliance with the principles of metrology, and therefore the substantial standard deviations in the obtained parameters attest to the fallibility of the device, which impacts the behavior of statistical tests during analysis, as well as the inference process itself). Another shortcoming of the study was the fact that the research was carried out at a single facility, which significantly extended the time of the project (nearly 3 years) and affected the final number of patients. A multi-facility project would have allowed access to a greater number of patients and a better selection, and would have substantially shortened the project duration. It may also be worthwhile to continue the work and gather greater populations in individual groups, in order to verify the obtained results using statistical parametric tests. A weakness of this study was also the relatively high measurement error during the observation of mobility of the hip joint and the lumbar region of the spine. When designing the study, we tried to reduce this deviation by making sure that all the measurements were made by the same person (a mean of 5 trials). However, the listed shortcomings certainly constituted significant limitations of the actions undertaken in this project. It must also be mentioned that the long-term follow-up observation (at 1 month and 3 months post-therapy) was extremely difficult and subject to certain limitations. During the trial, at different stages, (after qualification for treatment to a given group) 16 participants were successively excluded from the study. It is worth noting that as many as 14 people from this subpopulation were not able to comply with the requirement to discontinue analgesics for such a long period of time. The other 2 cases were a viral infection, which prevented the patient from systematic participation in treatments, and the sudden, unplanned departure of another patient, which also resulted in exclusion from the project. The abovementioned circumstances affected the final number of participants in the comparison groups.

In conclusion, further randomized clinical research trials regarding the application of magnetic fields in various areas should certainly be continued, in order to verify the findings of this study. No doubt, studies conducted by other institutions would enable the comparison of experience gained and a broadening of the knowledge on the subject.

Conclusions

Magnetic fields studied in the present clinical trial, in combination with specialist motor rehabilitation (5 times a week for 3 weeks), may be efficient in reducing certain symptoms of spinal discopathy at L5–S1, but the resulting remission is only acute and short-term (without further continuation of kinesiotherapy). The study has shown that application of magnetic therapy (10 mT, 50 Hz, 20 min) significantly reduces pain symptoms and leads to an improvement of functional ability in patients with low back pain, based on the analysis of both subjective and objective parameters. However, the application of magnetic therapy with an induction value of 5 mT and of magnetic stimulation appears to be ineffective and pointless in the treatment of lumbosacral discopathy (within the scope studied in this paper).

References

1. Krismer M, van Tulder M.; Low Back Pain Group of the Bone and Joint Health Strategies for Europe Project. Strategies for prevention and management of musculoskeletal conditions: Low back pain (non-specific). *Best Pract Res Clin Rheumatol*. 2007;21:77–91.
2. Calvo-Muñoz I, Gómez-Conesa A, Sánchez-Meca J. Prevalence of low back pain in children and adolescents: A meta-analysis. *BMC Pediatr*. 2013;13:14.
3. Borenstein DG. Epidemiology, etiology, diagnostic evaluation, and treatment of low back pain. *Curr Opin Rheumatol*. 2001;13:128–134.
4. Hoy D, Bain C, Williams G, et al. A systematic review of the global prevalence of low back pain. *Arthritis Rheum*. 2012;64:2028–2037.
5. Meucci RD, Fassa AG, Faria NMX. Prevalence of chronic low back pain: Systematic review. *Rev Saúde Pública*. 2015;49:1. doi:10.1590/S0034-8910.2015049005874
6. Zhang Y, Guo T, Guo X, Wu S. Clinical diagnosis for discogenic low back pain. *Int J Biol Sci*. 2009;5:647–658.
7. Garg A, Gerr F, Katz JN, Marras WS, Silverstein B. Low back pain and the workplace. *JAMA*. 2007;298:403–404.
8. Morton M. Spinal pain syndromes. *Przew Lek*. 2008;5:45–55.
9. Elder BD, Witham TF. Low back pain and spondylosis. *Semin Neurol*. 2016;36:456–461.
10. Allegri M, Montella S, Salici F, et al. Mechanisms of low back pain: A guide for diagnosis and therapy. *F1000 Research*. 2016;5. doi:10. 12688/f1000research.8105
11. Hoozemans MJM, Koppes LLJ, Twisk JWR, van Dieën JH. Lumbar bone mass predicts low back pain in males. *Spine*. 2012;37:1579–1585.
12. Golob AL, Wipf JE. Low back pain. *Med Clin North Am*. 2014;98: 405–428.
13. Goubert D, Oosterwijck JV, Meeus M, Danneels L. Structural changes of lumbar muscles in non-specific low back pain: A systematic review. *Pain Physician*. 2016;19:985–1000.
14. Furlan AD, Pennick V, Bombardier C, van Tulder M; Editorial Board, Cochrane Back Review Group. 2009 updated method guidelines for systematic reviews in the Cochrane Back Review Group. *Spine*. 2009;34:1929–1941.
15. Furlan AD, Yazdi F, Tsertsvadze A, et al. A systematic review and meta-analysis of efficacy, cost-effectiveness, and safety of selected complementary and alternative medicine for neck and low-back pain. *Evid-Based Complement Altern Med ECAM*. 2012;953139. doi: 10.1155/2012/953139
16. Chou R, Huffman LH; American Pain Society, American College of Physicians. Nonpharmacologic therapies for acute and chronic low back pain: A review of the evidence for an American Pain Society/American College of Physicians clinical practice guideline. *Ann Intern Med*. 2007;147:492–504.
17. Koes BW, van Tulder MW, Thomas S. Diagnosis and treatment of low back pain. *BMJ*. 2006;332:1430–1434.

18. Kuryliszyn-Moskal A. Management of low back pain: Treatment strategies. *Rheumatology*. 2009;47(6):368–371.
19. Rubinstein SM, van Middelkoop M, Kuijpers T, et al. A systematic review on the effectiveness of complementary and alternative medicine for chronic non-specific low-back pain. *Eur Spine J*. 2010;19: 1213–1228.
20. Delitto A, George SZ, Van Dillen LR, et al.; Orthopaedic Section of the American Physical Therapy Association. Low back pain. *J Orthop Sports Phys Ther*. 2012;42(4):A1–A57.
21. McCaskey MA, Schuster-Amft C, Wirth B, Suica Z, de Bruin ED. Effects of proprioceptive exercises on pain and function in chronic neck- and low back pain rehabilitation: A systematic literature review. *BMC Musculoskelet Disord*. 2014;15:382.
22. Standaert CJ, Friedly J, Erwin MW, et al. Comparative effectiveness of exercise, acupuncture, and spinal manipulation for low back pain. *Spine*. 2011;36:120–130.
23. Bouche K, Stevens V, Cambier D, Caemaert J, Danneels L. Comparison of postural control in unilateral stance between healthy controls and lumbar discectomy patients with and without pain. *Eur Spine J*. 2006;15:423–432.
24. Salavati M, Mazaheri M, Negahban H, et al. Effect of dual-tasking on postural control in subjects with nonspecific low back pain. *Spine*. 2009;34:1415–1121.
25. Mazaheri M, Coenen P, Parnianpour M, Kiers H, van Dieën JH. Low back pain and postural sway during quiet standing with and without sensory manipulation: A systematic review. *Gait Posture*. 2013;37:12–22.
26. Ruhe A, Fejer R, Walker B. Center of pressure excursion as a measure of balance performance in patients with non-specific low back pain compared to healthy controls: A systematic review of the literature. *Eur Spine J*. 2011;20:358–368.
27. Omar AS, Awadalla MA, El-Latif MA. Evaluation of pulsed electromagnetic field therapy in the management of patients with discogenic lumbar radiculopathy. *Int J Rheum Dis*. 2012;15:101–108.
28. Thuile C, Walzl M. Evaluation of electromagnetic fields in the treatment of pain in patients with lumbar radiculopathy or the whiplash syndrome. *NeuroRehabilitation*. 2002;17:63–67.
29. Oke KI, Umebese PFA. Evaluation of the efficacy of pulsed electromagnetic therapy in the treatment of back pain: A randomized controlled trial in a tertiary hospital in Nigeria. *West Indian Med J*. 2013;62: 205–209.
30. Ratajczak B, Ryfa R, Boerner E, Kuciel-Lewandowska J, Hawrylak A, Demidaś A. Assessment the influence of the lasertherapy and magnetotherapy in connection with kinesitherapy used by patients with the degenerative low back disease. *Adv Rehabil*. 2013;25:13–18.
31. Janiszewski M. Wpływ terapeutycznego systemu magnetostymulacyjnego (MRS 2000) na niektóre wskaźniki biomechaniczne narządu ruchu u pacjentów z chorobą zwyrodnieniową stawów. *Acta Bio-Opt Inf Med*. 1998;4:73–75.
32. Pasek J, Pasek T, Sieroń A. Some practical recommendations on the use of magnetic fields and light in physical medicine. *Acta Bio-Opt Inform Medica*. 2007;13:284–285.
33. Pasek J, Kwiatek P, Pasek T, Szajkowski S, Szewc A, Sieroń A. Application of magnetic field and visible light in the treatment of low back pain and sciatic neuralgia. *Curr Neurol*. 2012;12:65–68.
34. Kapłun E, Kapłun D, Majcher P, Fatyga M. Evaluation of magnetstimulation usefulness using VIOFOR JPS in rehabilitation of patients after stroke. *Adv Rehabil*. 2004;18.

Management of gastrointestinal stromal tumors: A 10-year experience of a single surgical department

Dariusz Janczak[1,2,A,F], Jacek Rać[1,B,D], Wiktor Pawłowski[1,2,A,D], Tadeusz Dorobisz[1,3,C,E], Agnieszka Ziomek[1,2,B], Dawid Janczak[3,C,D], Michał Leśniak[1,2,C,E], Mariusz Chabowski[1,2,D,F]

[1] Department of Surgery, 4th Military Teaching Hospital, Wrocław, Poland
[2] Division of Surgical Procedures, Department of Clinical Nursing, Faculty of Health Sciences, Wroclaw Medical University, Poland
[3] Division of Oncology and Palliative Care, Faculty of Health Sciences, Wroclaw Medical University, Poland

A – research concept and design; B – collection and/or assembly of data; C – data analysis and interpretation; D – writing the article; E – critical revision of the article; F – final approval of the article

Advances in Clinical and Experimental Medicine, ISSN 1899-5276 (print), ISSN 2451-2680 (online) *Adv Clin Exp Med*. 2018;27(5):667–671

Address for correspondence
Mariusz Chabowski
E-mail: mariusz.chabowski@gmail.com

Funding sources
None declared

Conflict of interest
None declared

Received on July 28, 2016
Reviewed on October 8, 2016
Accepted on January 29, 2017

Abstract

Background. Gastrointestinal stromal tumors (GISTs) are the most common mesenchymal tumors of the digestive system. The primary location of GISTs is mainly the gastrointestinal system. Clinical symptoms are nonspecific and mainly depend on the location and size of the tumor.

Objectives. The aim of this study was to conduct a clinical and pathological analysis of 18 cases of GISTs from the medical records of the Department of Surgery at the 4th Military Teaching Hospital in Wrocław, Poland.

Material and methods. The medical records were of women and men at the age of 36–84 years who were treated in the Surgical Clinic. The medical data that was gathered included clinical records, histopathological results and the type of surgical treatment. The study also encompassed the anatomical location and size of the tumor as well as microscopic examination of the tumor.

Results. In most cases, GISTs were located in the stomach. The most common symptoms were stomachaches and signs of bleeding into the digestive system. Usually, the tumor presented a diameter of <5 cm and a low grade of malignancy. Out of 18 patients, 16 were treated with laparoscopic resection, whereas in the remaining 2 cases, multiorgan resections were carried out, because the tumor was locally advanced.

Conclusions. It is essential to distinguish stromal tumors from other mesenchymal tumors, since GISTs are among the cancers that have a high risk of malignant progression. The conditions for successful treatment are a properly established histopathological diagnosis, accompanied by immunohistochemical tests for CD117, and a combination of antibodies for a differential diagnosis of other mesenchymal tumors.

Key words: gastrointestinal stromal tumor, CD117, tumorectomy, jejunal gastrointestinal stromal tumor, stomach gastrointestinal stromal tumor

DOI
10.17219/acem/68718

Copyright
© 2018 by Wroclaw Medical University
This is an article distributed under the terms of the Creative Commons Attribution Non-Commercial License (http://creativecommons.org/licenses/by-nc-nd/4.0/)

Introduction

Gastrointestinal stromal tumors (GISTs) are the most common mesenchymal cancers of the gastrointestinal tract. They derive from the precursors of the pacemaker interstitial cells of Cajal, which are responsible for intestinal peristaltic activity. They are characterized by the overexpression of the tyrosine kinase receptor KIT.[1] Primary GISTs are largely located along the gastrointestinal tract – over 80% of them. Most frequently, they are found in the stomach (40–70%) and small intestine (20–50%). This type of sarcoma less frequently develops in the retroperitoneal space (<15%). GISTs rarely occur in the colon (~5%) or esophagus (<5%). Approximately 30% of all gastrointestinal stromal tumors present signs of malignancy with evidence of infiltration and distant metastases, especially liver and peritoneal.

Primarily, GISTs develop within the wall of the gastrointestinal tract, below the mucosal layer. They are not attached to the intestinal mucosa, but as the disease advances, they may lead to infiltration and ulceration of the intestinal mucosa. The clinical symptoms of GISTs are nonspecific and depend on the size and anatomical location of the tumor. The most common presentations include abdominal pain, a palpable mass in the abdomen and gastrointestinal bleeding, which can be chronic or less frequently acute.[2–4] The most effective method of treatment is a complete resection of the tumor. Gastric GISTs are typically removed along with a part of the gastric wall by wedge resection with a margin of 1–2 cm. Metastases to regional lymph nodes are rare; they appear in <3% of patients, so systemic lymph node dissection is not generally required. The resectability rate of GISTs is high and varies from 70 to 80%.[5]

The aim of this study was to analyze the records of patients treated for stromal tumors in the Department of Surgery at the 4th Military Teaching Hospital in Wrocław (Poland) between 2005 and 2015.

Material and methods

Clinical data, histopathological results and information about the type of operation were collected from the medical records of 18 patients operated on in the Department of Surgery at the 4th Military Teaching Hospital in Wrocław. Clinical symptoms reported before the surgical treatment, the type of resection (R0, R1 or R2), the anatomical location, and the size of the tumor as well as the results of microscopic examination were analyzed.

The study group included 18 patients (11 men and 7 women) aged 36–84 years. The mean age of the study group was 62 years. In all patients, the histopathological diagnosis was determined after the surgical treatment. In the majority of cases, the GIST was located in the stomach (72%). In 2 patients, it was found in the mesentery; in the remaining single cases, it was located in the small intestine, rectum or retroperitoneal space (Table 1).

Table 1. Tumor location

Organ	Number of cases	Percentage [%]
Stomach	13	72
Small intestine	1	5.5
Rectum	1	5.5
Mesentery	2	11
Retroperitoneal space	1	5.5
Total	18	100

Table 2. Tumor size

Tumor size [cm]	Number of cases	Percentage [%]
<5	12	66.7
5–10	4	22.3
11–20	1	5.5
>20	1	5.5
Total	18	100

The most frequently reported symptoms were abdominal pain and signs of intestinal bleeding, such as anemia and tarry stools. One patient with a tumor in the mesentery presented with episodes of obstruction of the gastrointestinal tract. One woman sought medical advice because of a palpable abdominal tumor. Eight patients were qualified for surgical treatment on the basis of endoscopy suggesting a stomach tumor; however, the biopsy results indicated only inflammatory changes. Other patients were qualified for surgery based on the results of computed tomography imagery of the abdominal cavity. In the majority of cases (66.7%), the diameter of the tumor was <5 cm (Table 2).

All procedures were followed in accordance with the ethical standards and with the Helsinki Declaration of 1964 and later versions. Informed consent was obtained from all the patients included in the study.

Results

A laparotomy was conducted on 16 patients. In all cases of gastric GIST, a local tumor resection along with a part of the stomach wall or a wedge resection with an oncologic margin was performed. A multiorgan resection was done in 2 patients with locally advanced tumors – a tumor diameter of >10 cm and infiltration of the adjacent organs (Table 3). Two patients were operated on laparoscopically for gastric GIST. In the 1st case, a 3 cm pedunculated endophytic tumor of the fundus was excised; in the 2nd case, a 3.5 cm exophytic tumor of the anterior was removed.

In the majority of cases (12 patients, 67%), the diameter of the tumor was ≤5 cm and they were classified as low to very low risk. Two cases of GIST with a tumor diameter >10 cm were classified as high risk. The mitotic index

Table 3. Type of surgical operation

Type of surgery	Number of operations	Percentage [%]
Tumor resection with a margin including the stomach wall	11	68.75
Segmental resection of the small intestine	2	12.5
Anterior resection of the rectum	1	6.25
Multiorgan resection 1. Tumor resection with a margin including the stomach wall, splenectomy, segmental resection of the transverse colon 2. Resection of the gastric tumor, segmental resection of the transverse colon	2	12.5
Total	16	100

Table 4. The degree of tumor malignancy

Risk classification	Tumor size [cm]	Mitotic index	Number of cases	Percentage [%]
Very low	<2	<5/50	3	16.7
Low	2–5	<5/50	9	50
Intermediate	<5 5–10	6–10/50 <5/50	0 4	22.2
High	>5 >10 all	>5/50 all >10/50	0 2 0	11.1
Total			18	100

Table 5. Residual tumor distribution

Presence of residual tumor	Number of cases	Percentage [%]
R0	13	72
R1	5	28
R2	0	0

in all 18 cases remained below 5. The results of histopathological examination with risk assessment, mitotic index, and tumor size are presented in Table 4.

The final result of microscopic examination confirmed a complete R0 resection in 13 patients. Tumors located in the mesentery and in the retroperitoneal space were removed with surgical margins showing microscopic evidence of tumor cells (R1 resection). In the 2 cases of gastric GIST with a diameter of >10 cm, tumor rupture occurred during the procedure, but they were classified as R1 resections. All tumors were removed without any macroscopic residual tumor (Table 5).

In all 18 patients, the follow-up period lasted from 6 to 60 months. The postoperative period was uneventful in 17 cases. One case of postoperative death occurred in an 84-year-old man who presented symptoms of heart failure. During the follow-up, all patients were recurrence-free. One patient was lost for follow-up. Four patients qualified for adjuvant therapy with imatinib.

Discussion

Stromal gastrointestinal tumors are rare and challenging for clinicians because of their nonspecific symptoms and an oligosymptomatic clinical course. They are often discovered incidentally during an evaluation for other reasons. A definite histopathological diagnosis is obtained postoperatively due to the subserosal, intramural or submucosal growth of such tumors. In this study, the diagnoses were made postoperatively based on histopathological examination of the excised tissues. Obtaining a representative endoscopic biopsy may be difficult because of the nature of tumor growth. The preferred diagnostic methods are endoscopic ultrasound-guided fine-needle aspiration or Tru-Cut biopsy, especially for small tumors. The usefulness of endoscopic ultrasound-guided fine-needle aspiration was studied by Akahoshi et al. on a group of 53 patients. The overall sensitivity of this method was 82% (42 out of 53). The sensitivity in relation to tumor size was 71% for lesions up to 2 cm, 86% for lesions of 2–4 cm, and 100% for lesions over 4 cm.[6]

Discovering the presence of activating mutations in the *KIT* or platelet-derived growth factor receptor alfa (*PDGFRA*) genes is crucial for GIST diagnosis. The most important diagnostic tool for GIST is the evaluation of the immunohistochemical expression of *CD117*, which is found to be positive in 95% of those tumors. Mutations within the *PDGFRA* gene are detected in tumors with a mutation-free *KIT* gene.

The location of the GIST within the gastrointestinal tract is a significant prognostic factor. A gastric location is associated with a better prognosis (only 25% of such tumors are malignant) than locations in other organs, including the small intestine (50% of such tumors are malignant), esophagus and colon (the majority of these tumors are malignant). Less frequently, a GIST may appear outside the wall of the gastrointestinal tract, in which case it is found in the mesentery, omentum, retroperitoneum, or pelvic tissues. Typically, however, in those locations, metastases

of the stromal tumor are found. Histopathological examination requires information about the site of origin of the tumor.[7] In our study group, 3 primary tumors (16.7%) were located outside the gastrointestinal tract.

The risk stratification developed on the basis of expert experience from the National Institutes of Health (NIH) distinguishes tumors of very low, low, intermediate, and high risk of recurrence or metastasis. The key elements of this scheme include tumor size and mitotic count assessed in 50/HPF. Additionally, the prognosis takes into account the location of the tumor. Cut-off values for tumor size are 2, 5 and 10 cm, and 5 mitoses per 50 HPF. Tumors larger than 10 cm with high mitotic activity (over 10/50 HPF) are always of high risk.[8] In our study group, the majority of tumors (16 patients, 89%) were classified as not high risk. Only in 1 case (5.5%) was the tumor classified as high risk.

In the treatment of GISTs, radical surgery is the most effective therapeutic approach. In approx. 75% of patients, it is possible to perform the first operation with curative intent and remove the lesion with a margin free of tumor (R0 or R1 resection). Increasingly, laparoscopic or endoscopic procedures are being used. Researchers from Korea conducted a retrospective study on 406 patients who were treated surgically for GIST between March 1998 and March 2012. The mean tumor size was 4.9 cm (ranging from 0.3 to 29 cm). All patients underwent radical surgery. Laparoscopic resection was carried out in 156 patients (38.4%), while the remaining 250 (61.6%) required open resection. The mean tumor size in the patients treated laparoscopically was significantly smaller than in those who were treated with open surgery (3.45 cm vs 5.46 cm; $p < 0.001$). During the follow-up period, which lasted from 2 to 166 months (median 42.9 months), 11 (2.7%) cases of recurrence with metastases to the liver (9 cases) and peritoneum (2 cases) were observed in patients undergoing surgical resection.[9] Authors from China used endoscopic resection to treat small lesions up to 2 cm which were located in the stomach and grew into the gastrointestinal tract lumen. This procedure was shorter and associated with less blood loss and a faster recovery of intestinal peristalsis. In 3 out of 50 patients (6%) who underwent the endoscopic procedure, perforation occurred. One patient was reoperated on because of abdominal infection, while in the remaining patients conservative treatment was effective.[10] In turn, Honda et al. described a group of 78 patients (32 men, 46 women) with a mean age of 63 years who were treated with laparoscopic surgery for gastric GIST. The mean size of the tumors was 34.7 ±12.1 mm. In 92.3% of patients, tumor resection was performed with a pathologically negative margin, while in 7.7% of patients, gastrectomy was required. The mean operative time was 147.5 ±63.8 min, the mean estimated amount of blood loss was 17.8 ±47.9 mL and the mean length of hospitalization was 9.4 ±12.8 days. Complications such as anastomotic leakage occurred in 2 (2.6%) cases. During the follow-up period of 45.3 ±18.5 months, 1 patient experienced recurrence in the omentum and 4 other patients died due to other causes. These results convinced the author that laparoscopic resection is an appropriate therapeutic option for lesions up to 5 cm in diameter.[11]

Stromal tumors constitute approx. 20% of all tumors of the small intestine. The most common presentation of intestinal GIST is bleeding, while obstruction occurs rarely. Morrison and Hodgdon described 2 patients with a GIST who underwent emergency laparoscopy due to small intestine obstruction.[12] In a 59-year-old man, the obstruction was caused by an 8 cm pedunculated tumor, which provoked a rotation of the bowel and its mesentery. In another case of a 24-year-old woman, the obstruction resulted from intussusception of the lesion. Both patients underwent segmental resection of the small intestine affected by the tumor, then a side-to-side anastomosis was created using the Endo GIA™ stapler. There were no complications in either case. The authors believe that laparoscopic resection for obstructed intestinal tumors is a safe procedure and is associated with less blood loss, shorter hospital stays and less analgesic use in comparison to open surgery. When a small intestinal tumor is suspected in the computed tomography, the presence of GIST shall be considered. During surgery, special care shall be taken to avoid damage to the capsule of the tumor.[12]

In the adjuvant treatment of patients with intermediate and high clinical aggressiveness according to the NIH, tyrosine kinase inhibitors are used because of the high risk of recurrence.[13] Additionally, a spontaneous rupture of the tumor or rupture during resection increases the risk of peritoneal recurrence and is considered an unfavorable prognostic factor.[14] The introduction of imatinib has significantly improved prognosis and survival in such patients. Proper histopathological diagnosis, along with an immunohistochemical test for *CD117*, and a panel of antibodies helpful in differential diagnosis of other mesenchymal cancers are prerequisites to successful therapy. An increase in the incidence of disease progression with longer follow-up times in patients treated with imatinib for disseminated GIST has been observed; thus, attempts at combining imatinib with other invasive methods have been undertaken.[15] Hakime et al. described a group of 17 patients who underwent radiofrequency ablation of the liver for metastatic GIST. The mean max tumor diameter was 2.5 ±1 cm (range: 0.9–4.5 cm). The authors believe that their treatment modality is effective and safe in patients with GIST liver metastases who undergo imatinib treatment, and that the treatment should be applied at the appropriate time for the best clinical response.[16]

Conclusions

The most common location of GISTs is the stomach (72%). In the diagnosis of GISTs located in the stomach, endoscopic biopsy results are often negative and indicate the

inflammatory process of the gastric mucosa. Computed tomography of the abdominal cavity is the best diagnostic test. The majority of GISTs are of very low or low risk of recurrence and metastasis (67%).

References

1. Głuszek S, Rylski R, Kot M, et al. GIST: Risk of recurrence and dissemination. *Gastroenterol Rev*. 2008;3(4):176–184.
2. Prywinski S, Szopiński J, Wierzchowski P, Dąbrowiecki S. Gastrointestinal stromal tumor of small intestine as the cause of massive gastrointestinal hemorrhage: Case report. *Pol Surg*. 2008;10(2):107–112.
3. Wang YP, Li Y, Song C. Clinicopathological features and prognosis of small gastrointestinal stromal tumors outside the stomach. *Oncol Lett*. 2015;10(5):2723–2730.
4. Yacob M, Inian S, Sudhaker CB. Gastrointestinal stromal tumors: Review of 150 cases from a single centre. *Indian J Surg*. 2015;77(2):505–510.
5. Ruka W, Debiec-Rychter M, Rutkowski P, et al. Current diagnostic and therapeutic management of patients with gastrointestinal stromal tumor (GIST). *J Oncol*. 2007;57(2):181–189.
6. Akahoshi K, Sumida Y, Matsui N, et al. Preoperative diagnosis of gastrointestinal stromal tumor by endoscopic ultrasound-guided fine-needle aspiration. *World J Gastroenterol*. 2007;13(14):2077–2082.
7. Guzińska-Ustymowicz K, Nasierowska-Guttmejer A. Nowotwory podścieliskowe przewodu pokarmowego. *Pol J Pathol*. 2013;64(4) (Suppl 2):47–54.
8. Miettinen M, Sobin LH, Lasota J. Gastrointestinal stromal tumors of the stomach: A clinicopathologic, immunohistochemical, and molecular genetic study of 1765 cases with long-term follow-up. *Am J Surg Pathol*. 2005;29(1):52–68.
9. Kim IH, Kim IH, Kwak SG, Kim SW, Chae HD. Gastrointestinal stromal tumors (GISTs) of the stomach: A multicenter, retrospective study of curatively resected gastric GISTs. *Ann Surg Treat Res*. 2014;87(6):298–303.
10. Feng F, Liu Z, Zhang X, et al. Comparison of endoscopic and open resection for small gastric gastrointenstinal stromal tumor. *Transl Oncol*. 2015;8(6):504–508.
11. Honda M, Hiki N, Nunobe S, et al. Long-term and surgical outcomes of laparoscopic surgery for gastric gastrointestinal stromal tumors. *Surg Endosc*. 2014;28(8):2317–2322.
12. Morrison JE, Hodgdon IA. Laparoscopic management of obstructing small bowel GIST tumor. *JSLS*. 2013;17(4):645–650.
13. Din OS, Woll PJ. Treatment of gastrointestinal stromal tumor: Focus on imatinib mesylate. *Ther Clin Risk Manag*. 2008;4(1):149–162.
14. Matthews BD, Walsh RM, Kercher KW, et al. Laparoscopic vs open resection of gastric stromal tumors. *Surg Endosc*. 2002;16(5):803–807.
15. Fu C, Liu N, Deng Q, Tan Y, Ma K, Bie P. Successful treatment of gastrointestinal stromal tumor with multiple liver metastases with radiofrequency ablation and imatinib: A case report. *Oncol Lett*. 2015;10(2):875–878.
16. Hakime A, Le Cesne A, Deschamps F, et al. A role for adjuvant RFA in managing hepatic metastases from gastrointestinal stromal tumors (GIST) after treatment with targeted systemic therapy using kinase inhibitors. *Cardiovasc Intervent Radiol*. 2014;37(1):132–139.

F2-isoprostanes and F4-neuroprostanes as markers of intracranial aneurysm development

Anna Syta-Krzyżanowska[1,A–D,F], Iwona Jarocka-Karpowicz[2,C], Jan Kochanowicz[1,A,E,F], Grzegorz Turek[3,B], Robert Rutkowski[3,B], Krzysztof Gorbacz[3,B], Zenon Mariak[3,A,E], Elżbieta Skrzydlewska[2,C–F]

[1] Department of Invasive Neurology, Medical University of Bialystok, Poland
[2] Department of Analytical Chemistry, Medical University of Bialystok, Poland
[3] Department of Neurosurgery, Medical University of Bialystok, Poland

A – research concept and design; B – collection and/or assembly of data; C – data analysis and interpretation; D – writing the article; E – critical revision of the article; F – final approval of the article

Advances in Clinical and Experimental Medicine, ISSN 1899-5276 (print), ISSN 2451-2680 (online) *Adv Clin Exp Med*. 2018;27(5):673–680

Address for correspondence
Anna Syta-Krzyżanowska
E-mail: annasyta@op.pl

Funding sources
None declared

Conflict of interest
None declared

Received on October 9, 2016
Reviewed on November 29, 2016
Accepted on January 24, 2017

Abstract

Background. Intracranial aneurysms are common, occurring in about 1–2% of the population. Saccular aneurysm is a pouch-like pathological dilatation of an intracranial artery that develops when the cerebral artery wall becomes too weak to resist hemodynamic pressure and distends.

Objectives. The aim of this study was to determine whether the development of intracranial aneurysms and subarachnoid hemorrhage (SAH) affects neuronal phospholipid metabolism, and what influence different invasive treatments have on brain free radical phospholipid metabolism.

Material and methods. The level of polyunsaturated fatty acid (PUFA) cyclization products – F2-isoprostanes and F4-neuroprostanes – was examined using liquid chromatography – mass spectrometry (LC-MS) in the plasma of patients with brain aneurysm and resulting subarachnoid hemorrhage.

Results. It was revealed that an aneurysm leads to the enhancement of lipid peroxidation with a significant increase in plasma F2-isoprostanes and F4-neuroprostanes (more than 3-fold and 11-fold, respectively) in comparison to healthy subjects. The rupture of an aneurysm results in hemorrhage and an additional increase in examined prostaglandin derivatives. The embolization and clipping of aneurysms contribute to a gradual restoration of metabolic homeostasis in brain cells, which is visible in the decrease in PUFA cyclization products.

Conclusions. The results indicate that aneurysm development is associated with enhanced inflammation and oxidative stress, factors which favor lipid peroxidation, particularly in neurons, whose membranes are rich in docosahexaenoic acid, a precursor of F4-neuroprostanes.

Key words: isoprostanes, neuroprostanes, aneurysm, subarachnoid hemorrhage

DOI
10.17219/acem/68634

Copyright
© 2018 by Wroclaw Medical University
This is an article distributed under the terms of the Creative Commons Attribution Non-Commercial License (http://creativecommons.org/licenses/by-nc-nd/4.0/)

Introduction

Intracranial aneurysms are common, occurring in about 1–2% of the population. A saccular aneurysm is a pouch-like pathological dilatation of an intracranial artery that develops when the cerebral artery wall becomes too weak to resist hemodynamic pressure and distends. Unfortunately, the majority of them do not give characteristic symptoms, while vascular diagnostics is recommended only for patients with a family history of aneurysm or subarachnoid hemorrhage (SAH). Some intracranial aneurysms remain stable over time, but in others, mural cells die, the matrix degenerates, and eventually the wall ruptures, causing a life-threatening hemorrhage. Subarachnoid hemorrhage requires urgent diagnosis and treatment due to the high mortality and younger age of onset compared to other cardiovascular diseases. It is particularly important to prevent systemic and cerebral complications, which significantly worsen the prognosis and are associated with the occurrence of new neurological deficits, leading to disability in patients. The most favorable situation would be to diagnose and embolize or clip an aneurysm before SAH. The main problem is the lack of easily detectable, fast-emerging markers in the blood, imaging complications in the course of SAH.

The exact pathogenesis of cerebral aneurysms is not completely known, but it was shown that inflammatory and immunological mechanisms play a dominant role, and that the modifiable risk factors include smoking and high blood pressure.[1] Inflammation in connection with hypertension leads to disturbances in reduction–oxidation (redox) homeostasis in the arterial wall.[2] In such a situation, increased reactive oxygen species (ROS) generation results in oxidative modifications of lipids, proteins and DNA.[3] Brain susceptibility to oxidative stress results from the consumption of large amounts of oxygen, alteration of the blood–brain barrier and bio-activation of glial cells.[4] Moreover, the metabolism of the brain is characterized by the promotion of ROS due to its unique metabolic features, such as neurotransmitter oxidation.[5] Some glial cells and macrophages can produce the superoxide anion (O_2^-), nitric oxide (NO) and hydrogen peroxide (H_2O_2) indirectly through the cytokine activation.[6] Additionally, some brain regions have a high concentration of non-heme iron ions that can catalyze reactive hydroxyl radical formation from hydrogen peroxide.[7] In contrast to the easy triggering of ROS production in the brain, antioxidant defense is rather modest.[8] In particular, the levels of catalase and glutathione peroxidase, enzymes which participate in phospholipid protection, are low in most brain regions and in cerebrospinal fluid (CSF).[9] Therefore, oxidative damage to membrane phospholipids can easily occur in the central nervous system. Brain cells are susceptible to ROS action because of their high phospholipid polyunsaturated fatty acid content, primarily arachidonic acid (AA) and docosahexaenoic acid (DHA).[10] ROS may participate in non-specific lipid peroxidation that proceeds through chain reactions for lipid radicals, which react with oxygen to form a wide variety of products depending on the substrate oxidized. Cyclization and fragmentation are the main fatty acid transformations during free radical reactions.[11]

The main products of polyunsaturated fatty acid (PUFA) cyclization are prostaglandin derivatives, primarily F2-isoprostanes and F4-neuroprostanes, while fragmentation leads mainly to small-molecule unsaturated aldehydes. F2-isoprostanes are formed in all types of brain cells, mainly during the process of peroxidation of AA, while F4-neuroprostanes are derived from DHA, which is a main component of neuron phospholipids.[12] Both are generated in vivo independently of cyclooxygenases, primarily by free radical-induced peroxidation, and they are more stable than reactive aldehydes.[13] In addition, the products of cyclization have been found to exert potent biological actions, and hence may become mediators of diseases.[14] Therefore, their measurement is currently recognized as the most accurate method of assessing oxidative injury in vivo. It has been shown that the concentration of F2-isoprostanes and F4-neuroprostanes is increased in a number of human brain diseases.[15]

The pathogenesis of cerebral aneurysms is not fully understood, and we lack fast and cheap diagnostic tests for them. These facts justify the search for indicators which could also help to assess the metabolic consequences of aneurysms and the results of specific medical treatment. Therefore, in this study we examined the levels of the products of PUFA cyclization in the plasma of patients with aneurysmal SAH in order to determine whether and how the development of a cerebral aneurysm, with or without SAH, affects the neuronal metabolism of phospholipids. The influence of different invasive treatments on brain free radical phospholipid metabolism was also checked.

Material and methods

The plasma samples used in this study were collected from a group of 66 patients, including 35 women at a mean age of 54 years (range: 29–84 years) and 31 men at a mean age of 53 years (range: 38–66 years). Aneurysm was diagnosed in 33 patients (11 women and 22 men) at a mean age of 53 years (range: 29–69 years) and subarachnoid hemorrhage caused by the rupture of aneurysm was diagnosed in 33 patients (24 female and 9 men) at a mean age of 54 years (range: 31–84 years). Hemorrhage was diagnosed by brain computed tomography (CT) and aneurysm was diagnosed by angio-CT and angiography. SAH patients were evaluated at admission according to the Glasgow Coma Scale (GCS), the Hunt-Hess scale and World Federation of Neurosurgeons Scale (WFNS), which define neurological condition in relation to the size of hemorrhage.[16–18] The size of hemorrhage and cerebral edema in CT was rated on the Fisher scale.[19] The patient's medical history takes into account

information which could affect the marked parameters, such as chronic diseases, drugs used in the past month, smoking, and alcohol use. The routine tests included electrocardiography (ECG) and basic blood diagnostic tests.

The control group consisted of 66 healthy subjects – 35 women and 31 men, average age 54 years (range: 27––79 years) (Table 1). All the participants were matched for sex, age, diagnosis, and blood test results. The results of the parameters of healthy subjects and patients from all groups are outlined in Table 1. The exclusion criteria were as follows: pregnancy, lack of written consent or recent treatment with certain medications, including non-steroidal anti-inflammatory drugs, steroids and oral contraceptives.

The study commenced after obtaining approval from the Local Bioethics Committee at the Medical University of Bialystok (Poland), and written informed consent was obtained from all patients.

Samples and laboratory measurements

Blood samples were drawn by venipuncture and collected into heparinized and non-heparinized tubes. Samples were centrifuged at 2000 × g, at 4°C for 20 min to obtain plasma and serum. An antioxidant, butylhydroxytoluene (BHT), was added to the plasma samples before storing them to prevent oxidation. Samples were stored at –80°C until analyzed.

The serum samples were used to take laboratory measurements, including morphology, electrolyte and creatinine levels, and glucose and coagulation panels.

Biochemical assays

Total F2-isoprostane and F4-neuroprostane levels were quantified using the modified liquid chromatography-mass spectrometry (LC-MS) (Agilent, Santa Clara, USA) methods of Coolen and Fam, respectively, which have been described in detail.[13,20,21] In short, F2-isoprostanes and F4-neuroprostanes were isolated using the solid phase extraction (SPE) method, after an alkaline hydrolysis step. All analyses were performed using an Agilent 1290 ultra-performance liquid chromatography (UPLC) system interfaced with an Agilent 6460 triple quadrupole mass spectrometer with electrospray ionization source (ESI) (Agilent). The separation was performed using a reverse phase C18 column and linear gradient with water (pH 5.7) and acetonitrile (Sigma-Aldrich, Darmstadt, Germany). As an internal standard, 8-isoPGF2α–d4 (Cayman Chemical, Ann Arbor, USA) was used. F2-isoprostanes were analyzed in negative ion mode using multiple reaction monitoring (MRM). The plasma 8-isoPGF2 was determined as total 8-isoPGF2 containing free and esterified 8-isoPGF2. The limit of detection (LOD) was 30 pg/mL, at a signal-to-noise ratio of 3. The limit of quantitation (LoQ) for the standard F2-isoprostane was 60 pg/mL, at a signal-to-noise ratio of 10. The precision of LoQ was 8.25% (coefficient of variation – CV). The linear dynamic range was 60–6000 pg/mL. F4-neuroprostanes were analyzed by selected ion monitoring (SIM) in the m/z 357, as a series of peaks that have molecular masses and retention times expected for F4-neuroprostanes generated from the oxidation of DHA (Sigma-Aldrich) in vitro.

Table 1. Results of blood laboratory tests of healthy subjects and patients with aneurysm and SAH

Parameters	Healthy subjects n = 66	Aneurysm patients n = 33	SAH patients n = 33
WBC [10^3/mm^3]	5.27 ±1.16	8.60 ±3.6	11.34 ±3.77
RBC [10^6/µL]	4.15 ±0.31	4.30 ±0.39	4.08 ±0.56
PLT [×100 000/mm^3]	174 ±47	270 ±80	205 ±60
Sex (male : female)	31:35	22:11	9:24
Age (<50 years : >50 years)	25:41	11:22	13:20
Chronic diseases (– : +)	–	9:24	13:20
Smoking (– : +)	–	21:9	12:13
Number of aneurysms (1 : >1)	–	21:12	24:9
Size of aneurysm (<10 mm : >10 mm)	–	27:5	27:7
Embolization : clipping	–	–	19:14

WBC – white blood cells; RBC – red blood cells; PLT – blood platelets; SAH – subarachnoid hemorrhage.

Statistical analysis

Data pertaining to continuous variables were expressed as mean ±SD. The χ^2 test was used for testing hypotheses pertaining to categorical variables. The normal distribution of quantitative data was verified using the Kolmogorov-Smirnov test, with corrections performed by the Lilliefors test and the Shapiro-Wilk test. The significance of differences between the groups was tested with the Mann-Whitney U test and the Kruskal-Wallis test. For the comparison of dependent variables, the Friedman test was used with the adjusted Conover post hoc test. A p-value of <0.05 was considered statistically significant. All statistical analyses were performed using Stata/IC v. 13.0 (StataCorp, College Station, USA).

Results

The results obtained in this study seem to indicate that aneurysm development leads to a significant increase in the plasma level of lipid peroxidation products, such as F2-isoprostanes and F4-neuroprostanes (more than 2-fold and 8-fold, respectively). The rupture of an aneurysm additionally increases the level of these parameters in comparison to healthy subjects (Table 2).

Mean concentrations of F2-isoprostanes in patients with an unruptured aneurysm amounted to 235% of that found in the control group and to 264% of that in patients with

Table 2. The plasma F2-isoprostane and F4-neuroprostane levels

Parameters	F2-isoprostanes [pg/mL]			F4-neuroprostanes [pg/mL]		
	healthy subjects	aneurysm	SAH	healthy subjects	aneurysm	SAH
Plasma level	a) 470 ±126 (260–790) b) 442 ±119 (240–820)	991 ±617[a] (255–2526)	1079 ±654b[b] (186–2830)	a) 694 ±215 (390–1110) b) 660 ±194 (360–1010)	5758 ±2439 (1621–13097)	6220 ±3869 (1814–22417)
<50 years old	255 (152–432)	718 (255–1769)	1399* (303–2830)	493 (229–849)	5852 (1621–8636)	5978 (1814–22417)
>50 years old	332 (232–516)	1015 (366–2526)	696* (186–1774)	476 (278–723)	6066 (2985–13097)	5387 (2082–9628)
Male	282 (152–516)	644 (366–2526)	1256 (186–2212)	465 (230–849)	5873 (3122–13097)	4603 (1814–7572)
Female	335 (172–389)	754 (255–2013)	858 (283–2830)	610 (282–787)	6083 (1621–9606)	5744 (2082–22417)
1 aneurysm	–	579 (255–2013)	1110 (274–2830)	–	6566 (2985–9234)	5082* (3156–7572)
>1 aneurysm	–	758 (366–2526)	971 (303–1901)	–	5750 (1621–13097)	9810* (5934–13153)
Aneurysm size <10 mm	–	1202 (433–1856)	1180* (186–2830)	–	6606 (3568–13097)	5387 (1814–22417)
Aneurysm size >10 mm	–	721 (260–2526)	293* (274–1915)	–	5852 (1621–9234)	6179 (3145–13153)

[a] the control group for aneurysm; [b] the control group for SAH; * statistical difference.

subarachnoid hemorrhage. The difference in isoprostane concentration between patients with a ruptured and unruptured aneurysm was not as substantial, reaching merely 9%. The plasma concentration of F4-neuroprostanes was significantly higher than that of F2, reaching 1027% in the aneurysm group and 1141% in the aneurysm and SAH group as compared to healthy subjects. When comparing the patients with unruptured and ruptured aneurysms, the values for patients with SAH were found to be 10% higher.

The iso- and neuroprostane plasma levels with additional information concerning the patients are listed in Table 2.

Due to the mean age of 50.08 years in all treated patients, a concentration of oxidative stress parameters was rated above and below 50 years. Table 2 shows the values of F2-isoprostane and F4-neuroprostane levels in the age groups; the marked p-value for the healthy and aneurysm patients is not statistically significant, whereas in the group with hemorrhage, the concentration of F2-isoprostanes is significantly higher, with $p < 0.05$. The concentration of F2-isoprostanes and F4-neuroprostanes were also compared in diversity by gender, described using the Mann-Whitney U test, but there was no statistically significant difference between men and women.

The size of an intracranial aneurysm had a statistically significant impact on plasma F2-isoprostanes at the time of hemorrhage, with $p < 0.05$. The results are shown in Table 2. The values of F4-neuroprostanes are higher for several intracranial aneurysms at admission and discharge.

A number of factors have an effect on oxidative stress, including chronic diseases, inflammation, smoking, and alcohol abuse. The influence of the above-mentioned factors on the value of F2-isoprostanes and F4-neuroprostanes was taken into consideration in the group of patients with SAH at the time of onset and at discharge. These parameters are shown in Table 3. The group of alcohol-abusing patients was too small to carry out credible statistical analysis.

Each SAH patient was examined neurologically on admission to the Department of Neurosurgery (Clinical Hospital of Medical University of Bialystok, Poland), after their medical history was taken. Neck stiffness was observed in all patients and Kernig's sign was present in 64% of patients. We observed the following focal symptoms in 5 patients: hemiparesis, blurred vision, and speech impairment in the form of motor and mixed aphasia. The remaining patients presented only neck stiffness. The Hunt-Hess scale illustrates neurological condition in relation to the degree of impaired consciousness and changes in the brain CT scans. There was no statistically significant difference between these groups of patients, but the values of measured parameters decreased faster in patients with less neurological deficit.

Dependence of the iso- and neuroprostane concentration was assessed in relation to the WFNS. The clinical grading system is based on the GCS and on the presence of neurological symptoms. Grade I without motor deficit was observed in 24 people and was compared with patients in the other stages. We observed 2 patients in both grade II, with impaired orientation, and grade IV with motor deficit and significant impairment of consciousness. The results did not differ in these groups. Indeed, a statistical decrease was recorded during hospitalization.

The Fisher scale is based on changes observed in brain CT scans performed for each patient on hospital admission. Grades 1 or 2 were found in 11 patients with a small amount of blood in the subarachnoid space. Grade 3 was found in 4 of them with hematoma in the subarachnoid space and in 18 patients with blood perforation into the ventricular system. There was a statistically significant difference in the concentration of F4-neuroprostanes at discharge between grades 2 and 3 on the Fisher scale, with $p < 0.05$.

Edema was observed in brain CT scans of 20 patients with subarachnoid hemorrhage. The analyzed parameters of oxidative stress were higher in the case of F4-neuroprostanes, but showed no statistical significance, with $p > 0.05$. On the other hand, intracerebral hematoma appeared in 6 patients; its presence did not affect plasma isoprostanes ($p = 0.4975$) or neuroprostanes ($p = 0.3559$) in the blood. However, for patients without intracerebral hematoma, the value of the F4-neuroprostanes decreased significantly faster, visualizing higher expiration of oxidative stress, with $p < 0.05$.

Each patient hospitalized in the course of SAH was monitored by transcranial Doppler (TCD) for vasospasm. This complication occurred in 17% of patients; the evaluated iso- and neuroprostane levels are shown in Table 3. The average values of F4-neuroprostanes were higher at admission and discharge in the case of vasospasm, falling significantly during hospitalization only in patients without vasospasm.

Aneurysms were embolized in 19 patients; in the remaining 14 patients, aneurysms were successfully clipped after angiography in all cases. Additionally, stress parameters were measured for 23 patients after the surgical procedure. The mean concentration of F2-isoprostanes increased by 7.8% on average after aneurysm treatment, and at discharge it decreased by 30.9%, representing 25.5% below baseline. Comparing the types of surgical intervention, lower values of isoprostanes can be observed after embolization, with a direct decrease during hospitalization (Fig. 1).

The mean values of neuroprostanes are several times higher, falling gradually after onset (Fig. 2).

This decrease since hospital admission is more significant in the case of embolized aneurysms. The distribution of concentration for clipping is also connected with an initial postoperative increase, as in the case of F2-isoprostanes.

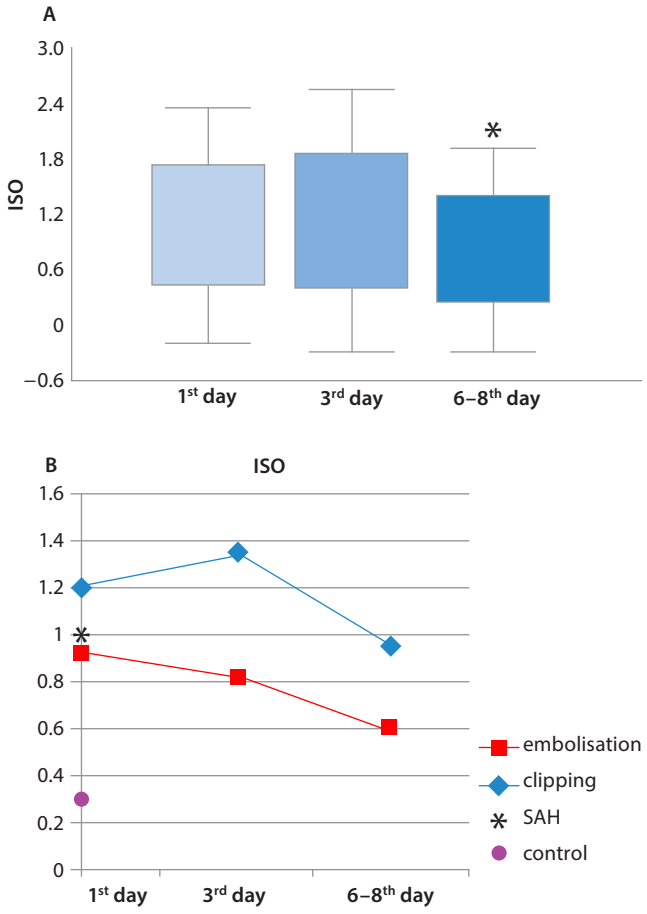

Fig. 1. The F2-isoprostanes (ISO) in patients with SAH before and after treatment

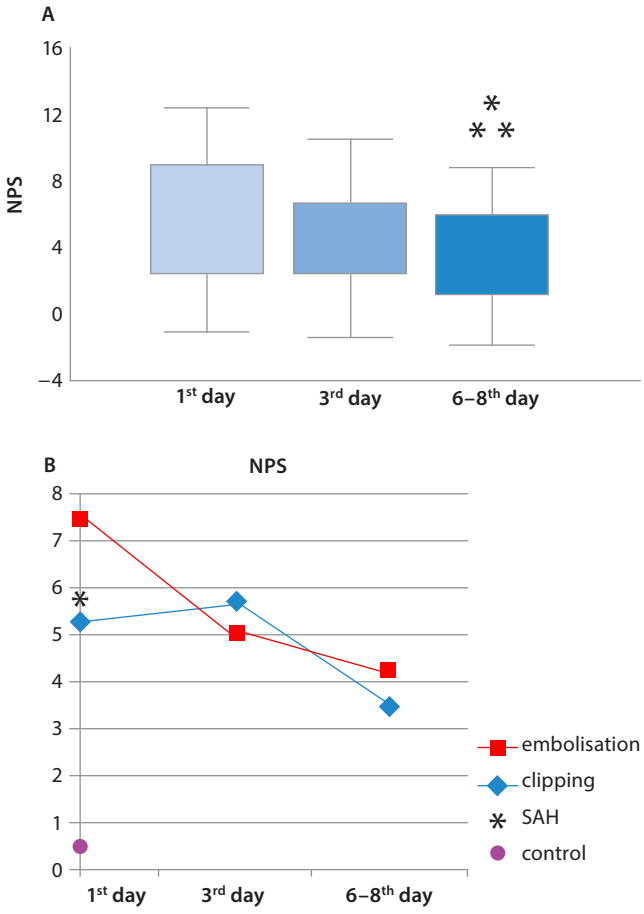

Fig. 2. The F4-neuroprostanes (NPS) in patients with SAH before and after treatment

Table 3. The plasma F2-isoprostane and F4-neuroprostane levels in SAH patients before and after treatment

Parameters		n	F2-isoprostanes [pg/mL]		F4-neuroprostanes [pg/mL]	
			1st day	6–8th day	1st day	6–8th day
Chronic disease	–	13	962 ±759 (274–2830)	625 ±410 (116–1454)	5834 ±3035 (1814–13153)	3542 ±2425 (1433–9518)
	+	20	961 ±595 (186–2212)	690 ±634 (171–2867)	5390 ±4656 (1953–22417)	3265 ±1690* (864–6112)
Smoking	–	12	1084 ±670 (283–2830)	690 ±751 (180–2867)	5610 ±5441 (2082–22417)	3110 ±1434 (864–9520)
	+	13	803 ±624 (186–2210)	553 ±438 (117–1562)	5834 ±2427 (1814–9628)	3680 ±2714 (1020–5740)
Kernig's sign	–	12	858 ±506 (274–1901)	559 ±398 (116–1454)	6854 ±5235 (3289–22417)	4890 ±2304* (1020–9518)
	+	21	1009 ±719 (186–2830)	680 ±621 (171–2867)	4603 ±2056 (1814–9984)	3112 ±1653* (864–7895)
Focal signs	–	28	985 ±631 (186–2830)	652 ±583 (116–2867)	5611 ±4179 (1814–22417)	3258 ±2139* (1020–9518)
	+	5	630 ±852 (404–2212)	553 ±412 (389–1374)	5122 ±3252 (1953–9984)	3542 ±1738 (864–5740)
Hunt-Hess scale	1	19	1192 ±473 (283–1901)	755 ±421* (116–1562)	5654 ±4681 (1814–22417)	3261 ±1745* (1020–7233)
	2–4	14	627 ±855 (186–2830)	542 ±717 (171–2867)	5167 ±2456 (1953–9984)	3480 ±2492 (864–9518)
WFNS	1	24	937 ±637 (186–2830)	625 ±444 (116–1562)	5654 ±4376 (1814–22417)	3680 ±2210* (1020–9518)
	2–4	9	825 ±724 (404–1965)	934 ±788 (171–2867)	5562 ±2647 (2082–9984)	3337 ±1283* (1206–4601)
Fisher Scale	1–2	11	889 ±579 (186–1897)	626 ±462 (116–1562)	5086 ±3417 (1814–13153)	4125 ±1880 (1433–7233)
	3–4	22	985 ±691 (274–2830)	788 ±602 (171–2867)	5654 ±4324 (1953–22417)	3340 ±2135* (864–9518)
Brain edema	–	12	1009 ±529 (186–1897)	625 ±718 (310–2867)	5086 ±1892 (2082–8715)	3256 ±1448 (1664–6112)
	+	21	858 ±723 (274–2830)	586 ±411 (116–1454)	5654 ±4752 (1814–22417)	3555 ±2375* (864–9518)
Hematoma	–	26	1105 ±639 (186–2830)	866 ±583 (116–2867)	6477 ±4314 (1814–22417)	3701 ±1623* (1020–7233)
	+	7	980 ±752 (274–2212)	571 ±393 (171–1177)	5151 ±2192 (1953–7572)	3874 ±3414 (864–9518)
Vasospasm	–	24	1192 ±575 (186–2212)	717 ±560* (171–2867)	5562 ±2446 (1814–10290)	3256 ±1853* (864–7895)
	+	5	449 ±1086 (274–2830)	310 ±90* (171–377)	6854 ±8596 (3156–22417)	3569 ±2996 (2101–9518)

* statistically different; WFNS – World Federation of Neurosurgeons Scale.

Discussion

An intracranial aneurysm, usually formed at cerebral artery bifurcations, is the result of pathological changes reducing the strength and stretching of the arterial wall, and hemodynamic blood flow, to which endothelial cells are exposed.[22,23] The loss of endothelium continuity and exposure to collagen leads to thrombus formation, in which blood cells get trapped. Trapped platelets release platelet growth factors that react with the receptors of muscle cells, leading to proliferation.[24] Moreover, the concomitant release of vascular endothelial growth factor (VEGF) increases endothelial permeability, thus facilitating the accumulation of lipids and plasma proteins, including antibodies and complement components in the arterial wall. Neutrophils, trapped in the thrombus, are a source of proteases and other cytotoxic and pro-inflammatory compounds which increase oxidative stress and damage the intima and media.[25] Therefore, it is suggested that chronic inflammation is the primary reason for arterial wall degeneration.[1] An increase in macrophage, T cell and leukocyte infiltration in the wall produces ROS that can modify the protein

and lipid components – extracellular as well as cellular – and in consequence, the atherosclerotic walls contain accumulated lipids. The accumulation of lipids and low-density lipoproteins (LDLs) in the intima of the cerebral artery walls over time leads to intimal thickening and to changes in their structure, and finally, their functions. It refers particularly to brain membrane phospholipids that contain a high content of highly PUFAs, including arachidonic acid, linoleic acid, and docosahexaenoic acid.[26] When they are attacked by ROS, peroxidation products are formed with peroxides first, and consequently, an increase in lipid peroxidation is observed.[27] Moreover, PUFA peroxidation is enhanced in the presence of transition metal ions, such as copper and iron ions. Iron is found throughout the brain, and damage to brain tissue releases iron ions in a form which is capable of catalyzing free radical reactions, such as hydroxyl radicals formed from hydrogen peroxide or lipid peroxidation. Unfortunately, CSF has no significant ability to bind any released iron ions, which further promotes lipid peroxidation in the central nervous system (CNS).[28] A relatively stable group of lipid peroxidation products is the prostaglandin-like compound group, including F2-isoprostanes and F4-neuroprostanes, whose levels are also significantly enhanced during aneurysm development, as was shown in this study. It confirms that the non-enzymatic mechanisms of oxidation of AA esterified at the sn-2 position of different cells of cellular and lipoprotein phospholipids, and DHA esterified at the sn-2 position of neuron phospholipids play an important role in brain diseases, since F2-isoprostanes are formed mainly during the peroxidation of AA, the most abundant in all types of cells, whereas F4-neuroprostanes are derived from DHA, in which neurons are particularly rich.[29] F2-isoprostanes and F4-neuroprostanes are recognized as specific markers of lipid peroxidation and are superior to other markers of oxidative damage. The elevated level of prostaglandin derivatives has been observed in a number of human CNS diseases linked to oxidative stress.[30,31] The level of these compounds was also significantly increased in the plasma of patients with aneurysm, where the F2-isoprostane and F4-neuroprostane levels were approx. 3-fold and 10-fold higher than in the controls.

Further endothelial dysfunction, loss of muscle cells and the infiltration of inflammatory cells escalate inflammation and matrix degradation in the wall of the aneurysm, and lead to its rupture.[32,33] This study revealed that aneurysm rupture was accompanied by an additional increase in F2-isoprostanes and F4-neuroprostanes. The number of such accidents increases with age. The average age for subarachnoid hemorrhage in the literature is 60 years. In this study, the average age for SAH was 54 years and women accounted for 72% of them. Female gender was also rated in the previous meta-analyses as a risk factor of rupture.[23] Another general factor influencing aneurysm rupture is smoking. Smoking patients made up half the cases in the study group, which also coincides with previous analyses, because in Europe, 45–75% of patients with ruptured aneurysms are smokers. In the general population, this incidence rate is 20–35%. The factors increasing the risk of rupture are polycyclic shape and size, the most commonly ruptured aneurysms being between 6 and 15 mm. Assessing the size, only 18% of ruptured aneurysms were larger than 10 mm. The extravasation of blood into the subarachnoid space during aneurysm rupture causes a decrease in superoxide dismutase (SOD) activity in erythrocytes, which reduces their antioxidant ability and is conducive to increased membrane lipid peroxidation. The disintegrating erythrocytes become a source of free iron ions released from hemoglobin, which may participate in the Fenton reaction, leading to the formation of hydroxyl radicals (•OH) and an increase in cascade radical reactions.[34] This is accompanied by the release of pro-inflammatory factors, leading to local and systemic inflammation.[35] As a result of this release from a ruptured artery and the migration in the course of inflammatory leukocytes, comes the mass overproduction of free radicals and increased oxidative stress. Irritation of the arteries by the breakdown of hemoglobin products manifested by spontaneous vasospasm is particularly hazardous.[36] The result might be brain tissue damage by ischemia-reperfusion or development of a delayed ischemic neurological deficit (DIND). The activated microglia and macrophages generate superoxide anion and hydrogen peroxide as well as the release of pro-inflammatory cytokines, such as IL-1, IL-6 and TNF-α, resulting in oxidative stress generation with subsequent lipid peroxidation. A particularly exacerbated inflammation and lipid peroxidation was observed in a study of younger patients (<50 years of age), suggesting a faster accumulation of systemic inflammatory responses. In addition, we observed a higher level of F4-neuroprostanes in the case of several cerebral aneurysms. Additional symptoms consistent with focal brain injury, such as hemiparesis, blurred vision, and motor and mixed aphasia, occurred in 5–15% of patients, much less than in the previous studies. The F2-isoprostane and F4-neuroprostane concentrations showed a greater decrease, providing for a faster stabilization of the prooxidative – antioxidative balance in asymptomatic patients with focal CNS injury, as well as in patients in the best condition according to the Hunt-Hess scale and the WFNS, based on the GCS. In our observation, the advancement of hemorrhagic and edemic changes observed in the brain in the course of SAH did not correlate with the parameters of oxidative stress in the blood, which has been observed in CSF.[37]

The neurosurgical treatment of SAH patients diagnosed with a ruptured aneurysm consists of clipping or coiling as less invasive techniques. Aneurysm embolization was performed in 19 patients, which accounted for 58% of patients. In the remaining 14 patients, the aneurysms were clipped after angiography. A gradual restoration of brain metabolic homeostasis by embolization and clipping is shown by a target decrease in the level of plasma F2-isoprostanes and F4-neuroprostanes.

A complication occurring in the course of SAH was vasospasm, observed in 17% of patients, imaged by TCD. This value is much lower than estimated in previous studies, which affects 67% of patients, with a focal onset of symptoms in 24–32% of patients.[36] The cause may be the quick exclusion of the aneurysm from the systemic circulation and the implementation of a "triple-H" treatment on hospital admission. In the case of vasospasm, the F4-neuroprostane level was higher with a slower decrease than in patients without this complication. In the recent publications, mortality was estimated at 30–40%.[38] The above study recorded only 1 death. This fact could have been due to the center's experience in aneurysm embolization and clipping conducted in the Neurosurgical Intensive Care Unit, and the prevention of complications.

In conclusion, it was revealed that aneurysm leads to an increase in the cyclized products of PUFA peroxidation (F2-isoprostanes and F4-neuroprostanes). However, the rupture of an aneurysm results in hemorrhage and an additional increase in the examined prostaglandin derivatives. Embolization and clipping of aneurysms contribute to a gradual restoration of metabolic homeostasis in brain cells, which is visible in the decreasing level of the examined lipid peroxidation products. These parameters, F4-isoprostanes in particular, could be useful in monitoring the onset of intracranial aneurysm development and the effectiveness of therapy.

References

1. Tulamo R, Frozen J, Hernesniemi J, Niemela M. Inflammatory changes in the aneurysm wall: A review. *J Neurointerv Surg*. 2010;2(2):120–130.
2. Chalouhi N, Hoh BL, Hasan D. Review of cerebral aneurysm formation, growth, and rupture. *Stroke*. 2013;44(12):3613–3622.
3. Aoki T, Nishimura M, Kataoka H, et al. Reactive oxygen species modulate growth of cerebral aneurysms: A study using the free radical scavenger edaravone and p47phox (–/–) mice. *Lab Invest*. 2009;89(7):730–741.
4. Nag S, Kapadia A, Stewart DJ. Review: Molecular pathogenesis of blood-brain barrier breakdown in acute brain injury. *Neuropathol Appl Neurobiol*. 2011;37(1):3–23.
5. Joseph JA, Shukitt-Hale B, Casadeus G, Fisher D. Oxidative stress and inflammation in brain aging: Nutritional considerations. *Neurochem Res*. 2005;30(6/7):927–935.
6. Li WJ. Research progress in the mechanism of brain self-repair [in Chinese]. *Zhongguo Dang Dai Er Ke Za Zhi*. 2011;13(7):606–611.
7. Sadrzadeh SMH, Saffari Y. Iron and brain disorders. *Am J Clin Pathol*. 2004;121:64–70.
8. Shila S, Kokilavani V, Subathra M, Panneerselvam C. Brain regional responses in antioxidant system to alpha-lipoic acid in arsenic intoxicated rat. *Toxicology*. 2005;210(1):25–36.
9. Kerman M, Cirak B, Ozguner MF, et al. Does melatonin protect or treat brain damage from traumatic oxidative stress? *Exp Brain Res*. 2005;163:406–410.
10. Mazza M, Pomponi M, Janiri L, Bria P, Mazza S. Omega-3 fatty acids and antioxidants in neurological and psychiatric diseases: An overview. *Prog Neuropsychopharmacol Biol Psychiatry*. 2007;31(1):12–26.
11. Catala A. Five decades with polyunsaturated fatty acids: Chemical synthesis, enzymatic formation, lipid peroxidation and its biological effects. *J Lipids*. 2013;2013:710290.
12. Nkiki E. Biomarkers of lipid peroxidation in clinical material. *Biochem Biophys Acta*. 2014;1840(2):809–817.
13. Fam SS, Murphey LJ, Terry ES, et al. Formation of highly reactive A-ring and J-ring isoprostane-like compounds (A4/J4-neuroprostanes) in vivo from docosahexaenoic acid. *J Biol Chem*. 2002;277(39):36076–36084.
14. Miller E, Morel A, Saso L, Saluk J. Isoprostanes and neuroprostanes as biomarkers of oxidative stress in neurodegenerative diseases. *Oxid Med Cell Longev*. 2014;2014:572491.
15. Milne GL, Yin H, Morrow JD. Human biochemistry of the isoprostane pathway. *J Biol Chem*. 2008;283(23):15533–15537.
16. Teasdale G, Jennett B. Assessment of coma and impaired consciousness: A practical scale. *Lancet*. 1974;2:81–84.
17. Hunt WE, Hess RM. Surgical risk as related to time of intervention in the repair of intracranial aneurysms. *J Neurosurg*. 1968;28(1):14–20.
18. Teasdale GM, Drake CG, Hunt W, et al. A universal subarachnoid hemorrhage scale: Report of a committee of the Word Federation of Neurosurgical Societies. *J Neurol Neurosurg Psych*. 1988;51(11):1457.
19. Fisher CM, Kistler JP, Davis JM. Relation of cerebral vasospasm to subarachnoid hemorrhage visualized by computerized tomographic scanning. *Neurosurg*. 1980;6:1–9.
20. Coolen SA, van Buuren B, Duchateau G, Upritchard J, Verhagen H. Kinetics of biomarkers: Biological and technical validity of isoprostanes in plasma. *Amino Acids*. 2005;29(4):429–436.
21. Łuczaj W, Moniuszko A, Rusak M, Pancewicz S, Zajkowska J, Skrzydlewska E. Lipid peroxidation products as potential bioindicators of Lyme arthritis. *Eur J Clin Microbiol Infect Dis*. 2011;30(3):415–422.
22. Juvela S, Poussa K, Porras M. Factors affecting formation and growth of intracranial aneurysms: A long-term follow-up study. *Stroke*. 2001;32(2):485–491.
23. Laaksamo E, Tulamo R, Liiman A, et al. Oxidative stress is associated with cell death, wall degradation, and increased risk of rupture of the intracranial aneurysm wall. *Neurosurgery*. 2013;72(1):109–117.
24. Nurden AT. Platelets, inflammation and tissue regeneration. *J Thromb Haemost*. 2011;105(Suppl 1):S13–S33.
25. Frosen J, Piippo A, Paetau A, et al. Remodeling of saccular cerebral artery aneurysm wall is associated with rupture: Histological analysis of 24 unruptured and 42 ruptured cases. *Stroke*. 2004;35(10):2287–2293.
26. Bourre JM. Diet, brain lipids, and brain functions: Polyunsaturated fatty acids, mainly omega-3 fatty acids. In: Lajtha A, Vizi SE, eds. *Handbook of Neurochemistry and Molecular Neurobiology*. New York, NY: Springer US; 2009:409–441.
27. Lajtha A, ed. *Handbook of Neurochemistry and Molecular Neurobiology: Neural Lipids*. New York, NY: Springer US; 2010.
28. Gueraud F, Atalay M, Bresgen N, et al. Chemistry and biochemistry of lipid peroxidation products. *Free Radical Res*. 2010;44(10):1098–1124.
29. Halliwell B. Reactive oxygen species and the central nervous system. *J Neurochem*. 1992;59(5):1609–1623.
30. Montuschi P, Barnes PJ, Roberts LJ. Isoprostanes: Markers and mediators of oxidative stress. *FASEB J*. 2004;18(15):1791–1800.
31. Nowak JZ. Oxidative stress, polyunsaturated fatty acids-derived oxidation products and bisretinoids as potential inducers of CNS diseases: Focus on age-related macular degeneration. *Pharmacol Rep*. 2013;65(2):288–304.
32. Halliwell B, Gutteridge J. *Free Radicals in Biology and Medicine*. 3rd ed. Oxford, UK: Oxford University Press; 1999.
33. Starke RM, Chalouhi N, Ali MS, et al. The role of oxidative stress in cerebral aneurysm formation and rupture. *Curr Neurovasc Res*. 2013;10(3):247–255.
34. Juvela S, Poussa K, Porras M. Natural history of unruptured intracranial aneurysms: Probability of and risk factors for aneurysm rupture. *J Neurosurg*. 2000;93(3):379–387.
35. Dimitrov JD, Vassilev TL, Andre S, et al. Functional variability of antibodies upon oxidative processes. *Autoimmun Rev*. 2008;7:574–578.
36. Nielsen MJ, Moestrup SK. Receptor targeting of hemoglobin mediated by the haptoglobins: Roles beyond heme scavenging. *Blood*. 2009;114(4):764–771.
37. Naraoka M, Matsuda N, Shimamura N, Asano K, Ohkuma H. The role of arterioles and the microcirculation in the development of vasospasm after aneurysmal SAH. *Biomed Res Int*. 2014;2014:253746.
38. Yu-Ping H, Chih-Lung L, An-Li S, et al. Correlation of F_4-neuroprostanes levels in cerebrospinal fluid with outcome of aneurysmal subarachnoid hemorrhage in humans. *Free Radic Biol Med*. 2009;47(6):814–824.

Adrenal hemorrhage: A single center experience and literature review

Izabela M. Karwacka[A–F], Łukasz Obołończyk[C–E], Krzysztof Sworczak[A,C–F]

Department of Endocrinology and Internal Diseases, Medical University of Gdańsk, Poland

A – research concept and design; B – collection and/or assembly of data; C – data analysis and interpretation;
D – writing the article; E – critical revision of the article; F – final approval of the article

Advances in Clinical and Experimental Medicine, ISSN 1899-5276 (print), ISSN 2451-2680 (online) *Adv Clin Exp Med*. 2018;27(5):681–687

Address for correspondence
Izabela M. Karwacka
E-mail: izabelakarwacka@gmail.com

Funding sources
None declared

Conflict of interest
None declared

Received on October 27, 2016
Reviewed on November 18, 2016
Accepted on February 9, 2017

Abstract

Background. Adrenal hemorrhage (AH) is a rare condition that can lead to acute adrenal insufficiency and may be fatal. The risk factors of AH include focal adrenal lesion, abdominal trauma and anticoagulation therapy. The clinical manifestation of AH varies widely; the symptoms may be related to adrenal insufficiency or may reflect multiple organ failure. However, in many cases, the course of AH is asymptomatic.

Objectives. The study is a retrospective analysis of 23 cases of AH, whose aim is to discuss the etiology and the management of selected patients, as well as a literature review.

Material and methods. The paper presents a retrospective analysis of 23 patients with AH confirmed by radiological and/or pathological examination. Epidemiological data, the results of laboratory tests, and radiological and pathological examinations were included in the analysis.

Results. The risk factors of AH were not established in 13 patients, 5 patients had experienced a trauma prior to AH diagnosis, 1 patient was diagnosed with sepsis, 2 patients had concomitant neoplastic disease, and in 2 patients, 2 risk factors were present. Among patients who required emergency admission, 5 patients were hospitalized due to acute abdominal pain, 1 patient due to sepsis and 1 patient due to symptoms of active endocrinopathy. In the remaining patients, diagnostic procedures were prompted by the detection of adrenal incidentaloma (AI). A total of 40% of patients underwent surgical treatment due to the magnitude of AH or clinical and laboratory evidence of overt endocrinopathy. In the remaining patients, conservative treatment and further observation was recommended. In 34.8% of these patients, follow-up examinations revealed a gradual regression.

Conclusions. It seems that there is a need to distinguish patients with AH who do not require surgical intervention. Follow-up radiological examination is necessary to reassess the lesion. The patients in whom shrinkage of the tumor can be observed are likely not to require surgical treatment.

Key words: adrenal glands, hemorrhage, pseudocyst, primary adrenal insufficiency, adrenal incidentaloma

DOI
10.17219/acem/68897

Copyright
© 2018 by Wroclaw Medical University
This is an article distributed under the terms of the Creative Commons Attribution Non-Commercial License (http://creativecommons.org/licenses/by-nc-nd/4.0/)

Introduction

Adrenal hemorrhage (AH) is a rare condition that can lead to acute adrenal insufficiency and may be fatal. It is potentially life-threatening when the adrenal glands are involved bilaterally, although at least 90% of each adrenal cortex must be compromised before this is clinically evident. The incidence of spontaneous AH based on data from autopsy studies is 0.14–1.1%. The risk factors of AH include focal adrenal lesion, abdominal trauma, anticoagulation therapy, congenital or acquired bleeding disorders, sepsis, and pregnancy.[1,2] Bleeding of an adrenal gland tumor is most frequently observed in pheochromocytoma and adrenal metastases.[1,3–6] Larger lesions of adrenal myelolipoma (>5 cm) rarely present with acute retroperitoneal AH.[6] The clinical manifestation of AH varies widely; the symptoms may be related to adrenal insufficiency or may reflect multiple organ failure. However, in many cases, the course of AH is asymptomatic.[7]

Until recently, AH diagnosis was often made at postmortem examination.[8] Currently, due to the increased availability of modern imaging techniques, AH is more frequently diagnosed intravitally and in many cases lesions in the adrenal glands are detected unexpectedly (adrenal incidentaloma – AI). The features of AH on radiological imaging are specific; therefore, its diagnosis based on imaging studies is relatively simple.[8,9]

Data on AH in the literature are scarce and management standards have not been precisely established. It seems that there is a need to redefine AH risk factors and to establish guidelines for the management of high-risk patients, particularly considering that some AH cases may be associated with metastases or pheochromocytoma.

This paper summarizes data on 23 cases of AH, and discusses the etiology and the management of selected patients.

Material and methods

This paper presents a retrospective analysis of 23 patients with AH confirmed by radiological and/or pathological examination. The study group included patients treated at the Department of Endocrinology and Internal Diseases and the Outpatient Clinic of the University Clinical Center in Gdańsk from 2002 to 2016. Epidemiological data, the results of laboratory tests, and radiological and pathological examinations were included in the analysis.

Results

The study group included 23 patients; 60.8% women and 39.2% men. The mean age was 60.6 years (Table 1).

The risk factors of AH were not established in 13 patients (56.6%), 5 patients (21.8%) had experienced a trauma prior to AH diagnosis, 1 patient (4.3%) was diagnosed with sepsis, 2 patients (8.7%) had concomitant neoplastic disease, and in 2 patients (8.7%), 2 risk factors were present: anticoagulant drugs and lung cancer, and trauma and chronic oral anticoagulation.

Among patients who required emergency admission, 5 patients (21.7%) were hospitalized due to acute abdominal pain, 1 patient (4.3%) due to sepsis and 1 patient (4.3%) due to symptoms of active endocrinopathy. In the remaining 16 patients (69.7%), diagnostic procedures were prompted by AI. The symptoms of adrenal insufficiency (in the course of sepsis) were confirmed in 1 patient, and 1 patient had treatment-resistant hypertension. The rest of the patients were asymptomatic.

The results of biochemical tests and hormone assays in serum and urine – e.g., cortisol, adrenocorticotropic hormone (ACTH), androstenedione, dehydroepiandrosterone sulfate, and metoxycatecholamine (MT) – and radiological images of the study participants were analyzed. In 13 patients (56.2%), laboratory test results were within the range of normal values. The remaining 10 patients had laboratory abnormalities, including biochemical markers of adrenal insufficiency (4.3%), hypercortisolemia (8.7%), elevated urinary MTs (mainly normetanephrine, 21.8%), and disorders of both the corticotropic axis and MT secretion (8.7%). In all patients, computed tomography (CT) examination was performed. A lesion in the right adrenal gland was found in 12 patients (52.2%), a lesion in the left adrenal gland was found in 10 patients (43.5%), and 1 patient had bilateral lesions. The diameter of the AH ranged from 17 to 150 mm (mean diameter: 60.6 mm) (Table 2).

Nine patients underwent surgical treatment (40%) due to the magnitude of AH or to clinical and laboratory evidence of overt endocrinopathy. The patient in whom both an elevated MT level and hypercortisolemia were found was disqualified from surgery due to the burden of concomitant diseases. It should be stressed that the results of radiological examinations did not raise any oncological concerns. Moreover, pathological assessment unequivocally indicated AH; only in 1 specimen was AH with the presence of neoplastic cells (a metastasis from lung cancer) found. In the remaining group of patients (n = 14; 60%) conservative treatment and further observation was recommended. In this group, specific risk factors were identified (sepsis, trauma and anticoagulation) and no clinical or laboratory evidence of endocrinopathy was observed, while the adrenal lesions were explicitly described in CT reports as AH. Follow-up examinations performed in 8 patients (34.8%) revealed a gradual regression of AH, and in the patient with bilateral lesions, a complete absorption of hematomas was found. Table 2 summarizes the clinical course of AH in the study population.

Discussion

The pathophysiological mechanism of AH remains unclear. The adrenal glands have unique vasculature providing abundant blood supply, which significantly increases

Table 1. Study group characteristics

No.	Age	Gender	Risk factor	Adrenal gland	Size on CT [mm]	Laboratory tests	Intervention	Additional information
1	38	female	trauma	right	30 × 17	normal	observation	none
2	70	male	anticoagulant drugs, lung cancer	right	55 × 40	elevated normetanephrine	observation	decreased size of mass to 25 mm at 18 months
3	60	female	urosepsis	bilateral	52 × 32	adrenal insufficiency	observation	resolution of mass at 12 months
4	87	male	unknown	right	115 × 70	normal	observation	decreased size of mass to 60 mm at 3 months
5	67	female	unknown	right	32 × 28	hypercortisolemia, elevated normetanephrine	observation	decreased size of mass to 25 mm at 12 months
6	55	male	unknown	right	150 × 10	normal	adrenalectomy	histologically hematoma
7	73	female	trauma	right	85 × 70	normal	adrenalectomy	histologically hematoma
8	65	male	trauma	left	76 × 65	hypercortisolemia, elevated normetanephrine	observation	decreased size of mass to 75 mm at 2 months
9	60	male	unknown	left	60 × 60	normal	adrenalectomy	histologically hematoma
10	51	female	unknown	right	64 × 48	normal	adrenalectomy	histologically hematoma
11	58	female	unknown	left	120 × 40	hypercortisolemia, elevated normetanephrine	adrenalectomy	histologically hematoma
12	62	female	unknown	right	62 × 52	normal	adrenalectomy	histologically hematoma
13	60	male	unknown	left	97 × 78	normal	adrenalectomy	histologically hematoma
14	67	female	unknown	left	35 × 25	normal	adrenalectomy	histologically hematoma
15	53	female	unknown	left	43 × 31	hypercortisolemia	adrenalectomy	histologically hematoma
16	61	female	anticoagulant drugs, trauma	left	60 × 60	elevated normetanephrine	observation	decreased size of mass to 57 mm at 10 months
17	58	female	unknown	left	21 × 13	elevated normetanephrine	observation	decreased size of mass to 18 mm at 20 months
18	64	male	unknown	right	1 × 1	elevated normetanephrine	observation	none
19	45	male	trauma	right	18 × 9	normal	observation	none
20	63	female	unknown	right	21 × 15	normal	observation	stable size of mass
21	60	female	lung cancer	left	60 × 23	normal	observation	none
22	60	male	colon cancer	right	35 × 25	normal	observation	none
23	57	female	trauma	left	48 × 33	normal	observation	none

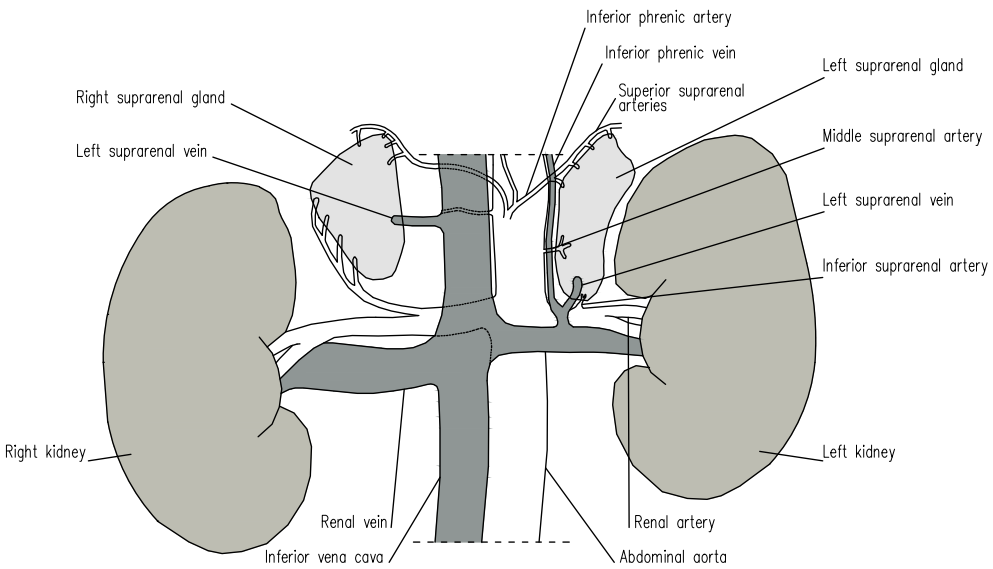

Fig. 1. Anatomical structure and blood supply of the adrenal glands

Table 2. Study group characteristics

Feature	Description	No.	%
Age (mean)	60.6 years	–	–
Gender	women	14	60.8
	men	9	39.2
Etiology	trauma	5	21.8
	sepsis	1	4.3
	anticoagulants + neoplasm	1	4.3
	anticoagulants + trauma	1	4.3
	neoplasm	2	8.7
	unknown	13	56.6
Adrenal gland involved	right adrenal gland	12	52.2
	left adrenal gland	10	43.5
	bilateral	1	4.3
Clinical presentation	acute abdominal pain	5	21.7
	asymptomatic (incidentaloma)	16	69.7
	infection	1	4.3
	evidence of active endocrinopathy	1	4.3
Laboratory parameters	normal	13	56.5
	hypercortisolemia	2	8.7
	elevated metoxycatecholamines	5	21.8
	hypercortisolemia + elevated metoxycatecholamines	2	8.7
	adrenocortical insufficiency	1	4.3
Intervention	observation	14	60
	surgical treatment	9	40

Table 3. Risk factors of adrenal hemorrhage

Conditions predisposing to AH	Examples
Trauma (80% of cases)	–
Stress	• burns • hypotension • surgery (particularly orthopedic surgery)
Infectious disease	• sepsis caused by *Neisseria meningitidis*, *Pseudomonas aeruginosa*, *Escherichia coli*, *Bacteroides fragilis*, *Streptococcus pneumoniae*
Medication	• anticoagulants • antiplatelets • nonsteroidal anti-inflammatory drugs • synthetic ACTH • glucocorticosteroids
Hematologic disorders	• antiphospholipid syndrome • systemic lupus erythematosus • heparin-induced thrombocytopenia • other thrombocytopathies • thrombocytosis
Obstetric causes	• pregnancy • postpartum period • pre-eclampsia
Perinatal injury	• asphyxia • perinatal hypoxia • sepsis • fetal hematologic disorders
Adrenal gland tumor	• primary: pheochromocytoma, adrenocortical cancer, myelolipoma, lipoma, hematoma, angioma, adenoma, pseudocyst • metastatic: lung cancer, renal cancer, breast cancer, colon cancer, thyroid cancer, gallbladder cancer, melanoma
Gastrointestinal diseases	• acute pancreatitis

AH – adrenal hemorrhage; ACTH – adrenocorticotropic hormone.

the propensity to bleeding. Each adrenal gland is supplied by 3 suprarenal arteries (the superior suprarenal artery, a branch of the inferior phrenic artery; the middle suprarenal artery, a direct branch of the abdominal aorta; and the inferior suprarenal artery, a branch of the renal artery).[3,8] It should be noted that venous outflow is provided by only 1 suprarenal vein tributary to the inferior vena cava.[10] Furthermore, it has been suggested that increased capillary resistance may be a significant factor predisposing an individual to AH. Elevated ACTH and MT levels, through their vasoconstrictive effect and excessive platelet activation, may lead to reperfusion and subsequent bleeding, mainly from distal capillary vessels (Fig. 1).[6,11]

Adrenal hemorrhages can be divided into primary (spontaneous or idiopathic) and secondary AHs (of known etiology, e.g., caused by trauma, sepsis or anticoagulation therapy).[1] The risk factors of AH are summarized in Table 3.

Based on a 25-year observation, Vella et al. divided a group of 141 patients with AH into 7 categories:

1. AH detected as AI – 28 cases;
2. spontaneous AH manifesting as acute hemorrhage to the abdominal cavity – 16 cases;
3. AH with concomitant hematological disease (antiphospholipid syndrome, systemic lupus erythematosus) – 20 cases;
4. postoperative AH (patients who underwent laparoscopic procedures or laparotomy, alloplastic joint replacement and prostatectomy) – 14 cases;
5. AH in patients treated with anticoagulants – 3 cases;
6. post-traumatic AH – 4 cases;
7. AH as a complication of sepsis and/or stress – 56 cases.[8]

The cases analyzed in our study were mainly AIs with non-established etiology (70% of patients), which were categorized as group 1 according to Vella's classification. The remaining patients were classified as group 2 or 7.

The clinical presentation reflects both the intensity of bleeding and the extent of adrenal gland injury.[1,9] The clinical course in bilateral massive hemorrhage to the adrenal glands is usually dramatic and, if recognized too late, may be fatal.[12] The patients in whom AH has been incidentally diagnosed usually do not develop a typical form of AH and the course of the disease may be asymptomatic.[8,13–16] In the analyzed group, 91.4% of cases were asymptomatic; only in 1 patient was clinically overt adrenal insufficiency observed.

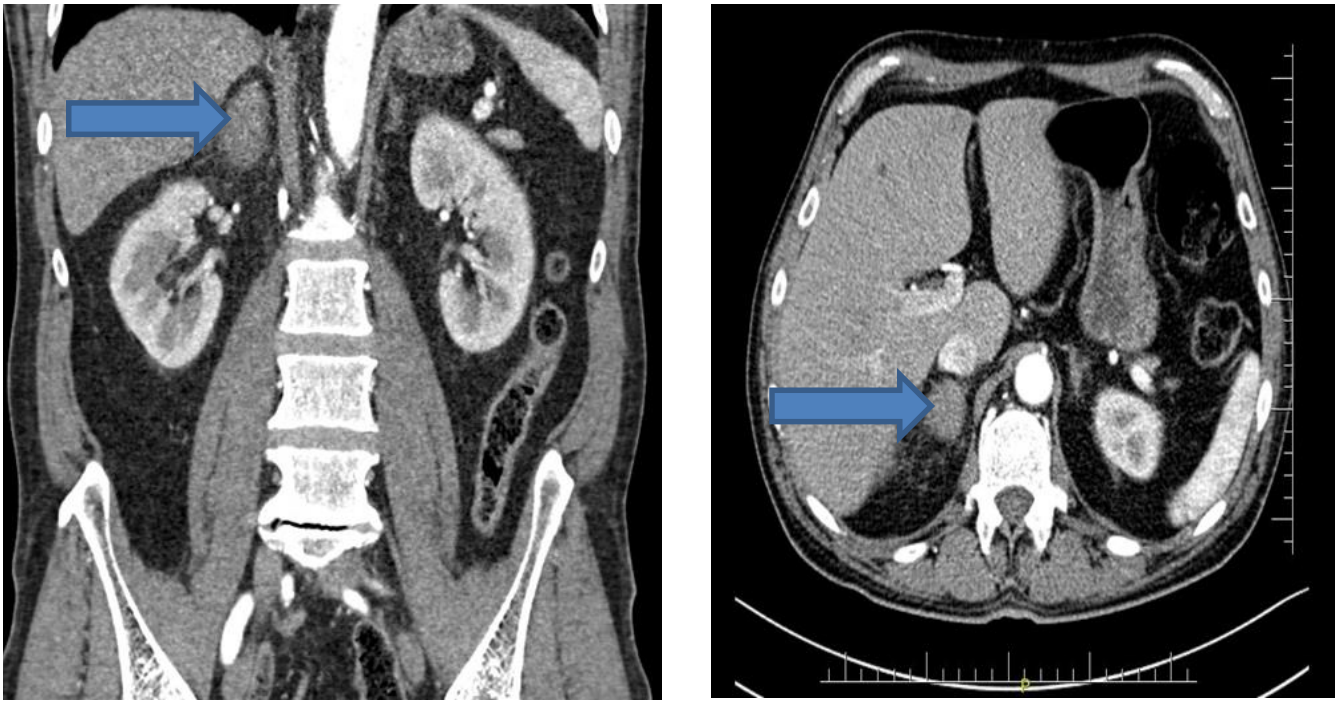

Fig. 2. Patient No. 22: right adrenal hematoma, 35 mm in diameter (arterial phase CT scan)

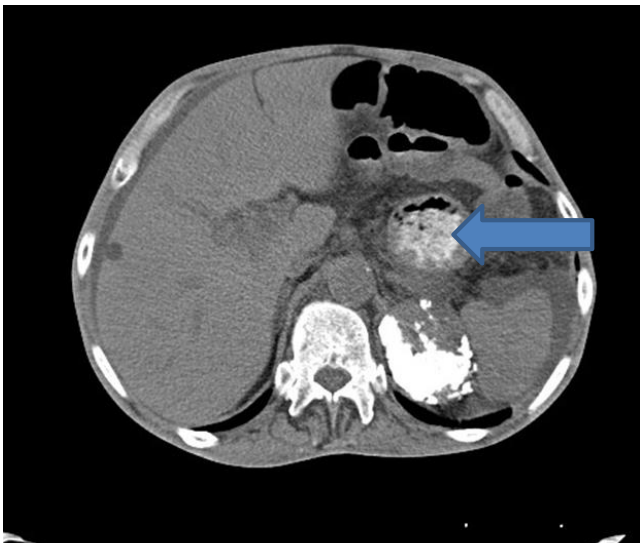

Fig. 3. Patient No. 8: left adrenal hematoma, 70 mm in diameter, with calcifications (arterial phase CT scan)

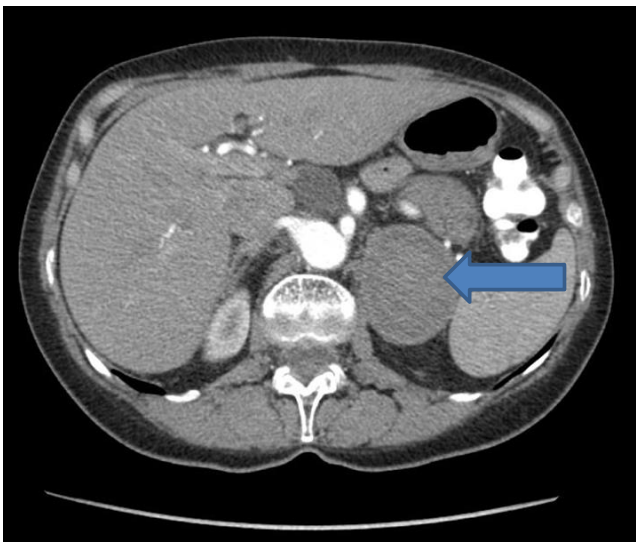

Fig. 4. Patient No. 16: left adrenal hematoma, 60 mm in diameter (arterial phase CT scan)

Abnormalities of laboratory parameters in patients with AH, such as hyponatremia, hyperkaliemia, hypercalcemia, and hypoglycemia, are biochemical markers of adrenal insufficiency. Anemia is observed in patients with massive bleeding. Thrombocytopenia and bleeding disorders occur in patients with antiphospholipid syndrome or lupus erythematosus.[8,17] Considering the risk of AH related to pheochromocytoma and adrenocortical cancer, in patients with these pathologies, the urine MT level measurement and the corticotropic axis assessment should be done.[1,18,19] In the study group, symptomatic adrenocortical insufficiency (in the patient with bilateral AH in the course of sepsis), increased secretion of MT and corticotropic axis disorders were found. Isolated hypersecretion of MT was observed in 5 patients, which could indicate an active neoplastic process (pheochromocytoma is the lesion where AH occurs most frequently);[4,5] however, MT levels only slightly exceeded normal laboratory range (50–100% above the upper limit of normal) and the patients did not present symptoms indicative of an excess of catecholamines. For this reason, the above abnormality was considered non-specific and could not be the basis for diagnosing

pheochromocytoma. Follow-up examination confirmed the spontaneous normalization of MT levels. It should be noted that 56.5% of patients had normal laboratory values. Similarly, in a group of 6 patients with AH described by Marti et al., 4 patients had normal laboratory test results.[1]

Undoubtedly, the increased availability of imaging examinations resulted in higher rates of AH diagnosis. The radiological image of AH depends on the patient's age and the duration and intensity of bleeding.[3,20] Despite the fact that ultrasonographic (USG) examination is a fast, inexpensive and widely available technique, its use in the diagnosis and monitoring of AH patients is limited to newborns and infants.[3] It has been reported that contrast-enhanced ultrasonography (CEUS) can also be used for the diagnosis of adrenal gland tumors, which might enhance the role of this technique in the detection of AH.[21,22] The method of choice for critically ill patients is CT scanning, because it allows preliminary differentiation of adrenal hemorrhagic tumors from malignant lesions (10% of pheochromocytomas, adrenocortical carcinoma and metastases).[23,24] On CT images, AH appears as a focal heterogeneous high-density (50–70 Hounsfield units) lesion (Fig. 2).[1,25,26] With the aging of the hematoma, its gradual shrinkage and even complete regression can be observed. Chronic AH can be seen as an adrenal mass with a hypodense center without calcification, known as an adrenal pseudocyst, and after a year, calcification is often found (Fig. 3). The lack of contrast enhancement allows the hemorrhagic nature of the lesion to be confirmed.[3] Moreover, Tan et al. presented 4 cases of non-traumatic AH which demonstrated features of prior adrenal congestion (adrenal gland thickening and periadrenal fat stranding) on CT scans (Fig. 4).[27] In some cases, magnetic resonance imaging (MRI) can be employed, which is particularly useful for differentiating acute bleeding from chronic bleeding.[22,25,26] The appearance of hemorrhage on MRI scans depends on the age of hemorrhage, with the signal intensity changing in relation to the progressive degradation of hemoglobin. In the acute phase (<2 days), hemorrhage is hypointense on T1-weighted images and hypointense on a T2 signal (Fig. 5). In the early subacute phase (2–7 days), AH is seen as a hyperintense T1 signal and a hypointense T2 signal. A chronic hematoma demonstrates peripheral low T1 and T2 signals due to intracellular hemosiderin, with central T2 hyperintensity and T1 isointensity.[28]

The management of patients with AH depends on their general health status. Hemodynamically unstable patients require intensive medical treatment for shock and adrenal insufficiency as well as qualification for surgical treatment. Surgery should be also considered in patients with the suspicion of pheochromocytoma and adrenocortical carcinoma, particularly if the size of the tumor in the adrenal gland exceeds 6 cm.[1,19,29] Conservative treatment should be considered in patients with bilateral AH, in patients whose AH was detected as AI, and in those with known

Fig. 5. Patient No. 3: bilateral adrenal hemorrhage; the lesions are 50 mm in diameter (MRI)

and reversible risk factors (e.g., AH caused by an overdose of anticoagulants).[5,30] Marti et al. described 6 cases of AH. In the group, 4 patients underwent surgical treatment, whereas the rest of the patients were re-examined.[1] One patient receiving conservative treatment was on anticoagulation therapy and, burdened with lung cancer metastasizing to the adrenal gland and adrenal hematoma, was qualified for chemotherapy. During the 6-month follow-up examination, a marked regression of the adrenal lesion was found. In another patient who had a history of septic shock complicated with neutropenia and colon perforation, and whose CT scan showed a hematoma with a pseudocyst, a complete regression of the adrenal lesion was observed at the 6-month follow-up visit. Bharucha et al. described bilateral AH with subclinical course in a patient on warfarin therapy in whom conservative treatment proved to be successful.[9] There are reports on cases of spontaneous bilateral AH manifesting with acute abdominal pain, in which the introduction of hydrocortisone replacement therapy and the withholding of surgical treatment resulted in a significant regression of the lesion confirmed by follow-up imaging.[11,24]

Among the patients included in the analysis, 9 (40%) underwent surgical treatment, and the decision was made based on the tumor size and the suspicion of active endocrinopathy. The remaining 14 patients (60%) were only examined again at follow-up. The factors that determined the choice of conservative treatment were known AH risk factors, an absence of clinical and laboratory markers of endocrinopathy, and a description of the adrenal lesion in the CT report, which unequivocally indicated AH. In 34.8% of these patients, follow-up imaging examinations showed a partial or total regression of the lesion.

Therefore, it seems that there is a need to distinguish patients with AH who do not require surgical treatment, because the natural course of AH may result in spontaneous hematoma resorption and recovery. Follow-up radiological examination is necessary in order to reassess the lesion. The patients in whom shrinkage of the tumor can be observed are likely not to require surgical treatment.

References

1. Marti JL, Millet J, Sosa JA, Roman SA, Carling T, Udelsman R. Spontaneous adrenal hemorrhage with associated masses: Etiology and management in 6 cases and a review of 133 reported cases. *World J Surg*. 2012;36:75–82.
2. Simon DR, Pales M. Clinical update on the management of adrenal hemorrhage. *Curr Urol Rep*. 2009;10:78–83.
3. Kawashima A, Sandler CM, Ernst RD, et al. Imagining of nontraumatic hemorrhage of the adrenal gland. *Radiographics*. 1999;19:949–963.
4. Jacobs LM, Williams LF, Hinrichs HR. Hemorrhage into a pheochromocytoma. *JAMA*. 1978;239(12):1156.
5. Nicholls K. Massive adrenal haemorrhage complicating adrenal neoplasm. *Med J Aust*. 1979;2:560–562.
6. Kumar S, Jayant K, Prasad S, et al. Rare adrenal gland emergencies: A case series of giant myelolipoma presenting with massive hemorrhage and abscess. *Nephrourol Mon*. 2015;7(1):e22671.
7. Kerkhofs TM, Haak HR, Roumen RM, Demeyere TB, van der Linden AN. Adrenal tumors with unexpected outcome: A review of the literature. *Int J Endocrinol*. 2015;2015:710514.
8. Vella A, Nippoldt TB, Morris JC III. Adrenal hemorrhage: A 25-year experience at the Mayo Clinic. *Mayo Clin Proc*. 2001;76:161–168.
9. Bharucha T, Broderick C, Easom N, Roberts C, Moore D. Bilateral adrenal haemorrhage presenting as epigastric and back pain. *JRSM Short Rep*. 2012;3:15.
10. Milewicz A. *Endokrynologia kliniczna*. Wrocław: Polskie Towarzystwo Endokrynologiczne; 2011:364–366.
11. Dhawan N, Bodukam VK, Thakur K, Singh A, Jenkins D, Bahl J. Idiopathic bilateral adrenal hemorrhage in a 63-year-old male: A case report and review of the literature. *Case Rep Urol*. 2015;2015:503638,1–4.
12. Moore MA, Biggs PJ. Unilateral adrenal hemorrhage: An unusual presentation. *South Med J*. 1985;78:989–992.
13. Christoforides C, Petrou A, Loizou M. Idiopathic unilateral adrenal haemorrhage and adrenal mass: A case report and review of the literature. *Hindawi Pub Corp*. http://dx.doi.org/10.1155/2013/567186. Accessed March 27, 2013.
14. Hoeffel C, Legmann P, Luton JP, Chapuis Y, Bonnin A. Spontaneous unilateral adrenal hematomas: 10 cases. *Presse Med*. 1994;23:1023–1026.
15. Bednarczuk T, Bolanowski M, Sworczak K, et al. Adrenal incidentaloma in adults: Management recommendations by the Polish Society of Endocrinology. *Endokrynol Pol*. 2016;67:234–258.
16. Babińska A, Siekierska-Hellmann M, Błaut K, et al. Hormonal activity in clinically silent adrenal incidentalomas. *Arch Med Sci*. 2012;8:97–103.
17. Potter EL, Barnes SL, Chunilal SD. Acute adrenal failure due to bilateral adrenal haemorrhage associated with lupus anticoagulant antibodies. *Intern Med J*. 2015;45:119–120.
18. Trauffer PM, Malee MP. Adrenal pseudocyst in pregnancy: A case report. *J Reprod Med*. 1996;41:195–197.
19. Dworakowska D, Drabarek A, Wenzel I, Babińska A, Świątkowska-Stodulska R, Sworczak K. Adrenocortical cancer (ACC): Literature overview and own experience. *Endokrynol Pol*. 2014;65:492–502.
20. Dunnick NR. Adrenal imaging: Current status. *AJR Am J Roentgenol*. 1990;154:927–936.
21. Cantisani V, Petramala L, Ricci P, et al. A giant hemorragic adrenal pseudocyst: Contrast-enhanced examination (CEUS) and computed tomography (CT) features. *Eur Rev Med Pharmacol Sci*. 2013;17:2546–2550.
22. Friedrich-Rust M, Schneider G, Bohle RM, et al. Contrast-enhanced sonography of adrenal masses: Differentiation of adenomas and non-adenomatous lesions. *Am J Roentgenol*. 2008;191:1852–1860.
23. Rao RH, Vagnucci AH, Amico JA. Bilateral massive adrenal hemorrhage: Early recognition and treatment. *Ann Intern Med*. 1989;110:227–235.
24. Wolverson MK, Kannegiesser H. CT of bilateral adrenal hemorrhage with acute adrenal insufficiency in the adult. *AJR Am J Roentgenol*. 1984;142:311–314.
25. Hiroi N, Yanagisawa R, Yoshida-Hiroi M, et al. Retroperitoneal hemorrhage due to bilateral adrenal metastases from lung adenocarcinoma. *J Endocrinol Invest*. 2006;29:551–554.
26. Goldman HB, Howard RC, Patterson AL. Spontaneous retroperitoneal hemorrhage from a giant adrenal myelolipoma. *J Urol*. 1996;155:639.
27. Tan GX, Sutherland T. Adrenal congestion preceding adrenal hemorrhage on CT imaging: A case series. *Abdom Radiol*. 2016;41:303–310.
28. Hammond NA, Lostumbo A, Adam SZ, et al. Imaging of adrenal and renal hemorrhage. *Abdom Imaging*. 2015;40:2747–2760.
29. Kashiwagi S, Amano R, Onoda N, et al. Nonfunctional adrenocortical carcinoma initially presenting as retroperitoneal hemorrhage. *BMC Surg*. 2015;15:46.
30. Kasperlik-Zauska AA, Rosłonowska E, Słowinska-Srzednicka J, et al. Incidentally discovered adrenal mass (incidentaloma): Investigation and management of 208 patients. *Clin Endocrinol (Oxf)*. 1997;46:29–37.

Spirometry testing among the homeless

Jerzy Romaszko[1,A–D,F], Adam Buciński[2,C,E,F], Anna M. Romaszko[3,B,D,F], Anna Doboszyńska[3,A,E,F]

[1] Family Medicine Unit, University of Warmia and Mazury, Olsztyn, Poland
[2] Department of Biopharmacy, Nicolaus Copernicus University in Toruń, Collegium Medicum in Bydgoszcz, Poland
[3] Department of Pulmonary Medicine and Infectious Diseases, University of Warmia and Mazury, Olsztyn, Poland

A – research concept and design; B – collection and/or assembly of data; C – data analysis and interpretation;
D – writing the article; E – critical revision of the article; F – final approval of the article

Advances in Clinical and Experimental Medicine, ISSN 1899-5276 (print), ISSN 2451-2680 (online) *Adv Clin Exp Med*. 2018;27(5):689–693

Address for correspondence
Jerzy Romaszko
E-mail: jerzy.romaszko@uwm.edu.pl

Funding sources
None declared

Conflict of interest
None declared

Acknowledgments
The authors wish to thank the study participants for their cooperation.

Received on December 27, 2016
Reviewed on January 16, 2017
Accepted on May 4, 2017

Abstract

Background. Many literature reports have indicated the fact that the percentage of active smokers among the homeless is high, often several times higher than that of the general population. The homeless are known to have worse spirometric parameters than the general population.

Objectives. The question of what the principal and exclusive cause of airway obstruction among the homeless is remains unanswered. Verification of the above-mentioned hypothesis is possible by comparing the spirometric parameters in homeless people with those in the general population, based on the data related to subgroups with similar tobacco smoke exposure, which are homogenous in terms of sex, race and age.

Material and methods. The spirometric parameters in 58 homeless male smokers were compared with those in 55 male smokers living normal lives. Neither group differed in age, duration of smoking or the number of pack-years. All of the subjects were Caucasian.

Results. The mean values of forced expiratory volume in 1 s (FEV1), forced vital capacity (FVC) and FEV1/FVC, both corrected and expressed as absolute figures, were lower amongst the smoking homeless men than amongst men living normal lives. In 27.59% of the homeless subjests not receiving treatment for lung diseases, airway obstruction was identified.

Conclusions. Our results suggest that smoking is not the only cause of the worse spirometric parameters found among the homeless.

Key words: homeless, spirometry, smoking

DOI
10.17219/acem/70915

Copyright
© 2018 by Wroclaw Medical University
This is an article distributed under the terms of the Creative Commons Attribution Non-Commercial License (http://creativecommons.org/licenses/by-nc-nd/4.0/)

Introduction

In the 21st century, diseases of the respiratory system have become a worldwide challenge for the medicine. Commonly known environmental factors are causing the problem to grow, and because most of these diseases are incurable, an increasing emphasis is being placed on their prevention. Atypical subpopulations, ones that exaggerate the extent of the problem, can be useful in the assessment of the effectiveness of preventive measures. Homeless people are such a subpopulation when it comes to many disease entities. Leaving aside the ethical and social aspects, the homeless population attracts the interest of researchers from a medical point of view due to the unique epidemiology of diseases of social significance. Given the limited access to medical assistance and the poor care for homeless people's own health, certain diseases are particularly prevalent among them and their diagnosis is often delayed.[1,2] Homeless people are characterized by a very high incidence of tuberculosis, an increased risk of HIV infection, a risk of various types of dependence syndromes (alcohol, illicit drugs, nicotine), a high percentage of individuals with mental problems, and high mortality.[3–5]

Apart from certain shared features which are independent of the geographical location of a study (such as the marked predominance of males among the homeless), there are also certain differences.[6] American and Western European authors most commonly deal with younger populations than authors from Central European countries do.[7] Drug dependence is more commonly reported by American authors, while alcohol dependence prevails in European publications.[3] Racial differences are also significant. American authors report that 70–90% of the homeless population is made up of African Americans, while this particular ethnicity is practically nonexistent in the Eastern European countries.[6]

Authors of multiple publications also observe that the percentage of active smokers among the homeless is high. Being estimated at 70–90%, irrespective of where the particular study was conducted, this percentage is several times higher than that in the general population.[8–10] Smoking is the strongest risk factor for the development of chronic obstructive pulmonary disease (COPD).[11] Taken together, these 2 facts clearly imply that COPD must be more prevalent among the homeless.

This was noticed by Snyder and Eisner, who performed spirometry in 67 homeless people in San Francisco (USA) and showed that obstructive lung disease (OLD) was twice as prevalent in this subpopulation as compared to the general population.[12] A report by Badiaga et al. from Marseilles (France) presented a similar conclusion suggesting an obvious pathophysiological association with smoking, which in this study was declared by 78% of the homeless compared to 30% of the members of the general population.[13] The problem is that such a combination of facts suggests a causal relationship, with homeless people developing OLD more often, because they smoke more. Meanwhile, this relationship has not been proven or, more precisely, the fact that there is a well-documented relationship between smoking and OLD does not make it the only reason why this highly smoke-exposed subpopulation develops OLD more often. Verification of this hypothesis is possible by comparing the spirometric parameters in homeless people with those in the general population and by studying the data related to subgroups with a similar exposure to tobacco smoke (homogenous in terms of sex, race and age).

Material and methods

Study population

A total of 53 homeless males from the city of Olsztyn (Poland) were included in the analysis. Olsztyn has a population of approx. 175,000; that – according to the 2014 data published by the Regional Center for Social Policy in Olsztyn – includes 153 homeless people falling within the European Typology on Homelessness and Housing Exclusion (ETHOS) operational categories: 1 – people living rough; 2 – people in emergency accommodation (a night shelter); and 3 – people living in accommodation for the homeless, in our case in a homeless hostel.[14] A set of basic demographic and medical data was collected from each of the subjects. Participation in the study was entirely voluntary and each subject was free to refuse to answer any of the questions, without providing a reason, at any stage of the study. The study protocol was approved by the Bioethics Committee of the University of Warmia and Mazury in Olsztyn, Poland (No. 38/2013).

The control group consisted of 578 individuals who had been examined during routine prophylactic campaigns carried out as part of Polish Spirometry Day. The examinations were performed at several different locations in Olsztyn (such as Old Market Square, City Hall, the Provincial Governor's Office, the Pulmonology Hospital, and others). Participation in the study was entirely voluntary and free. Each of the subjects completed a questionnaire which included questions about the subject's sociodemographic data, risk factors and respiratory symptoms. The volunteers were free to refuse to answer any of the questions. For the purposes of the study, all male current and ever-smokers over 35 years of age were selected, making a total of 55 people.

The reason why we chose 35 years as the lower age limit was because it was necessary to enable comparisons in the analogous age groups. This way, only 1 much younger person was excluded from the study group (the homeless group). Both groups consisted of subjects who considered themselves healthy and had never been treated for COPD or asthma.

Spirometry

Measurements of vital capacity (VC) and the flow – volume curve were carried out by medical staff experienced in performing spirometry, in accordance with the ATS/ERS 2005 guidelines.[15] Testing was performed using a Microlab CareFusion MK8 spirometer (Medicom, Zabrze, Poland); it was calibrated each day before the testing.

Before the start of the study, each subject was informed about the spirometry testing procedure. The spirometry was carried out with the patient in a sitting position. Only the results that met the criteria of a correctly conducted test according to ATS/ERS were included in the statistical analysis.

Statistical analysis

Statistical analysis was performed using STATISTICA software v. 12 (StatSoft Inc., Tulsa, USA). The Shapiro-Wilk test was used to check for normality. The homogeneity of variance in the groups being compared was assessed using the Levene's test. Where the assumptions of normality and homogeneity of variance were met, the Student's t-test for independent samples was used. Otherwise, the non-parametric alternative, namely the Mann-Whitney U test, was employed. A significance level of 0.05 was adopted as the borderline value of acceptable error level.

Results

Of the total of 58 homeless individuals examined, 53 homeless ever-smokers were included in the analysis. This group was compared with 55 male ever-smokers leading a normal lifestyle.

Table 1 summarizes the mean values in the homeless and control groups.

This was followed by an analogous comparison among current smokers; the results of the comparison are given in Table 2.

Furthermore, in our homeless group, we identified 11 cases with mild, 1 case with moderate, 2 cases with moderately severe, and 2 cases with severe airway obstruction (i.e., a total of 16 cases). We did not identify any case with very severe obstruction. In the control group, on the other hand, we only identified 8 cases with mild obstruction.

Table 1. Mean values and their comparison among ever-smokers in the homeless group and the control group

Variable	Homeless group			Control group			p-value
	mean	SD	n	mean	SD	n	
FEV1 [dm^3/s]	2.82	0.73	53	3.41	0.75	55	0.000
FEV1 [%]	84.83	17.79	53	99.75	17.20	55	0.000
FVC [dm^3/s]	3.71	0.80	53	4.43	0.86	55	0.000
FVC [%]	89.23	15.53	53	102.78	17.70	55	0.000
FEV1/FVC	75.76	11.36	53	79.53	11.50	55	0.090
Age [years]	57.21	9.83	53	57.84	12.12	55	0.768
Years of smoking	35.65	13.11	51	27.94	12.42	50	0.003
Pack/days	0.85	0.34	51	1.12	0.71	55	0.014
Pack/years	29.60	16.72	52	30.30	23.04	55	0.860

FEV1 – forced expiratory volume in 1 s; FVC – forced vital capacity.

Table 2. Mean spirometry values in the current smokers group

Variable	Homeless group			Control group			p-value
	mean	SD	n	mean	SD	n	
FEV1 [dm^3/s]	2.77	0.73	48	3.69	0.73	31	0.000
FEV1 [%]	82.65	16.84	48	103.06	14.96	31	0.000
FVC [dm^3/s]	3.69	0.80	48	4.69	0.87	31	0.000
FVC [%]	87.94	15.39	48	104.32	18.92	31	0.000
FEV1/FVC	75.07	11.49	48	80.35	10.77	31	0.044
Age [years]	56.90	9.19	48	53.84	13.36	31	0.232
Years of smoking	36.25	11.81	48	30.48	13.25	29	0.051
Pack/days	0.82	0.31	48	1.05	0.66	31	0.040
Pack/years	30.28	15.89	48	29.44	20.74	31	0.840

FEV1 – forced expiratory volume in 1 s; FVC – forced vital capacity.

Discussion

The current Global Initiative for Chronic Obstructive Pulmonary Disease (GOLD) criteria require post-bronchodilator spirometry for the diagnosis of COPD.[11] A simple spirometry test allows for the identification of obstruction or restriction, but is not sufficient for establishing a diagnosis of a specific disease. The specific nature of work with the homeless makes it very difficult to satisfy the GOLD criteria and is very likely to be one of the reasons why, to the best of our knowledge, no such studies have been conducted. In one of the published studies, which was based on spirometry results among the homeless, Snyder and Eisner reported a much higher percentage of subjects meeting the criteria of airway obstruction than would be expected in the general population.[12] Another study, already mentioned in the introduction, was conducted by measuring the peak flow, a tool that is much easier to use in this group of people.[13] Our study is therefore eligible for comparison with the report by Snyder and Eisner. In such a comparison, despite the fact that our study group was much older ($p = 0.000$), the mean values of forced expiratory volume in 1 s (FEV1), forced vital capacity (FVC) and FEV1/FVC in our study were not significantly different from those reported by Snyder and Eisner .[12]

Our study material, however, allowed us to make a more interesting comparison, namely a comparison between homeless males and males living normal lives.

Our results demonstrated much worse spirometric parameters among the homeless than in the control group (Tables 1, 2), even though these 2 groups did not differ significantly in age or in exposure to tobacco smoke expressed in pack-years.

In their report, Snyder and Eisner considered several explanations for the poorer spirometric parameters observed in the homeless. Some of them, such as the considerable percentage of African Americans among the homeless, who usually have worse spirometric parameters, can be directly negated.[16] In our database, both in the study group and in the control group, 100% of the subjects were Caucasian. It is also questionable that such considerable differences can be explained by the statement that OLD may be one of the causes of homelessness. Spirometric parameters physiologically decline with age. Our database primarily included chronically homeless subjects (98%), aged 57 years on average, while only few of them (5.17%) met the criterion of severe obstruction (even before checking the reversibility criterion).

What we agree with is the statement regarding delayed diagnosis or no diagnosis of OLD among the homeless and the impact of respiratory tract infections. We are likely to be dealing here with a similar situation to that with the course of tuberculosis. The poor care for one's own health is one of the reasons for delayed diagnosis.[17] In our database, which included subjects considering themselves to be healthy, we identified a total of 16 cases of airway obstruction among the homeless (27.59%), with only 8 such cases in the control group (15.55%). And although this difference was borderline significant ($p = 0.0506$; $n = 53$ vs 55 homeless vs control group, respectively), the quantitative comparison did not take into account the severity of the obstruction. A total of 5 cases of more than moderate obstruction (including 2 cases of severe obstruction) were identified among the homeless compared to 0 in the control group. This difference is best reflected by comparing the mean values (Tables 1, 2).

The issue that is most interesting here, however, is smoking. Our results negate the hypothesis according to which spirometric parameters among the homeless are worse, because homeless individuals smoke more. It is very likely that the high cost of tobacco products limits their availability to this group of people, so that despite the longer duration of smoking (Table 1 – current and ex-smokers), the number of pack-years in both groups is the same. The analysis of current smokers (Table 2) showed that the total duration of exposure to tobacco smoke in both groups was the same. Without negating the already proven relationship between smoking and OLD, it seems that in this case, this relationship is not responsible for the differences observed.[18]

It should, however, be kept in mind that it is not possible to objectively – quantitatively or qualitatively – assess the exposure to passive smoking. It may be assumed to be particularly high in this group (especially during the winter months, when survival of the homeless depends on their stay at various types of night shelters). On the other hand, we did not attempt to assess the exposure to passive smoking in the control group, either. This unconfirmed suggestion concerning the impact of passive smoking among the homeless requires further studies, especially since this is an area in which prophylactic activities are feasible and would require appropriate training to be provided to social workers employed in night shelters.

Limitations

Our sample size of homeless people is too small to allow a reliable statistical analysis of the subgroup of homeless male non-smokers and the subgroups of female smokers and female non-smokers, who were not included in our study. For this reason, we limited the focus of the analysis to smoking males. This limitation results from the demographic regularities already mentioned in the introduction. The inclusion of females, due to their considerably lower proportion (approx. 10%), would require a multicenter study assessing approx. 1,000 homeless subjects, which still would not include a subgroup of non-smoking females, whose number would be too small for statistical analysis.

Conclusions

The apparently obvious conclusion that homeless people have worse spirometric parameters, because they smoke too much seems incorrect. Our results have demonstrated

much worse spirometric parameters among male homeless smokers than in the control group including male smokers leading normal lives, in spite of the fact that these 2 groups did not differ significantly in terms of age or exposure to tobacco smoke. Our study does not explain this fact, but points to the existence of other causes in addition to exposure to tobacco smoke.

The considerable percentage (27.59%) of homeless male subjects with airway obstruction not receiving treatment for lung diseases suggests the need to place this group under detailed observation and to provide them with treatment.

References

1. Tan de Bibiana J, Rossi C, Rivest P, et al. Tuberculosis and homelessness in Montreal: A retrospective cohort study. *BMC Public Health*. 2011;11:833.
2. Romaszko J, Buciński A, Kuchta R, Bednarski K, Zakrzewska M. The incidence of pulmonary tuberculosis among the homeless in north-eastern Poland. *Cent Eur J Med*. 2013;8(2):283–285.
3. Fazel S, Khosla V, Doll H, Geddes J. The prevalence of mental disorders among the homeless in western countries: Systematic review and meta-regression analysis. *PLoS Med*. 2008;5(12):e225.
4. Romaszko J, Siemaszko A, Bodzioch M, Buciński A, Doboszyńska A. Active case finding among homeless people as a means of reducing the incidence of pulmonary tuberculosis in general population. *Adv Exp Med Biol*. 2016;911:67–76.
5. Krausz RM, Clarkson AF, Strehlau V, Torchalla I, Li K, Schuetz CG. Mental disorder, service use, and barriers to care among 500 homeless people in 3 different urban settings. *Soc Psychiatry Psychiatr Epidemiol*. 2013;48(8):1235–1243.
6. Busch-Geertsema V, Benjaminsen L, Hrast MF, Pleace N. Extent and profile of homelessness in european member states: A statistical update: FEANTSA; 2014. https://pure.sfi.dk/ws/files/294722/Feantsa_Studies_04_WEB.pdf. Accessed December 27, 2016.
7. Rhoades H, Wenzel SL, Golinelli D, et al. The social context of homeless men's substance use. *Drug Alcohol Depend*. 2011;118(2):320–325.
8. Baggett TP, Rigotti NA. Cigarette smoking and advice to quit in a national sample of homeless adults. *Am J Prev Med*. 2010;39(2):164–172.
9. Chen Q, Wan M, Ban C, Gao Y. Retrospective assessment of the prevalence of cardiovascular risk factors among homeless individuals with schizophrenia in Shanghai. *Shanghai Arch Psychiatry*. 2014;26(3):149–156.
10. Wincup E, Buckland G, Bayliss R. *Youth Homelessness and Substance Use: Report to the Drugs and Alcohol Research Unit*. London: Home Office Research, Development and Statistics Directorate; 2003.
11. Vestbo J, Hurd SS, Agusti AG, et al. Global strategy for the diagnosis, management, and prevention of chronic obstructive pulmonary disease: GOLD executive summary. *Am J Respir Crit Care Med*. 2013;187(4):347–365.
12. Snyder LD, Eisner MD. Obstructive lung disease among the urban homeless. *Chest*. 2004;125(5):1719–1725.
13. Badiaga S, Richet H, Azas P, et al. Contribution of a shelter-based survey for screening respiratory diseases in the homeless. *Eur J Public Health*. 2009;19(2):157–160.
14. Amore K, Baker M, Howden-Chapman P. The ETHOS definition and classification of homelessness: An analysis. *Europ J Homeless*. 2011;5(2)19–37.
15. Miller MR, Hankinson J, Brusasco V, et al. Standardisation of spirometry. *Eur Respir J*. 2005;26(2):319–338.
16. Hankinson JL, Odencrantz JR, Fedan KB. Spirometric reference values from a sample of the general U.S. population. *Am J Respir Crit Care Med*. 1999;159(1):179–187.
17. Villa L, Trompa IM, Montes FN, Gomez JG, Restrepo CA. Analysis of mortality caused by tuberculosis in Medellin, Colombia, 2012. *Biomedica*. 2014;34(3):425–432.
18. Forey BA, Thornton AJ, Lee PN. Systematic review with meta-analysis of the epidemiological evidence relating smoking to COPD, chronic bronchitis and emphysema. *BMC Pulm Med*. 2011;11:36.

Venous insufficiency: Differences in the content of trace elements. A preliminary report

Agnieszka Rusak[1,B–D], Ewa Karuga-Kuźniewska[2,A,E], Benita Wiatrak[3,D,E], Maria Szymonowicz[4,C,D], Mateusz Stolarski[5,B], Małgorzata Radwan-Oczko[6,B], Rafał J. Wiglusz[7,C–F], Paweł Pohl[8,A,C], Zbigniew Rybak[4,D–F]

[1] Division of Histology and Embryology, Department of Human Morphology and Embryology, Wroclaw Medical University, Poland
[2] Division of Infectious Diseases of Animals and Veterinary Administration, Department of Epizootiology and Clinic of Bird and Exotic Animals, Faculty of Veterinary Medicine, Wroclaw University of Environmental and Life Sciences, Poland
[3] Department of Basic Medical Sciences, Wroclaw Medical University, Poland
[4] Department of Experimental Surgery and Biomaterials Research, Wroclaw Medical University, Poland
[5] Department of Trauma Surgery, Knappschaftskrankenhaus Bochum-Langendreer, University Hospital Bochum, Germany
[6] Department of Periodontology, Wroclaw Medical University, Poland
[7] Institute of Low Temperature and Structure Research, Polish Academy of Sciences, Wrocław, Poland
[8] Division of Analytical Chemistry and Chemical Metallurgy, Faculty of Chemistry, Wroclaw University of Science and Technology, Poland

A – research concept and design; B – collection and/or assembly of data; C – data analysis and interpretation; D – writing the article; E – critical revision of the article; F – final approval of the article

Advances in Clinical and Experimental Medicine, ISSN 1899-5276 (print), ISSN 2451-2680 (online) *Adv Clin Exp Med*. 2018;27(5):695–701

Address for correspondence
Agnieszka Rusak
E-mail: rusakagn@gmail.com

Funding sources
Financial support of the National Science Centre (Poland) in the course of realization of the project "Preparation and characterization of nanoapatites doped with rare earth ions and their biocomposites" (No. UMO-2012/05/E/ST5/03904).

Conflict of interest
None declared

Received on September 15, 2016
Reviewed on December 14, 2016
Accepted on February 9, 2017

DOI
10.17219/acem/68902

Copyright
© 2018 by Wroclaw Medical University
This is an article distributed under the terms of the Creative Commons Attribution Non-Commercial License (http://creativecommons.org/licenses/by-nc-nd/4.0/)

Abstract

Background. Venous insufficiency is still a serious clinical problem. The exact cause and molecular mechanisms of this disease are still unknown. In this study, we try to identify whether there is a difference in the level of trace elements between healthy and pathological veins. Our results show that insufficient veins have different levels of some trace elements: magnesium, calcium, manganese, and silicon compared to control samples. This study could lead to a better understanding of the molecular causes of venous insufficiency and may help to develop better methods of treatment.

Objectives. Nowadays, venous diseases are a very common clinical phenomenon. Venous insufficiency is thought to be one of the most common vein diseases. The exact mechanisms of its etiology are still unknown, although from a clinical point of view some risk factors include gender, age, changing hormone levels, heredity, and standing or sitting for long periods. An imbalance in trace elements could also play a crucial role in the development and/or progression of venous insufficiency.

Material and methods. The trace element content in varicose vein walls and in normal vein walls was measured using an inductively coupled plasma-optical emission spectrometer (ICP-OES) after sample mineralization. Statistical analysis (the Mann-Whitney U test and the Friedman ANOVA) was performed to compare insufficient veins to controls (healthy veins).

Results. This study found statistically significant higher magnesium (Mg) ion levels in varicose veins compared to controls ($p = 0.0067$) and differences close to statistical significance in calcium (Ca), manganese (Mn), and silicon (Si) ion levels.

Conclusions. The results obtained could indicate oxidative stress occurring in chronic venous insufficiency as well as free radical neutralization pathways due to superoxide dismutase (SOD) activity with Mg, Mn and copper (Cu) ion involvement. Our results are consistent with literature data and are preliminary in nature.

Key words: trace elements, venous insufficiency, venous pathology

Introduction

Venous disease with concomitant varicose veins is presently a very common clinical phenomenon consisting of the destruction of vein valves, backward blood flow (venous reflux) and dilated veins.[1] This in turn, may lead to serious complications, such as thrombosis, skin changes and leg ulcers. There are many genetic, hormonal and environmental factors affecting the development of varicose veins. The exact mechanism of their formation has not been identified. The main destructive factor is venous hypertension, which may lead to the remodeling of vein walls and vein valves.[2,3] It is thought that long-term high pressure in veins may activate matrix metalloproteinases (MMPs), initiate coagulation and complement cascades, and activate platelets, leukocytes and macrophages as well.[1,2,4] Matrix metalloproteinases destroy the extracellular matrix, affect smooth muscle cells, and change the properties of the endothelium layer. These processes tend to reduce the flexibility of vein walls. Activated leukocytes escape via damaged endothelium outside the capillaries, starting inflammatory processes. Then, proteins like fibrinogen build a cuff around the capillaries, interfering with the gas exchange between the blood and the extracellular environment, which then leads to further damage of vein walls.[1,2]

The role of trace elements in vein pathology is not yet fully understood, but it is known that they play a significant role in tissue metabolism. Many studies suggest that iron (Fe) could be important in the development of venous diseases, but the cause of these iron deposits in the legs of patients with venous diseases is not yet known.[5] It has been suggested that this process is connected with activated MMPs or free radicals.[5–7] There is also a hypothesis that iron is not a direct cause of venous abnormalities, but only a factor which intensifies the autoimmune response.[8] Zinc (Zn), manganese (Mn) and copper (Cu) ions are associated with an active center of superoxide dismutase (SOD) and participation in free radical neutralization.[9–11] It is thought that reactive oxygen species (ROS) play a significant role in the development of the endothelial dysfunctions which are connected with venous diseases, such as varicose veins and venous ulcers.[12–14] Zinc, Cu and Fe ions also participate in free oxygen radical formation and may be involved in damage leading to chronic venous insufficiency.[7,15] Zinc is an important trace element for the immune system.[16,17] In in vitro tests, high levels of Zn led to cell apoptosis. Most of the zinc (90%) in the human body is contained in the muscles and bones.[16] Copper is also an important trace element for human health – the body needs Cu in the appropriate amount, but excessive amounts are confirmed to have toxic properties.[18,19] Copper deficiency causes many abnormalities, e.g., problems with the absorption of iron leading to cellular iron deficiency, disorders of the immune system and weakness of the walls of the blood vessels.[7,20,21] Copper is needed as a structural component or catalyst by many proteins.[7] One of the important copper-containing proteins relevant to the construction of the blood vessels is lysyl oxidase. It is responsible for stiffness and elasticity as a result of the fact that it allows bonding between collagen and elastin.[7,22] Manganese is needed for the proper functioning and metabolism of cells.[23] However, in vivo and in vitro studies showed the toxic properties of Mn in high doses, especially for the central nervous system and PC12 cells (used as an in vitro model of neuronal cells).[23–25]

Age-related changes were previously reported in the arteries and veins.[26] The magnesium (Mg) content in the veins increases with aging, which may play a role in the development of vein wall diseases.[27] Magnesium Mg^{2+} ions are known as an enzyme cofactor.[28] Signaling pathways, ATPase activity, and the channel and metabolic regulation of the cell cycle are all dependent on Mg^{2+} content. Magnesium deficiency is connected with the occurrence of many disorders, such as osteoporosis, hypertension, heart arrhythmia, impaired glucose tolerance, and serum cholesterol.[29–31] A reduced level of magnesium also increases oxidative stress and can reduce erythrocyte SOD concentrations.[30]

Calcium (Ca) is involved in many metabolic processes. It occurs in the human body mainly in the bones and teeth in the form of calcium hydroxyapatite. Accumulated calcium in the bones constitutes a reserve for the functioning of the body.[32] Calcium ions are used to carry cellular signals and as transporters across cell membranes.[33,34] They also regulate intracellular mechanisms by binding to proteins. The cellular level of Ca^{2+} is precisely regulated – a significant increase in the calcium level can lead to apoptotic changes.[34] Metabolic processes involving Ca ions are critical for the functioning of the vessels, muscles, nerves, and the endocrine system.[32]

Silicon (Si) is an important element in the biology of all living organisms – small amounts of this element are essential for their proper functioning.[35,36] It plays an important role in the connective tissue (bone, cartilage, skin, and blood vessels).[37,38] It is believed that Si is associated with the content of collagen and glycosaminoglycans in the connective tissue matrix.[38,39] Changes in the Si level of pathological tissues have been observed (e.g., in atherosclerotic tissue).[40] In vitro studies suggest that Si could have neuroprotective or neurotoxic properties (depending on the concentration).[41]

In our study, we determined the content of trace elements – Cu, Fe, Mn, Mg, Zn, Ca, and Si – found in human veins affected by chronic venous insufficiency and compared this data with the levels of the same trace elements found in healthy, sufficient human veins. It was confirmed that the concentrations of elements in tissue are often correlated with each other.[42] For this reason, the opportunity to check the correlation of various trace elements in healthy and pathological veins was taken.

Material and methods

This study was conducted over a span of 2 years, between 2013 and 2014, at the Wroclaw Medical University and the Institute of Low Temperature and Structure Research, Polish Academy of Sciences. It was performed in compliance with the ethical principles of the Declaration of Helsinki and Good Clinical Practice. Legal representatives read, signed and dated the form before taking part in any study activity. Consent from the Bioethical Commission of Wroclaw Medical University was granted for the study (No. KB-87/2013).

Reagents and solutions

EMSURE® ACS grade reagents, i.e., concentrated HNO_3 (65%), HCl (36%) and H_2O_2 (30%) solutions were purchased from Merck Millipore (Merck KGaA, Darmstadt, Germany). Aqua regia was freshly prepared by mixing concentrated HCl and HNO_3 solutions at a 3:1 volume ratio. Deionized water from an EASYpure™ water purification system (Barnstead Thermolyne Corp., Dubuque, USA) was used throughout. A Certipur® multi-element stock (1000 µg/mL) ICP standard solution IV (Merck KGaA) was used for preparing simple and matrix-matching standard solutions for the calibration of the inductively coupled plasma-optical emission spectrometry (ICP-OES) instrument.

Samples and their preparation

An inorganic solution, made directly from human veins, was fabricated using microwave-assisted wet digestion, whereby the disinfected human veins were combined with HNO_3 and H_2O as well as NH_4OH, for pH control. First of all, the received disinfected human veins were subjected to thermal treatment using an electric furnace at a temperature of 550°C for 1 h. Following typical preparation procedures for a final product containing all microelements, the inorganic powder was first dissolved in an excess of HNO_3 in order to create an inorganic solution. This inorganic solution was then transferred into a teflon vessel and placed in a microwave reactor. After 60 min of microwave-stimulated hydrothermal processing at 200°C, and under an autogenous pressure of 45 atm, the pH of the dispersion was then adjusted to approx. 7 with the addition of NH_4OH. The resulting composition of the prepared solutions was then determined by inductively coupled plasma-optical emission spectrometry (ICP-OES).

Apparatus

A bench-top optical emission spectrometer, model 720 (Agilent, Santa Clara, USA), with an axially viewed Ar-ICP and a 5-channel peristaltic pump, was used to measure the concentrations of Cu, Mn, Fe, Mg, Zn, Ca, and Si (trace elements). The instrument was equipped with a high-resolution echelle-type polychromator and a VistaChip II CCD detector (Agilent) cooled down to –35°C on a triple-stage Peltier device. The plasma was sustained in a standard 1-piece, low-flow, extended quartz torch with a 2.4 mm inside diameter injector tube. A single-pass glass cyclonic spray chamber and a OneNeb pneumatic concentric nebulizer made of a high-tech PFA and PEEK polymers were used to introduce the sample solutions by pneumatic nebulization. Operating conditions recommended by the manufacturer for solutions containing high levels of dissolved solids were applied: an RF power of 1200 W, a plasma gas flow rate of 15.0 L min^{-1}, an auxiliary gas flow rate of 1.5 L min^{-1}, a nebulizer gas flow rate of 0.75 L min^{-1}, a sample flow rate of 0.75 mL min^{-1}, a stabilization delay of 15 s, a sample uptake delay of 30 s, a rinse time of 10 s, a replicate read time of 1 s, and 3 replicates. A fitted background mode with 7 points per line profile was applied for the background correction. Background-corrected intensities of analytical lines were used for calibration graphs.

Characteristic of groups

In this study, 2 different groups of patients were enrolled. One group of 11 patients (study group) was referred for surgery due to symptomatic vein insufficiency in 1 or both legs according to Clinical, Etiological, Anatomical, and Pathophysiological (CEAP) classification C2S, Ep, As, or Pr. The other group, consisting of 14 patients (control group), underwent cardiac coronary bypass grafting due to symptomatic arterial coronary insufficiency. The proximal and distal segments of the great saphenous vein were obtained from patients via a striping procedure (study group), while the patients with healthy veins (control group) underwent elective coronary artery bypass grafting, whereby excess vein was obtained from the proximal and distal vein segments. Patients were matched for age, sex and major risk factors (data not shown). Vessel segments were harvested using a non-touch technique before surgical distension or rapid removal. The segments were immediately transferred to physiological saline solution and stored in a refrigerator at a temperature of –20°C.

Statistical analysis

The results were statistically analyzed using the STATISTICA v. 12 software (StatSoft, Tulsa, USA). The Shapiro-Wilk test showed no normal distribution in the samples. The Mann-Whitney U test, Spearman's rank order correlation (R), Friedman ANOVA, and Kendall's coefficient of concordance were applied.

Results

Differences in the levels of elemental ions in insufficient veins compared to control samples were observed and analyzed in each group (the Friedman ANOVA) (Fig. 1).

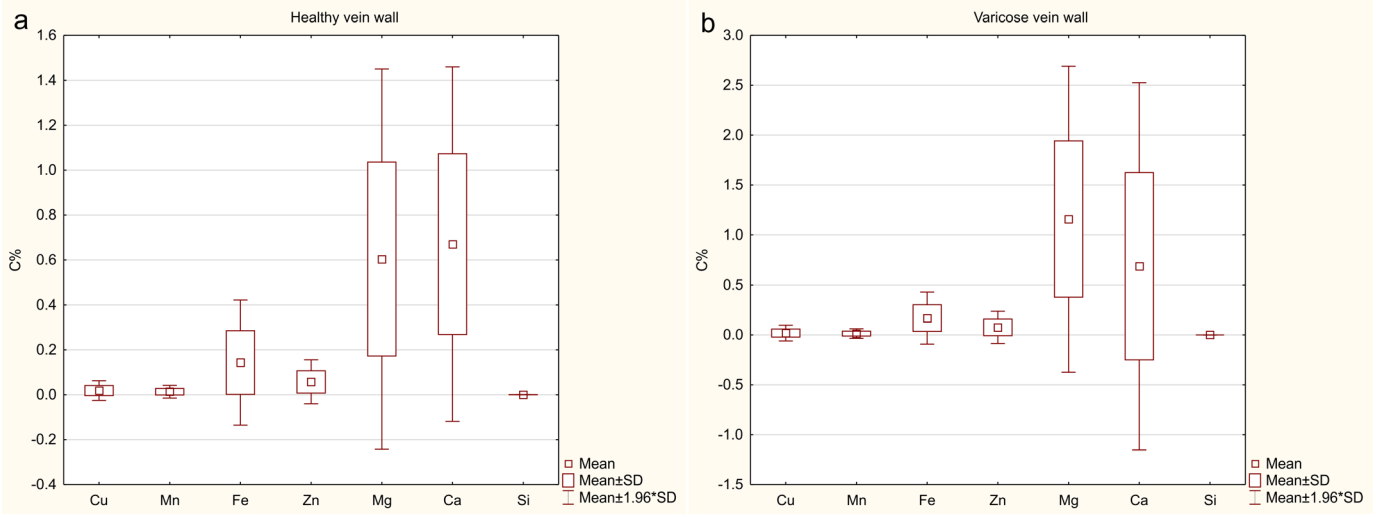

Fig. 1. Distribution of trace elements in: a) the group of insufficient veins, Friedman ANOVA (N = 11, df = 6) p = 0.000, Kendall's coefficient of concordance: p = 0.970; and b) the group of normal, healthy veins (control group), Friedman ANOVA (N = 14, df = 6) p = 0.00000, Kendall's coefficient of concordance: p=0.925

C% – mean % mass concentration; SD – standard deviation.

Table 1. Spearman's rank order correlation (R) in the study group of insufficient veins

Trace element	Cu	Mn	Fe	Zn	Mg	Ca	Si
Cu	1.00	0.13 (p = 0.73)	−0.01 (p = 0.99)	0.05 (p = 0.88)	0.16 (p = 0.65)	0.10	−0.10
Mn	0.13 (p = 0.73)	1.00	0.48 (p = 0.13)	0.46 (p = 0.15)	0.65 (p = 0.03)*	0.71 (p = 0.01)*	0.75 (p = 0.008)*
Fe	−0.01 (p = 0.99)	0.48 (p = 0.13)	1.00	0.36 (p = 0.27)	0.33 (p = 0.32)	0.37 (p = 0.26)	0.15 (p = 0.67)
Zn	0.05 (p = 0.88)	0.46 (p = 0.15)	0.36 (p = 0.27)	1.00	0.93 (p = 0.00004)*	0.93 (p = 0.00004)*	0.45 (p = 0.17)
Mg	0.16 (p = 0.65)	0.65 (p = 0.03)*	0.33 (p = 0.32)	0.93 (p = 0.00004)*	1.00	0.98 (p = 8.4E−08)*	0.59 (p = 0.05)
Ca	0.10 (p = 0.78)	0.71 (p = 0.01)*	0.37 (p = 0.26)	0.93 (p = 0.00004)*	0.98 (p = 8.4E−08)*	1.00	0.61 (p = 0.04)*
Si	−0.10 (p = 0.78)	0.75 (p = 0.008)*	0.15 (p = 0.67)	0.45 (p = 0.17)	0.59 (p = 0.05)	0.61 (p = 0.04)*	1.00

* statistically significant values (p < 0.05).

Statistically significant differences (the Mann-Whitney U test) compared to controls were observed (Fig. 2). A statistically significant difference (p = 0.007) in the Mg ion level in varicose veins compared to controls was noted (Fig. 2e). Differences in Mn (p = 0.067), Ca (p = 0.085) and Si (p = 0.075) levels were close to the margin of statistical significance (Fig. 2b, 2f, 2g). The concentrations of microelements in the studied human veins are presented as mean % mass concentration (C%) of trace elements in the mineral part of tissue samples.

A statistically significant (p > 0.05), positive and strong correlation (Spearman's rank order correlation) between the levels of some trace elements were observed for the study group (Table 1) and control group (Table 2). In the investigated group, correlations between the Ca and Mn ion levels (R = 0.71; p = 0.01), and the Ca and Zn levels (R = 0.93; p = 0.00004) were observed. In the control group, a correlation between these pairs was also observed (R = 0.58; p = 0.03 and R = 0.88; p = 0.00003, respectively), with a common correlation for both groups being noted.

Discussion

Similar research has already been done, but there is very little literature available for comparison. The pioneer study of ferrous content in veins was performed by Krzyściak et al.[6] One of the mechanisms involved in chronic venous disease is the destructive effect of free oxygen and free nitrogen radicals. The authors showed that Fe ions were involved in the oxidative damage mechanism which caused tissue altering via the Fenton reaction. Oxidative stress correlated with insufficiency in the venous tissue, and increased SOD activity was observed compared to normal venous tissue.[15] An increased level of iron in the skin of patients with chronic venous disease was described

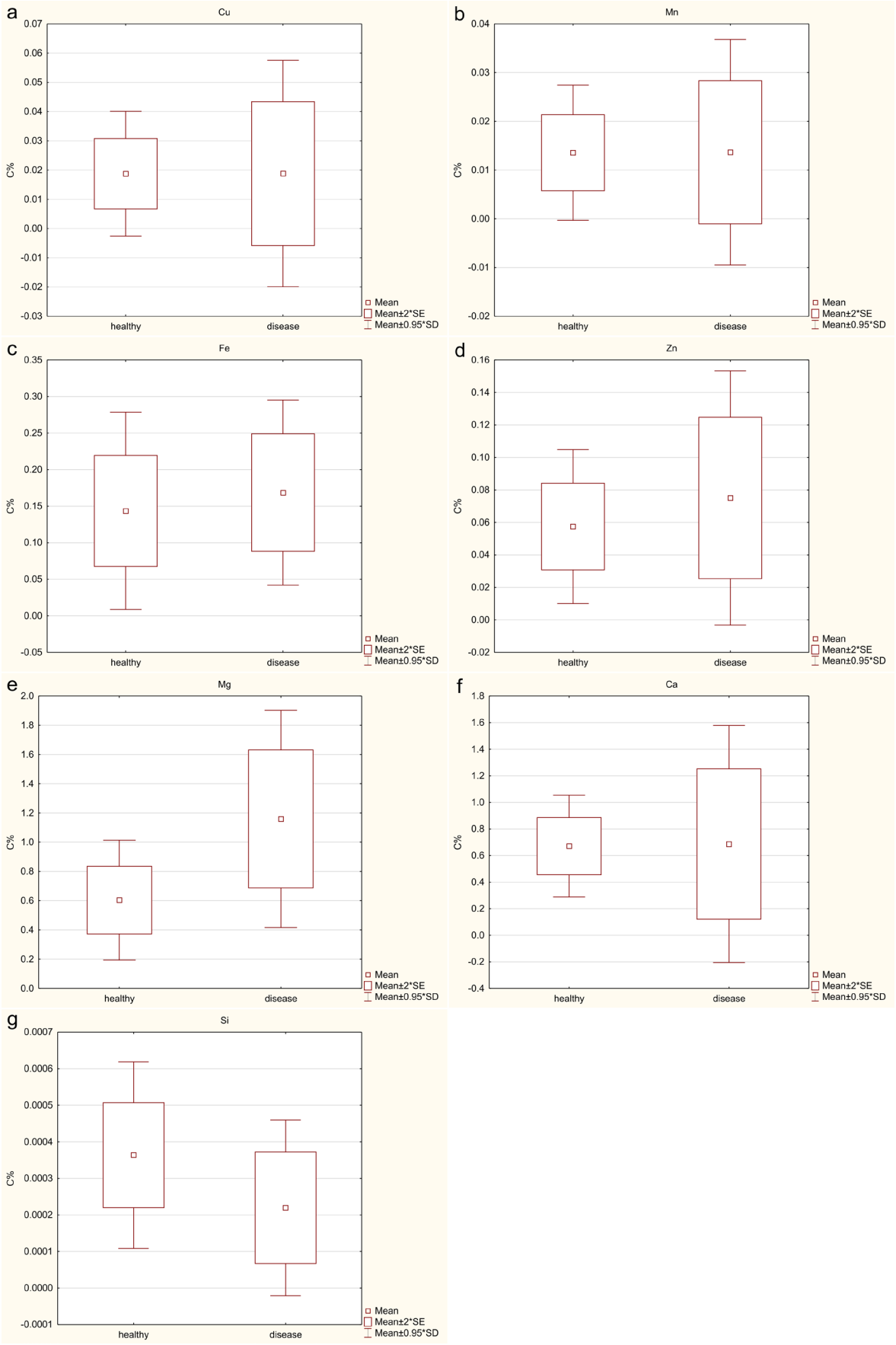

Fig. 2. Levels of ions, presented as mean % mass concentration (C%) of trace elements in the mineral part of tissue samples in insufficient veins compared to healthy veins (Mann-Whitney U test): a) Cu ions (p = 0.723); b) Mn ions (p = 0.067); c) Fe ions (p = 0.529); d) Zn ions (p = 0.848); e) Mg ions (p = 0.007); f) Ca ions (p = 0.085); and g) Si ions (p = 0.075)

SE – standard error; SD – standard deviation.

Table 2. Spearman's rank order correlation (R) in the control group (c) of normal veins

Trace element	Cu c	Mn c	Fe c	Zn c	Mg c	Ca c	Si c
Cu c	1.00	0.32 (p = 0.27)	−0.006 (p = 0.98)	0.74 (p = 0.002)*	0.13 (p = 0.65)	0.59 (p = 0.02)*	0.29 (p = 0.31)
Mn c	0.32 (p = 0.27)	1.00	0.16 (p = 0.56)	0.54 (p = 0.05)*	0.08 (p = 0.78)	0.58 (p = 0.03)*	0.23 (p = 0.42)
Fe c	−0.006 (p = 0.98)	0.16 (p = 0.56)	1.00	0.40 (p = 0.16)	0.90 (p = 0.00001)*	0.33 (p = 0.25)	0.16 (p = 0.59)
Zn c	0.74 (p = 0.002)*	0.54 (p = 0.05)*	0.40 (p = 0.16)	1.00	0.46 (p = 0.09)	0.88 (p = 0.00003)*	0.61 (p = 0.02)*
Mg c	0.13 (p = 0.65)	0.08 (p = 0.78)	0.90 (p = 0.00001)*	0.46 (p = 0.09)	1.00	0.26 (p = 0.36)	0.18 (p = 0.54)
Ca c	0.59 (p = 0.02)*	0.58 (p = 0.03)*	0.33 (p = 0.25)	0.88 (p = 0.00003)*	0.26 (p = 0.36)	1.00	0.50 (p = 0.07)
Si c	0.29 (p = 0.31)	0.23 (p = 0.42)	0.16 (p = 0.59)	0.61 (p = 0.02)*	0.18 (p = 0.54)	0.50 (p = 0.07)	1.00

* statistically significant values ($p < 0.05$).

by Myers in 1966.[43] Degradation of hemoglobin, as well as Fe release, was associated with erythrocyte dysfunction. Moosavi et al. showed increased concentrations of iron and copper in the walls of varicose veins compared to controls, using a proton-induced X-ray emission (PIXE) analysis.[44]

Determining the content of trace elements in tissues is still a subject of research, though environmental contamination due to metal ions and the bioaccumulation ratio needs to be assessed as well.[45,46] The level of trace elements in tissue is a reflection of the general health and metabolic status of the individual.[47] The level of metal ions significantly depends on the type and location of the tissue being measured. Determining the level of trace elements may have a diagnostic application in such tissues as brain and blood serum.[47,48]

The level of SOD, oxidative DNA damage, and increased levels of iron, copper and zinc ions were also observed.[27,30] SOD functions as a free radical scavenger. In oxidative stress conditions, increased antioxidant activity must be correlated with increased levels of enzymatic cofactors like Zn, Mn and Cu ions.[15]

The analysis of our results shows the differences between normal and insufficient veins. The Cu, Zn, Mn, and Ca ion levels had higher maximum values and slightly higher mean values compared to normal. Increased levels of these ions were observed in chronic venous insufficiency (CVI). Moreover, the Mn and Ca ion levels were close to being statistically significantly different from the control. These results are consistent with the literature and suggest a role of an SOD-, Cu-, Mn-, and Zn-dependent enzyme in CVI. Even though only a few articles dealing with a similar subject were found, the results obtained in this study were consistent with the data in the existing literature.[6,15]

The iron ion levels were the highest detected, but the difference between altered and normal veins was not statistically significant.

The reduction of vein wall elasticity is one of the symptoms of venous insufficiency, which, in our opinion, could be associated with a decreased level of silicon, considering the role of this trace element in fiber synthesis. Our study shows decreased levels of Si in insufficient veins. These levels were considerably lower, as predicted, and the results were close to statistically significant. To our knowledge, at present, there are no other reports in the literature about the Si levels in similar research.

We found that the magnesium ion levels were higher in varicose veins compared to the control ($p = 0.0067$). This result may suggest that magnesium ions play an important role in the mechanism which occurs during venous insufficiency, and very probably in vein wall structures as well.

Differences in the correlation patterns of trace elements between normal and varicose veins may suggest homeostatic destabilization associated with vein disease. In addition, they could also suggest a significant role of trace elements in chronic venous disease.

The current study is only a preliminary one. There is a need to perform further research, with an increased size of the study and control groups. Future studies are planned to assess the impact of gender on the levels of trace elements in a larger group.

Conclusions

This paper shows the levels of certain ions in insufficient and normal veins, particularly the differences between the concentrations of Mg, Mn, Ca, and Si. This study is preliminary in nature, but the data obtained suggests that the oxidative damage mechanism is involved in the development of varicose veins and chronic venous insufficiency.

References

1. Raffetto JD, Khalil RA. Mechanisms of varicose vein formation: Valve dysfunction and wall dilation. *Phlebology*. 2008;23:85–98.
2. Kucukguven A, Khalil RA. Matrix metalloproteinases as potential targets in the venous dilation associated with varicose veins. *Curr Drug Targets*. 2013;14:287–324.
3. Simka M. Cellular and molecular mechanisms of venous leg ulcers development: The "puzzle" theory. *Int Angiol*. 2010;29:1–19.
4. Raffetto JD, Qiao X, Koledova VV, Khalil RA. Prolonged increases in vein wall tension increase matrix metalloproteinases and decrease constriction in rat vena cava: Potential implications in varicose veins. *J Vasc Surg*. 2008;48:447–456.
5. Zamboni P, Izzo M, Tognazzo S, et al. The overlapping of local iron overload and HFE mutation in venous leg ulcer pathogenesis. *Free Radic Biol Med*. 2006;40:1869–1873.
6. Krzyściak W, Kowalska J, Kózka M, Papież MA, Kwiatek WM. Iron content (PIXE) in competent and incompetent veins is related to the vein wall morphology and tissue antioxidant enzymes. *Bioelectrochemistry*. 2012;87:114–123.
7. Arredondo M, Núñez MT. Iron and copper metabolism. *Mol Aspects Med*. 2005;26:313–327.
8. Simka M, Rybak Z. Hypothetical molecular mechanisms by which local iron overload facilitates the development of venous leg ulcers and multiple sclerosis lesions. *Med Hypotheses*. 2008;71:293–297.
9. Skrzycki M, Czeczot H. The role of superoxide dismutase in the arising of tumors. *Postępy Nauk Med*. 2005;4:7–15.
10. Xu B, Wu SW, Lu CW, et al. Oxidative stress involvement in manganese-induced alpha-synuclein oligomerization in organotypic brain slice cultures. *Toxicology*. 2013;305:71–78.
11. Prasad AS, Beck FW, Bao B, et al. Zinc supplementation decreases incidence of infections in the elderly: Effect of zinc on generation of cytokines and oxidative stress. *Am J Clin Nutr*. 2007;85:837–844.
12. Ojeda R, Aljama PA. Chronic microinflammation and endothelial damage in uremia. *Nefrologia*. 2008;28:583–586.
13. Chiu JJ, Chien S. Effects of disturbed flow on vascular endothelium: Pathophysiological basis and clinical perspectives. *Physiol Rev*. 2011; 91:327–387.
14. Karatepe O, Unal O, Ugurlucan M, et al. The impact of valvular oxidative stress on the development of venous stasis ulcer valvular oxidative stress and venous ulcers. *Angiology*. 2010;61:283–288.
15. Krzyściak W, Kózka M, Kowalska J, Kwiatek WM. Role of Zn, Cu-trace elements and superoxide dismutase (SOD) in oxidative stress progression in chronic venous insufficiency (CVI). *Przegląd Lek*. 2010;67: 446–449.
16. Plum LM, Rink L, Haase H. The essential toxin: Impact of zinc on human health. *Int J Environ Res Public Health*. 2010;7:1342–1365.
17. Chasapis CT, Loutsidou AC, Spiliopoulou CA, Stefanidou ME. Zinc and human health: An update. *Arch Toxicol*. 2012;86:521–534.
18. Leone N, Courbon D, Ducimetiere P, Zureik M. Zinc, copper, and magnesium and risks for all-cause, cancer, and cardiovascular mortality. *Epidemiology*. 2006;17:308–314.
19. Tisato F, Marzano C, Porchia M, Pellei M, Santini C. Copper in diseases and treatments, and copper-based anticancer strategies. *Med Res Rev*. 2010;30:708–749.
20. Saari JT, Schuschke DA. Cardiovascular effects of dietary copper deficiency. *Biofactors*. 1999;10:359–375.
21. Gupta A, Lutsenko S. Human copper transporters: Mechanism, role in human diseases and therapeutic potential. *Future Med Chem*. 2009; 1:1125–1142.
22. Cromwell GL. Copper as a nutrient for animals. In: Richardson HW, ed. *Handbook of Copper Compounds and Applications*. Boca Raton, FL: CRC Press; 1997.
23. Tuschl K, Mills PB, Clayton PT. Manganese and the brain. *Int Rev Neurobiol*. 2013;110:277–312.
24. Hirata Y. Manganese-induced apoptosis in PC12 cells. *Neurotoxicol Teratol*. 2002;24:639–653.
25. Erikson KM, Aschner M. Manganese neurotoxicity and glutamate-GABA interaction. *Neurochem Int*. 2003,43:475–480.
26. Tohno S, Tohno Y, Minami T, et al. A high accumulation of minerals in human internal jugular vein. *Biol Trace Elem Res*. 1998;62:17–23.
27. Tohno S, Tohno Y, Masuda M, et al. A possible balance of magnesium accumulations among bone, cartilage, artery, and vein in single human individuals. *Biol Trace Elem Res*. 1999;70:233–241.
28. Pilotelle-Bunner A, Cornelius F, Sebban P, Kuchel PW, Clarke RJ. Mechanism of Mg^{2+} binding in the Na^+, K^+-ATPase. *Biophys J*. 2009;96: 3753–3761.
29. Rude RK, Singer FR, Gruber HE. Skeletal and hormonal effects of magnesium deficiency. *J Am Coll Nutr*. 2009;28:131–141.
30. Nielsen FH, Milne DB, Klevay LM, Gallagher S, Johnson L. Dietary magnesium deficiency induces heart rhythm changes, impairs glucose tolerance, and decreases serum cholesterol in post menopausal women. *J Am Coll Nutr*. 2007;26:121–132.
31. Kolte D, Vijayaraghavan K, Khera S, Sica DA, Frishman WH. Role of magnesium in cardiovascular diseases. *Cardiol Rev*. 2014;22:182–192.
32. Ross AC, Taylor CL, Yaktine AL, Del Valle HB. *Dietary Reference Intakes for Calcium and Vitamin D*. Washington, DC: National Academies Press; 2011.
33. Yáñez M, Gil-Longo J, Campos-Toimil M. Calcium binding proteins. *Adv Exp Med Biol*. 2012;740:461–482.
34. Brini M, Ottolini D, Calì T, Carafoli E. Calcium in health and disease. *Met Ions Life Sci*. 2013;13:81–137.
35. Pruksa S, Siripinyanond A, Powell JJ, Jugdaohsingh R. Silicon balance in human volunteers: A pilot study to establish the variance in silicon excretion versus intake. *Nutr Metab (Lond)*. 2014;11(1):4. doi: 10.1186/1743-7075-11-4
36. Martin KR. Silicon: The health benefits of a metalloid. *Met Ions Life Sci*. 2013;13:451–473.
37. Jugdaohsingh R, Watson AIE, Pedro LD, Powell JJ. The decrease in silicon concentration of the connective tissues with age in rats is a marker of connective tissue turnover. *Bone*. 2015;75:40–48.
38. Gropper S, Smith J. *Nonessential Trace and Ultratrace Elements*. *Advanced Nutrition and Human Metabolism*. 6th ed. Belmont, CA: Wadsworth; 2013.
39. Mertz W, ed. *Trace Elements in Human and Animal Nutrition. Volume 2*. 5th ed. Orlando, FL: Academic Press; 2012.
40. Nakashima Y, Kuroiwa A, Nakamura M. Silicon contents in normal, fatty streaks and atheroma of human aortic intima: Its relationship with glycosaminoglycans. *Br J Exp Pathol*. 1985;66:123–127.
41. Garcimartín A, Merino JJ, Santos-López JA, et al. Silicon as neuroprotector or neurotoxic in the human neuroblastoma SH-SY5Y cell line. *Chemosphere*. 2015;135:217–224.
42. Tohno S, Tohno Y, Moriwake Y, Azuma C, Ohnishi Y, Minami T. Quantitative changes of calcium, phosphorus, and magnesium in common iliac arteries with aging. *Biol Trace Elem Res*. 2001;84:57–66.
43. Myers HL. Topical chelation therapy for varicose pigmentation. *Angiology*. 1966;17:66–68.
44. Moosavi K, Vatankhah S, Salimi J, Moradi M. A proton induced X-ray emission (PIXE) analysis of concentration of trace elements in varicose veins. *Int J Radiat Res*. 2010;8:117–121.
45. Aubail A, Méndez-Fernandez P, Bustamante P, et al. Use of skin and blubber tissues of small cetaceans to assess the trace element content of internal organs. *Mar Pollut Bull*. 2013;76:158–169.
46. Heidari B, Riyahi Bakhtiari A, Shirneshan G. Concentrations of Cd, Cu, Pb and Zn in soft tissue of oyster (*Saccostrea cucullata*) collected from the Lengeh Port coast, Persian Gulf, Iran: A comparison with the permissible limits for public health. *Food Chem*. 2013;141:3014–3019.
47. Döker S, Hazar M, Uslu M, Okan İ, Kafkas E, Boşgelmez İl. Influence of training frequency on serum concentrations of some essential trace elements and electrolytes in male swimmers. *Biol Trace Elem Res*. 2014;158:15–21.
48. Krebs N, Langkammer C, Goessler W, et al. Assessment of trace elements in human brain using inductively coupled plasma mass spectrometry. *J Trace Elem Med Biol*. 2014;28:1–7.

Serum concentrations of VEGF and bFGF in the course of propranolol therapy of infantile hemangioma in children: Are we closer to understand the mechanism of action of propranolol on hemangiomas?

Lidia Babiak-Choroszczak[1,A–F], Kaja Giżewska-Kacprzak[1,A,C–F], Elżbieta Gawrych[1,A,C–F], Katarzyna Fischer[2,B,E,F], Anna Walecka[3,B,E,F], Lidia Puchalska-Niedbał[4,B,E,F], Justyna Rajewska-Majchrzak[1,A,E,F], Maciej Bagłaj[5,D–F]

[1] Department of Pediatric and Oncological Surgery, Pomeranian Medical University in Szczecin, Poland
[2] Independent Laboratory of Rheumatic Diagnostics, Pomeranian Medical University in Szczecin, Poland
[3] Department of Diagnostic Imaging and Interventional Radiology, Pomeranian Medical University in Szczecin, Poland
[4] Department of Ophthalmology, Pomeranian Medical University in Szczecin, Poland
[5] Department of Pediatric Surgery and Urology, Wroclaw Medical University, Poland

A – research concept and design; B – collection and/or assembly of data; C – data analysis and interpretation; D – writing the article; E – critical revision of the article; F – final approval of the article

Advances in Clinical and Experimental Medicine, ISSN 1899-5276 (print), ISSN 2451-2680 (online) *Adv Clin Exp Med*. 2018;27(5):703–710

Address for correspondence
Kaja Giżewska-Kacprzak
E-mail: k.gizewska@gmail.com

Funding sources
None declared

Conflict of interest
None declared

Received on November 7, 2017
Reviewed on December 15, 2017
Accepted on January 26, 2018

Abstract

Background. Propranolol has become the treatment of choice for infantile hemangiomas (IH). Neither the pathogenesis of IH nor the mechanism of action of propranolol on them are well understood. Possible explanations include the inhibition of angiogenesis by decreasing vascular endothelial growth factor (VEGF) and basic fibroblast growth factor (bFGF), induction of vascular endothelial cell apoptosis and vasoconstriction.

Objectives. The aim of the study was to assess serum concentrations of VEGF and bFGF in the course of propranolol therapy of IH in children, and to assess their clinical implications.

Material and methods. The study included 51 children with IH treated with propranolol. The participants were assessed before, during and after the therapy with Hemangioma Activity Score (HAS), Doppler ultrasound (US) of the lesions, as well as VEGF and bFGF serum concentrations.

Results. All children showed clinical improvement measured in the HAS. A complete involution of the IH was reported in 32 (63%) children at the time of decision of the gradual withdrawing of propranolol, and in 28 (61%) patients at the end of the treatment (out of 46 patients present at the follow up after 1.5 months). Doppler US at the follow-up showed a complete disappearance of the blood flow in the lesion in 24 (52%) children and its reduction in 12 (26%) children. There was a significant decrease in VEGF and bFGF during and after treatment compared to pretreatment values. There was a correlation between the outcome of the Doppler US and changes in bFGF during and after treatment. Changes in VEGF during treatment did not correlate with changes in the Doppler US.

Conclusions. Serum concentrations of VEGF and bFGF decreased during the propranolol treatment of IH, which may indicate the effect of propranolol on both. However, the statistical analysis showed their low prognostic value as biochemical markers of propranolol treatment. Clinical evaluation combined with Doppler US is the most valuable method of monitoring the therapy.

Key words: infantile hemangioma, propranolol, vascular growth factor, vascular endothelial growth factor, basic fibroblast growth factor

DOI
10.17219/acem/84800

Copyright
© 2018 by Wroclaw Medical University
This is an article distributed under the terms of the Creative Commons Attribution Non-Commercial License (http://creativecommons.org/licenses/by-nc-nd/4.0/)

Introduction

Infantile hemangiomas (IH) are the most common childhood soft tissue tumors – they affect about 10% of infants, including 20–30% of premature babies.[1–4] The pathogenesis of hemangiomas remains unclear.[2–5] The 3 most common theories, which do not exclude each other, are: a hypoxia theory, a theory about the small-vessel embolization by cells from the placenta, and a theory of angiogenesis and vasculogenesis increase by the activity of vascular endothelial growth factor (VEGF) and basic fibroblast growth factor (bFGF).[3] The unique feature of IH is its natural development, which includes a phase of intensive growth (proliferation) lasting up to 18 months, and a phase of slow disappearance (involution).[5] Unfortunately, both the beginning of the involution phase and its duration are unpredictable. Only in 40% of children the disappearance of the hemangioma leaves no trace or minimal residue, resulting in a good cosmetic effect. Most often, IH disappears, leaving telangiectasias, scars, excess skin, or the so-called fatty fibrous residue.[5,6] Lesions of the periocular region or face, extensive in size, affecting inner organs or threatening life function, are particularly problematic. There is a high complication rate if no treatment is applied.[5] As most of them are classified as inoperable, alternative treatment options have been sought. In 2008, Léauté-Labreze et al. introduced propranolol (β-blocker) as an alternative treatment option for IH.[7] Since then, propranolol has successfully become the treatment of choice.[8,9] However, the mechanism of action of propranolol on IH is still not well understood.

According to Storch and Hoeger, the drug has 3 mechanisms of action that affect the lesion.[4] The early effects (lightening of the IH and reduction of tension), seen in the first 3 days of treatment, are attributed to vasoconstriction as a result of reduced nitric oxide release. The intermediate effect is the inhibition of vascular tumor growth, most likely associated with a blockade of proangiogenic growth factors, such as VEGF, bFGF or metalloproteinase-2/9. The regression of the lesion classified as the long-term effect is caused by apoptosis of the proliferating endothelial cells.

The aim of the study was to assess serum concentrations of VEGF and bFGF in the course of propranolol therapy of IH in children as an attempt to assess their practical role as a biochemical marker of successful treatment.

Material and methods

The analysis included a group of 51 infants with IH, diagnosed and treated between 2011 and 2014.

The criteria for inclusion in the research project were IHs that had to be: nonoperative, extensive in size, ulcerative, resulting in an impairment of important vital functions, causing a significant cosmetic defect, or with lesions affecting internal organs.

The Bioethics Committee of the Pomeranian Medical University in Szczecin, Poland, approved the study protocol, and reviewed and approved the consent forms. Written informed consent was obtained from the legal guardians of all of the study participants and recorded in the patient files.

Methods

After history taking of the occurrence and growth of the IH and coexistence of risk factors for IH, clinical interventions were applied before, during and at the follow-up (1.5 months) after treatment, including:

- clinical examination with assessment of location, size, color and consistency, assessment in terms of Hemangioma Activity Score (HAS) (Table 1), and ophthalmic examination performed in lesions of the periocular region[1];
- photographic documentation;
- doppler US assessing the size and blood flow in the lesion with a ranking system applied: initial size of the IH ranked as 2, reduction during treatment which was less than 50% ranked as 1.5, reduction greater than 50% ranked as 1, and complete involution ranked as 0; the intensity of the blood flow was defined as increased (++), moderate (+) or absent (–);
- serum concentrations of VEGF and bFGF before starting the treatment, at 6th month of treatment and 1.5 months after treatment, carried out using the immunoenzyme method (ELISA);
- cardiological examination with electrocardiography, echocardiography and basic laboratory tests; blood

Table 1. Hemangioma Activity Score (HAS)[1]

The assessed feature of the infantile hemangioma (IH)	Points
Deep swelling: tense IH (6) "neutral" IH at t = 0 or less than 50% reduction at follow up ≥50% reduction at follow-up no more swelling at follow-up	 4 6 2 0
Bright red/shining red IH	5
Bright red edge	4
Matt red/reddish-purple IH/matt red edge	3
Blue IH or blue shining through in deep IH	2
Grey IH	1
Skin coloured after activity	0
Total score	
Number of items scored	
Preliminary HAS = total score/number of items scored	
Ulcer score ulcer ≤1 cm^2 ulcer 1–25 cm^2 ulcer ≥25 cm^2	 0.5 1 2
HAS = preliminary HAS + ulcer score	

IH – infantile hemangioma.

morphology, ionogram, serum glucose, aspartate aminotransferase (AST), and alanine aminotransferase (ALT) were performed for the safety of the therapy;
– oral propranolol introduced in 2 divided doses (at 8 AM and 8 PM), according to the following protocol:
  • 1st day: 0.5 mg/kg/day;
  • 2nd day: 1 mg/kg/day;
  • 3rd day: 1.5 mg/kg/day;
  • 4th day: 2.0 mg/kg/day.

Treatment was introduced in hospital conditions for 4–5 days with monitoring of vital functions, including blood glucose levels, and then continued in outpatient settings.

Statistical analysis

All continuous variables were checked for the normality of the distributions by Kolmogorov-Smirnov test. These variables are described by means, medians, standard deviations (SD), quartiles, as well as minimum and maximum values. The statistical differences between the 2 groups were tested by Student's t-test and Mann-Whitney U test. Multiple variances (ANOVA), covariance (ANCOVA) or Kruskal-Wallis test were used for multiple groups. Variables in the same patient were tested with the Wilcoxon test or the t-test of dependent variables. Discrete variables were described by the amount and frequency. The Pearson's χ^2 test was used to study the statistical relationships between discrete variables. For the study of the correlation between discontinuous and orderly variables (coded variables: 0/1), the Spearman's rank correlation coefficient was applied.

The results are described by the correlation coefficient (r) and the probability value (p). The statistically significant differences in all the tests performed were those with a probability value of $p < 0.05$. Significance level with p-value between 0.051 and 0.099 was designated as a trend at the limit of statistical significance.

Statistical analysis was carried out using Stata 11 statistical program (StataCorp LLC, College Station, USA; license No. 30110532736).

Results

The study group included 51 children, 36 (71%) girls and 15 (29%) boys. The age of patients at the time of introduction of propranolol ranged from 7 weeks to 21.8 months (mean 5.8 months). In the study, 39 (75%) children – the largest group of patients – were 7 weeks to 6 months old (mean 3.6 months). In all cases, the evolutionary history was characteristic for IH. The burden of risk factors included: prematurity of birth, low birth weight (<2500 g in 17.6% of children) and children born from twin pregnancies (3 children, 5.8%). Obstetric risk factors were reported by 5 mothers (9.8%); other reported factors were (number of cases in brackets): invasive prenatal examination (1), cigarette smoking (2), alcohol use (1), and taking pharmaceuticals during pregnancy (28). There was a family history of IH in 11 children (21.5%).

The hemangiomas were isolated in 39 (76.5%) patients, while in the remaining 12 (23.5%) cases multifocal lesions were found. A total number of 79 IHs were present in 51 patients. More than half of the patients had a lesion of the head. The localizations included (number of lesions in brackets): upper eyelid (9), lower eyelid (3), parotid gland (4), nose (7), upper and lower lip (7), other head areas (8), crotch area (7), upper limb (8), lower limb (5), trunk (17), neck (1), oral cavity (2), and liver (1). Twelve children (23.5%) had lesions complicated with ulceration.

The lesions that were less than 0.5 × 0.5 cm in size or affected internal organs (liver) were excluded from evaluation in HAS. Before the treatment, HAS ranged from 3 to 6.5 points. The clinical improvement was expressed as a percentage; it presented the difference between the evaluation moment and pretreatment measurement. Significant clinical improvement (from 80% to 99%) corresponded with almost complete disappearance of IH, with only slight skin discoloration, telangiectasia or excess skin. The result of 100% was an equivalent of a total disappearance of the hemangioma (Fig. 1). All children showed clinical improvement with a statistically significant reduction in HAS (Fig. 2). The best results were present at the

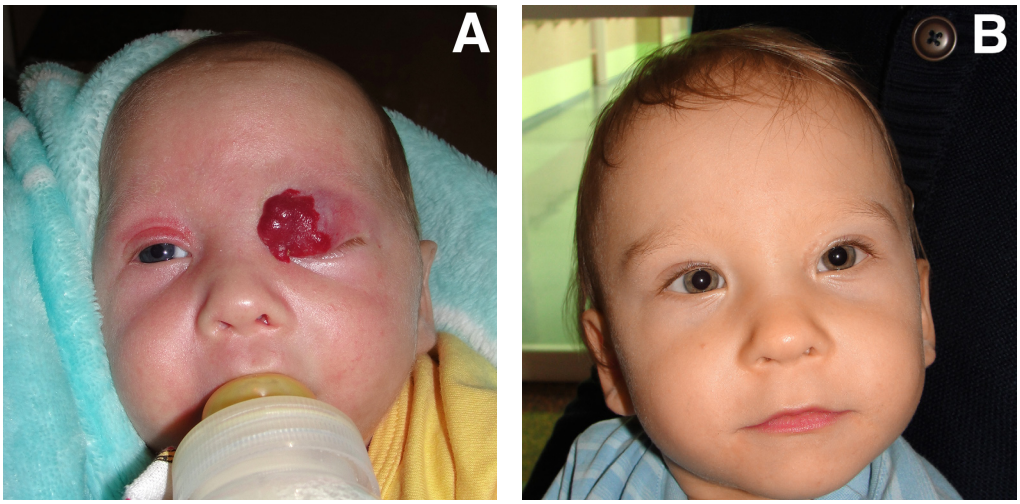

Fig. 1. Patient with hemangioma of the left upper eyelid causing severe ptosis

A – 2-month old child at admission (HAS: 4.3);
B – after 12 months of propranolol treatment (HAS: 0);
HAS – Hemangioma Activity Score.

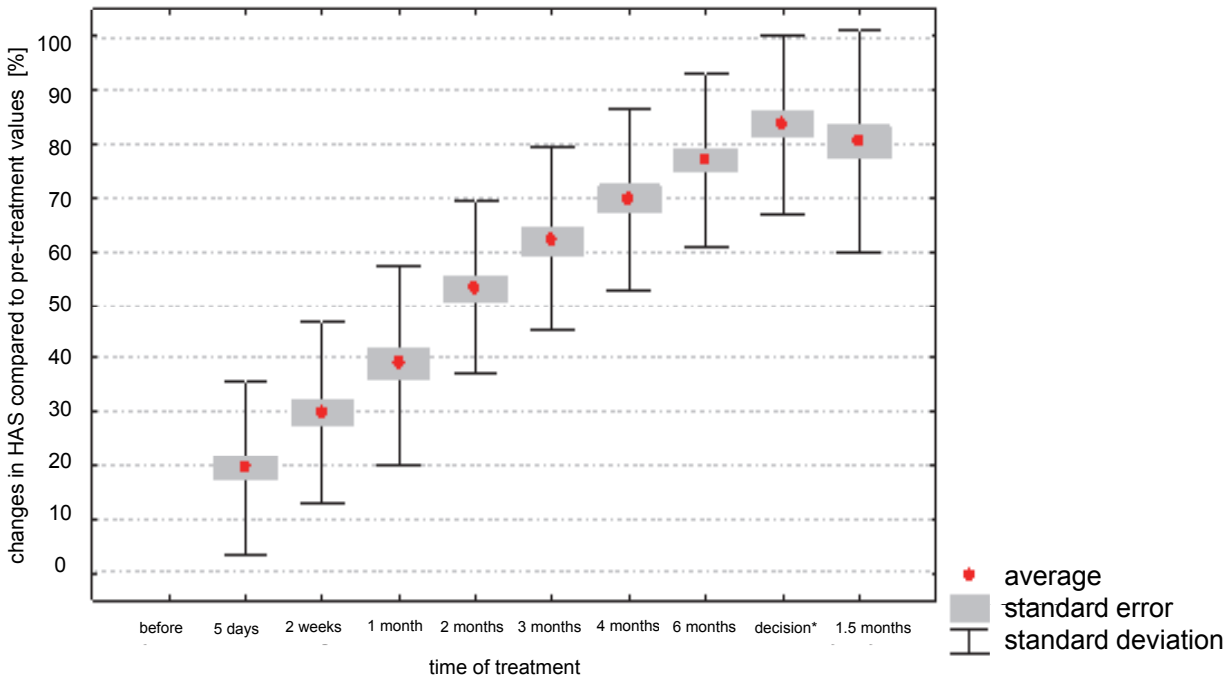

Fig. 2. Changes in Hemangioma Activity Score (HAS) throughout the propranolol treatment

* decision of gradual withdrawal of propranolol.

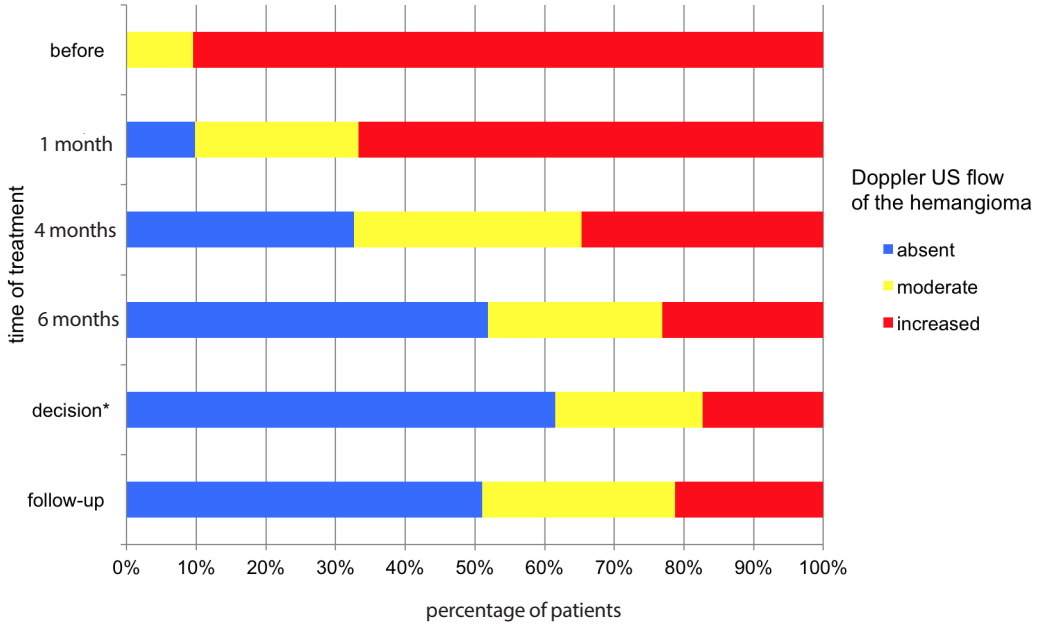

Fig. 3. Doppler US vascular flows in the hemangioma throughout the propranolol treatment

* decision of gradual withdrawal of propranolol.

moment of the decision of graduate cessation of therapy. In 32 (63%) patients disappearance of IH (80–100%) was observed, including a complete involution in 16 patients (32%). Only in 1 case the therapeutic effect was assessed below 50% (33%). Forty-six patients were present at a follow-up 1.5 months after treatment, where the average change was 80.6%. A complete involution was recorded in 28 children (60.9%). In 12 (26.1%) children, there was a slight recurrence.

The best therapeutic effect was achieved in the group of infants who started treatment in early infancy. In this group (7 weeks to 6 months of age) the final therapeutic effect of a complete involution was present in 69% of children. In the group aged 6–12 months, the analogous percentage was 56%. Among children who started treatment at 1 year of age, only 25% of patients had a complete effect. The most spectacular effect, the highest change measured in HAS, was observed in the first month of therapy (19.2%). A gradual decrease was present in later months.

At baseline, hypertensive vascular flow was observed in Doppler US in 47 (92.2%) cases, the remaining 4 (7.8%) were moderate. Changes in vascular flows in subsequent

studies are shown in Fig. 3. There was a statistically significant decrease in vascular flow in the IH, as compared to baseline p = 0.00001 and p = 0.00688 – before vs 1 month of treatment. A negative correlation was observed between the decrease in vascular flow and the length of therapy (r = –0.53; p = 0.00001). The highest correlation coefficient (r = –0.76) was obtained between the study of the flow at the time of withdrawal of therapy and the study prior to initiation of the therapy. Significant reductions in the size of IH measured in Doppler US (at 0 to 2, corresponding to their percentage change from the baseline) were observed during therapy (p < 0.015). At the end of treatment, the change in the size of the lesion (slight increase) was not statistically significant (p = 0.8385). The highest percentage of lack of vascular flow (69%) was observed in the youngest group of patients (Fig. 4).

Values of VEGF and bFGF were evaluated in 47 children. Values of serum VEGF levels before starting the treatment ranged from 40.862 pg/mL to 1151.928 pg/mL, after 6 months of treatment – from 33.589 pg/mL to 1093.84 pg/mL, after treatment ended – from 24.73 pg/mL to 722.074 pg/mL. There was a statistically significant decrease in mean VEGF concentration during and after treatment compared to pretreatment values (p < 0.05). There was a slight decrease in VEGF concentrations during and after treatment (p = 0.11923). Mean values of VEGF did not correlate with number of lesions, location of IH, age of the patients, or dose of propranolol.

The serum bFGF levels before starting the treatment ranged from 0 pg/mL to 30.125 pg/mL, after 6 months of treatment – from 0 pg/mL to 40.92 pg/mL, at the end of treatment – from 1.409 pg/mL to 25.472 pg/mL. It was found that the mean pretreatment bFGF values differed significantly from the treatment and follow-up values (p = 0.0152 and p = 0.0139, respectively). No statistically significant change in bFGF values was observed during and after treatment, with a slight increase in follow-up after treatment (p = 0.1322). Mean values of bFGF did not correlate with the number of lesions or their location. At the border of statistical significance, lower values of bFGF were obtained in pediatric patients receiving the highest doses (1.86–2 mg/kg/day) of the drug during treatment (p = 0.0558). Furthermore, it was found that mean bFGF values were dependent on patient age both before and during treatment (p = 0.007 and p = 0.0001, respectively). The bFGF values were higher in the oldest group of children (18–21 months).

There was a statistically significant correlation between the outcome of the treatment and the changes in bFGF values during and after treatment. In the case of lack of flow in the Doppler US after treatment, a significant decrease in bFGF value was observed (p = 0.0206). In contrast, an increase in bFGF was noted in the case of persistently high blood flow in the post-treatment (p = 0.0121) study (p-value was calculated with control of doses and age). There was no correlation between changes in VEGF values during and after treatment and vascular flows in Doppler US.

The target therapeutic dose was 2 mg/kg/day in 2 divided doses. In 6 children, the therapy was started at a lower dose (1.3–1.6 mg/kg/day) due to younger age, low body weight and low serum glucose levels, and problems with normalization of the pulse during propranolol introduction. In 5 of these children, the dose was increased to the target dose after 1 month without any side effects.

Six children treated with full-dose therapy required a reduction in the therapeutic dose to 0.9–1.6 mg/kg/day due to adverse events (frequent cough and vomiting, sleep disorders, frequent respiratory infections, symptomatic hypoglycemia, reflux, and suspected asthma).

On average, the full dose was applied for 8.7 months and the total treatment time regarding the gradual withdrawal of the drug was 12 months. The drug was discontinued within 1.5–3 months, with gradual reduction of the dose.

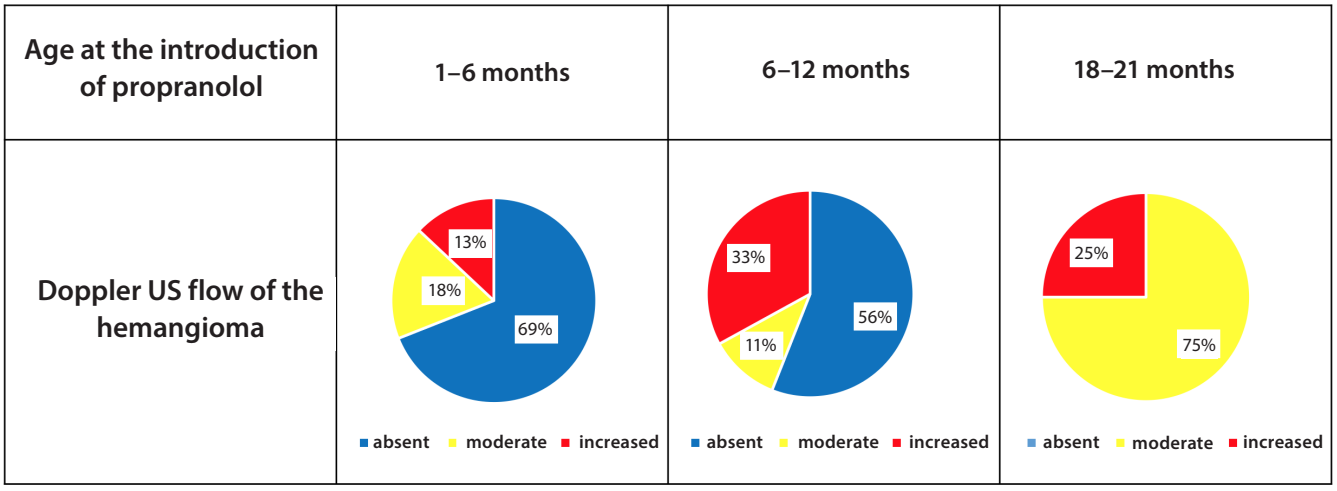

Fig. 4. Relation between age of the child at introduction of propranolol and Doppler US examination at the time of decision of gradual withdrawal of treatment

Discussion

In 2007, Chang et al. and Kleinman et al. published studies on the effect of tissue hypoxia on the development of IH.[10,11] According to those studies, hypoxia increases the expression of hypoxia-inducible factor 1-alpha (HIF-1-alpha), which increases vascular endothelial growth factor A (VEGF-A) production by the non-oxidized endothelial cells. Both hypoxia and stromal cell-derived factor 1-alpha (SDF-1 alpha) increase the differentiation and proliferation of endothelial progenitor cells, leading to the development of hemangioma.[10,11] Hypoxia is probably the strongest factor inducing angiogenesis and the formation of hemangioma. Multiple pregnancy, alcohol consumption, nicotinism, drug use during pregnancy, shortening of the pregnancy, low birth weight, and consequently poor general condition of the newborn are risk factors for IH and may be associated with increased tissue hypoxia.[2]

Elevated estrogens in the mother increase the risk of IH in a child.[12] Estrogens stimulate endothelial cell division and increase the concentration of, i.a., metalloproteinase 9 and VEGF, as well as bFGF and nitric oxide (NO), directly and indirectly, and affect endothelial cell migration and angiogenesis.[12] In the literature, the incidence of IH is higher in females, which is consistent with the dominance of girls in our study group.[1]

During proliferation, cells that build hemangioma (multipotent stem cells – $CD133^+$, pericytes – SMA^+, dendritic cells, mesenchymal cells, and immature endothelial cells – $CD31^+$) behave as if they were in the embryonic stage, multiplying much faster than the cells of the remaining tissues. Their intensive proliferation is linked to the activity of VEGF and bFGF. Proteases (collagenase type IV and urokinase) and adhesion molecules play role in the proliferation as well.[2,3,5,13,14] Hu et al. demonstrated elevated serum VEGF levels in children with IH in the proliferative phase.[15] However, other authors have reported increased bFGF in both hemangioma tissue and urine in the proliferation phase, and normalization in the involuting phase.[14,16,17]

Research into the mechanism of action of propranolol on early hemangiomas is still ongoing. The clinical implications of finding a prognostic marker may include determining effective dosage and optimal age for treatment initiation and completion. Takahashi et al. analyzed 9 factors that can have an influence on angiogenesis.[14] The study material consisted of biopsies at different stages of development (proliferation or involution). The research focused on the proangiogenic or antiangiogenic properties of the individual factors, and, consequently, determining their effect on the growth or disappearance of the IH. The presence of VEGF, type IV collagenase and proliferating cell nuclear antigen (PCNA) was only observed in the period of intense proliferation of choroidal lesions, whereas tissue metalloproteinase inhibitor (TIMP) was recorded only in the angiogenesis phase. The presence of bFGF was found both in the proliferative phase and in the involuting phase, without observing its presence after complete disappearance.[14] These observations allowed the authors to assume that the selected factors may have a prognostic significance in determining the growth phase or involution. However, the invasive character of the surgical biopsy of lesions limits the use of this method.

Zhang et al. analyzed serum VEGF concentrations both in the proliferative phase and in the involuting phase.[18] The results were compared with the values in healthy children. The authors demonstrated significantly higher VEGF values in patients with IH during the period of intensive proliferation compared to the values in healthy children. A similar dependence was observed by other authors, although they found remarkably low levels of this factor in the material taken directly from the hemangioma, both in the proliferative phase and in the involution.[19,20]

The proangiogenic properties of VEGF, as well as the effect of glucocorticoids on angiogenesis and vasculogenesis, have been reported in animal models.[21] After the implantation of stem cells producing vascular endothelial growth factor A (VEGF-A) in mice and simultaneous administration of dexamethasone, other researchers observed a decrease in VEGF value and symptoms of atrophic decompression. These authors measured the angiogenic factors solely from angiogenic lesions.[21] It is, therefore, possible that VEGF is responsible for the proliferation process. In the same way, the mechanism of action of propranolol can be explained. Multipotent stem cells from the hemangioma have vascular endothelial growth factor receptor 1 (VEGFR-1) receptors specific for VEGF-A. Linking them with VEGF-A protein induces the differentiation of these cells into vascular endothelial cells and subsequent vascular formation.[22] According to Zhang et al., propranolol reduces VEGF expression in stem cells derived from hemangioma, which inhibits angiogenesis.[23] The amount of VEGF produced by these cells decreases with the propranolol dose and is markedly reduced even at very low drug concentrations.

Our results confirm the correlation between high levels of VEGF and the phase of intensive proliferation. VEGF levels were also assessed in the study group during the proliferative phase, during which the possibility of correlation of VEGF values and patients' age was also analyzed. There was no statistically significant association between VEGF values and patient age. VEGF values in the course of treatment were significantly lower, which may indicate the efficacy of propranolol therapy. The observed lower VEGF values during the first 6 months and after treatment differed significantly from the values found before treatment. Similar results were obtained by Chinese researchers.[24,25]

The importance of bFGF in the proliferation and suppression of apoptosis of cells in the period of involution are to be emphasized. High concentrations are reported in the urine of patients with hemangiomas, whereas the decrease in urinary values is observed during treatment with interferon alpha 2.[17,26] Therefore, the decrease of this

factor should have a beneficial effect on the disappearance of the hemangioma. Przewratil et al. did not find a statistically significant difference in serum bFGF values in children with hemangiomas in the proliferative phase compared to the involuting phase.[19] In addition, no difference was observed between healthy children compared to children with a vascular malformation. Subsequent studies by the same author showed statistically significant lower values of serum bFGF in the proliferative phase (median bFGF values of 19.445 pg/mL) as compared to children with IH in the involuting phase (32.034 pg/mL). In addition, the author noted higher values of bFGF in the blood taken directly from hemangiomas than in the peripheral blood of the patients.[27]

In our study, low concentrations of bFGF were noted (mean 9.59 pg/mL). There was also a statistically significant decrease in the value of this factor during the treatment (mean 6.45 pg/mL). Evaluation of bFGF values before and after the treatment showed a statistically significant difference and may indicate the efficacy of propranolol in the treatment of early hemangiomas. In addition, bFGF level was found to be related to the age of the child – it was higher in older children. This relationship was not observed by other authors.[27] The observed correlation between the decrease in bFGF concentrations after treatment and the disappearance of vascular flow in Doppler US has little prognostic value as it relates to changes that occurred after treatment was completed.

Although IHs undergo a natural involution, the generally accepted principle of "wait and see" is not always beneficial. Finn et al. divided the hemangiomas into those that involute by the age of 6, and those whose disappearance lasted much longer.[6] The early introduction of propranolol suppresses the stage of intense angiogenesis, reducing the possibility of cosmetic defects. However, in the absence of a full therapeutic effect, surgery or laser therapy is necessary. As a rule, it is considered that about 30% of hemangiomas disappear by 3 years of age and 50% by 5 years of age.[5] According to Rajewska et al., only 17% of patients not treated and only monitored for 14.5 months showed the complete disappearance of the hemangioma.[28] In the presented study group, there was a 3-fold increase in the rate of complete disappearance in 8.7 months of treatment, both in the clinical assessment and Doppler US. This indicates the important contribution of propranolol to the hastened process of involution.

Visible assessment of involution of IH does not always correspond with Doppler US of the lesion. Monitoring effects of propranolol should include both methods, especially at the time of the decision to cease therapy.

Propranolol is usually introduced in hospital settings, although there are reports of safe procedures in outpatient settings.[29] The therapeutic dose should be in the range of 1–3 mg/kg/day, in 3 or 2 divided doses.[30–32] In the study group, the treatment was started in the hospital for 4–5 days, starting from 0.5 mg/kg/day of propranolol until a maximum dose of 2 mg/kg/day in 2 divided doses, with final high effectiveness of such protocol.

The best efficacy of therapy is observed in children who started it before 1 year of age.[30] However, Zvulunov et al. have reported good results of treatment introduced after 1 year of age.[33] Our observations indicate that early initiation of therapy, even before the 6th month of life, results in a faster disappearance of IH, which is evident in both physical examination and Doppler US. However, all patients who received treatment after 1 year of age experienced significant clinical improvement, but no complete involution was observed.

The effect of propranolol is usually rapid, often seen in the early days of therapy.[7,34–36] Visible changes between the 1st and the 3rd day of therapy are explained with vasospasms following the reduction of nitric oxide release.[4] In the study group, a change of color or reduction of tension in the 1st week of treatment was observed in 70% of patients, while at the end of the 1st month it was noted in over 90% of children.

Probably, the observed lack of IH growth is an effect of the inhibition of bFGF and VEGF by acting on β-adrenergic receptors. An increase in the size of the hemangiomas during the treatment in 2 of our patients, confirmed by increased vascular perfusion in the Doppler US, could be caused by a decreased dose.

Complete involution is observed at different times from the introduction of the treatment. The treatment should last 6–8 months, but may be extended to 1–2 years.[7,8,34,35] The treatment should be continued until the end of the proliferative phase, to a minimum of 1 year of age, and in periocular hemangiomas until the defect (astigmatism) is corrected.[35,37,38] Too early or rapid withdrawal may result in recurrence.[29,36] In the study group, the mean duration of the treatment with the full therapeutic dose was 8.7 months. The best results were obtained by comparing the status between the beginning of the drug withdrawal and the pretreatment condition ($r = -0.76$). The duration of therapy was prolonged by gradual withdrawal, lasting 1–3 months, to minimize the recurrence risk and maintain a good therapeutic effect. Storch and Hoeger explain the absence of the recurrence by capillary vascular endothelial cell apoptosis induced by non-selective β-blockers.[4] Kum and Khan have shown that only vascular endothelial cells undergo apoptosis, while stem cells – derived from arteries that are precursors of angiogenesis cells – do not.[39] This may explain recurrence after the treatment, seen in about 20% of children.[22]

The limitations of this study include a small number of patients and lack of a control group. Nowadays, with the well-documented beneficial effects of propranolol therapy in IH, it would be impossible, from an ethical point of view, to construct a methodology that would include a control group of children with IH not receiving any treatment.

Conclusions

VEGF and bFGF values decrease during propranolol treatment of IH, which may indicate the effect of propranolol on the change in both. However, the results of the statistical tests show a low prognostic value of VEGF and bFGF as possible biochemical markers for monitoring the treatment. Clinical evaluation combined with Doppler US is the most valuable method of monitoring the therapy.

References

1. Janmohamed SR, de Waard-van der Spek FB, Madern GC, et al. Scoring the proliferative activity of haemangioma of infancy: The Haemangioma Activity Score (HAS). *Clin Exp Dermatol*. 2011;36(7): 715–723.
2. Janmohamed SR, Madern GC, de Laat PCJ, et al. Educational paper: Pathogenesis of infantile haemangioma, an update 2014 (part I). *Eur J Pediatr*. 2015;174:97–103.
3. Lechańska J. Naczyniaki niemowlęce – od etiologii do postępowania terapeutycznego. DoveMed website. http://www.dovemed.pl/uploads/sfMediaBrowser//porady/naczyniaki-niemowl-ce.pdf. Accessed October 22, 2017.
4. Storch CH, Hoeger PH. Propranolol for infantile haemangiomas: Insights into the molecular mechanisms of action. *Br J Dermatol*. 2010;163(2):269–274.
5. Wyrzykowski D, Bukowski M, Jaśkiewicz J. Guzy naczyniowe i wrodzone malformacje naczyniowe [in Polish]. *Cancer Surg*. 2009;1(1): 1–17. http://cancersurgery.pl/pdf/200901a02.pdf. Accessed October 22, 2017.
6. Finn MC, Glowacki J, Mulliken JB. Congenital vascular lesions: Clinical application of a new classification. *J Pediatr Surg*. 1983;18(6): 894–900.
7. Léauté-Labrèze C, Dumas de la Roque E, Hubiche T, et al. Propranolol for severe hemangiomas of infancy. *N Engl J Med*. 2008;358(24):2649–2651.
8. Janmohamed SR, Madern GC, de Laat PC, et al. Educational paper: Therapy of infantile haemangioma – history and current state (part II). *Eur J Pediatr*. 2015;174:259–266.
9. Drolet BA, Frommelt PC, Chamlin SL, et al. Initiation and use of propranolol for infantile hemangioma: Report of a consensus conference. *Pediatrics*. 2013;131(1):128–140.
10. Chang E, Chang E, Thangarajah H, et al. Hypoxia, hormones, and endothelial progenitor cells in hemangioma. *Lymphat Res Biol*. 2007;5(4): 237–243.
11. Kleinman M, Greives M, Churgin S, et al. Hypoxia-induced mediators of stem/progenitor cell trafficking are increased in children with hemangioma. *Arterioscler Thromb Vasc Biol*. 2007;27:2664–2670.
12. Zhi-Yong S, Li Y, Cheng-Gang Y, et al. Possibilities and potential roles of estrogen in the pathogenesis of proliferation hemangiomas formation. *Med Hypotheses*. 2008;71:286–292.
13. Frieden IJ, Haggstrom AN, Drolet BA. Infantile hemangiomas: Current knowledge, future directions. Proceedings of a research workshop on infantile hemangiomas. April 7–9, 2005, Bethesda, Maryland, USA. *Pediatr Dermatol*. 2005;22(5):383–406.
14. Takahashi K, Mulliken J, Kozakewich H, et al. Cellular markers that distinguish the phases of hemangioma during infancy and childhood. *J Clin Invest*. 1994;93:2357–2364.
15. Hu Q, Lin X, Shang Q, et al. The determination and significance of VEGF in the serum of hemangioma patients. *Arch Neurol*. 2003;60:1613–1618.
16. Bielenberg DR, Bucana CD, Sanchez R, et al. Progressive growth of infantile cutaneous hemangiomas is directly correlated with hyperplasia and angiogenesis of adjacent epidermis and inversely correlated with expression of the endogenous angiogenesis inhibitor, IFN-beta. *Int J Oncol*. 1999;14:401–408.
17. Marler JJ, Fishman SJ, Kilroy SM, et al. Increased of urinary matrix metalloproteinases parallels the extent and activity of vascular anomalies. *Pediatrics*. 2005;116(1):38–45.
18. Zhang L, Lin X, Wang W, et al. Circulating level of vascular growth factor in differentiating hemangioma from vascular malformation patients. *Plast Reconstr Surg*. 2005;116(1):200–205.
19. Przewratil P, Sitkiewicz A, Wyka K, et al. Serum levels of vascular endothelial growth factor and basic fibroblastic growth factor in children with hemangiomas and vascular malformations – preliminary report. *Pediatr Dermatol*. 2009;26(4):399–404.
20. Przewratil P, Sitkiewicz A, Andrzejewska E. Local serum levels of vascular endothelial growth factor in infantile hemangioma: Intriguing mechanism of endothelial growth. *Cytokine*. 2010;49(2):141–147.
21. Greenberger S, Boscolo E, Adini I, et al. Corticosteroid suppression of VEGF-A in infantile hemangioma-derived stem cells. *N Engl J Med*. 2010;362:1005–1013.
22. Kum JJ, Khan ZA. Mechanisms of propranolol action in infantile hemangioma. *Dermatoendocrinol*. 2015;6(1):e979699.
23. Zhang L, Mai HM, Zheng J, et al. Propranolol inhibits angiogenesis via down-regulating the expression of vascular endothelial growth factor in hemangioma-derived stem cell. *Int J Clin Exp Pathol*. 2013;7(1): 48–55.
24. Chen XD, Ma G, Huang JI, et al. Serum-level changes of vascular endothelial growth factor in children with infantile hemangioma after oral propranolol therapy. *Pediatr Dermatol*. 2013;30(5):549–553.
25. Yuan WL, Jin ZL, Wei JJ, et al. Propranolol given orally for proliferating infantile haemangiomas: Analysis of efficacy and serological changes in vascular endothelial growth factor and endothelial nitric oxide synthase in 35 patients. *Br J Oral Maxillofac Surg*. 2013;51(7):656–661.
26. Chang E, Boyd A, Nelson CC, et al. Successful treatment of infantile hemangiomas with interferon-alpha 2b. *J Pediatr Hematol Oncol*. 1997;19:237–244.
27. Przewratil P, Sitkiewicz A, Andrzejewska E. Serum levels of basic fibroblastic growth factor (bFGF) in children with vascular anomalies: Another insight into endothelial growth. *Clin Biochem*. 2010;43(10-11): 863–867.
28. Rajewska J, Gawrych E, Fischer K, et al. Estimation of vascular endothelial growth factor and placental growth factor serum levels in infant with hemangioma and population of healthy infants. *Ann Acad Med Stetin*. 2012;58:5–10.
29. Haider KM, Plager DA, Neely DE, Eikenberry J, Haggstrom A. Outpatient treatment of periocular infantile hemangiomas with oral propranolol. *J AAPOS*. 2010;14(3):251–256.
30. Hoeger PH, Harper JI, Baselga E, et al. Treatment of infantile haemangiomas: Recommendations of a European expert group. *Eur J Pediatr*. 2015;174(7):855–865.
31. Léauté-Labreze Ch, Hoeger P, Mazereeuw-Hautier J, et al. A randomized, controlled trial of oral propranolol in infantile hemangioma. *N Engl J Med*. 2015;372(8):735–746.
32. Andrzejewska E, Bacewicz L, Bagłaj M, et al. Zastosowanie propranololu w leczeniu naczyniaków krwionośnych wczesnodziecięcych – program wieloośrodkowej oceny skuteczności. *Stand Med Probl Chir Dziec*. 2011;1:19–22.
33. Zvulunov A, McCuaig C, Frieden IJ, et al. Oral propranolol therapy for infantile hemangiomas beyond the proliferation phase: A multicenter retrospective study. *Pediatr Dermatol*. 2011;28(2):94–98.
34. Snir M, Reich U, Siegel R, et al. Refractive and structural changes in infantile periocular capillary haemangioma treated with propranolol. *Eye (Lond)*. 2011;25(12):1627–1634.
35. Thoumazet F, Léauté-Labrèze C, Colin J, et al. Efficacy of systemic propranolol for severe infantile haemangioma of the orbit and eyelid: A case study of eight patients. *Br J Ophthalmol*. 2012;96:370–374.
36. Claerhout I, Buijsrogge M, Delbeke P, et al. The use of propranolol in the treatment of periocular infantile haemangiomas: A review. *Br J Ophthalmol*. 2011;95(9):1199–1202.
37. Fabian ID, Ben-Zion I, Samuel C, et al. Reduction in astigmatism using propranolol as first-line therapy for periocular capillary hemangioma. *Am J Ophthalmol*. 2011;151(1):53–58.
38. Babiak-Choroszczak L, Giżewska-Kacprzak K, Puchalska-Niedbał L, et al. Propranolol as an effective treatment for inoperable periocular haemangiomas in children. *Pomeranian J Life Sci*. 2016;62:16–20.
39. Kum JJ, Khan ZA. Propranolol inhibits growth of hemangioma-initiating cells but does not induce apoptosis. *Pediatr Res*. 2014;75(3): 381–388.

Assessment of quality of life in patients with laryngeal cancer: A review of articles

Mateusz Kolator[A–F], Patrycja Kolator[A–F], Tomasz Zatoński[A–F]

Department and Clinic of Otolaryngology Head and Neck Surgery, Jan Mikulicz-Radecki University Teaching Hospital, Wrocław, Poland

A – research concept and design; B – collection and/or assembly of data; C – data analysis and interpretation;
D – writing the article; E – critical revision of the article; F – final approval of the article

Advances in Clinical and Experimental Medicine, ISSN 1899-5276 (print), ISSN 2451-2680 (online) *Adv Clin Exp Med*. 2018;27(5):711–715

Address for correspondence
Mateusz Kolator
E-mail: mateusz.kolator@gmail.com

Funding sources
None declared

Conflict of interest
None declared

Received on November 26, 2016
Reviewed on January 22, 2017
Accepted on March 22, 2017

Abstract

This article presents a review of the medical literature published between 1994 and 2014 with the use of the PubMed database concerning quality-of-life instruments for head and neck cancer patients used to assess general well-being of patients with laryngeal cancer. The PubMed database was searched for articles containing the keywords "quality of life", "laryngeal neoplasm" and "questionnaires". The resulting articles were reviewed and analyzed. After the identification of questionnaires, an additional search was performed. The articles and questionnaires were described and analyzed. In 43 articles, the authors used questionnaires specific to the head and neck regions in order to assess the quality of life in patients with laryngeal cancer. Four different questionnaires were identified. The European Organization for Research and Treatment of Cancer (EORTC) questionnaire is most commonly used to assess the quality of life in patients with laryngeal cancer. Questionnaires are generally used in order to select from a range of different treatment methods. There are a few head and neck cancer-related quality-of-life instruments which are widely used to assess the quality of life in patients with laryngeal cancer, but they are not dedicated to that region of the body. Today, there is much more attention paid to the quality of life; therefore, there is a real need to develop specific scales for different types of cancer.

Key words: literature review, health-related quality of life, quality of life questionnaire, head and neck neoplasms, laryngeal neoplasm

DOI
10.17219/acem/69693

Copyright
© 2018 by Wroclaw Medical University
This is an article distributed under the terms of the Creative Commons Attribution Non-Commercial License (http://creativecommons.org/licenses/by-nc-nd/4.0/)

Introduction

The group of neoplasms called head and neck cancers (HNC) – mainly because of their location – is the 10th most common group of cancers worldwide. They mostly begin in the squamous cells in mucosal organs in the head and neck area, such as the oral cavity, the pharynx, the larynx, the paranasal sinuses, the nasal cavity, and the salivary glands. Laryngeal cancer is the most commonly occurring neoplasm in this group. Symptoms may include a lump or sore that does not heal, a sore throat, difficulty in swallowing, and hoarseness in the voice. People who use tobacco, drink alcohol, or are exposed to the human papilloma virus are at risk of developing the disease. Treatment of laryngeal cancer because of its radical and traumatic type in every stage of the disease or therapy, i.e surgery, radiotherapy and chemotherapy, can have an effect on the quality of life even a few years later.[1,2]

Quality of life (QoL) is described as the quality of an individual's daily life. It is an evaluation of a person's well-being or lack thereof. This consists of the emotional, social, and physical aspects of a person's life. In healthcare, QoL is an assessment of how different aspects of an individual's life can be affected by a disease or a disability. Over the years, the concept of health-related QoL has evolved to encompass all aspects that can be proven to affect one's physical or mental health. Measuring QoL can deliver an enormous amount of information which has great value in modifying treatments, selecting drugs, avoiding side effects, and preventing disease.[3]

The aim of this study was to review the specific instruments used to assess the QoL in patients with laryngeal cancer.

Description of current knowledge

Numerous international organizations have undertaken to create instruments which would be able to accurately assess an individual's health-related QoL. There is a wide range of factors which need to be covered by this kind of questionnaire. The various tools for measuring QoL can be divided into 2 groups: general and specific. General scales assess QoL without recording the impact of the disease in particular, i.e., regardless of the pathologies. Specific scales are focused on a group of diseases, a single disease, factor, or even symptom.[4]

In this study, the PubMed database was searched using the MeSH keywords "quality of life", "laryngeal neoplasms" and "questionnaires" for articles published from 1990 to 2015. In total, 119 articles were found. Articles in any language other than English were not considered. Evaluation of the title and abstract excluded 76 studies, leaving 43 eligible for review. In the second search, the database was searched for properties and validations of these instruments.

Four different QoL questionnaires were identified. All questionnaires were specific to head and neck oncology, but were used for patients with laryngeal cancer. Some publications have reported the use of the European Organization for Research and Treatment of Cancer (EORTC) QLQ-C30 and H&N modules, the University of Washington Quality of Life Questionnaire (UW-QOL v4), the Functional Assessment of Cancer Therapy for patients with head and neck cancer (FACT-H&N), and the University of Michigan Head and Neck specific Quality of Life Instrument (HNQoL). The most widely used questionnaire is the EORTC QLQ-H&N module, followed by the UW-QOL (Table 1).

Table 1. Usage of head and neck scales

Questionnaire	Citations (No./%)
European Organization for Research and Treatment of Cancer (EORTC QLQ-H&N)	29/67.44
University of Washington Quality of Life Questionnaire (UW-QLQ v4)	10/23.25
Functional Assessment of Cancer Therapy for head and neck cancer (FACT-H&N)	3/6.97
University of Michigan Head and Neck specific Quality of Life Instrument (HNQoL)	1/2.33

There are a few studies where a specific region of the larynx (like the glottis or the hypolarynx) was assessed, but there are many more where the whole larynx as a region was taken into consideration. The authors mostly use these instruments to compare different methods of treatment. There are also a few studies where the authors have assessed voice quality, mental disorders, dysphagia, or sexual functioning (Table 2).[5–47]

Quality of life assessment tools

In 1994, Bjordal et al. developed the European Organization for Research and Treatment of Cancer questionnaire module to assess QoL in HNC patients. That module was specifically designed to be used before, during and after radiotherapy or surgery. The preliminary questionnaire was tested in patients from more than 5 European countries. The result was a questionnaire consisting of 37 items concerning disease- and treatment-related symptoms, social functioning and sexual functioning.[48] Hammerlid et al. showed that the QLQ-C30 questionnaire was well received by patients and that the results seemed to be sensitive to changes during the one-year study. Symptoms like difficulty swallowing, hoarse voice, sore mouth, dry mouth, and problems with the sense of taste showed the greatest variability in HNC patients.[49] The reliability and validity of the EORTC head and neck cancer module (QLQ-H&N35) and v. 3.0 of the EORTC Core Questionnaire

Table 2. Purposes and regions for which questionnaires were used

Authors	Questionnaire	Region	Purpose of use	Ref. No.
Zheng et al.	EORTC	supraglottic	swallowing assessment	5
Kucuk et al.	EORTC	larynx	comparison of treatment methods	6
Vilaseca et al.	UW-QLQ v4	larynx	comparison of treatment methods	7
Laoufi et al.	EORTC	glottis	voice quality assessment	8
Risberg-Berlin et al.	EORTC	larynx	rehabilitation results assessment	9
Robertson et al.	UW-QLQ v4	larynx	quality of life dependence on the stage of tumor after treatment	10
Filipovska-Mušanović et al.	EORTC	larynx/hypolarynx	comparison of treatment methods	11
Kanatas et al.	UW-QLQ v4	oral/oropharyngeal/laryngeal	quality of life assessment process	12
Gilbert et al.	EORTC	larynx	comparison of treatment methods	13
Mallis et al.	EORTC	larynx	comparison of treatment methods	14
Hamid et al.	EORTC	larynx	comparison of treatment methods	15
Azevedo et al.	UW-QLQ v4	larynx/hypolarynx	voice quality	16
Johansson et al.	EORTC	larynx	mental adjustment to cancer	17
Danker et al.	EORTC	larynx	alcohol consumption assessment	18
Guibert et al.	EORTC	hypopharyngeal/laryngeal	different treatment methods	19
Bajaj et al.	UW-QLQ v4	glottis	voice quality assessment	20
Robertson et al.	UW-QLQ v4	larynx	voice quality assessment	21
Varghese et al.	EORTC	larynx	voice quality, rehabilitation results assessment	22
Maclean et al.	UW-QLQ v4	larynx	dysphagia assessment	23
Singer et al.	EORTC	larynx	sexual functioning assessment	24
Singer et al.	EORTC	larynx	quality of life assessment process	25
Johansson et al.	EORTC	larynx	communication problems assessment	26
Minovi et al.	EORTC	larynx	comparison of treatment methods	27
Boscolo-Rizzo et al.	EORTC	larynx	comparison of treatment methods	28
Bindewald et al.	EORTC	larynx	comparison of treatment methods	29
Singer et al.	EORTC	larynx	mental disorders assessment	30
Ringash et al.	FACT-H&N	larynx	quality of life assessment process	31
Bahannan et al.	EORTC	glottis	comparison of treatment methods	32
Mowry et al.	UW-QLQ v4	larynx/oropharynx	comparison of treatment methods	33
Scalet et al.	EORTC	larynx	mental disorders assessment	34
Derks et al.	EORTC	larynx	mental disorders assessment	35
Loughran et al.	UW-QLQ v4	glottis	different treatment methods	36
Sewnaik et al.	EORTC	larynx	different treatment methods	37
Ringash et al.	FACT-H&N	larynx	quality of life assessment process	38
Derks et al.	EORTC	larynx	comparison of treatment methods	39
Muller et al.	EORTC	larynx	comparison of treatment methods	40
Paleri et al.	HNQoL	larynx	comparison of treatment methods	41
Zotti et al.	EORTC	larynx	comparison of treatment methods	42
Stoeckli et al.	EORTC	larynx	comparison of treatment methods	43
Ringash et al.	FACT-H&N	larynx	comparison of treatment methods	44
Allal et al.	EORTC	larynx/hypopharynx	comparison of treatment methods	45
Deleyiannis et al.	UW-QLQ v4	larynx	quality of life assessment process	46
Hammerlid et al.	EORTC	larynx	comparison of treatment methods	47

EORTC – European Organization for Research and Treatment of Cancer; UW-QLQ v4 – University of Washington Quality of Life Questionnaire; FACT-H&N – Functional Assessment of Cancer Therapy for head and neck cancer; HNQoL – Head and Neck specific Quality of Life Instrument.

(QLQ-C30) were confirmed in studies of large groups of patients from many different countries with HNC in different stages of treatment. The EORTC QLQ-C30 and head and neck module (QLQ-H&N35) demonstrates reliability and sensitivity to different groups of patients and types of treatment.[50,51]

The University of Washington Quality of Life Scale (UW-QOL) was first published in 1993, and since then it has been developed to its current stage. It consists of 12 domains: pain, appearance, activity, recreation, swallowing, chewing, speech, shoulder, taste, saliva, mood, and anxiety; each of these are followed by an importance rating scale over the past 7 days. The third part of the questionnaire consists of 3 questions: 1 asking how patients are feeling in comparison to the month before they developed cancer, 1 question about QoL related to health and 1 about their overall QoL.[52]

The Functional Assessment of Cancer Therapy for Head and Neck Cancer Scale (FACT-H&N) is one of many scales developed by the Functional Assessment of Chronic Illness Therapy (FACIT) measurement system. This questionnaire is specific to the head and neck region and consists of 5 domains; 4 of them are rather general, including "physical wellbeing", "social/family wellbeing", "emotional wellbeing", and "functional wellbeing", while the last domain is known as "additional concerns" – it strictly regards symptoms connected to the disease. The validity and reliability of this scale have also been confirmed.[53]

The University of Michigan Head and Neck-Specific Quality of Life Instrument includes 20 items scored on a 5-point rating scale: 0 – not at all, 1 – slightly, 2 – moderately, 3 – a lot, and 4 – extremely. Items are grouped into 4 domains: eating and swallowing, communication, head and neck pain, and emotional wellbeing. It also has additional optional questions A–G which are useful for deeper insight into the patient's health and their attitudes towards the treatment.[54]

Conclusions

Nowadays, there is a large variability in the QoL assessment tools specific to HNC which have been translated and validated in many different countries and languages. However, among these, there are not many which are specific to patients with laryngeal cancer. Because of its location and functional importance, the larynx plays a critical role in the maintenance of such cardinal physiological functions as phonation, the regulation of respiratory airflow, airway protection, and swallowing. Both the laryngeal cancer itself and the impact of its treatment can affect laryngeal functions. QoL should be taken into account in the selection of treatment. It affords the possibility of choosing the treatment which has not only had the best results in clinical trials, but has also had the best effect on QoL in patients after treatment. All of the scales are similar: they concern many of the same domains, but are grouped differently. The European Organization for Research and Treatment of Cancer Quality of Life Questionnaire and the University of Washington Quality of Life Questionnaire are the most commonly used ones in the assessment of patients with laryngeal cancer, but they are not strictly specific to that neoplasm. The QLQ-C30 module in connection with QLQ-H&N35 seem to cover most of the important aspects, but the disadvantages of this questionnaire are the large number of questions (65), the time needed to complete the questionnaire, and the complicated scoring algorithm. The UW-QOL is commonly used because of its simplicity, which makes it useful for patients. This questionnaire consists of 12 domains, but QoL in each domain is calculated on the basis of only 1 question, one which might not exactly describe the person's feelings. The FACT-H&N is only divided into functional scales, and though it includes questions about symptoms, it is impossible to compare QoL based on symptomatic scales. The University of Michigan Head and Neck Instrument, in turn, is calculated into only 1 simple result, which does not allow QoL comparison across different domains. None of the instruments described above seem to be sensitive or specific enough to cover all the changes in the larynx's functioning caused by cancer and the impact of different types of treatment. This is confirmed by the fact that the literature describes the use of different questionnaires focused on specific symptoms, such as voice-related QoL or swallowing-related QoL, as a supplement to head and neck cancer questionnaires.

Standardization in QoL assessment and the ability to choose 1 or 2 widely used and well-known questionnaires would more readily facilitate the comparison of results from different studies in research centers around the world.

References

1. Head and Neck Cancers – National Cancer Institute. http://www.cancer.gov/types/head-and-neck/head-neck-fact-sheet. Accessed December 10, 2015.
2. Sanderson RJ, Ironside JAD. Squamous cell carcinomas of the head and neck. *BMJ*. 2002;325(7368):822–827.
3. CDC – Concept – HRQOL. http://www.cdc.gov/hrqol/concept.htm. Accessed December 10, 2015.
4. Heutte N, Plisson L, Lange M, Prevost V, Babin E. Quality of life tools in head and neck oncology. *Eur Ann Otorhinolaryngol Head Neck Dis*. 2014;131(1):33–47.
5. Zheng Y, Liu M, Li M, et al. The influence of the 'patient-to-patient model' on swallowing problems in patients with supraglottic laryngeal cancer. *ORL J Otorhinolaryngol Relat Spec*. 2014;76(3):171–177.
6. Kucuk H, Kurnaz SC, Kutlar G. Treatment expectations and quality of life outcomes of patients with laryngeal cancer based on different treatment methods. *Eur Arch Otorhinolaryngol*. 2015;272(5):1245–1250.
7. Vilaseca I, Bernal-Sprekelsen M, Him R, Mandry A, Lehrer E, Blanch JL. Prognostic factors of quality of life after transoral laser microsurgery for laryngeal cancer. *Eur Arch Otorhinolaryngol*. 2015;272(5):1203–1210.
8. Laoufi S, Mirghani H, Janot F, Hartl DM. Voice quality after treatment of T1a glottic cancer. *Laryngoscope*. 2014;124:1398–1401.
9. Risberg-Berlin B, Karlsson TR, Tuomi L, Finizia C. Effectiveness of olfactory rehabilitation according to a structured protocol with potential of regaining pre-operative levels in laryngectomy patients using nasal airflow-inducing manoeuvre. *Eur Arch Otorhinolaryngol*. 2014;271(5):1113–1119.

10. Robertson SM, Yeo JCL, Sabey L, Young D, MacKenzie K. Effects of tumor staging and treatment modality on functional outcome and quality of life after treatment for laryngeal cancer. *Head Neck*. 2013;35(12):1759–1763.
11. Filipovska-Mušanović M, Hodžić D, Hrnčić N, Hatibović H. Quality of life in patients with larygeal/hypopharyngeal cancer following total/partial laryngectomy. *Med Glas (Zenica)*. 2012;9(2):287–292.
12. Kanatas A, Ghazali N, Lowe D, et al. Issues patients would like to discuss at their review consultation: Variation by early and late stage oral, oropharyngeal and laryngeal subsites. *Eur Arch Otorhinolaryngol*. 2013;270(3):1067–1074.
13. Gilbert RW, Goldstein DP, Guillemaud JP, Patel RS, Higgins KM, Enepekides DJ. Vertical partial laryngectomy with temporoparietal free flap reconstruction for recurrent laryngeal squamous cell carcinoma: Technique and long-term outcomes. *Arch Otolaryngol Head Neck Surg*. 2012;138(5):484–491.
14. Mallis A, Goumas PD, Mastronikolis NS, et al. Factors influencing quality of life after total laryngectomy: A study of 92 patients. *Eur Rev Med Pharmacol Sci*. 2011;15(8):937–942.
15. Hamid OA, El Fiky LM, Medani MM, Abdelhady A, Ali HH. Laryngeal cancer in Egypt: Quality of life measurement with different treatment modalities. *Head Neck*. 2011;33:1162–1169.
16. Azevedo EHM, Montoni N, Gonçalves Filho J, Kowalski LP, Carrara-de Angelis E. Vocal handicap and quality of life after treatment of advanced squamous carcinoma of the larynx and/or hypopharynx. *J Voice*. 2012;26:e63–71.
17. Johansson M, Rydén A, Finizia C. Mental adjustment to cancer and its relation to anxiety, depression, HRQL and survival in patients with laryngeal cancer – A longitudinal study. *BMC Cancer*. 2011;11:283.
18. Danker H, Keszte J, Singer S, et al. Alcohol consumption after laryngectomy. *Clin Otolaryngol*. 2011;36:336–344.
19. Guibert M, Lepage B, Woisard V, Rives M, Serrano E, Vergez S. Quality of life in patients treated for advanced hypopharyngeal or laryngeal cancer. *Eur Ann Otorhinolaryngol Head Neck Dis*. 2011;128(5):218–223.
20. Bajaj Y, Uppal S, Sharma RK, et al. Evaluation of voice and quality of life after transoral endoscopic laser resection of early glottic carcinoma. *J Laryngol Otol*. 2011;125(7):706–713.
21. Robertson SM, Yeo JCL, Dunnet C, Young D, MacKenzie K. Voice, swallowing, and quality of life after total laryngectomy – Results of the west of Scotland laryngectomy audit. *Head Neck*. 2012;34:59–65.
22. Varghese BT, Mathew A, Sebastian P, Iype EM, Vijay A. Comparison of quality of life between voice rehabilitated and nonrehabilitated laryngectomies in a developing world community. *Acta Otolaryngol*. 2011;131(3):310–315.
23. Maclean J, Cotton S, Perry A. Dysphagia following a total laryngectomy: The effect on quality of life, functioning, and psychological well-being. *Dysphagia*. 2009;24:314–321.
24. Singer S, Danker H, Dietz A, et al. Sexual problems after total or partial laryngectomy. *Laryngoscope*. 2008;118:2218–2224.
25. Singer S, Wollbrück D, Wulke C, et al. Validation of the EORTC QLQ-C30 and EORTC QLQ-H&N35 in patients with laryngeal cancer after surgery. *Head Neck*. 2009;31(1):64–76.
26. Johansson M, Rydén A, Finizia C. Self evaluation of communication experiences after laryngeal cancer – A longitudinal questionnaire study in patients with laryngeal cancer. *BMC Cancer*. 2008;8:80.
27. Minovi A, Ural A, Nowak C, Pearson M, Dazert S, Brors D. Long-term quality of life evaluation after laser microsurgery with or without adjuvant radiotherapy for laryngeal carcinoma. *Kulak Burun Bogaz Ihtis Derg*. 2008;18(6):362–366.
28. Boscolo-Rizzo P, Maronato F, Marchiori C, Gava A, Da Mosto MC. Long-term quality of life after total laryngectomy and postoperative radiotherapy versus concurrent chemoradiotherapy for laryngeal preservation. *Laryngoscope*. 2008;118:300–306.
29. Bindewald J, Oeken J, Wollbrueck D, et al. Quality of life correlates after surgery for laryngeal carcinoma. *Laryngoscope*. 2007;117:1770–1776.
30. Singer S, Danker H, Dietz A, et al. Screening for mental disorders in laryngeal cancer patients: A comparison of 6 methods. *Psychooncology*. 2008;17:280–286.
31. Ringash J, O'Sullivan B, Bezjak A, Redelmeier DA. Interpreting clinically significant changes in patient-reported outcomes. *Cancer*. 2007;110:196–202.
32. Bahannan AA, Zábrodsky M, Cerny L, Chovanec M, Lohynska R. Quality of life following endoscopic resection or radio-therapy for early glottic cancer. *Saudi Med J*. 2007;28:598–602.
33. Mowry S, Lotempio M, Sadeghi A, Wang K, Wang M. Quality of life outcomes in laryngeal and oropharyngeal cancer patients after chemoradiation. *Otolaryngol Head Neck Surg*. 2005;132(6):948–953.
34. Scalet D, Braz A, Ribas MM, et al. Quality of life and depression in patients undergoing total and partial laryngectomy. *Clinics*. 2005;60:135–142.
35. Derks W, Leeuw JRJ, Hordijk GJ, Winnubst JAM. Differences in coping style and locus of control between older and younger patients with head and neck cancer. *Clin Otolaryngol*. 2005;30:186–192.
36. Loughran S, Calder N, MacGregor FB, Carding P, MacKenzie K. Quality of life and voice following endoscopic resection or radiotherapy for early glottic cancer. *Clin Otolaryngol*. 2005;30:42–47.
37. Sewnaik A, Van Den Brink JL, Wieringa MH, Meeuwis CA, Kerrebijn JDF. Surgery for recurrent laryngeal carcinoma after radiotherapy: Partial laryngectomy or total laryngectomy for a better quality of life? *Otolaryngol Head Neck Surg*. 2005;132:95–98.
38. Ringash J, Bezjak A, O'Sullivan B, Redelmeier DA. Interpreting differences in quality of life: The FACT-H&N in laryngeal cancer patients. *Qual Life Res*. 2004;13(4):725–733.
39. Derks W, Leeuw JRJ, Hordijk GJ, Winnubst JAM. Reasons for nonstandard treatment in elderly patients with advanced head and neck cancer. *Eur Arch Otorhinolaryngol*. 2005;262(1):21–26.
40. Müller R, Paneff J, Köllner V, Koch R. Quality of life of patients with laryngeal carcinoma: A post-treatment study. *Eur Arch Otorhinolaryngol*. 2001;258:276–280.
41. Paleri V, Stafford FW, Leontsinis TG, Hildreth AJ. Quality of life in laryngectomees: A post-treatment comparison of laryngectomy alone versus combined therapy. *J Laryngol Otol*. 2001;115:450–454.
42. Zotti P, Lugli D, Vaccher E, Vidotto G, Franchin G, Barzan L. The EORTC quality of life questionnaire-head and neck 35 in Italian laryngectomized patients. European organization for research and treatment of cancer. *Qual Life Res*. 2000;9:1147–1153.
43. Stoeckli SJ, Guidicelli M, Schneider A, Huber A, Schmid S. Quality of life after treatment for early laryngeal carcinoma. *Eur Arch Otorhinolaryngol*. 2001;258:96–99.
44. Ringash J, Redelmeier DA, O'Sullivan B, et al. Quality of life and utility in irradiated laryngeal cancer patients. *Int J Radiat Oncol*. 2000;47:875–881.
45. Allal AS, Dulguerov P, Bieri S, Lehmann W, Kurtz JM. Assessment of quality of life in patients treated with accelerated radiotherapy for laryngeal and hypopharyngeal carcinomas. *Head Neck*. 2000;22:288–293.
46. Deleyiannis FW, Weymuller EA, Coltrera MD, Futran N. Quality of life after laryngectomy: Are functional disabilities important? *Head Neck*. 1999;21:319–324.
47. Hammerlid E, Mercke C, Sullivan M, Westin T. A prospective quality of life study of patients with laryngeal carcinoma by tumor stage and different radiation therapy schedules. *Laryngoscope*. 1998;108:747–759.
48. Bjordal K, Ahlner-Elmqvist M, Tollesson E, et al.; EORTC Quality of Life Study Group. Development of a European Organization for Research and Treatment of Cancer (EORTC) questionnaire module to be used in quality of life assessments in head and neck cancer patients. *Acta Oncol*. 1994;33:879–885.
49. Hammerlid E, Bjordal K, Ahlnerelmqvist M, et al. Prospective, longitudinal quality-of-life study of patients with head and neck cancer: A feasibility study including the EORTC QLQ-C30. *Otolaryngol Head Neck Surg*. 1997;116(6 Pt 1):666–673.
50. Sherman AC, Simonton S, Adams DC, Vural E, Owens B, Hanna E. Assessing quality of life in patients with head and neck cancer. *Arch Otolaryngol Neck Surg*. 2000;126:459.
51. Bjordal K, de Graeff A, Fayers P, et al. A 12 country field study of the EORTC QLQ-C30 (version 3.0) and the head and neck cancer specific module (EORTC QLQ-H&N35) in head and neck patients. EORTC Quality of Life Group. *Eur J Cancer*. 2000;36(14):1796–1807.
52. Rogers SN, Lowe D. The University of Washington Quality of Life Scale. In: *Handbook of Disease Burdens and Quality of Life Measures*. New York, NY: Springer New York; 2010:101-128.
53. List MA, D'Antonio LL, Cella DF, et al. The performance status scale for head and neck cancer patients and the functional assessment of cancer therapy-head and neck scale: A study of utility and validity. *Cancer*. 1996;77:2294–2301.
54. Ronis DL, Fowler KE, Bradford CR, et al. Clinical predictors of quality of life in patients with head and neck cancer. *Arch Otolaryngol Head Neck Surg*. 2004;130(4):401–408.

The expression of marker genes during the differentiation of mesenchymal stromal cells

Aleksandra Zołocińska[A–F]

Department of Regenerative Medicine, Maria Skłodowska-Curie Memorial Cancer Center, Warszawa, Poland

A – research concept and design; B – collection and/or assembly of data; C – data analysis and interpretation;
D – writing the article; E – critical revision of the article; F – final approval of the article

Advances in Clinical and Experimental Medicine, ISSN 1899-5276 (print), ISSN 2451-2680 (online) *Adv Clin Exp Med*. 2018;27(5):717–723

Address for correspondence
Aleksandra Zołocińska
E-mail: aleksandradebska88@gmail.com

Funding sources
The work was supported by OPUS UMO-2013/11/B/ST8/03401, National Science Center.

Conflict of interest
None declared

Received on August 23, 2016
Reviewed on January 2, 2017
Accepted on January 10, 2017

Abstract

Mesenchymal stromal cells (MSCs) are an excellent and easily accessible source of precursor cells that have applications in regenerative medicine. They can be obtained from almost any tissue; however, bone marrow, Wharton's jelly and adipose tissue are the most frequently used sources of MSCs. Increased interest in using MSCs in medical procedures has resulted in a pressing need to identify the genetic elements that can indicate the presence and the characteristics of MSCs. Genomic profiling enables the identification and characterization of MSCs as well as finding biomarkers and key molecules involved in all processes occurring in the cell. This knowledge is essential for developing a stem cell approach for tissue engineering and can improve the development of new clinical applications of MSCs. This review is an attempt to give an overview of key genetic markers indicating the main directions of MSC differentiation. The expression of these genes provides information about the direction and progress of differentiation and about interactions with the surrounding environment as well as specific molecular pathways that MSCs are involved in.

Key words: gene expression, mesenchymal stem cells, regenerative medicine, genetic markers

DOI
10.17219/acem/68386

Copyright
© 2018 by Wroclaw Medical University
This is an article distributed under the terms of the Creative Commons Attribution Non-Commercial License (http://creativecommons.org/licenses/by-nc-nd/4.0/)

Introduction

Mesenchymal stem cells (MSCs) are multipotent progenitor cells that are capable of differentiating into osteogenic, chondrogenic, and adipogenic lineages at least (Fig. 1).[1] It has been noted that MSCs may demonstrate plasticity beyond their traditional mesodermal lineage and that under specific conditions they can differentiate into neural cells, cardiomyocytes, pancreatic islet beta-cells, and hepatocytes.[2–5] According to the definition of the International Society for Cellular Therapy (ISCT), MSCs are plastic-adherent cells, expressing a panel of surface markers while lacking expression of hematopoietic-related antigens.[1] Their phenotype is characterized by a synthesis of surface markers: $CD73^+$, $CD90^+$, $CD105^+$, $CD45^-$, $CD34^-$, $CD14^-$ or $CD11b^-$, and $CD79a^-$ or $CD19^-$. Knowledge of these surface markers is crucial for their identification, characteristics and isolation by sorting.[6] Initially, MSCs were identified in mice bone marrow aspirates, the spleen and the thymus, but further studies have revealed the presence of MSCs in most organs of the adult body as well as in cord blood, Wharton's jelly, the perivascular area, and under the amniotic membrane of the umbilical cord, the placenta, and the amniotic fluid.[6,7] However, the only MSCs with a practical application are cord blood MSCs, Wharton's jelly MSCs (WJ-MSCs), bone marrow stromal cells (BM-MSCs) and adipose-derived stromal cells (ASCs). In particular, a number of studies have reported that the isolation of stromal cells from adipose tissue is endowed with a high proliferative capacity and differentiation potential; ASCs are also easily isolated from lipoaspirate.[8]

Mesenchymal stromal cells are an easily accessible source of precursor cells that can find applications in regenerative medicine, improving myocardial function, therapies of Crohn's disease, and neurodegenerative disorders.[9] Adipose-derived stromal cells are also used for adipose tissue regeneration in patients following breast cancer surgery,[10] the acceleration of skin wound healing, regenerative treatment of widespread traumatic calvarial bones defects, the repair of tracheomediastinal fistulas caused by cancer ablation, the treatment of chronic ulcers caused by radiation therapy and controlling graft-versus-host disease (GVHD), and the treatment of osteoarthritis (OA).[9,10]

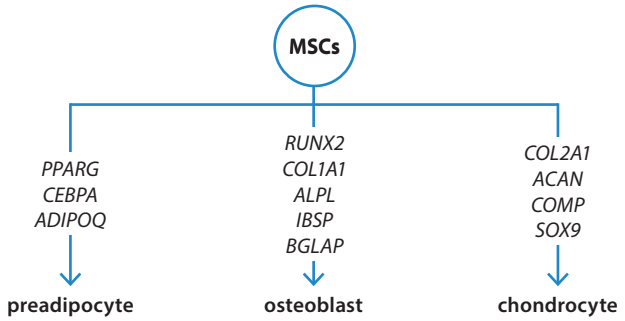

Fig. 1. Scheme of genes activated during MSCs differentiation into adipogenic, osteogenic, and chondrogenic lineages

The main function of MSCs is considered to be generating connective tissue and forming the stromal cells for bone marrow. Recent studies also revealed that MSCs are able to modulate the functions of the immune system. Taking into account the growing interest in using MSCs in medical procedures, there is a pressing need to identify the genetic elements that can indicate the presence of MSCs and their differentiation into various tissues. Numerous studies have examined the genomic profiles of MSCs, identifying potential biomarkers and key molecules that regulate biological processes involved in cell growth, development and survival. The knowledge gained from these studies may help in the development of strategies of improving the tissue regeneration potential of MSCs for various clinical applications.[11]

There are several methods that enable the detection of the directions of MSCs differentiation. The simplest method is staining differentiated cells using specific dyes. Mesenchymal stromal cells differentiated into osteogenic lineage can be detected by alizarin red staining, which detects the formation of extracellular matrix calcification. A differentiation toward an adipocyte phenotype can be assessed by Oil Red O staining in order to visualize the presence of lipid droplets. The acquisition of a chondrogenic phenotype can be evaluated with the use of alcian blue. Staining, however, is not reliable enough to be the only method that determines the directions of differentiation: it has to be confirmed by more specific techniques like real-time polymerase chain reaction (RT-PCR), immunocytochemistry, or the comparison of miRNA expression profiles.[12] Immunocytochemistry is the most common method of detecting MSCs in the examined tissue, because it enables an analysis of the presence and location of any antigens in the cell and the identification of particular cell types by combining the fluorophore-labeled antibody with a suitable surface antigen. This method, however, has some disadvantages, such as the possibility of false positive or negative results as well as non-specific fluorescence. Besides, direct immunocytochemical methods have a poor sensitivity and a high cost, while in turn, an indirect method procedure is very complex and long; they also have higher risk of non-specific binding of secondary antibody resulting in background staining.[13]

Very precise methods include the comparative genome-wide gene expression profile analysis and microRNA expression profiling. It is known that these small non-coding RNA molecules' occurrence is specific to cell type and that they modulate gene expression and/or protein synthesis, but little is known about their global expression profiles in mesenchymal stromal cells. Therefore, mRNA expression data, when combined with genome-wide gene expression profiles, can provide a great deal of information about transcriptional networks and differentiation processes in MSCs.[14] RNA-seq, using NGS (next generation sequencing) to indicate the presence and quantity of RNA as well as cDNA microarrays, are other very accurate methods of assessing the gene expression level; however, they are

expensive and their results require difficult data analysis. In comparison to these methods, real-time PCR seems to be the most appropriate way to define the differentiating potential of MSCs through measuring the expression of marker genes specific for particular tissue.

Quantitative assessment of the expression of marker genes

Real-time PCR technology enables the determination of the cell differentiation stage by gene expression monitoring, which allows us to detect an active differentiation mechanism very early, depending on the chosen marker genes. Quantitative real-time PCR is a high-throughput, sensitive and fast method that can measure the increase in DNA copy numbers in real time.[15] For the detection of the number of cDNA copies in tested samples, researchers use molecules that emit light after binding to double-stranded DNA, e.g., SYBR Green or ethidium bromide. However, using primers and SYBR Green dye may result in binding non-specific sequences, which gives false results because SYBR Green emits light when bound to any double-stranded DNA.

A more specific and reliable method involves the use of fluorescent probes, e.g., TaqMan™ probes, which are labeled with 2 different fluorescent dyes: a reporter dye at the 5' and a quenching dye at the 3'. In order to generate light emission, the reporter dye molecule must be separated from the quencher dye molecule. Primers and probes sequences are available in multiple publications; they can also be designed using specialized software, based on sequences in the National Center for Biotechnology Information (NCBI) or the Ensembl database. Real-time PCR is an integral method, widely used in molecular diagnostics. This technique is extremely sensitive and allows for simultaneous expression analysis of several samples. In addition, the results generated by the software and obtained from different experiments can be combined and compared with each other. However, this technique has some disadvantages, as the accuracy of the results depends largely on the probes and endogenous control used. The choice of a proper internal control gene is essential for obtaining reliable results, because a critical factor for creating reliable data in relative quantification is the normalization of the expression data of the genes of interest. This selection is particularly important when the expression differences are slight or when the samples derive from different histological origins or stages of development. Reference genes are called "house-keeping genes" and their expression in tissue is stable, irrespective of the conditions.[16]

Progenitor cells undergo a series of stable identity transitions on their way to becoming fully differentiated cells with unique identities. The gene expression profile determines the mode of cell differentiation; it is the most fundamental level at which a genotype gives rise to a phenotype. At the beginning of the gene expression, transcription factors initiate transcription and RNA polymerase binds to the promoter sequence in order to synthesize pre-mRNA. Due to post-transcriptional processes, mature mRNA is formed and transported from the nucleus to the ribosomes in a cytoplasm, where translation begins and the information encoded in mRNA is translated to an amino acid chain.

Using quantitative real-time PCR, the differentiation potential of MSCs can be confirmed very early, at every step of gene expression before the formation of protein, producing results for several studied genes at once very fast and easily.

Differentiation marker genes

During cell differentiation, certain genes specific to the tissue are expressed (Table 1). To determine if MSCs differentiate into a particular tissue, a few differentiation-related genes have to be chosen. Molecular basis and transcription factors activated during the differentiation of particular tissues of mesodermal origin have been broadly described. While examining the differentiation of MSCs, the expression of genes involved in the direction of differentiation is checked. Gene expression analysis can be performed using primers or probes for selected genes or prepared gene expression arrays for specific biological processes, e.g., RT² Profiler™ PCR Array, with assays for differentiation-associated genes and assays for endogenous control genes. The second option is easy and it does not require the selection of appropriate marker genes or the matching of endogenous controls, but the cost is very high and 3–5 marker genes are sufficient to check whether there is a differentiation process. Designing primers or probes, however, is associated with a risk, because the accuracy of results depends on the quality of the used primers or probes and the endogenous control.[17]

Table 1. List of markers of MSCs differentiation into osteogenic, adipogenic, and chondrogenic lineages

Direction of MSCs differentiation	Activated genes	References
Chondrogenic	*COL2A1* *ACAN* *COMP* *SOX9*	Hamid et al.[32] de Crombrugghe et al.[33] Lin et al.[34] Mwale et al.[35]
Adipogenic	*PPARG* *CEBPA* *ADIPOQ*	Graneli et al.[19] Ntambi et al.[20] Hu et al.[21]
Osteogenic	*RUNX2* *COL1A1* *ALPL* *IBSP* *BGLAP*	Graneli et al.[11] Qi et al.[23] Marom et al.[25] Mizuno et al.[26] Tsai et al.[27] Eid et al.[28] Gordon et al.[29] Maes et al.[31]

MSCs – mesenchymal stem cells.

Adipogenic differentiation

Mesenchymal stromal cells differentiate in vitro at least toward adipogenic, osteogenic and chondrogenic lineages when treated with established lineage-specific factors. The selective differentiation of these cells depends on specific environmental cues, usually a combination of growth factors and cytokines, which are supplied in vitro. In order to differentiate MSCs toward the adipogenic lineage, cells must be cultured in fetal bovine serum (FBS) containing Dulbecco's modified Eagle's medium (DMEM), supplemented with dexamethasone, insulin, and isobutylmethylxanthine (IBMX) and/or indomethacin and thiazolidinedione (TZD).[12,18]

One of the most commonly used marker genes in the detection of adipogenic differentiation of MSCs is *PPARG* (peroxisome proliferator-activated receptor gamma). The PPARG gamma protein, encoded by this gene, is a transcription factor, the main switch in adipogenic differentiation of MSCs, and has been implicated in the pathology of such diseases as obesity, diabetes, atherosclerosis and cancer. It is reported that the expression of the *PPARG* gene has a negative effect on osteogenic differentiation and that its inhibition of *PPAR-γ* during the induction of osteogenesis leads to increased osteogenic differentiation of human MSCs.[19] The expression of the *PPAR-γ* gene is transcriptionally induced within 2 days following the induction of differentiation and lasts until day 3 to 4 at the latest. The *PPAR-γ* expression is mediated by the activity of *C/EBP β* and *δ*, which also mediate the expression of *C/EBP α* – another marker gene of adipogenic differentiation.[20] *C/EBP β* and *δ* are the first transcription factors induced after preadipocyte exposure to a differentiation medium, as their expression starts increasing a few hours after induction. Once the induction medium is removed from the culture, the expression of *C/EBP δ* dissipates over the subsequent 48 h, whereas the decline of *C/EBP β* is more gradual, with its expression approximating 0% of maximal levels by day 8. The expression of *C/EBP α* increases from undetectable levels in preadipocytes to detectable levels 2 days after stimulation with adipogenesis-specific factors, and to full expression 5 days after differentiation is initiated. The genes of the *C/EBP* family are involved in directing the process of differentiation during adipogenesis and, together with *PPAR-γ*, are required for full adipocyte differentiation.[20] Therefore, the *C/EBP* family genes and *PPAR-γ* are markers of early adipogenesis. One late adipogenesis marker gene is *ADIPOQ*, whose expression is highly specific to adipose tissue and is observed exclusively in mature fat cells as the stromal-vascular fraction of fat tissue does not contain *ADIPOQs* mRNA. The expression of *ADIPOQs* mRNA is a late event in adipogenesis, first appearing on approx. day 4 after the induction of differentiation.[21]

Osteogenic differentiation

The most promising area for MSCs application is bone reconstruction and regeneration. Osteogenesis is a complex process that involves the differentiation of mesenchymal cells into pre-osteoblasts and osteoblasts, which ultimately leads to the synthesis and deposition of bone matrix proteins.[22] In order to differentiate mesenchymal stromal cells toward the osteogenic lineage, cells need to be cultured in osteogenic medium, containing dexamethasone, ascorbate-2-phosphate, β-glycerophosphate, l-glutamine, ascorbic acid, and/or vitamin D_3.[12,22]

Bone formation is known to occur through the activation of molecules as the runt-related transcription factor 2 (RUNX2), type I collagen (COL1A1), alkaline phosphatase (ALPL), integrin-binding sialoprotein (IBSP), and bone gamma-carboxyglutamate (gla) protein (BGLAP), which orchestrate the differentiation of MSCs into functional osteoblasts. The most important transcription factor in osteogenesis is RUNX2, which plays a crucial role in the formation of the mineralized skeleton during embryogenesis and regulates the maturation of the osteoblast phenotype.[23,24] It is crucial for the formation of mineralized tissue and its expression is usually associated with the early phases of osteogenic differentiation.[11] *RUNX2* is the main regulator of the osteogenic differentiation of MSCs and it regulates the transcription of osteocalcin (*BGLAP*). Osteocalcin is a matrix protein that regulates osteoclast activity; it is highly specific for mineralization and is a good marker of the osteoblastic phenotype.[25,26] The *BGLAP* gene encodes a protein associated with the mineralized bone matrix, secreted by the calcified tissue and regulated by vitamin D_3; it indicates the activity of osteoblasts and it is known as a marker of late osteogenesis.

Another gene which is activated by RUNX2 is *COL1A1*. Collagen I is the pervading protein of the bone matrix, and its expression and secretion is crucial to the mineralization process. Attachment to collagen I is mediated through integrins that activate kinase signaling pathways, thus supporting osteoblast cell proliferation and bone growth.[25] *COL1A1* is essential for osteoblast adhesion and bone growth.[26] Furthermore, type I collagen is the main constituent of the organic part of the extracellular matrix (ECM).[11] The next most frequently used marker of osteogenic differentiation, alkaline phosphatase (*ALP*), is the effector protein responsible for the mineralization of the extracellular matrix.[11] Alkaline phospatase is an early bone marker protein and an essential enzyme for ossification. As *ALP* is widely used as a marker of osteoblasts, an increase in its activity should be associated with osteoblastic differentiation. When the mineralization process is well progressed, the *ALP* level increases and then decreases; the peak of its expression falls on day 7 after induction.[27] *ALP* is closely related to pre-osseous cellular metabolism and to the elaboration of calcified bone matrix.[28]

Integrin-binding sialoprotein (IBSP) is an acidic, non-collagenous glycoprotein abundantly expressed in mineralized tissues and a major structural protein of the bone matrix.[29] This protein binds to calcium and hydroxyapatite through its acidic amino acid clusters and mediates cell

binding through an arginylglycylaspartic acid (RGD) sequence, which recognizes the vitronectin receptor.[30]

Generally, *IBSP* and *BGLAP* are late markers of osteogenesis, as are osteopontin (*OPN*) and msh homeobox 2 (*MSX2*), whereas *RUNX2*, *COL1A1* and ALP are markers of early osteogenesis, along with the Sp7 transcription factor (OSX) and transforming growth factor-beta 1 (*TGFB1*).[22–31]

Chondrogenic differentiation

Cartilage defects caused by trauma, tumor ablation or age-related abrasion lead to constant pain and functional limitations, causing a decreased quality of life. It is known that even small lesions can affect the structure and function of the articular cartilage, predisposing it to the development of osteoarthritis (OA). The reason for this is a lack of vascularization and enervation in the articular cartilage tissue, which inhibits repair processes like inflammation and fibrin clot formation. Only chondrocytes and synoviocytes residing in the local environment can fill up the defects by slow proliferation and matrix deposition.[31] Troubles caused by the nature of cartilage tissue have inspired further studies, which focus on the possibilities of regeneration of this tissue. Mesenchymal stromal cells are one of the most promising research areas. Chondrogenic differentiation requires a high density cell culture and monolayer culture reduces the ability of differentiation towards chondrogenic lineage; therefore, the best solution is 3-dimensional culture created using scaffolds made of natural or synthetic materials. The chondrogenic induction medium is enriched with glutamax (Invitrogen Carlsbad, USA), vitamin C, insulin-transferrin-selenium-X (ITS), insulin-like growth factor 1 (IGF-1), ascorbate-2-phosphate, L-proline, TGF-β, and dexamethasone.[32]

At the beginning of chondrogenesis, MSCs aggregate and condensate, while expressing various extracellular matrix components, including type II collagen (COL2A1), aggrecan core protein (ACAN), cartilage oligomeric protein (COMP), and SRY-box 9 (SOX9). After differentiating into chondrocytes, the cells begin to produce ECM materials rich in aggrecan core protein and cartilage oligomeric protein, forming cartilage tissue.[32]

Type II collagen is an early marker of chondrogenesis, expressing in chondroprogenitor cells and in chondrocytes[33]; the expression of the *COL2A1* gene was reduced at the 2nd and 3rd week of the culture.[32] The *SOX9* expression, however, reached the highest level at the 3rd week of culture, promoting a production of cartilage matrix. This protein also expresses in chondroprogenitor cells and chondrocytes, but there is no *SOX9* expression in hypertrophic chondrocytes.[33] Lin et al. confirms that the expression of *COL2A1* and *SOX9* is an early and unique marker of chondrogenesis.[34] Another early marker of chondrogenesis is *COMP*, whose expression reaches the highest level 1 week after chondrogenic induction.[32] In contrast, aggrecan and type X collagen are markers of late chondrogenesis, related to chondrocyte hypertrophy.[35]

Chondrogenesis in mesenchymal stem cells is most prominent after 1 week of chondrogenic induction, and longer stimulation can induce chondrocyte hypertrophy.[32]

Other differentiation directions

Mesenchymal stromal cells seem to be an easily accessible source of precursor cells that can be expanded in vitro and used for many clinical applications. As mentioned above, MSCs may demonstrate plasticity beyond their traditional mesodermal lineage. Under specific conditions, they are able to differentiate into mesodermal lineage cells (adipocytes, chondrocytes, osteoblasts, tenocytes, or myocytes), endodermal lineage cells (astrocytes or neurons) or ectodermal lineage cells (hepatocytes or islet beta cells).[3–6] There is a need to create a panel of markers for each direction of MSC differentiation. The expression of *MYOD1* (myogenic differentiation 1), *MYF5* (myogenic factor 5) and *MYOG* (myogenin) transcription factors is crucial for myogenic differentiation and a high expression of *TNC* (tenascin C), *SCX* (scleraxis bHLH transcription factor), *DCN* (decorin), and *COL1A2* (collagen type I alpha 2 chain) genes occurs during tenogenic differentiation of MSCs.[6,36] During neurogenic differentiation of MSCs, there is an expression of genes related to nervous system development: nestin, used to identify neural stem and early progenitor cells, *GFAP* – a structural element of fibrillary astrocytes – and *NeuN*, a neuronal nuclear antigen.[2] Mesenchymal stromal cells induced to differentiate into a islet beta cell phenotype express genes which encode hormones specific for the pancreas: *ISL1* (insulin), *NGN3* (an early pancreatic progenitor marker), *SST* (somatostatin), and *GCG* (glucagon) – a specific endocrine marker.[4] Differentiation into hepatocytes results in the expression of *AFP* (alpha-fetoprotein) and *HNF1β* (hepatocyte nuclear factor 1β).[5]

Reference genes

Gene expression analyses are essential to the discovery and characterization of the roles for known genes and to understanding the processes occurring in cells. Regarding the study of the development of different tissues, gene expression analyses can provide insights into complex regulatory networks that coordinate in cells such processes as proliferation, cell commitment, differentiation, and apoptosis. Genes which exhibit constant expression levels among all tissues regardless of conditions are reference genes. The perfect reference gene should have similar expression levels regardless of experimental conditions, mainly developmental stages, composition of cell types and sample treatments.

The most commonly used reference genes are *β-actin* and *GAPDH*; however, recent studies have shown that these common reference genes are not stably expressed under all experimental conditions. Ideally, reference genes

should show stable expression levels in all studied cell types and tissues, and transcription should be constant relative to the general cellular transcription rates under different experimental conditions.

Nonetheless, research has proven that the expression of individual reference genes varies among samples under different experimental conditions. Therefore, it is relevant to select a proper reference gene for normalization, according to experimental settings. In recent years, it has been found that gene expression should be normalized using at least 3 reference genes to ensure that the experiment results are reliable.[37]

Summary

Tissue engineering offers potential methods of repairing damaged tissues, and it is a rapidly growing field of regenerative medicine. The ability to differentiate in multiple directions, the immunomodulation properties and the regulation of endogenous tissue repair make MSCs very attractive for regenerative medicine. In recent years, the use of adipose-derived stromal cells have particularly gained popularity. Adipose tissue can be described as an easily available source of stromal vascular fraction (SVF), which contains preadipocytes, endothelial progenitor cells, T cells, B cells, mast cells, adipose tissue macrophages, and MSCs. In 2001, Zuk et al. demonstrated that adipose-derived stromal cells are capable of differentiating into adipo-, chondro-, osteo-, and myogenic lineages.[38] A year later, the same authors proved that ASCs express the same surface markers as bone marrow: derived mesenchymal stromal cells (BM-MSCs): CD29, CD44, CD71, CD90, and CD105, lacking the expression of CD31, CD34, and CD45.[39]

Real-time PCR enables the definition of the common genetic profile of BM-MSCs and ASCs, and the examination of a complex network of molecules which regulate the homing and communication of MSCs with their environment by activating signaling pathways that play a crucial role in maintaining their stemness properties. Saulnier et al. identified 190 cohort modulated transcripts, which may be molecular MSCs' stemness signature. Among them, there were genes involved in basic biological mechanisms like embryogenesis, signal transduction, cell adhesion, and inter-cellular communication.[8]

The biggest advantage of ASCs over BM-MSCs lies in the collection of a much larger number of cells with less of the risk associated with surgical procedure. Cells derived from lipoaspirate are also a more homogenic population than those derived from bone marrow, which makes ASC applications more efficient than the use of BM-MSCs. ASCs as well as BM-MSCs have already been used for cell-based therapies, including orthopedic disorders, cardiovascular diseases, graft vs host disease, and Crohn's disease.[3,9] The use of stem cells in medicine is growing, so there is a need for an accurate characterization of these cells. Knowledge of rapid changes in gene expression during stem cell differentiation will provide a better understanding of the potential of these cells for regenerative medicine.

Numerous studies have examined genomic profiles of MSCs collected from different tissues, which differ in their ability to proliferate and differentiate into various lineages. Genomic profiling enables the characterization of MSCs and the identification of biomarkers and key molecules involved in the regulation of cell survival, growth and development. The knowledge gained from these studies will improve the understanding of basic processes occurring in the stem cell and may help in the development of strategies for improving the clinical applications of MSCs.[2–10]

Comprehensive knowledge of the biological processes involved in tissue repair is essential for developing a stem cell approach for tissue regeneration. Understanding their molecular regulation during the repair process is crucial in order to achieve the desired clinical outcomes. Overall, molecular studies on differentiating MSCs identify potential markers that can be used to isolate and purify MSCs from heterogeneous cell populations. They also provide data on potential genomic indicators involved in specific differentiation pathways that can disclose information about the stage of differentiation of the tested cells. Importantly, however, the detection of differentiation-related gene expression is insufficient for successful phenotypic differentiation. Further experiments are required in order to confirm the differentiation.[11–16]

In conclusion, gene expression analysis during MSCs differentiation provides information regarding the direction and progress of differentiation and exhibits the activation of specific molecular pathways MSCs are involved in as well as their interactions with the surrounding environment.

References

1. Horwitz EM, Le Blanc K, Dominici M, et al. Clarification of the nomenclature for MSC: The International Society for Cellular Therapy position statement. *Cytotherapy*. 2005;7(5):393–395.
2. Safford KM, Hicok KC, Safford SD, et al. Neurogenic differentiation of murine and human adipose-derived stroll cells. *Biochem Biophys Res Commun*. 2002;294:371–379.
3. Toma C, Pittenger MF, Cahill KS, Byrne BJ, Kessler PD. Human mesenchymal stem cells differentiate to a cardiomyocyte phenotype in the adult murine heart. *Circulation*. 2002;105:93–98.
4. Chen LB, Jiang XB, Yang L. Differentiation of rat marrow mesenchymal stem cells into pancreatic islet beta-cells. *World J Gastroenterol*. 2004;10:3016–3020.
5. Ji R, Zhang N, You N, et al. The differentiation of MSCs into functional hepatocyte-like cells in a liver biomatrix scaffold and their transplantation into liver-fibrotic mice. *Biomaterials*. 2012;33:8995–9008.
6. Pojda Z, Machaj E, Kurzyk A, et al. Mesenchymal stem cells. *Postepy Biochem*. 2013;59(2):187–197.
7. Friedenstein AJ, Gorskaja JF, Kulagina NN. Fibroblast precursors in normal and irradiated mouse hematopoetic organs. *Exp Hematol*. 1976;4:267–274.
8. Saulnier N, Puglisi MA, Lattanzi W, et al. Gene profiling of bone marrow- and adipose tissue-derived stromal cells: A key role of Kruppel-like factor 4 in cell fate regulation. *Cytotherapy*. 2011;13:329–340.
9. Mizuno H. Adipose-derived stem cells for tissue repair and regeneration: Ten years of research and literature review. *J Nippon Med Sch*. 2009;76(2):56–66.

10. Włodarski K, Włodarski P, Galus R, Mazur S. Adipose mesenchymal stem cells. Their characteristics and potential application in tissue repair. *Pol Orthop Traumatol*. 2012;77:97–99.
11. Graneli C, Thorfve A, Ruetschi U, et al. Novel markers of osteogenic and adipogenic differentiation of human bone marrow stromal cells identified using a quantitative proteomics approach. *Stem Cell Res*. 2014;12:153–165.
12. Huang SJ, Fu RH, Shyu WC, et al. Adipose-derived stem cells: Isolation, characterization, and differentiation potential. *Cell Transplant*. 2013;22:701–709.
13. Luongo de Matos L, Trufelli DC, Luongo de Matos MG, da Silva Pinhal MA. Immunohistochemistry as an important tool in biomarkers detection and clinical practice. *Biomark Insights*. 2010;5:9–20.
14. Bae S, Ahn JH, Park CW, et al. Gene and microRNA expression signatures of human mesenchymal stromal cells in comparison to fibroblasts. *Cell Tissue Res*. 2009;335:565–573.
15. Heid CA, Stevens J, Livak KJ, Williams PM. Real time quantitative PCR. *Genome Res*. 1996;6:986–994.
16. Walder RY, Wattiez AS, White SR, de Prado BM, Hamity MV, Hammond DL. Validation of four reference genes for quantitative mRNA expression studies in a rat model of inflammatory injury. *Mol Pain*. 2014;10:55.
17. Wu L, Cai X, Zhang S, Karperien M, Lin Y. Regeneration of articular cartilage by adipose tissue derived mesenchymal stem cells: Perspectives from stem cell biology and molecular medicine. *J Cell Physiol*. 2013;228;938–944.
18. Taha MF, Hedayati V. Isolation, identification and multipotential differentiation of mouse adipose tissue-derived stem cells. *Tissue Cell*. 2010;42:211–216.
19. Graneli C, Karlsson C, Brisby H, Lindahl A, Thomsen P. The effects of PPAR-γ inhibition on gene expression and the progression of induced osteogenic differentiation of human mesenchymal stem cells. *Connect Tissue Res*. 2014;55(4):262–274.
20. Ntambi JM, Kim YC. Adipocyte differentiation and gene expression. *J Nutr*. 2000;130:3122S–3126S.
21. Hu E, Liang P, Spiegelman BM. AdipoQ is a novel adipose-specific gene dysregulated in obesity. *J Biol Chem*. 1996;271(18):10697–10703.
22. Sila-Asna M, Bunyaratvej A, Maeda S, Kitaguchi H, Bunyaratvej N. Osteoblast differentiation and bone formation gene expression in strontium-inducing bone marrow mesenchymal stem cell. *Kobe J Med Sci*. 2007;53(1–2):25–35.
23. Qi H, Aguiar DJ, Williams SM, La Pean A, Pan W, Verfaillie CM. Identification of genes responsible for osteoblast differentiation from human mesodermal progenitor cells. *Proc Natl Acad Sci U S A*. 2003;100(6);3305–3310.
24. Prince M, Banerjee C, Javed A, et al. Expression and regulation of Runx2/Cbfa1 and osteoblast phenotypic markers during the growth and differentiation of human osteoblasts. *J Cell Biochem*. 2001;80:424–440.
25. Marom R, Shur I, Solomon R, Benayahu D. Characterization of adhesion and differentiation markers of osteogenic marrow stromal cells. *J Cell Physiol*. 2005;202:41–48.
26. Mizuno M, Kuboki Y. Osteoblast-related gene expression of bone marrow cells during the osteoblastic differentiation induced by type I collagen. *J Biochem*. 2001;129:133–138.
27. Tsai MT, Li WJ, Tuan RS, Chang WH. Modulation of osteogenesis in human mesenchymal stem cells by specific pulsed electromagnetic field stimulation. *J Orthop Res*. 2009;27(9):1169–1174.
28. Eid AA, Hussein KA, Niu LN, et al. Effects of tricalcium silicate on osteogenic differentiation of human bone marrow-derived mesenchymal stem cells in vitro. *Acta Biomater*. 2014;10:3327–3334.
29. Gordon JAR, Tye CE, Sampaio AV, Underhill TM, Hunter GK, Goldberg HA. Bone sialoprotein expression enhances osteoblast differentiation and matrix mineralization in vitro. *Bone*. 2007;41:462–473.
30. http://www.uniprot.org/uniprot/P21815. Published May 1, 1991. Updated February 28, 2018. Accessed April 15, 2018.
31. Maes C, Kobayashi T, Selig MK, et al. Osteoblast precursors, but not mature osteoblasts, move into developing and fractured bones along with invading blood vessels. *Dev Cell*. 2010;19:329–344.
32. Hamid AA, Idrus RBH, Saim AB, Sathappan S, Chua KH. Characterization of human adipose-derived stem cells and expression of chondrogenic genes during induction of cartilage differentiation. *Clinics*. 2012;67(2);99–106.
33. de Crombrugghe B, Lefebvre V, Behringer RR, Bi W, Murakami S, Huang W. Transcriptional mechanisms of chondrocyte differentiation. *Matrix Biol*. 2000;19:389–394.
34. Lin Y, Luo E, Chen X, at al. Molecular and cellular characterization during chondrogenic differentiation of adipose tissue-derived stromal cells in vitro and cartilage formation in vivo. *J Cell Mol Med*. 2005;9(4):929–939.
35. Mwale F, Stachura D, Roughley P, Antoniou J. Limitations of using aggrecan and type X collagen as markers of chondrogenesis in mesenchymal stem cell differentiation. *J Orthop Res*. 2006;24:1791–1798.
36. Burk J, Gittel C, Heller S, at al. Gene expression of tendon markers in stromal cells derived from different sources. *BMC Res Notes*. 2014;7:826.
37. An Y, Reimers K, Allmeling C, Liu J, Lazaridis A, Vogt PM. Validation of differential gene expression in muscle engineered from rat groin adipose tissue by quantitative real-time PCR. *Biochem Biophys Res Commun*. 2012;421:736–742.
38. Zuk PA, Zhu M, Mizuno H, et al. Multilineage cells from human adipose tissue: Implications for cell-based therapies. *Tissue Eng*. 2001;7:211–226.
39. Zuk PA, Zhu M, Ashjian P, et al. Human adipose tissue is a source of multipotent stem cells. *Mol Biol Cell*. 2002;13:4279–4295.

Multiple primary lung cancer: A literature review

Anna M. Romaszko[A–F], Anna Doboszyńska[A–F]

Department of Pulmonary Medicine and Infectious Diseases, Faculty of Medical Sciences, University of Warmia and Mazury, Olsztyn, Poland

A – research concept and design; B – collection and/or assembly of data; C – data analysis and interpretation;
D – writing the article; E – critical revision of the article; F – final approval of the article

Advances in Clinical and Experimental Medicine, ISSN 1899-5276 (print), ISSN 2451-2680 (online) *Adv Clin Exp Med*. 2018;27(5):725–730

Address for correspondence
Anna Romaszko
E-mail: annama90@wp.pl

Funding sources
None declared

Conflict of interest
None declared

Received on August 3, 2016
Reviewed on December 5, 2016
Accepted on January 24, 2017

Abstract

Nowadays, lung cancer is a leading cause of death in both men and women worldwide. There is no clear explanation for its mortality rate. However, it is already known that genetic and environmental factors as well as oncological treatment are involved. As the incidence of lung cancer soars, the number of patients diagnosed with multiple primary lung cancers (MPLC) is also rising. While differentiating between MPLC and intrapulmonary metastasis of lung cancer is important for treatment strategy and prognosis, it is also quite complicated, particularly in the cases with similar histologies. It is also important not to delay the diagnosis. The aim of this paper was to discuss MPLC in general, and the differentiation between MPLC and intrapulmonary lung cancer metastasis in particular. Based on a review of statistical data and the current literature, we discuss the diagnostic criteria and the molecular, genetic and radiographic methods used to distinguish between MPLC and intrapulmonary metastases.

Key words: lung cancer, intrapulmonary metastasis, multiple primary lung cancer

DOI
10.17219/acem/68631

Copyright
© 2018 by Wroclaw Medical University
This is an article distributed under the terms of the
Creative Commons Attribution Non-Commercial License
(http://creativecommons.org/licenses/by-nc-nd/4.0/)

Introduction

Lung cancer is a leading cause of death in both men and women worldwide.[1] About 1.6 million people die of lung cancer each year and the overall 5-year survival rate is only 15%.[1,2] Most lung cancers are detected at an advanced stage. During or after the treatment of one cancer, the patient may develop another one, including lung cancer. In patients with synchronous multiple primary lung cancer (MPLC) and contraindications to surgical treatment, the mean survival time is 31 months.[3] Distinguishing between intrapulmonary metastases and a new primary cancer may be difficult (especially when the tumor histologies are similar). It is estimated that about 50.8–57.9% of MPLCs have similar histologies.[4,5] It may be even more difficult to discriminate between a subsequent primary lung tumor and an intrapulmonary metastatic tumor if the former develops at a location previously treated with radiotherapy, due to the morphological changes that have taken place there.

Definition of multiple primary lung cancers

The first diagnostic criteria of MPLC were published by Martini et al. in 1975.[6] According to these criteria, synchronous and metachronous MPLC can be distinguished. Synchronous cancers are separate neoplastic processes, histologically identical or different, but occurring in different segments, lobes, or lungs. If they originate from carcinomas in situ, they do not metastasize to the lymph nodes; moreover, extrapulmonary metastases are not present at the time of diagnosis. Metachronous cancers are neoplastic processes with identical or different histologies which develop at an interval of at least 2 years or which originate from carcinomas in situ, or in which the 2nd tumor is located in another lobe or lung, there is no evidence of lymph node metastases, and no extrapulmonary metastases are present at the time of diagnosis. The development of new diagnostic methods has led to modifications of these criteria. Since 1995, MPLC has been defined according to Antakli et al.[4] A diagnosis of MPLC is established if the tumors have different or similar histologies and meet at least 2 of the following 5 criteria:

– different histological locations;
– premalignant lesion;
– no metastases;
– no mediastinal infiltration; or
– different DNA ploidy.

Metachronous lung cancers are the most common MPLC, accounting for 50–70% of all cases.[7]

A case of multiple primary cancers in a single patient was first reported in the literature by Billroth in 1898, while a report on the first case of MPLC was published by Beyreuther in 1924.[8,9]

Various cancer registries have been created since then, enabling the collection of statistical data on the incidence of multiple primary cancers and allowing the prediction of the most likely development of subsequent cancers. This may prove useful in guiding the diagnostic process and preventing the development of further tumors in patients already diagnosed with primary cancers. The registries include:

– the Vaud Cancer Registry, a cancer registry covering the Swiss canton of Vaud and designed to facilitate the risk assessment of the 2nd metachronous cancer;
– The Italian Association of Cancer Registries (AIRTUM), an Italian association of cancer registries providing data on the demographic situation, statistics, incidence, and mortality from cancer in Italy;
– European Cancer Registry (EUROCARE), a registry providing information on the survival of cancer patients based on data collected in population registries; and
– Surveillance, Epidemiology, and End Results Program (SEER), a National Cancer Institute (NCI) population analysis providing information on the statistics of cancer in the US population.

Epidemiology

The development of multiple cancers is determined by many different factors. The treatment administered for the initial cancer is thought to be the primary factor which affects the development of subsequent malignancies. The likelihood of developing the 2nd cancer increases with the duration of survival after the completion of treatment for the primary cancer. The risk is higher in patients diagnosed with the primary cancer below the age of 60 years and in patients with lower-stage primary cancers, in whom the chances of recovery are considerably higher. The process of subsequent neoplasia – apart from genetic factors – is largely determined by carcinogens, such as tobacco smoke and alcohol, which contribute to disseminated lesions in the tissues permanently exposed to these substances.

Smoking is one commonly known factor responsible for the development of cancer. It is particularly related to the direct exposure of the respiratory tract to carcinogenic substances. Many years of smoking may also contribute to the simultaneous development of several cancers at any point after resection of the primary cancer tumor.[10] Despite considerable expenditure on the primary prevention of lung cancer (smoking cessation programs), this malignancy still ranks 1st in terms of incidence and cancer-related mortality worldwide.[11] In the vast majority of cases (85–90%), lung cancer is associated with smoking – including passive smoking by never-smokers.[11,12] Moreover, in a large percentage of cases, lung cancer is diagnosed in former smokers, as the risk of this malignancy continues to increase for many years after smoking cessation.[13]

Retrospective studies have shown an increased risk of subsequent lung cancer after the diagnosis of the 1st lung

cancer. In patients with non-small-cell lung carcinoma (NSCLC), the risk of developing another cancer has been estimated at 1–2% per year, while the risk of another lung cancer in patients with successfully cured small-cell lung carcinoma (SCLC) has been reported at 2–14% per year.[14,15]

In patients who have undergone primary surgical resection for lung cancer, the risk of MPLC is approx. 16%. The risk is obviously not very high, but this is explained by the fact that most patients diagnosed with primary lung cancer die before they develop another type of cancer. If we consider only those patients who survive more than 3 years after the diagnosis of the initial cancer, we can observe that 10–25% of them will develop another lung cancer.[16]

The effects of genetic factors on the development of lung cancer

Recent advances in the analysis of the lung cancer genome have profoundly changed our understanding of this disease on a molecular level. The most important genes responsible for the development of lung cancer are: *EGFR*, *KRAS*, *MET*, *LKB1*, *BRAF*, *PIK3CA*, *ALK*, *RET*, and *ROS1*.[17]

Mutations in *EGFR*, *KRAS*, and *ERBB2* have been demonstrated in adenocarcinoma of the lung.[18] It is often the case that *EGFR* mutations are present in the primary lung cancer but not in its metastases.[19] The *EGFR* gene was screened for mutation in exons 18, 19, 20, and 21 in a female patient with a recent diagnosis of lung adenocarcinoma and a previous lung adenocarcinoma. Mutation analysis of the *EGFR* gene revealed a different mutation in each tumor (on exon 19) confirming the diagnosis of 2 metachronous primary lung cancers.[20,21] Both *EGFR* and *RAS* mutations contribute to the development of NSCLC.[22,23]

KRAS mutations are rare in squamous cell carcinoma of the lung, but may be found in approx. 15–25% of lung adenocarcinomas.[24] In most cases, this is a missense mutation introducing an amino acid substitution at position 12, 13 or 61, which is associated with a poorer prognosis and resistance to erlotinib and gefitinib.[25] Yoon et al. described a case with synchronous triple primary lung cancers with wild-type *EGFR/KRAS* and anaplastic lymphoma kinase mutation.[26]

The tyrosine kinase receptor c-Met plays a significant role in the development of many solid tumors, including SCLC, involved in the processes of neoplasia, cell motility, scattering, invasion, and metastatic spread.

Loss-of-function mutations in *LKB1* were initially only associated with Peutz-Jeghers syndrome, an autosomal dominant genetic disorder.[27] Sanchez-Cespedes et al., however, have demonstrated that *LKB1* mutation is also present in 1/3 of all lung adenocarcinomas.[28]

In NSCLC, *BRAF* mutations have been identified in 1–3% of samples collected from patients. V600E mutations (50%) are the most common, followed by G469A mutations (39%) and D594G (11%).[29] An analysis of the *BRAF* gene sequences in 127 patients with lung adenocarcinoma has shown 2 specific mutations: one in exon 11 (G465V) and the other in exon 15 (L596R).[30]

Kawano et al., in a study of 135 patients with a diagnosis of lung cancer, showed that *PIK3CA* exon 9 mutation occurred in about 3.4% of the patients.[31] This mutation was more common in squamous cell carcinoma of the lung than in adenocarcinoma (6.5% vs 1.5%), and its presence did not correlate with the patient's sex or smoking history.

Less frequent mutations, such as *ROS1* and *RET* mutations in patients with NSCLC, have been reported to occur at a rate of 2% and 1%, respectively.[32,33] *ROS1* mutations are almost always exclusively concomitant with *KRAS*, *EGFR*, and *ALK* mutations.[34,35]

Oncogenetic lung cancer research will lead to new considerations, such as diagnostic tools and therapies. In the near future, more research is needed to more accurately characterize lung cancer mutations in order to generate information that can significantly change the future clinical management of this disease. This can contribute to reducing the incidence of MPLC and improving its detectability. Based on the difference in the expression of the mutated genes, a new primary tumor can be differentiated from an intrapulmonary metastasis, as discussed below.

Screening tests

Preventing lung cancer is much more important than screening for it. Randomized clinical trials have shown that obtaining a chest radiograph does not increase the survival of patients diagnosed with lung cancer. Recent studies, however, have demonstrated that annual screening for lung cancer with chest computed tomography (CT) decreases mortality in patients with a history of strong nicotine dependence.[36] The efficacy of intensive surveillance by means of annual chest CT scanning to detect subsequent lung cancers or lung cancer metastases has not been formally demonstrated, although subsequent annual CT scans are often performed and recommended by the National Comprehensive Cancer Network (NCCN) guidelines. This data, however, is insufficient to conclusively support this common practice. More sensitive diagnostic measures, such as lung imaging fluorescence endoscopy (LIFE), are being investigated to establish their usefulness for the detection of synchronous tumors.[37]

How to differentiate multiple primary lung cancers from disseminated primary tumor

The incidence of synchronous or metachronous lung cancers has been increasing over the past few years. This has been due to technological progress and the increasing

availability of novel diagnostic methods, such as computed tomography and positron emission tomography. What continues to be challenging is the differentiation of a subsequent lung cancer from intrapulmonary metastases of the 1st lung cancer. According to the current TNM classification (8th edition) for lung cancer, in the event that the tumor nodules are found in the same lobe as the main tumor, the tumor is categorized as T3; if the tumor is found in a different lobe but on the same side – T4; and if it is located on a contralateral side – M1a.[38] When multiple primary lung tumors are present, it is quite difficult to distinguish multicentric lung cancer from a primary cancer in a different organ.[39] Currently, based on histopathology, many of the subsequent lung cancers are erroneously diagnosed, especially if the patient develops a multiple lung malignancy that is histologically impossible to differentiate.[3] Such differentiation, however, is possible using genetic and immunohistochemical methods, and a correct diagnosis is necessary for the selection of suitable treatment. Many studies have reported differences in certain cancer gene mutations, chromosome aberrations, and microsatellite alterations between different MPLCs.[40,41]

A study of 19 metachronous and 11 synchronous multiple lung tumors investigated the overexpression and genetic abnormalities of the *p53* gene.[42] The results have shown that some of the multiple tumors were of different clonal origins, although their histological type was the same. Mitsudomi et al. analyzed the phenotypes in 16 patients with *p53* gene mutation using polymerase chain reaction (PCR) and single-strand conformation polymorphism (SSCP).[43] At least one *p53* gene mutation in the lung tumor was demonstrated in 9 of these patients. The *p53* mutation statuses were incongruent in these patients. This suggested a different clonal origin, even though 6 of them had nearly identical histological features. In lung cancer, the *p53* gene has so far been considered one of the most commonly mutated genes, with mutations present in 50% of NSCLC patients and in nearly all SCLC patients.[44] Another advantage offered by testing for *p53* gene mutation is that the mutation can be demonstrated relatively early in the course of lung cancer, especially its squamous cell variety, because the mutation plays a role in developing the malignant phenotype.[45] Once acquired, this phenotype is well-preserved during progression and metastasis.[46] In addition to the *p53* gene mutation, several other molecular methods are currently available for clonal analysis of lung tumors. The analysis of X-chromosome inactivation, which occurs in the early phase of lung cancer development, is interesting. It is only possible, however, to investigate it in females.[47] In addition, testing for the loss of heterozygosity (LOH) in certain arms of chromosomes, such as 3p, 5q, 9q, 11p, 13q, 17p, or 18q, or for *RAS* mutations is currently being performed.

Many studies have shown that phenomena based on microsatellite instability (MSI) and on LOH can be used to differentiate between a disseminated primary tumor and a subsequent primary tumor, both in the early and late stages of the disease.[48–50] Both of these phenomena, MSI and LOH, represent molecular abnormalities acquired by the cell during neoplastic transformation. Shen et al. carried out a molecular analysis of 2 lung tumors in a single patient (one tumor located in the right lower lobe and the other in the right upper lobe) based on microsatellite allele D2S1363, which was detected in the 1st tumor, but not in the other. In both tumors, the same allelic background for 5 microsatellite markers was established, although it did differ in 1 microsatellite marker – D2S1363 – which was detected in the 1st, but not in the other tumor.[51] This finding was concluded to substantiate the fact that the 2nd lesion was indeed a metastatic lesion originating from the 1st tumor, which was histologically confirmed.

Wang et al. investigated genetic material from 70 lung tumors in 30 patients.[52] In each of the 30 patients, LOH was demonstrated in 1–4 of the 6 microsatellite markers. Twenty-three of the 30 patients (77%) were shown to have identical genetic abnormalities consistent with a monoclonal origin of different tumors.

Molecular analysis of different alleles and microsatellite polymorphic markers can therefore be used to differentiate metastatic tumors from MPLCs.

Differential diagnosis of tumors can also be carried out on the basis of *EGFR* mutations.[53] Takuwa et al. published a case report on the simultaneous presence of 2 adenocarcinomas, each at a different location.[54] One tumor, located in the middle lobe, showed the L858R mutation in *EGFR* exon 21, which was identical to the mutation in the cells sampled from the subcarinal lymph nodes. No such mutation, however, was detected in the other tumor, located in the upper lobe. Based on that, a diagnosis of dual primary lung cancer was established. This is a known hotspot mutation and accounts for more than 40% of *EGFR* mutations reported in Asian lung adenocarcinoma patients.[55]

In the area of low-dose CT screening for lung cancer, though, the search for a non-invasive tool to differentiate primary lung cancer and granulomatous nodules has intensified.[56,57]

Positron emission tomography (PET) can be used to differentiate multiple primary synchronous tumors from disseminated primary tumors. Dijkman et al. conducted a study in 37 patients in which they demonstrated a significantly higher ΔSUV (difference between standardized uptake values) in those with the 2nd primary tumor compared to those with a metastatic tumor (58% vs 28%, $p < 0.001$).[58] Furthermore, Hsu et al. showed that tumor size itself may have a strong influence on potential local progression or metastasis, and that the combination of SUV_{max} and size together identified a subgroup of patients at higher risk for recurrence after surgical resection.[59] The SUV values from images acquired using ^{18}F-FDG PET can therefore be useful in differentiating metastatic tumors from other primary tumors in patients with synchronous lung cancer.[60]

Summary

Patients diagnosed with their 1st lung cancer should be carefully monitored in order to allow the early detection of a subsequent malignancy. The diagnosis of MPLC may be delayed or incorrect in patients with lung cancer with intrapulmonary spread. Novel methods of differential diagnosis of the intrapulmonary spread of a primary tumor vs MPLC may provide valuable diagnostic clues. Undoubtedly, molecular methods in the near future will have a growing role and will optimize the management of patients with multiple neoplasms. However, the current knowledge about MPLC oncogenetics is still insufficient. We hope that future studies will provide a deeper understanding of this problem, and thus contribute to better prevention and earlier diagnosis. Precise determination of the clonal origin of MPLC might help rationalize the treatment and improve the prognosis of patients.

References

1. Jemal A, Siegel R, Ward E, et al. Cancer statistics, 2008. *CA Cancer J Clin*. 2008;58:71–96.
2. World Health Organization. Cancer fact sheet, 2010. http://www.who.int/mediacentre/factsheets/fs297/en/. Accessed May 30, 2016.
3. Griffioen GH, Lagerwaard FJ, Haasbeek CJ, Smit EF, Slotman BJ, Senan S. Treatment of multiple primary lung cancers using stereotactic radiotherapy, either with or without surgery. *Radiother Oncol*. 2013;107:403–408.
4. Antakli T, Schaefer RF, Rutherford JE, Read RC. Second primary lung cancer. *Ann Thorac Surg*. 1995;59:863–836.
5. Riquet M, Cazes A, Pfeuty K, et al. Multiple lung cancers prognosis: What about histology? *Ann Thorac Surg*. 2008;86:921–926.
6. Martini N, Melamed M. Multiple primary lung cancers. *J Thorac Cardiovasc Surg*. 1975;70:606–612.
7. Tsunezuka Y, Matsumoto I, Tamura M, et al. The results of therapy for bilateral multiple primary lung cancers: 30 years' experience in a single centre. *Eur J Surg Oncol*. 2004;30:781–785.
8. Billroth T. General surgical pathology and therapy: Guidance for students and physicians. Lecture [in Russian]. *Khirurgiia*. 1991;10:136–143.
9. Beyreuther H. Multiplicität von Carcinomen bei einem Fall von sog. "Schneeberger" Lungenkrebs mit Tuberkulose. *Virchows Arch Pathol Anat Physiol Klin Med*. 1924;250:230–243.
10. Polednak AP. Obtaining smoking histories for population based studies on multiple primary cancers: Connecticut, 2002. *Int J Cancer*. 2006;119:233–235.
11. Fontham ET, Correa P, Reynolds P, et al. Environmental tobacco smoke and lung cancer in nonsmoking women: A multicenter study. *JAMA*. 1994;271:1752–1759.
12. Alberg AJ, Samet JM. Epidemiology of lung cancer. *Chest*. 2003;123:21S–49S.
13. Tong L, Spitz MR, Fueger JJ, Amos CI. Lung carcinoma in former smokers. *Cancer*. 1996;78:1004–1010.
14. Johnson BE. Second lung cancers in patients after treatment for an initial lung cancer. *J Natl Cancer Inst*. 1998;90:1335–1345.
15. Li X, Hemminki K. Familial and second lung cancers: A nationwide epidemiologic study from Sweden. *Lung Cancer*. 2003;39:255.
16. Van Bodegom PC, Wagenaar S, Corrin B, Baak J, Berkel J, Vanderschueren R. Second primary lung cancer: Importance of long term follow up. *Thorax*. 1989;44:788–793.
17. El-Telbany A, Ma PC. Cancer genes in lung cancer racial disparities: Are there any? *Genes Cancer*. 2012;3:467–480.
18. Ding L, Getz G, Wheeler DA, et al. Somatic mutations affect key pathways in lung adenocarcinoma. *Nature*. 2008;455:1069–1075.
19. Han HS, Eom DW, Kim JH, et al. EGFR mutation status in primary lung adenocarcinomas and corresponding metastatic lesions: Discordance in pleural metastases. *Clin Lung Cancer*. 2011;12:380–386.
20. Vaz D, Conde S, Tente D, Machado JC, Barroso A. Role of epidermal growth factor mutational status for distinction between recurrent lung cancer and second primary lung cancer: Case report. *Clin Respir J*. 2017;11(6):854–858.
21. Yang Y, Shi C, Sun H, et al. Elderly male smokers with right lung tumors are viable candidates for KRAS mutation screening. *Sci Rep*. 2016;6:18566. doi:10.1038/srep18566
22. Yang Y, Yin W, He W, et al. Phenotype-genotype correlation in multiple primary lung cancer patients in China. *Sci Rep*. 2016;6:36177. doi:10.1038/srep36177
23. Wang L, Hu H, Pan Y, et al. PIK3CA mutations frequently coexist with EGFR/KRAS mutations in non-small cell lung cancer and suggest poor prognosis in EGFR/KRAS wildtype subgroup. *PloS One*. 2014;9(2):e88291. https://doi.org/10.1371/journal.pone.0088291
24. Aviel-Ronen S, Blackhall FH, Shepherd FA, Tsao MS. K-ras mutations in non-small-cell lung carcinoma: A review. *Clin Lung Cancer*. 2006;8:30–38.
25. Riely GJ, Kris MG, Rosenbaum D, et al. Frequency and distinctive spectrum of KRAS mutations in never smokers with lung adenocarcinoma. *Clin Cancer Res*. 2008;14:5731–5734.
26. Yoon HJ, Lee HY, Han J, Choi YL. Synchronous triple primary lung cancers: A case report. *Korean J Radiol*. 2014;15:646–650.
27. Hemminki A, Markie D, Tomlinson I, et al. A serine/threonine kinase gene defective in Peutz–Jeghers syndrome. *Nature*. 1998;391:184–187.
28. Sanchez-Cespedes M, Parrella P, Esteller M, et al. Inactivation of LKB1/STK11 is a common event in adenocarcinomas of the lung. *Cancer Res*. 2002;62:3659–3662.
29. Paik PK, Arcila ME, Fara M, et al. Clinical characteristics of patients with lung adenocarcinomas harboring BRAF mutations. *J Clin Oncol*. 2011;29:2046–2051.
30. Naoki K, Chen TH, Richards WG, Sugarbaker DJ, Meyerson M. Missense mutations of the BRAF gene in human lung adenocarcinoma. *Cancer Res*. 2002;62:7001–7003.
31. Kawano O, Sasaki H, Endo K, et al. PIK3CA mutation status in Japanese lung cancer patients. *Lung Cancer*. 2006;54:209–215.
32. Bergethon K, Shaw AT, Ou SHI, et al. ROS1 rearrangements define a unique molecular class of lung cancers. *J Clin Oncol*. 2012;30:863–870.
33. Kohno T, Ichikawa H, Totoki Y, et al. KIF5B-RET fusions in lung adenocarcinoma. *Nat Med*. 2012;18:375–377.
34. Warth A, Muley T, Dienemann H, et al. ROS1 expression and translocations in non-small-cell lung cancer: Clinicopathological analysis of 1478 cases. *Histopathology*. 2014;65:187–194.
35. Shaw AT, Ou SH, Bang YJ, et al. Crizotinib in ROS1-rearranged non-small-cell lung cancer. *N Engl J Med*. 2014;371:1963–1971.
36. Pastorino U, Rossi M, Rosato V, et al. Annual or biennial CT screening versus observation in heavy smokers: 5-year results of the MILD trial. *Eur J Cancer Prev*. 2012;21:308.
37. van Rens MT, Schramel FM, Elbers JR, Lammers JW. The clinical value of lung imaging fluorescence endoscopy for detecting synchronous lung cancer. *Lung Cancer*. 2001;32:13.
38. Edge SB & American Joint Committee on Cancer. *AJCC Cancer Staging Manual*. 8th ed. New York, NY: Springer-Verlag New York; 2017.
39. Asamura H. Multiple primary cancers or multiple metastases, that is the question. *J Thorac Oncol*. 2010;5:930–931.
40. Murphy SJ, Aubry MC, Harris FR, et al. Identification of independent primary tumors and intrapulmonary metastases using DNA rearrangements in non-small-cell lung cancer. *J Clin Oncol*. 2014;32:4050–4058.
41. Rekhtman N, Borsu L, Reva B, et al. Unsuspected collision of synchronous lung adenocarcinomas: A potential cause of aberrant driver mutation profiles. *J Thorac Oncol*. 2014;9:e1–e3.
42. Hiroshima K, Toyozaki T, Kohno H, Ohwada H, Fujisawa T. Synchronous and metachronous lung carcinomas: Molecular evidence for multicentricity. *Pathol Int*. 1998;48:869–876.
43. Mitsudomi T, Yatabe Y, Koshikawa T, et al. Mutations of the P53 tumor suppressor gene as clonal marker for multiple primary lung cancers. *J Thorac Cardiovasc Surg*. 1997;114:354–360.
44. Gazdar AF. The molecular and cellular basis of human tumors: A review. *Cancer Res*. 1990;50:1355–1360.
45. Sozzi G, Miozzo M, Donghu R, et al. Deletion of 17p and p53 mutation in preneoplastic lesion of the lung. *Cancer Res*. 1992;52:6079–6082.

46. Reichel MB, Oghaki H, Petersen I, Kleihues P. p53 mutation in primary human lung tumors and their metastases. *Mol Carcinog*. 1986;89: 25s–32s.
47. Wainscoat JS, Fey MF. Assessment of clonality in human tumor: A review. *Cancer Res*. 1990;50:1355–1360.
48. Geurts TW, Nederlof PM, van den Brekel MW, et al. Pulmonary squamous cell carcinoma following head and neck squamous cell carcinoma: Metastasis or second primary? *Clin Cancer Res*. 2005;11:6608–6614.
49. Shen C, Wang X, Tian L, Che G. Microsatellite alteration in multiple primary lung cancer. *J Thorac Dis*. 2014;6:1499.
50. Dacic S, Ionescu DN, Finkelstein S, Yousem SA. Patterns of allelic loss of synchronous adenocarcinomas of the lung. *Am J Surg Pathol*. 2005;29:897–902.
51. Shen C, Wang X, Tian L, et al. "Different trend" in multiple primary lung cancer and intrapulmonary metastasis. *Eur J Med Res*. 2015;20:17.
52. Wang X, Wang M, MacLennan GT, et al. Evidence for common clonal origin of multifocal lung cancers. *J Natl Cancer Inst*. 2009;101:560–570.
53. Liu Y, Zhang J, Li L, et al. Genomic heterogeneity of multiple synchronous lung cancer. *Nat Commun*. 2016;7:13200.
54. Takuwa T, Tanaka F, Yoneda K, et al. Diagnosis of synchronous primary lung adenocarcinomas based on epidermal growth factor (EGFR) gene status: A case report. *Lung Cancer*. 2010;68:498–500.
55. Mok TS, Wu YL, Thongprasert S, et al. Gefitinib or carboplatin-paclitaxel in pulmonary adenocarcinoma. *N Engl J Med*. 2009;361:947–957.
56. Sharma N, Ray AK, Sharma S, et al. Segmentation and classification of medical images using texture primitive features: Application of BAM-type artificial neutral network. *J Med Phys*. 2008;33:119–126.
57. Dennie C, Thornhill R, Sethi-Virmani V, et al. Role of quantitative computed tomography texture analysis in the differentiation of primary lung cancer and granulomatous nodules. *Quant Imaging Med Surg*. 2016;6(1):6–15.
58. Dijkman BG, Schuurbiers OC, Vriens D, et al. The role of 18F-FDG PET in the differentiation between lung metastases and synchronous second primary lung tumors. *Eur J Nucl Med Mol Imaging*. 2010;37: 2037–2047.
59. Hsu HH, Ko KH, Chou YC, et al. SUVmax and tumor size predict surgical outcome of synchronous multiple primary lung cancers. *Medicine* (*Baltimore*). 2016;95:e2351.
60. Obando JA, Samii JM, Yasrebi M. A case of two synchronous primary lung tumors demostrated by FDG positron emission tomography. *Clin Nucl Med*. 2008;33:775–777.

Advances
in Clinical and Experimental
Medicine